NASA SP-474

Voyager 1 and 2 Atlas of Six Saturnian Satellites

Raymond M. Batson

Associate Authors

Image Processing

Ella M. Lee
Kevin F. Mullins
Brian A. Skiff

Airbrush Cartography

Patricia M. Bridges
Jay L. Inge

Nomenclature

Harold Masursky
Mary E. Strobell

NASA Scientific and Technical Information Branch 1984
National Aeronautics and Space Administration
Washington, DC

Library of Congress Cataloging in Publication Data

Batson, Raymond M.
Voyager 1 and 2 atlas of six Saturnian satellites.

(NASA SP–474)
Bibliography: p. 141
Includes index.
1. Satellites—Saturn—Atlases. 2. Project Voyager—Atlases. I. Title.
QB405.B37 1984 523.9'86 84–11580

For sale by the National Technical Information Service
Springfield, Va. 22151

Preface

The exploration of the outer solar system by the two U.S. Voyager spacecraft marks an important turning point in understanding the universe. Prior to the Voyager and Pioneer missions, the planetary exploration program concentrated on the terrestrial bodies of the inner solar system: Mercury, the Moon, and Mars. The Moon and Mercury, now geologically dead, display ancient battered crusts developed under the torrential bombardment of debris remaining from the accretion of the solar system. Both display evidence of fleeting episodes of early volcanism as they cooled down. Mars, to a large degree, exhibits the same basic pattern. Owing to its tenuous carbon dioxide atmosphere and moderate amount of water, Mars shows evidence of additional processes: sand dunes and wind scour, and features that appear to be related to glacial action and brief fluvial episodes. We were trained by these experiences to expect the planets of the solar system (and, by implication, of the universe) to belong to a fairly narrow spectrum in terms of the types of geologic processes and histories they could have. Armed with this perspective, we journeyed with the Voyager spacecraft to the environs of Jupiter and Saturn, inspecting many things along the way, including the miniature planetary systems consisting of the Jovian and Saturnian arrays of moons. The Voyager spacecraft arrived first at Jupiter, where we examined Io, Europa, Ganymede, and Callisto. Two of them we knew to be roughly the size and density of our own Moon; the other two we knew to be the size of Mercury, but to consist roughly of half water or water ice. In this cold setting, we expected lifeless, plain, simple, geologic styles and histories that would interest only the most esoteric planetary geologists. To our surprise we discovered an intensely volcanically active moon laced with sulfur and sulfur dioxide driven volcanoes (Io); a moon with a complex, intricate, interwoven network of stretch marks and cycloidal ridges (Europa); and a moon with a bizarre jumble of forms driven by a process of ice-raft tectonics that resembles in some aspects Earth's own process of continental drift (Ganymede). The two spacecraft flew on to Saturn. Here the moons were even smaller. The bodies we would examine geologically have diameters that range from less than half the diameter of our Moon down to only a few hundred kilometers. Evidence indicated that these objects could not have substantial geologic variability or complex geologic histories. How could an object the size of Enceladus, with only 10 millionths the mass of Earth, in a deep freeze at only 90 K (−300° F), composed of water ice frozen to the consistency of the hardest rocks, display substantial activity? The maps presented in this atlas portray the diversity that we found. Examination of three of the smallest classical Saturnian moons, Mimas, Enceladus, and Hyperion, reveals a diversity many times broader than the narrow terrestrial view we had held prior to the Voyager missions. Mimas is close to what we expected—a frozen, pockmarked ball of cold rubble. Hyperion (not yet mapped in detail and hence not included in the atlas) is about the same size as Mimas but shows a highly irregular shape indicating that it is a fragment torn from a much larger, rigid object. On Enceladus, the greatest surprise, regions of cratered plains suggest great antiquity, yet other regions are free of craters, at least to the limit of resolution. Our best models indicate that this tiny body must have been active in the geologically recent past and is probably, at least from time to time, geologically active today. The lesson we learned is that wherever we look, we will find energy sources that will drive the geologic engines of planets: some radiogenic, some accretional heat, some gravitational, and, probably, some chemical and some electromagnetic. We have also learned that no matter how cold the ambient environment, materials are available to serve as lubricants to mobilize the interiors of the planets. On the Saturnian satellites, the likely lubricants are methane and ammonia. As you peruse the materials in this atlas, remember how limited our expectations of the Saturnian moons were compared to what we found; imagine how diverse planetary objects throughout the universe must truly be.

Laurence A. Soderblom
Deputy Chief, Voyager Imaging Team

Acknowledgments

The image processing and preliminary mapping contained in this atlas were supported by funding from the Voyager Imaging Team, in cooperation with the National Aeronautics and Space Administration under contract WO–8395. Preparation of this atlas for publication was supported by funding from the Planetary Geology Programs Office of the National Aeronautics and Space Administration under contract W–13,709.

Digital image processing of the Voyager pictures was done in the Flagstaff Image Processing Facility. The programs and techniques that were used have been developed over a period of several years by many scientists and programmers, but most of the critical Voyager radiometric calibration programming was done by Eric M. Eliason, and most of the geometric programming is by Kathleen Edwards. Ellen M. Sanchez developed the sequencing and control programs for the Level 1 image processing, and Lynda B. Sowers supervised the computer production phases of the work. Photoprocessing support was supervised by Karl A. Zeller and photomechanical processing by Hugh F. Thomas. Roger D. Carroll supervised preparation of map linework. Many other people, too numerous to mention here, contributed to the preparation of this atlas. To all contributors, named and unnamed, the authors extend their heartfelt thanks.

We are also indebted to Merton E. Davies of the Rand Corp. and Paul D. Spudis of the U.S. Geological Survey for critical reviews and many helpful suggestions.

Earth:
Mercury
Gemini
Apollo
Landsat
Skylab
Mariner 10
Galilean satellites:
Voyagers 1 and 2
Galileo
Mercury:
Mariner 10
Moon:
Ranger
Lunar Orbiter
Apollo
Mariner 10
Venus:
Mariner 10
Venus Pioneer
Venus Mapper
Mars:
Mariner 4
Mariners 6 and 7
Mariner 9
Viking Orbiters
Saturnian satellites:
Voyagers 1 and 2

Contents

Introduction

This atlas contains preliminary maps of six satellites of Saturn and includes the pictures and other data gathered primarily by the Voyager 1 and 2 spacecraft that were used to compile the maps. These satellites are the only ones for which a sufficiently comprehensive set of pictures is currently available for this kind of work. Maps have not yet been made of the irregularly shaped satellites because conventional map projection techniques are useful only for spherical or at least spheroidal bodies. Maps of Saturn and its largest satellite, Titan, cannot be made with Voyager pictures because they show only the dense clouds that cover those bodies. Voyager passed so far from the remaining satellites that the pictures taken are not adequate to support the compilation of maps.

Two versions of each satellite picture and two versions of each map are contained in the atlas. In addition, a grid showing the latitude-longitude system for each satellite, in the perspective view of each picture, is included. The two versions of each picture include a contrast-enhanced unfiltered version, and a contrast-enhanced high-pass filtered version. These two versions provide significantly different presentations of the images to augment the study and interpretation of the data. Appendix C discusses the computer-processing methods used to produce these pictures.

The two map versions include Mercator and polar stereographic projections of each map as well as Lambert azimuthal equal-area projections. The Mercator and polar stereographic projections are termed "conformal" by cartographers and are useful because the correct shapes of small features are preserved. Equal-area projections, on the other hand, are preferred for measuring surface areas. For example, a coin placed anywhere on an equal-area map will always cover the same number of square kilometers, even though the shapes of features may appear to be foreshortened near the edges of the maps.

Part or all of 14 planets and satellites have now been mapped with data from American spacecraft (Batson, 1980). Figure 1 is a montage of these objects, with Earth included for scale. The size of the image of each object is correct in proportion to the others. The names of American spacecraft with sensors capable of providing map data are shown next to the planets and satellites they have visited. Galileo and Venus Mapper had not flown at the time of this writing. Figure 2 shows the total known mappable area in our solar system. Planets that may not have solid surfaces beneath their cloudy atmospheres are not mappable in the traditional sense and are, therefore, excluded. Figure 3 shows the size of the Earth-Moon system with respect to the Saturnian system, along with the geometry of the Voyager trajectories with respect to the Saturnian system.

The process of mapping another planet involves special computer processing of spacecraft television pictures, making mosaics of those pictures, selecting names for newly discovered features, and compiling a co-

Figure 1 (*facing page*). The planets and satellites visited by American spacecraft. Each of the bodies is shown at its correct size relative to others. The names of spacecraft with sensors capable of collecting map data are also listed next to the image of the body. The Galileo and Venus Mapper spacecraft (labeled in blue) had not flown at the time of this writing.

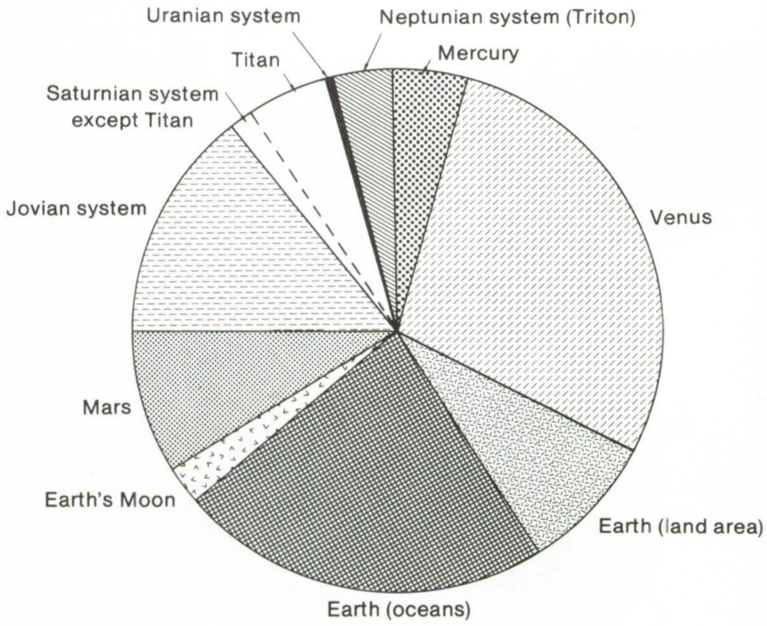

Figure 2. The total known mappable area in the solar system ($\cong 1.6 \times 10^6$ km^2). Planets that may not have solid (mappable) surfaces (Jupiter, Saturn, Uranus, and Neptune) are not included. Pluto and its satellite, Charon, would add only a minuscule amount to this diagram.

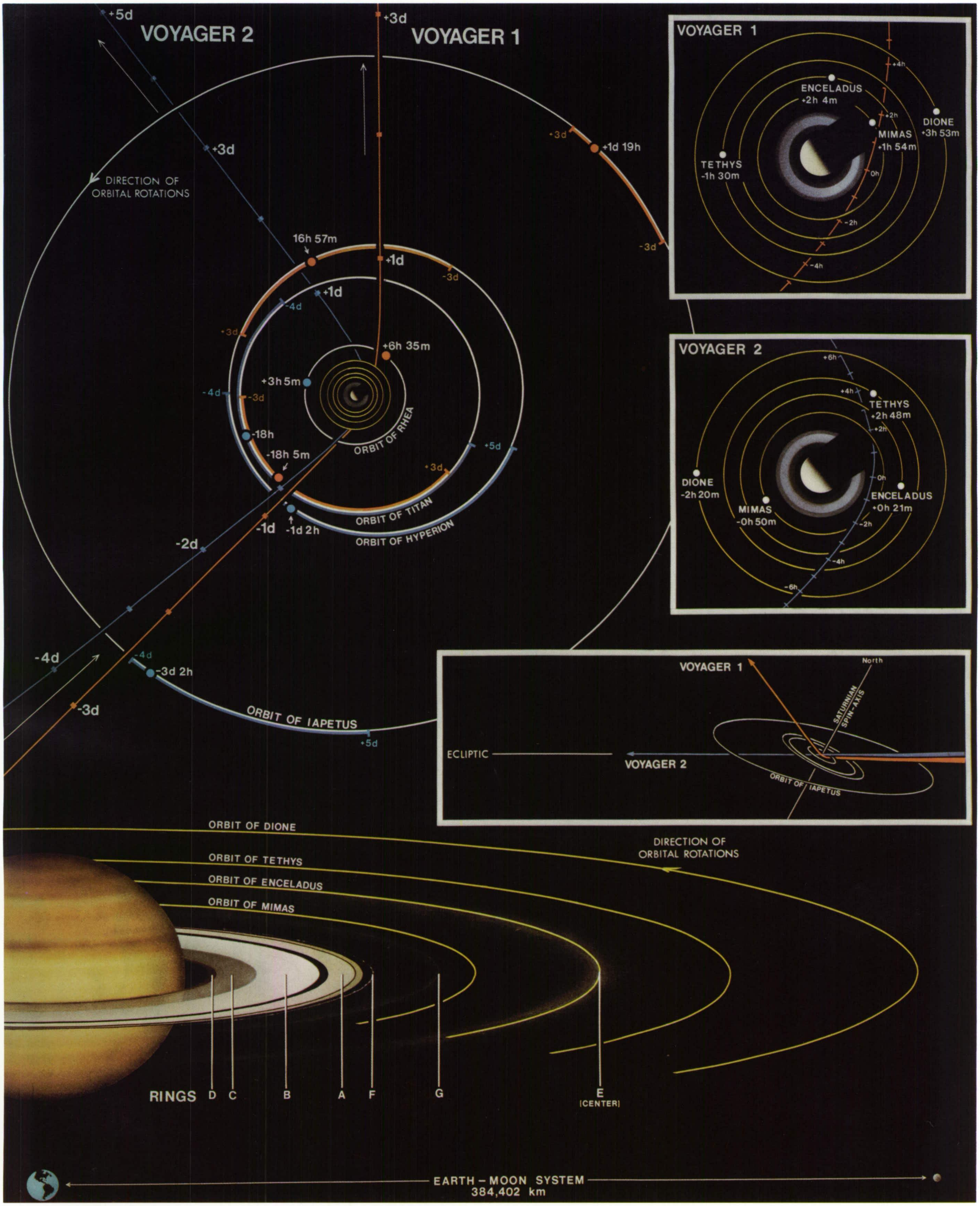

VOYAGER 2
VOYAGER 1
+5d
+3d
DIRECTION OF ORBITAL ROTATIONS
+1d 19h
16h 57m
+1d
+6h 35m
+3h 5m
-18h
-18h 5m
ORBIT OF RHEA
ORBIT OF TITAN
ORBIT OF HYPERION
-1d
-1d 2h
-2d
-4d
-3d
-3d 2h
ORBIT OF IAPETUS
ENCELADUS +2h 4m
DIONE +3h 53m
MIMAS +1h 54m
TETHYS -1h 30m
TETHYS +2h 48m
DIONE -2h 20m
ENCELADUS +0h 21m
MIMAS -0h 50m
North
SATURNIAN SPIN-AXIS
ECLIPTIC
ORBIT OF DIONE
ORBIT OF TETHYS
ORBIT OF ENCELADUS
ORBIT OF MIMAS
RINGS D C B A F G E (CENTER)
EARTH – MOON SYSTEM 384,402 km

Table 1. Resolution of Available Voyager 1 and 2 Image Coverage of Six Satellites of Saturn

Satellites	Dimension of picture elements										Total surface area, 10^3 km^2
	0.5 to 2 km		2 to 5 km		5 to 20 km		20 to 40 km		>40 km		
	Percent of planet	Area, 10^3 km^2	Percent of planet	Area, 10^3 km^2	Percent of planet	Area, 10^3 km^2	Percent of planet	Area, 10^3 km^2	Percent of planet	Area, 10^3 km^2	
Mimas	7.7	37	17	82	38.7	18.7	11.9	57	24.7	119	482
Enceladus	10.6	83	39.3	309	22.5	177	7.8	61	19.8	155	785
Tethys	—	—	3.3	116	53.5	1888	24.2	854	19	671	3529
Dione.............	4.5	177	12.8	504	32.7	1289	30.3	1194	19.7	776	3940
Rhea..............	11.5	846	17	1250	13.3	978	14.4	1059	43.8	3221	7354
Iapetus............	—	—	—	—	10.4	696	1067	0	79.6	5330	6696

herent portrayal of the surface on an appropriate map projection using airbrush drawing techniques. These techniques are discussed in appendixes C and D, and further information is contained in publications listed in the references section. The discussions are intended to provide a basic reference and orientation to readers who may be unfamiliar with some aspects of the mapping project. Appendix C, covering digital image processing, in particular was purposely written at an elementary level for the benefit of readers unfamiliar with many of the concepts of digital image processing. Full technical details of the processing are beyond the scope of the atlas.

The striking variations in the amount of detail shown on the maps are a direct function of the resolution of Voyager 1 and 2 pictures taken at different distances from the satellite. Some areas are portrayed with intricate detail, whereas others show only diffuse mottling, or nothing at all. Maps showing the resolution of available Voyager pictures are included at the beginning of the section for each satellite. Table 1 is a tabulation of the same information. The term "resolution" is used here to define the size of the area covered by a single picture element (pixel) on a planet or satellite. A surface feature must usually be large enough to be covered by at least two pixels if it is to be detected in the image. True resolution is more complicated: It varies as a function of scene contrast, the optical quality of the camera lens, various electronic recording and transmission factors in the camera and spacecraft, and the viewing geometry at the time a picture is taken.

The two most important visual aspects of an image of a cloudless planet or satellite are the surface forms, or topography, and the surface coloration, or albedo. Albedo is a measure of light reflected from surface materials (charcoal has a low albedo; snow has a high albedo) and is easiest to see and measure when the Sun is directly behind the observer or camera, so that shadows are not mixed with albedo markings. Albedo patterns sometimes vary in color, resulting in apparent differences between black and white pictures taken through different color filters. Albedo patterns cover vast areas on planets and satellites, and can usually be mapped from very low resolution data. Topography, on the other hand, is most visible when the Sun strikes the surface at an oblique angle, thus producing shadows, and is most sharply defined along the terminator, a line on the surface that divides day and night. Landforms tend to be much smaller than albedo patterns and, therefore, require much higher resolution to detect. They are rarely discernible on images in which each picture element covers an area that is more than 20 km in diameter.

Just as our Moon always presents the same face to Earth, the six moons in this atlas always present the same face to Saturn. The phenomenon of libration probably causes the sub-Saturn point to oscillate by some amount, undetectable through Voyager data. The International Astronomical Union (IAU) defines the prime meridian on each satellite by reference to a great circle line that passes through a specified, observable surface feature and the intercepts of the spin axis with the surface of the satellite (i.e., the North

Figure 3 (*facing page*). The Earth-Moon system compared with the Saturnian system, and the geometry of the Voyager trajectories through the Saturnian system. Earth, Moon, Saturn, Titan, and all orbits are shown to scale. Most of the Saturnian satellites are too small to be shown to scale in this figure (Illustration by J. L. Inge, W. T. Borgeson, and C. E. Isbell) and South poles) (Davies et al., 1980). Astronomical convention defined by the IAU also specifies that longitude values increase in the direction of the movement of the Sun as viewed from the surface. Thus, if the Sun appears to rise in the east and move to the west, longitude values increase to the west (IAU, 1971). The terms "Saturn facing," "anti-Saturn facing," "leading," and "trailing" hemisphere are used in this atlas to specify areas on the satellites. The leading hemisphere is to the west of the central meridian, because the satellites revolve in a counterclockwise direction as viewed from above Saturn's north pole.

Some of Saturn's moons are not so orderly. Phoebe, for example, moves in the opposite direction to the other satellites in an orbit that is highly inclined to its orbital plane. There is evidence that the spin axis of Hyperion is highly inclined to the plane of its orbit, and that it does not always present the same face to Saturn.

Maps and photographs in this atlas are available to the public through Government distribution centers. Maps published by the U.S. Geological Survey, including many lunar and planetary maps in addition to those of the Saturnian satellites, are available at the following addresses:

U.S. Geological Survey Branch of Distribution Denver Federal Center Denver, Colo. 80225	*or*	U.S. Geological Survey Branch of Distribution 1200 South Eads St. Arlington, Va. 22202

Maps are ordered by the "I-number" shown on the captions.

Various enhancements of the pictures in the atlas are available from—

National Space Science Data Center
Code 601
Goddard Space Flight Center
Greenbelt, Md. 20771

Images are ordered by "picno," the picture number shown in each caption.

PART 1

Mimas

Diameter	394 km (245 miles)
Density	1.4
Albedo	0.6
Distance from Saturn	188 224 km (116 957 miles)
Orbital period	23 hr, 8 min, 20 sec
Voyager 1 closest approach	88 440 km (54 954 miles)
Voyager 1 pictures used in mapping	9
Voyager 2 closest approach	309 990 km (192 618 miles)
Voyager 2 pictures used in mapping	0

Mimas is the smallest and innermost of the spherical satellites of Saturn. Its orbit lies between the newly discovered Rings G and E. Its most distinctive feature is a giant crater 130 km in diameter, nearly one-third the diameter of Mimas itself. The walls of the crater have an average height of 5 km, and the crater may be more than 10 km deep. It is nearly centered on the leading hemisphere of Mimas. Smaller craters are abundant and appear to be more or less uniformly distributed.

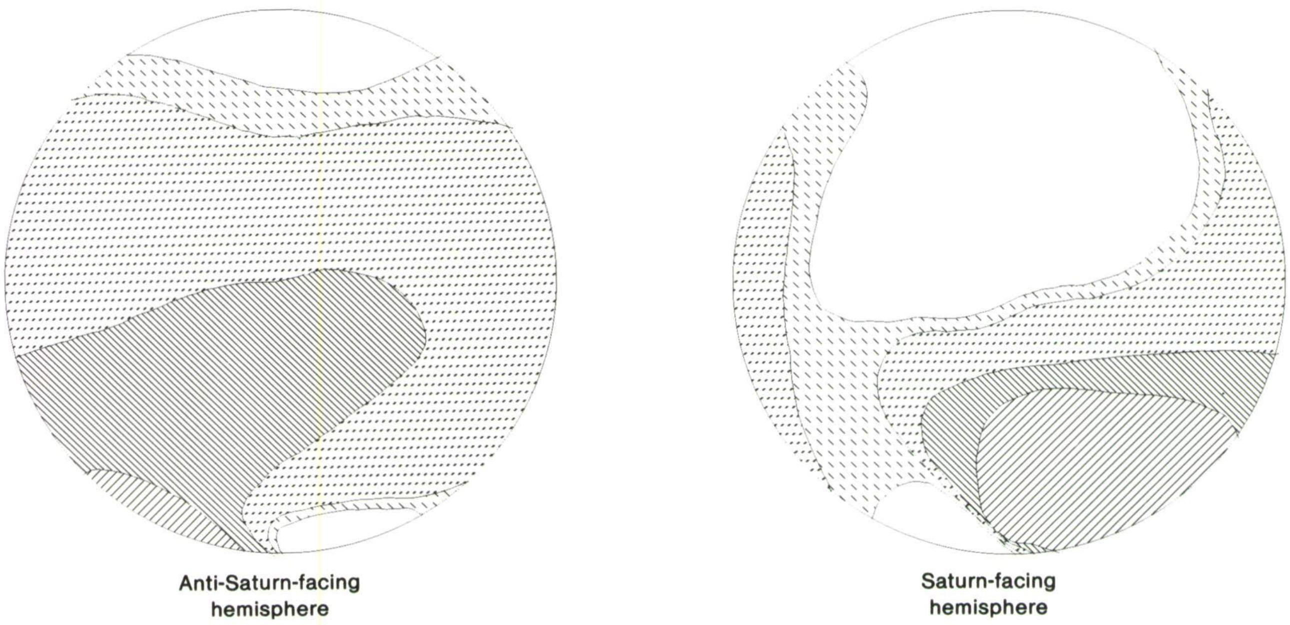

Resolution, km/pixel	Area, km^2	Percent of total
0.5 to 2	37 000	7.7
2 to 5	82 000	17.0
5 to 20	187 000	38.7
20 to 40	57 000	11.9
>40	119 000	24.7

Figure 1–1. Resolution of Voyager pictures on Mimas in terms of aerial coverage.

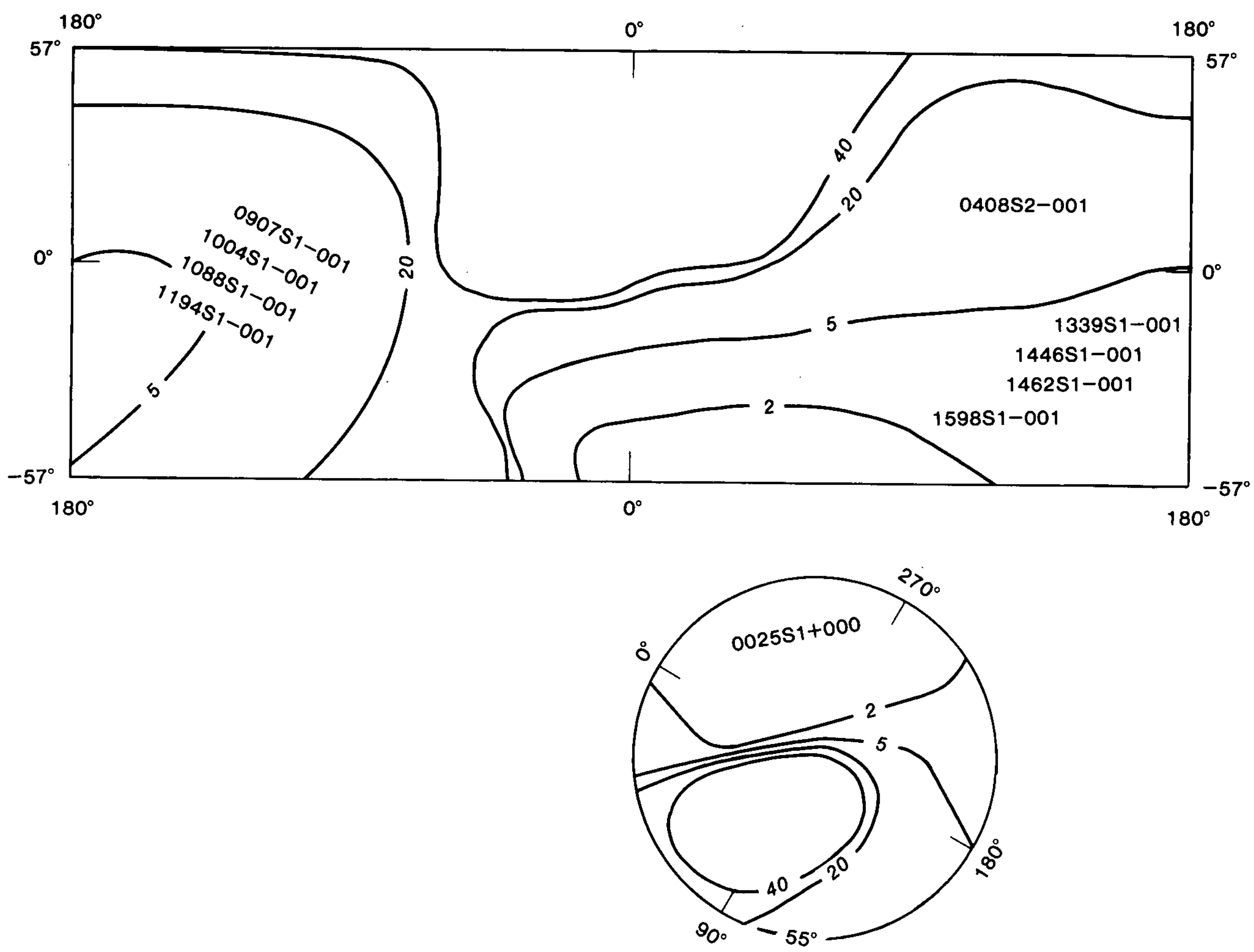

Figure 1–2. Index of Voyager 1 and 2 pictures used to compile the maps of Mimas. Picture numbers indicate the subspacecraft point at the time the pictures were taken. Contour lines indicate the approximate resolution of available images in kilometers per picture element. (See also fig. 1–1.)

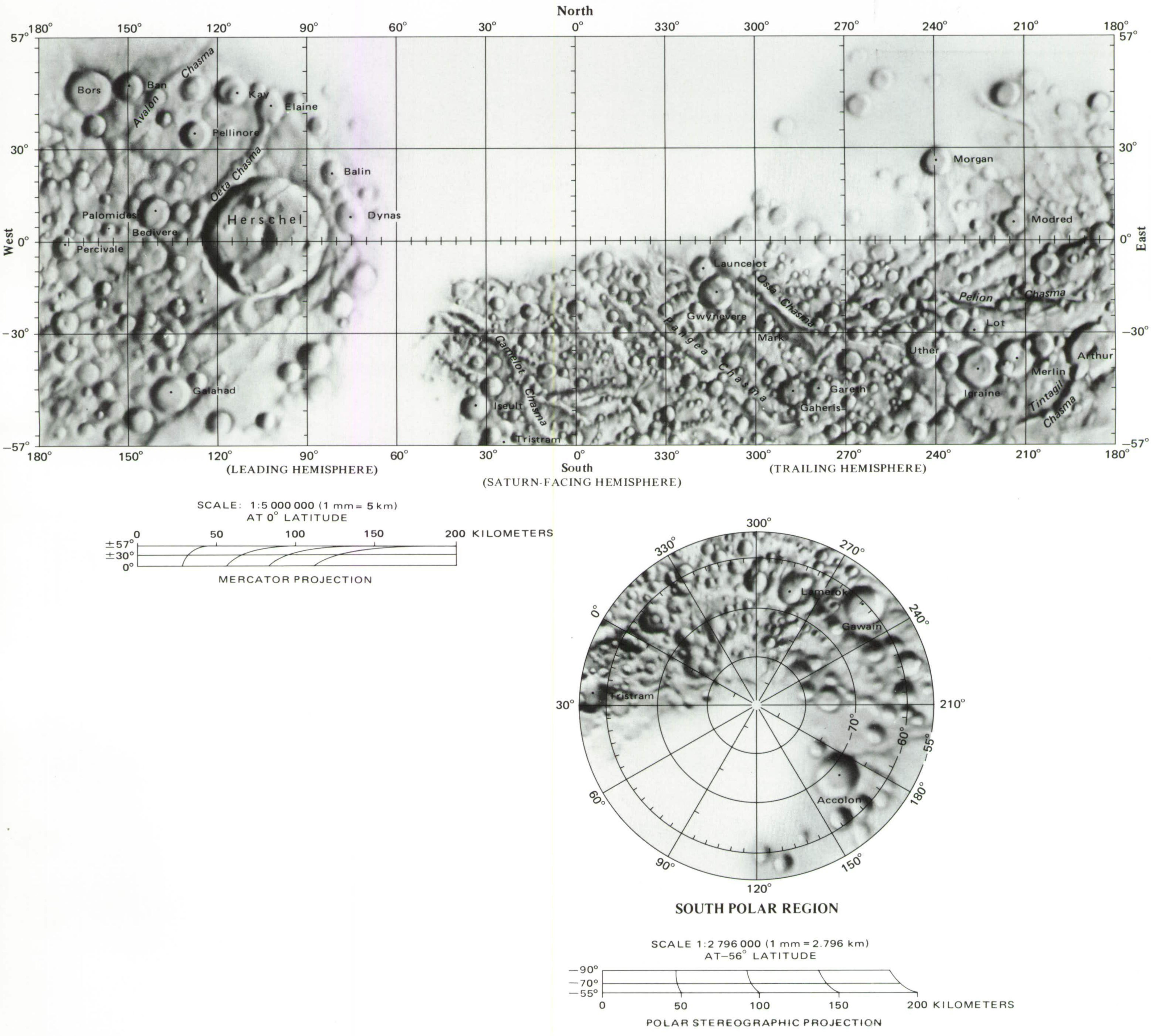

Figure 1–3. Maps of Mimas on conformal projections (map I–1489).

(a)

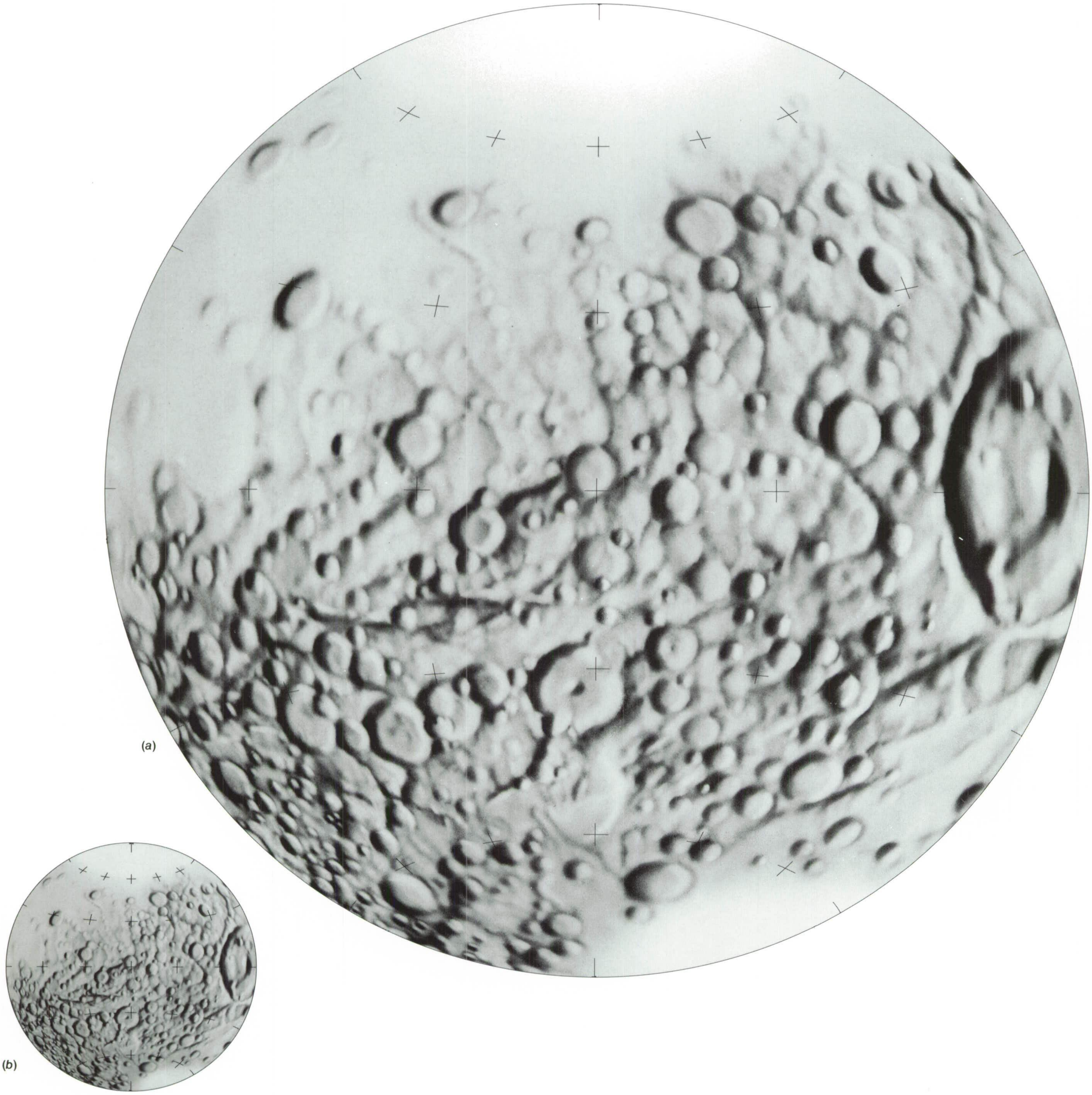

(b)

Figure 1–4. Maps of the anti-Saturn-facing hemisphere of Mimas on a Lambert azimuthal equal-area projection. Nomenclature is not shown, to avoid obscuring detail. (*a*) Scale 1:2 580 000 (1 mm^2 = 6.648 km^2; 1 in^2 = ~1656 mi^2). (*b*) Scale 1:10 000 000 (1 mm^2 = 100 km^2; 1 in^2 = ~25 000 mi^2).

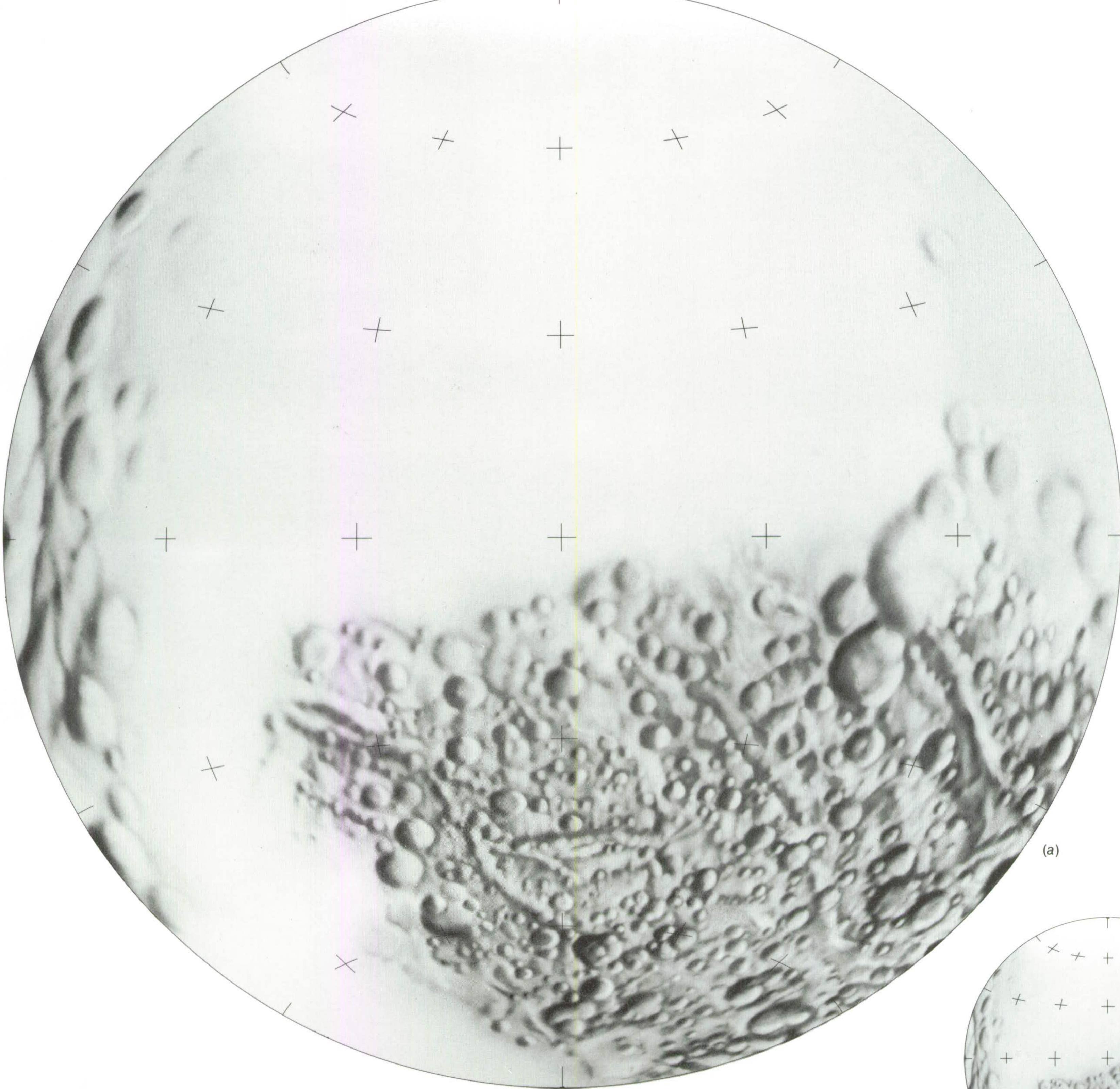

(a)

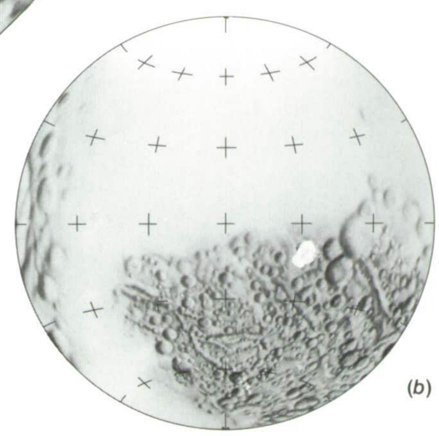

(b)

Figure 1–5. Maps of the Saturn-facing hemisphere of Mimas on a Lambert azimuthal equal-area projection. Nomenclature is not shown, to avoid obscuring detail. (*a*) Scale 1:2 580 000 (1 mm^2 = 6.648 km^2; 1 in^2 = ~1656 mi^2). (*b*) Scale 1:10 000 000 (1 mm^2 = 100 km^2; 1 in^2 = ~25 000 mi^2).

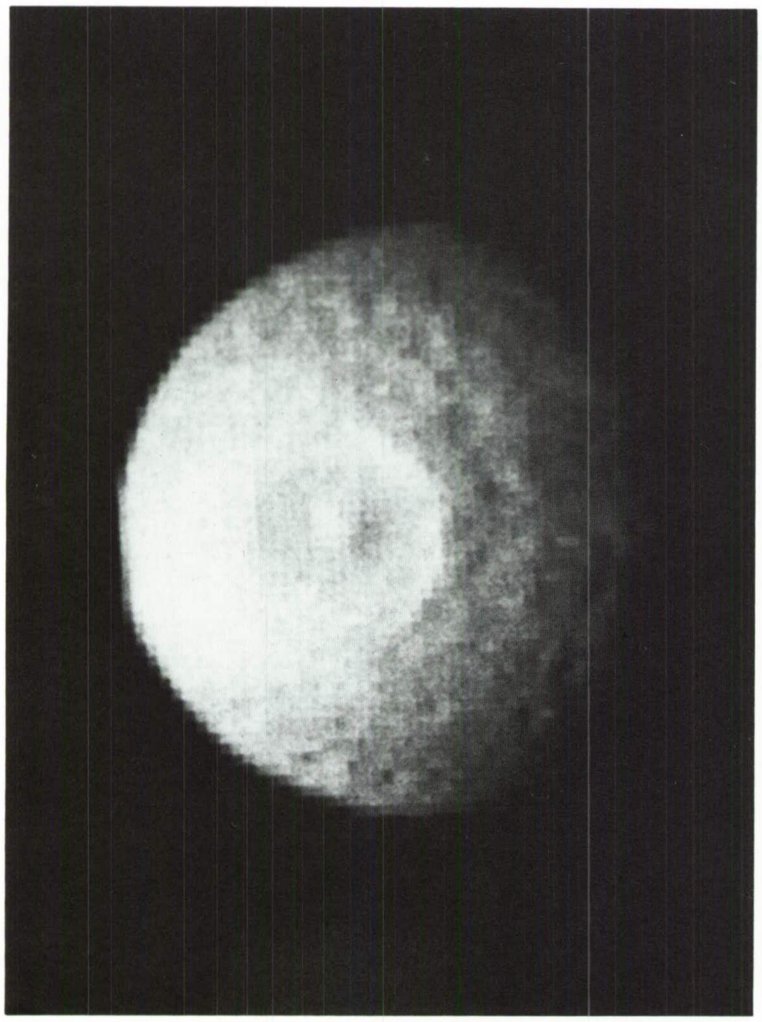

(a)

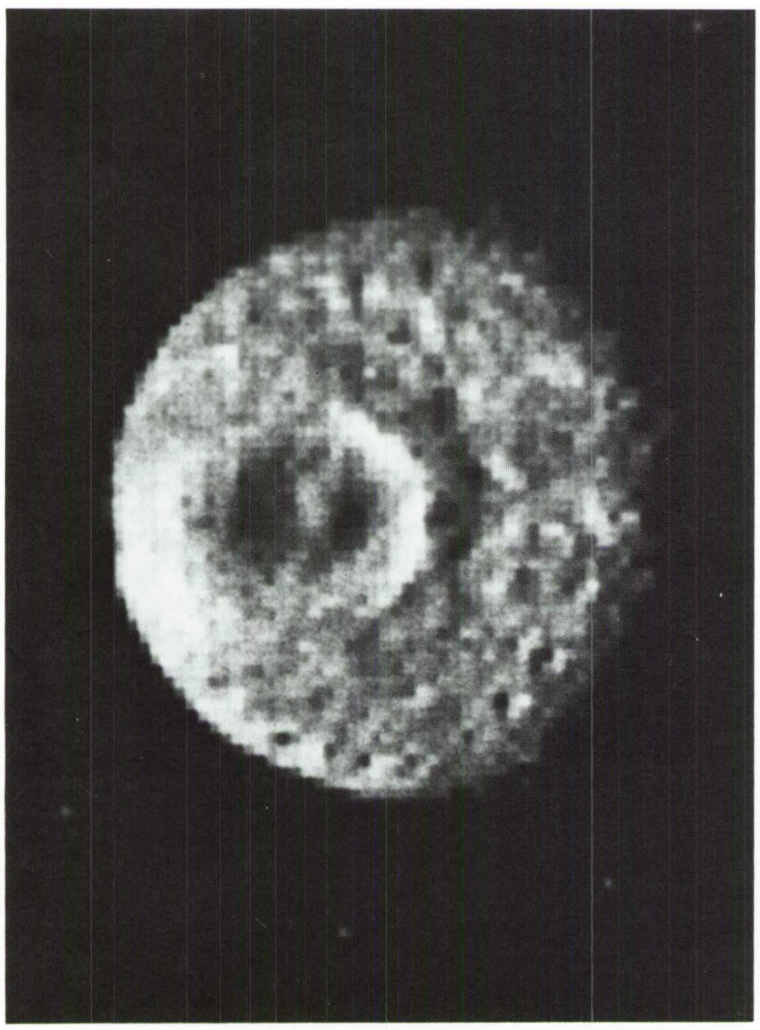

(b)

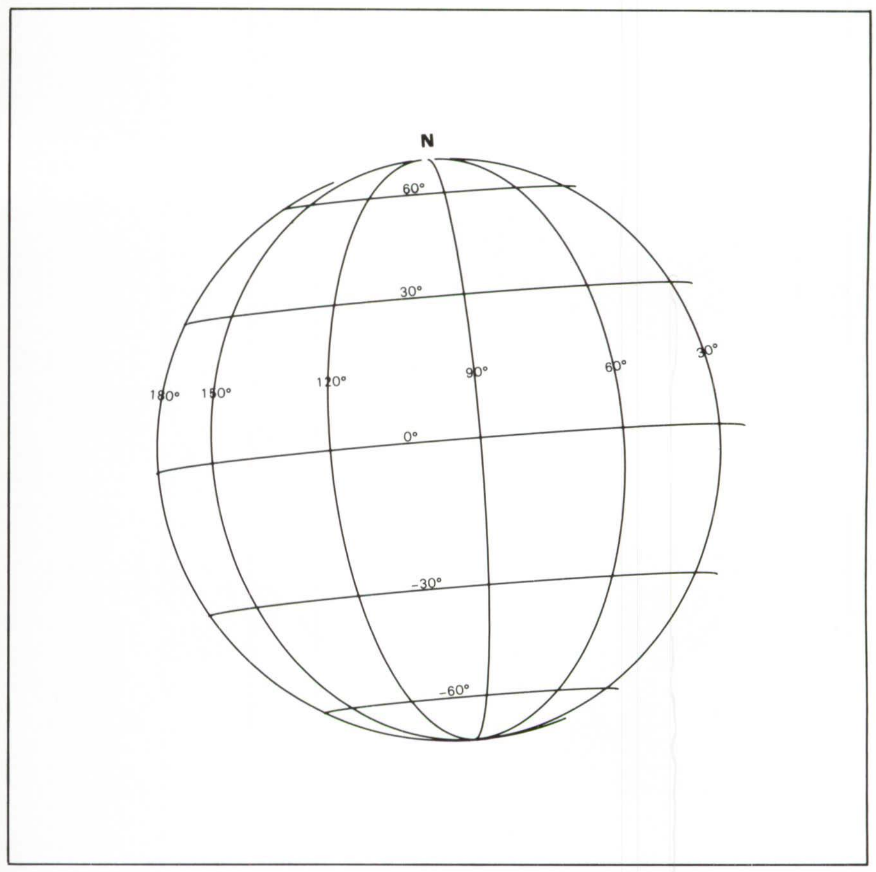

(c)

Picno	0907S1—001
FDS	34929.03
Range, km	791 531
Subspacecraft latitude/longitude, degrees	−2/96
Subsolar latitude/longitude, degrees	5/135
Resolution, km/pixel	7
Filter size, pixels	15 × 15
Filter size, km	110
Scale	1:5 000 000

Figure 1–6. Picno 0907S1—001. (*a*) Unfiltered image. (*b*) High-pass filtered image. (*c*) Perspective grid.

(a)

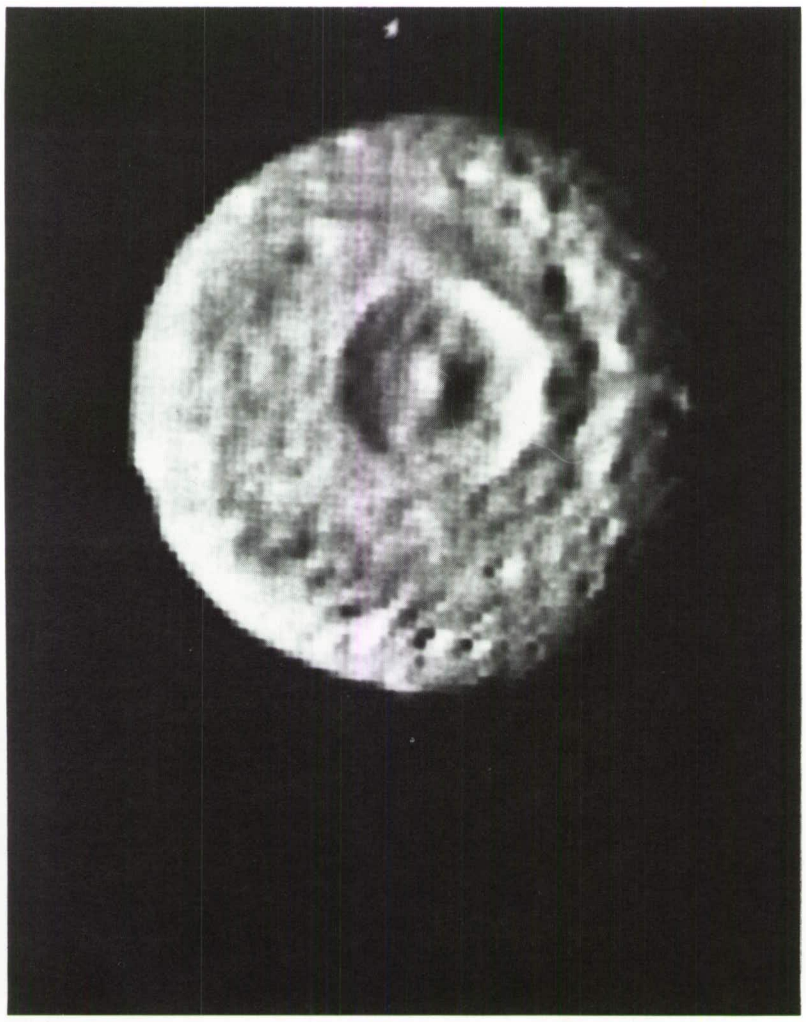

(b)

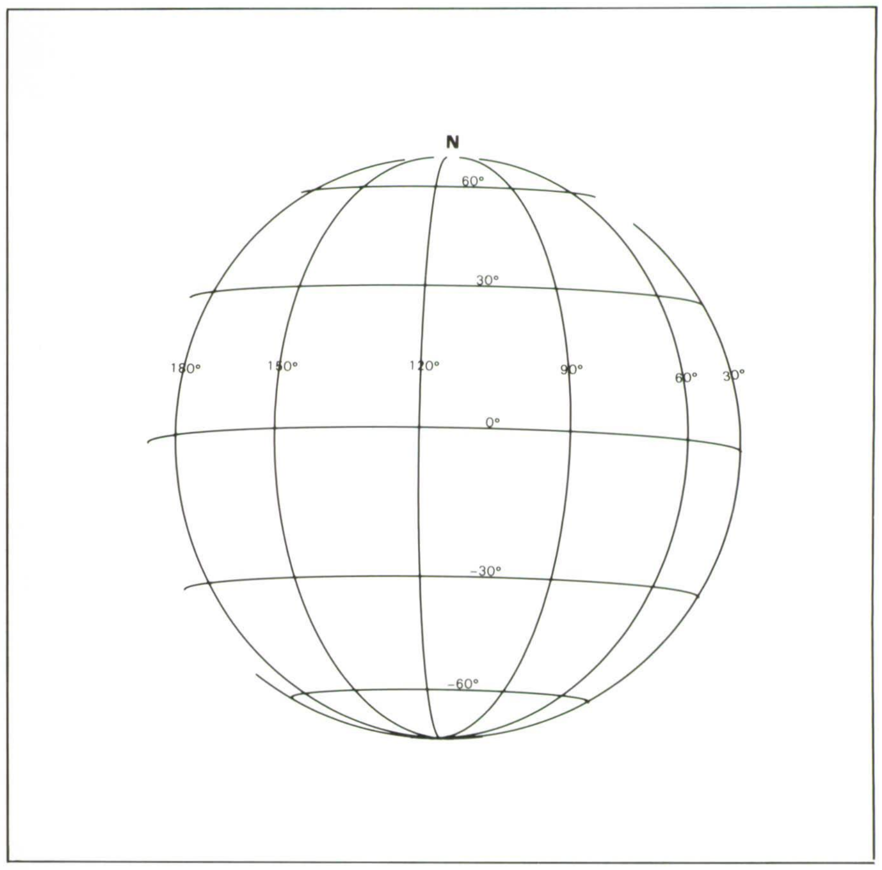

(c)

Picno	1004S1−001
FDS	34930.40
Range, km	656 422
Subspacecraft latitude/longitude, degrees	−4/115
Subsolar latitude/longitude, degrees	5/156
Resolution, km/pixel	6
Filter size, pixels	15 × 15
Filter size, km	91
Scale	1:5 000 000

Figure 1–7. Picno 1004S1−001. (*a*) Unfiltered image. (*b*) High-pass filtered image. (*c*) Perspective grid.

(a)

(b)

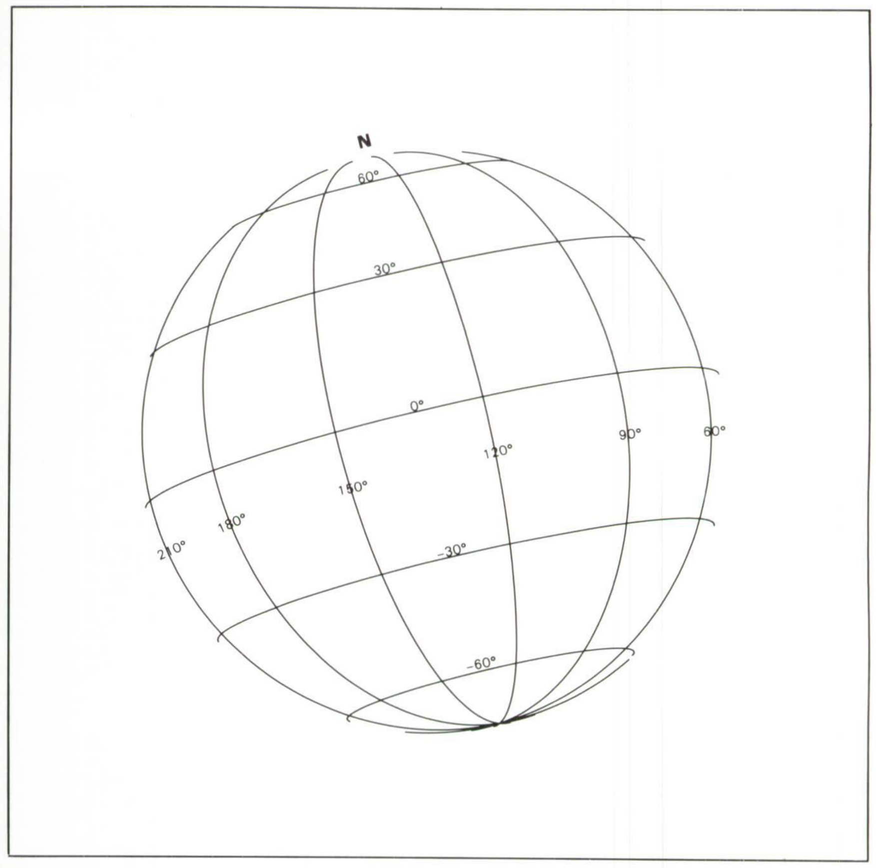

(c)

Picno	1088S1−001
FDS	34932.04
Range, km	546 552
Subspacecraft latitude/longitude, degrees	−6/132
Subsolar latitude/longitude, degrees	5/173
Resolution, km/pixel	5
Filter size, pixels	15 × 15
Filter size, km	76
Scale	1:5 000 000

Figure 1–8. Picno 1088S1−001. (*a*) Unfiltered image. (*b*) High-pass filtered image. (*c*) Perspective grid.

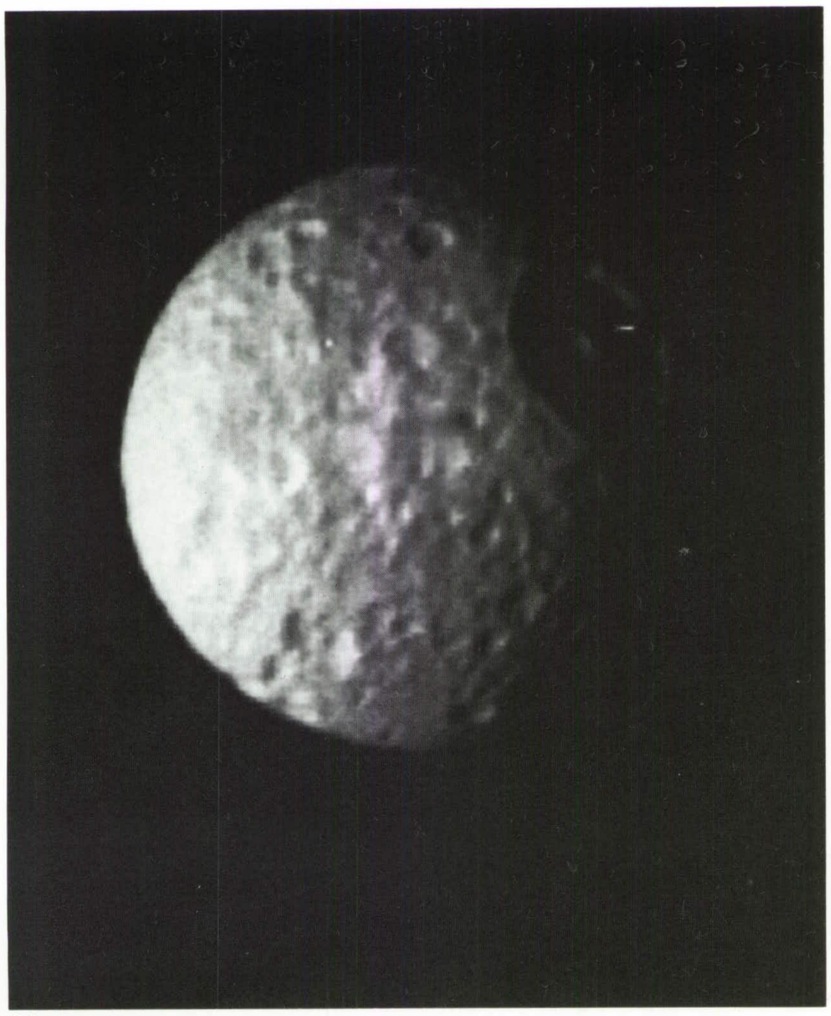

(a)

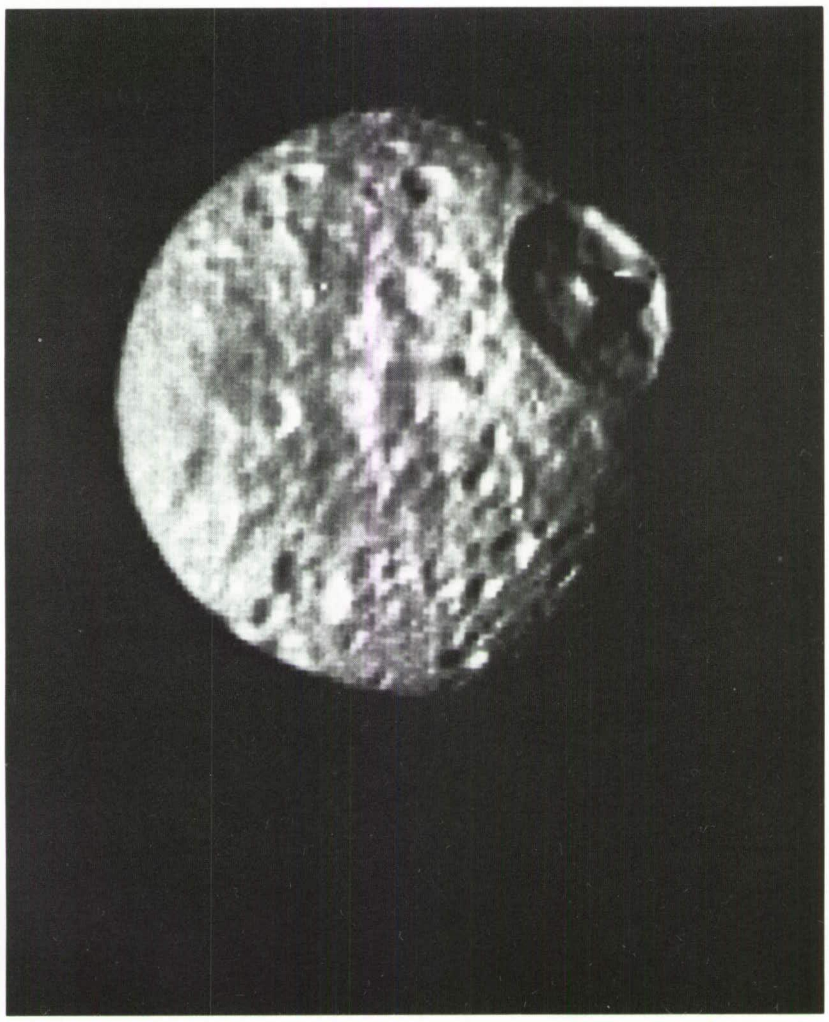

(b)

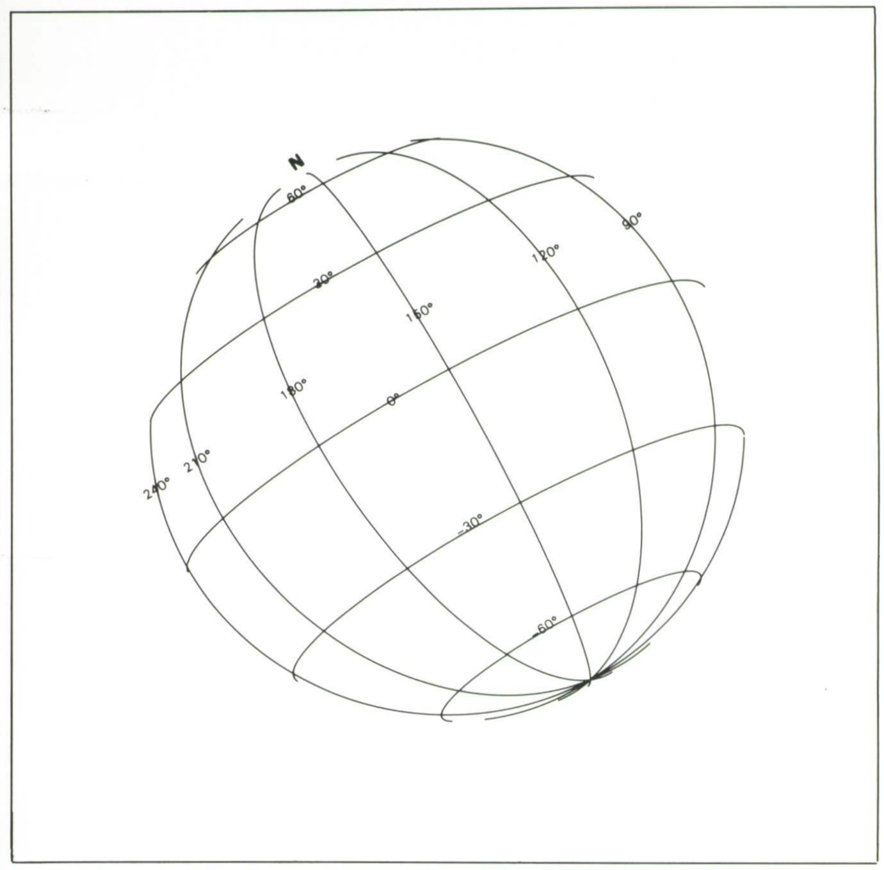

(c)

Picno	1194S1–001
FDS	34933.50
Range, km	424 514
Subspacecraft latitude/longitude, degrees	−10/156
Subsolar latitude/longitude, degrees	5/196
Resolution, km/pixel	4
Filter size, pixels	41 × 41
Filter size, km	161
Scale	1:5 000 000

Figure 1–9. Picno 1194S1–001. (*a*) Unfiltered image. (*b*) High-pass filtered image. (*c*) Perspective grid.

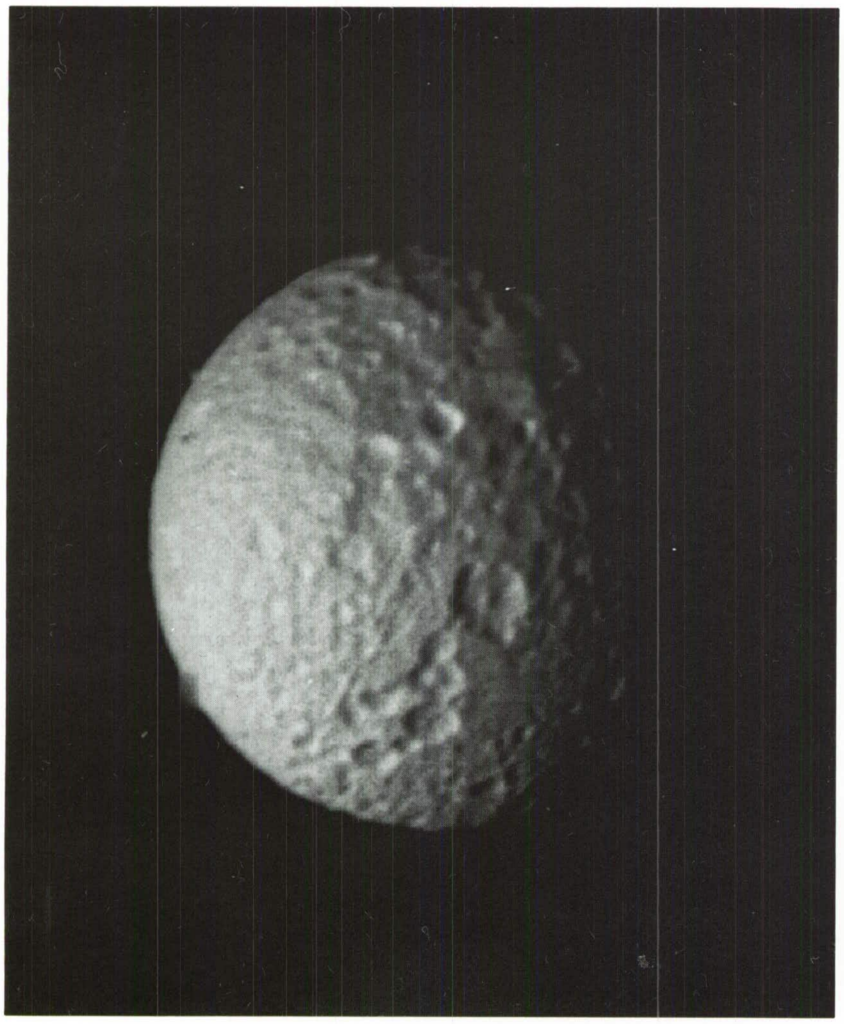

(a)

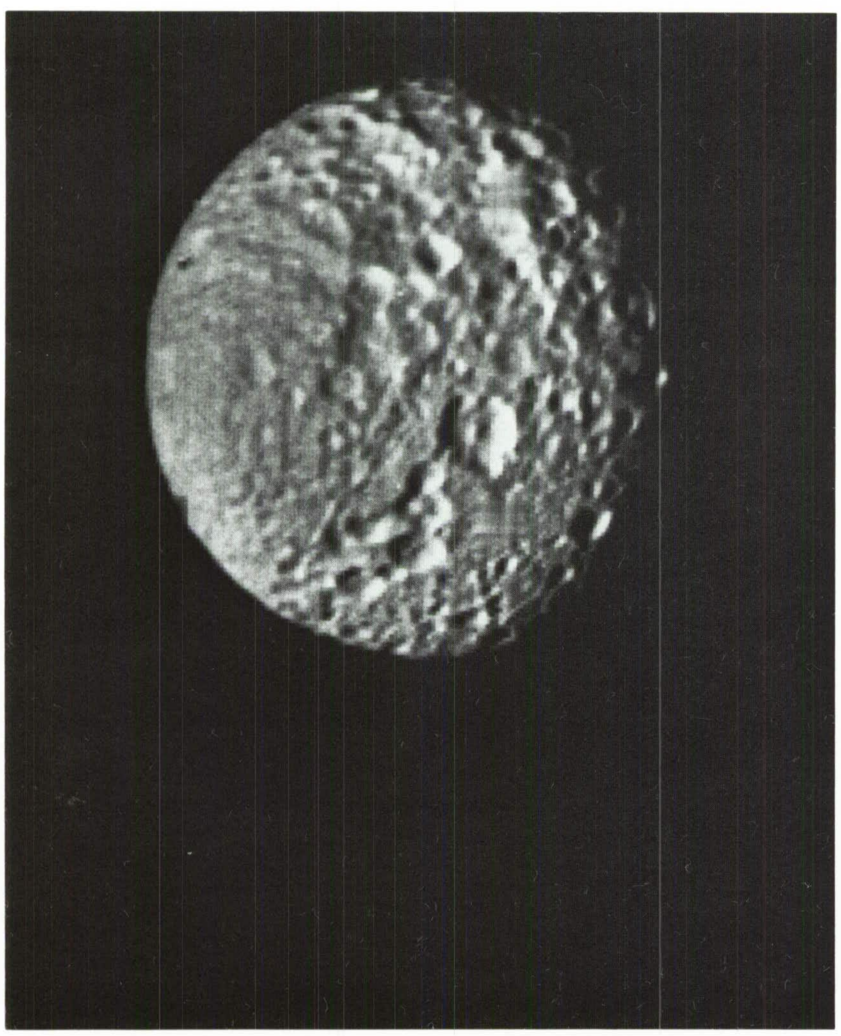

(b)

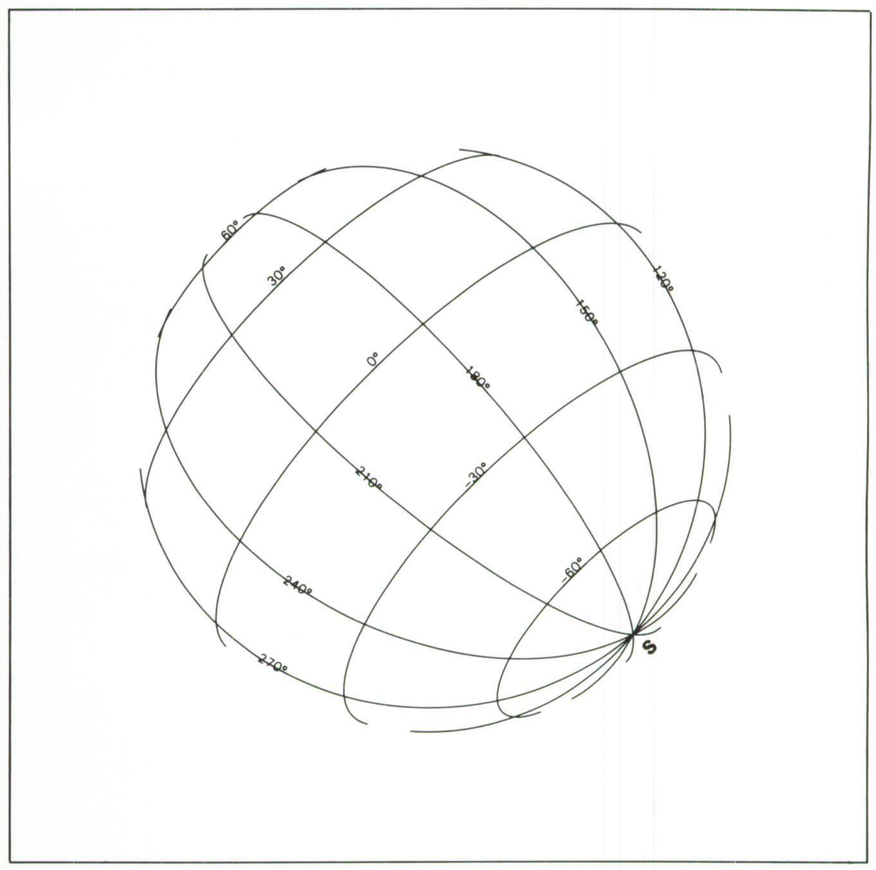

(c)

Picno	1339S1−001
FDS	34936.15
Range, km	302 106
Subspacecraft latitude/longitude, degrees	−18/195
Subsolar latitude/longitude, degrees	5/227
Resolution, km/pixel	2
Filter size, pixels	41 × 41
Filter size, km	114
Scale	1:5 000 000

Figure 1–10. Picno 1339S1−001. (*a*) Unfiltered image. (*b*) High-pass filtered image. (*c*) Perspective grid.

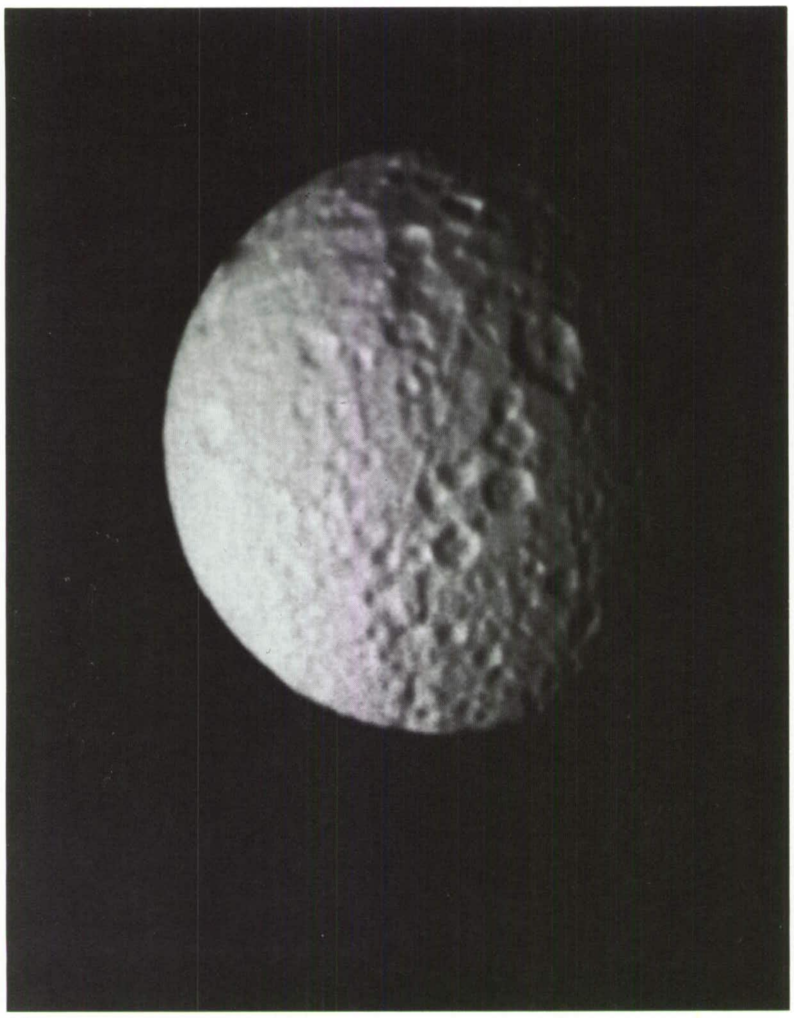

(a)

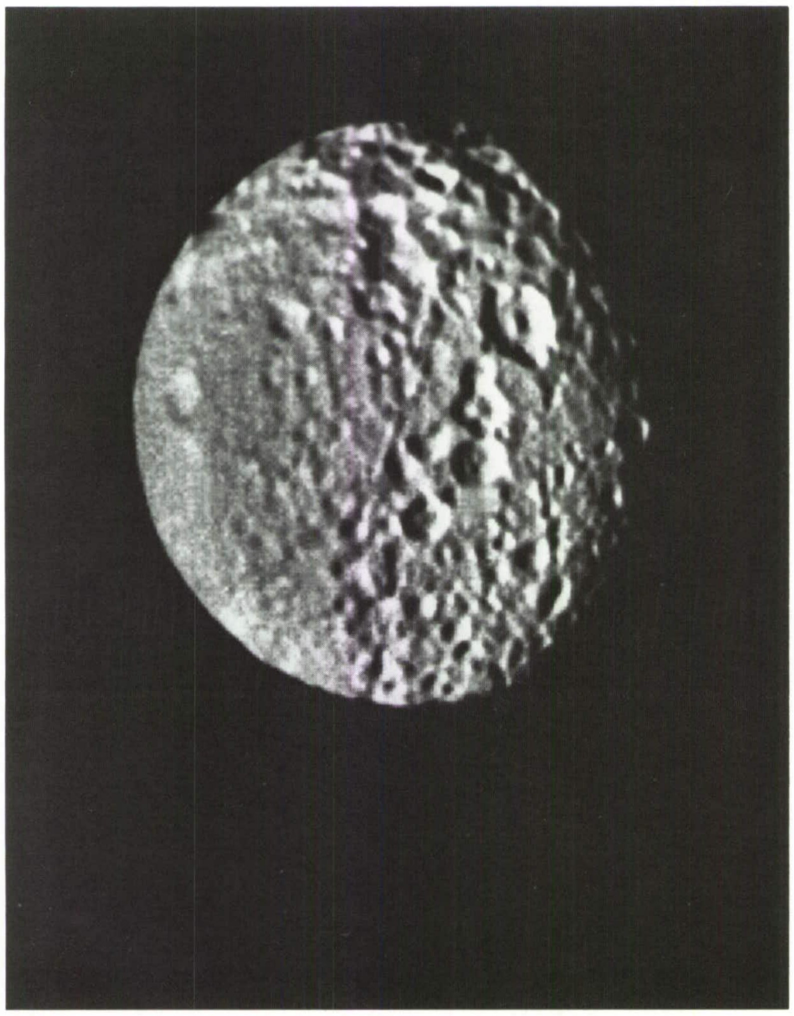

(b)

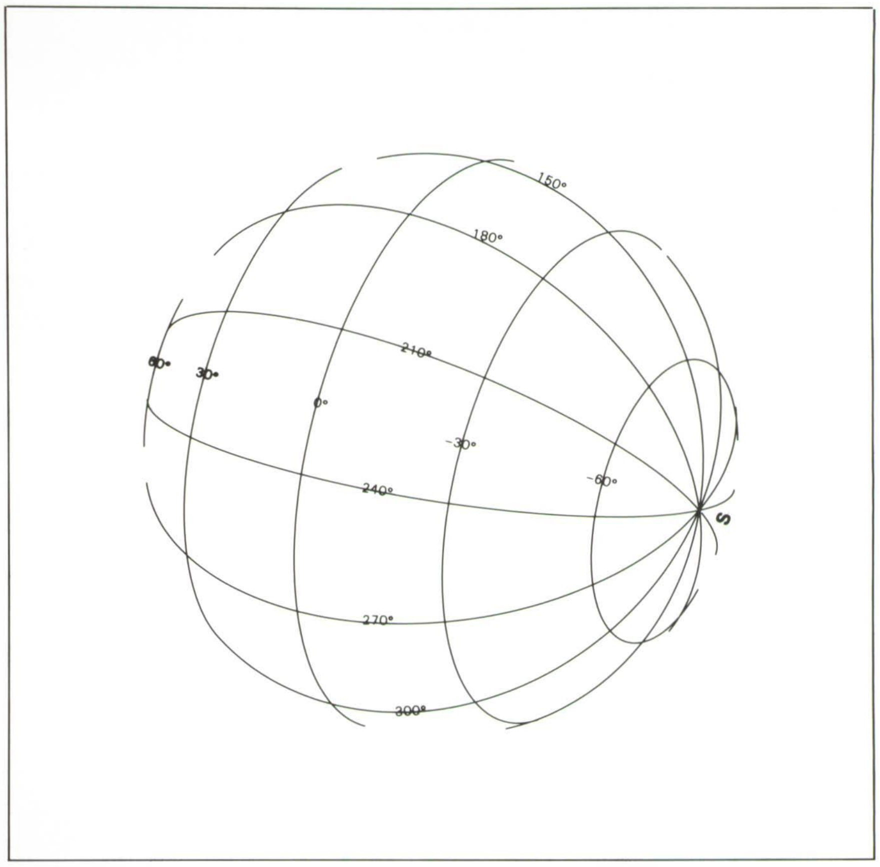

(c)

Picno	1446S1−001
FDS	34938.02
Range, km	249 646
Subspacecraft latitude/longitude, degrees	−26/228
Subsolar latitude/longitude, degrees	5/249
Resolution, km/pixel	2
Filter size, pixels	41 × 41
Filter size, km	94
Scale	1:5 000 000

Figure 1–11. Picno 1446S1−001. (*a*) Unfiltered image. (*b*) High-pass filtered image. (*c*) Perspective grid.

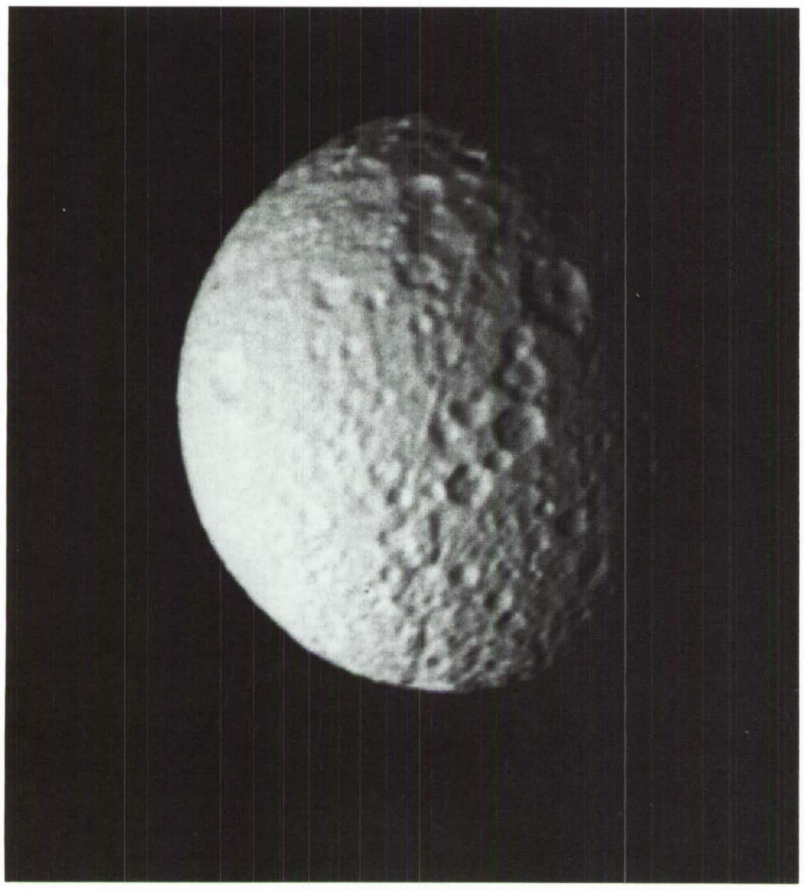

(*a*)

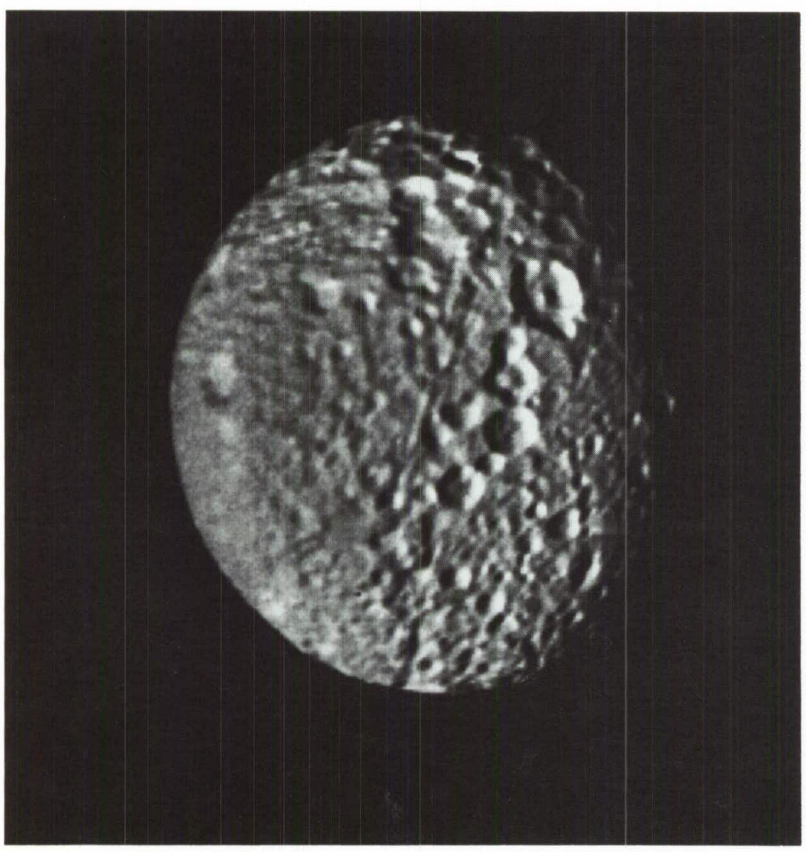

(*b*)

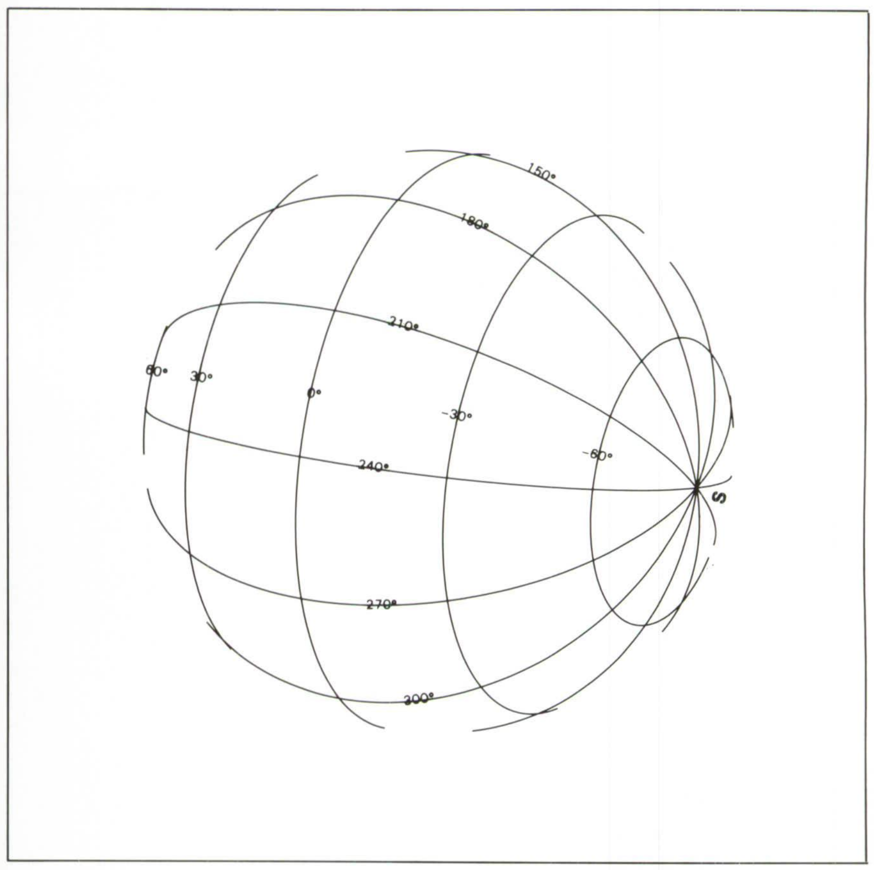

(*c*)

Picno	1462S1−001
FDS	34938.18
Range, km	244 121
Subspacecraft latitude/longitude, degrees	−27/232
Subsolar latitude/longitude, degrees	5/253
Resolution, km/pixel	2
Filter size, pixels	51 × 51
Filter size, km	115
Scale	1:5 000 000

Figure 1–12. Picno 1462S1−001. (*a*) Unfiltered image. (*b*) High-pass filtered image. (*c*) Perspective grid.

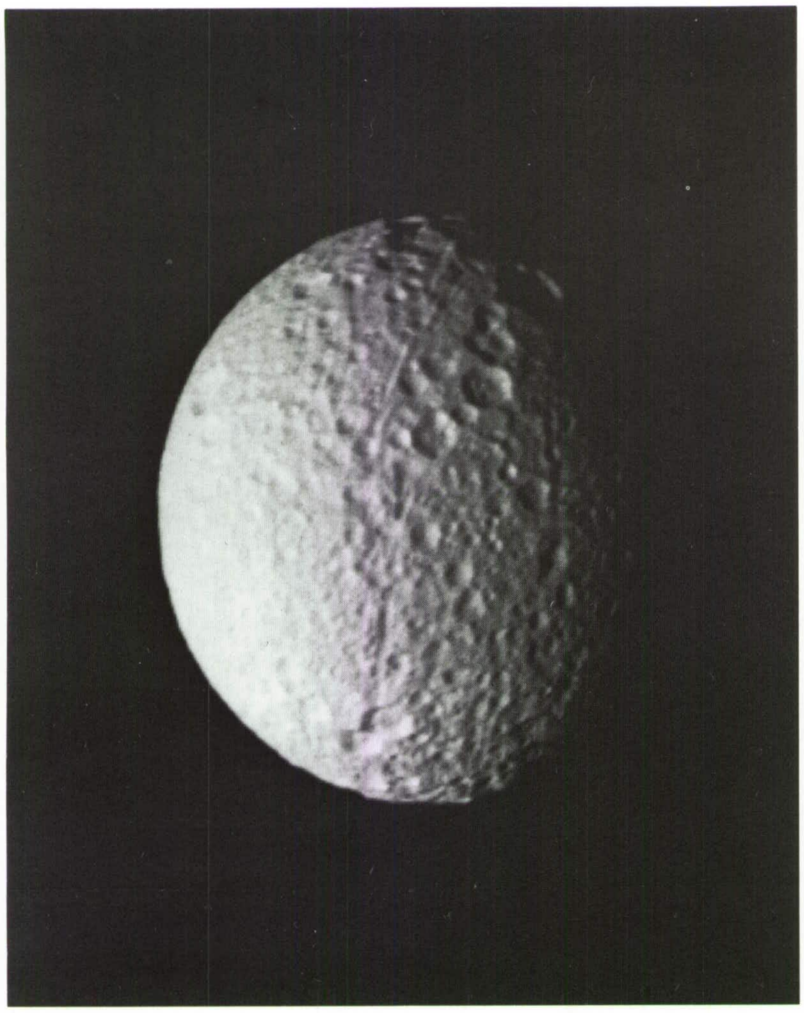

(a)

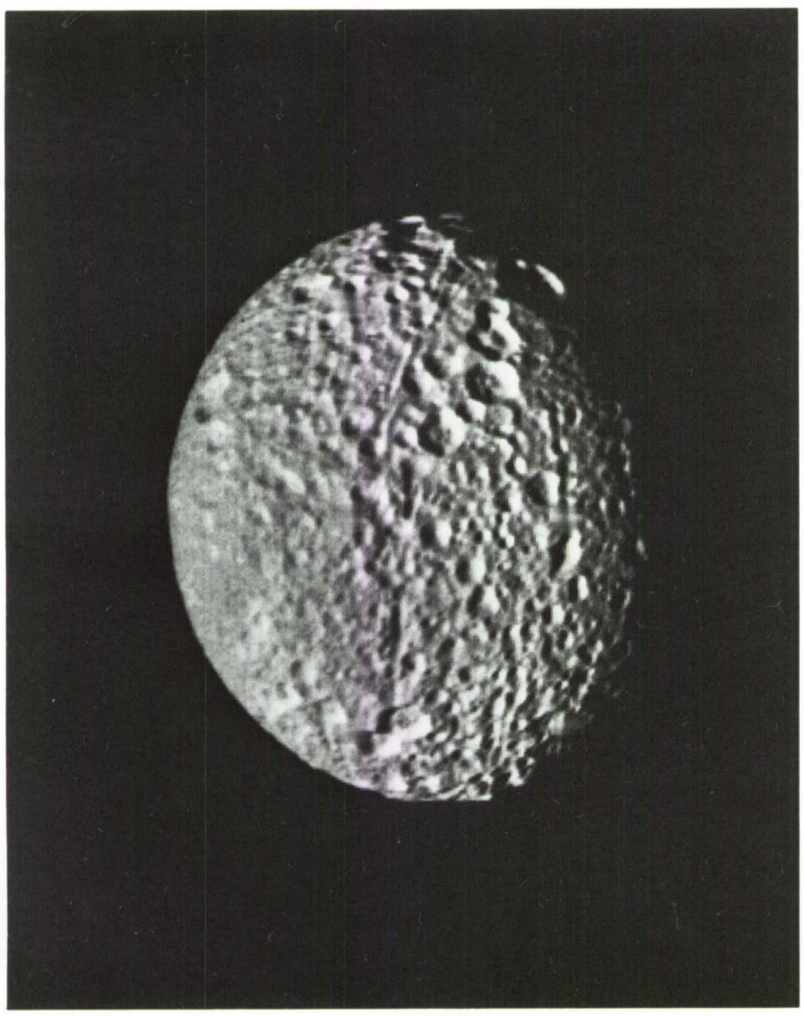

(b)

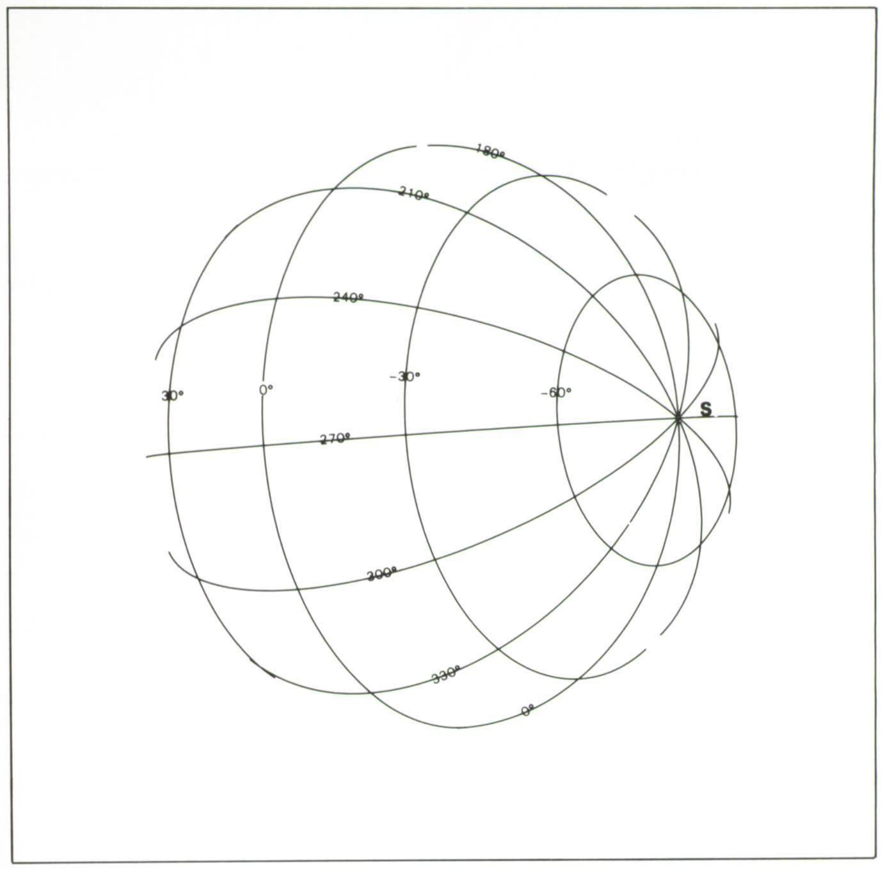

(c)

Picno	1598S1−001
FDS	34940.34
Range, km	208 440
Subspacecraft latitude/longitude, degrees	−37/271
Subsolar latitude/longitude, degrees	5/282
Resolution, km/pixel	2
Filter size, pixels	57 × 57
Filter size, km	110
Scale	1:5 000 000

Figure 1–13. Picno 1598S1−001. (*a*) Unfiltered image. (*b*) High-pass filtered image. (*c*) Perspective grid.

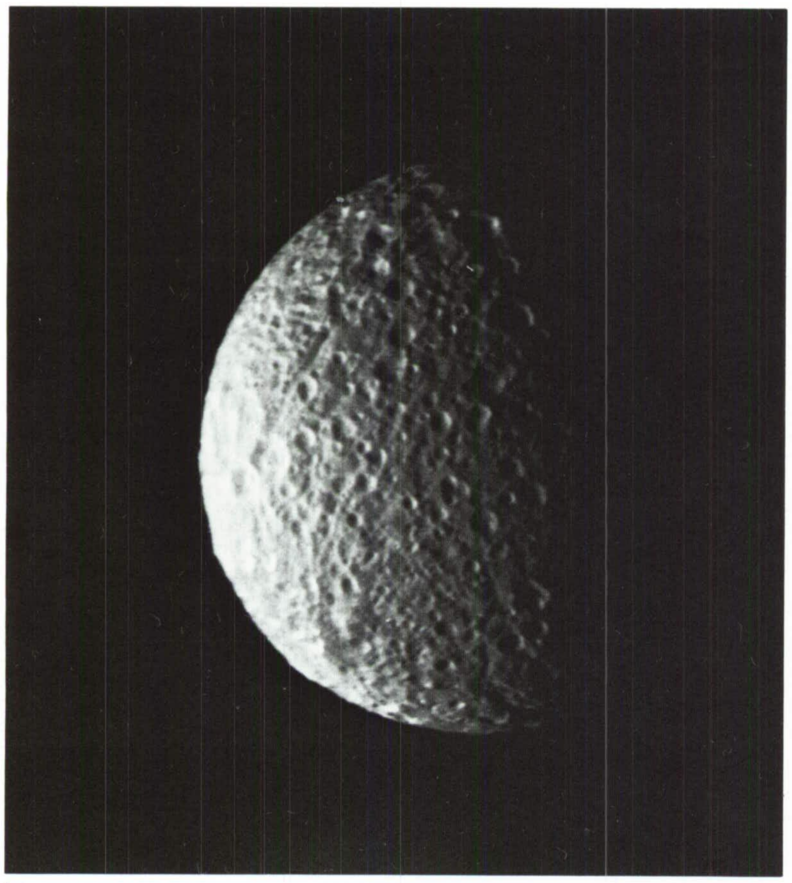

(a)

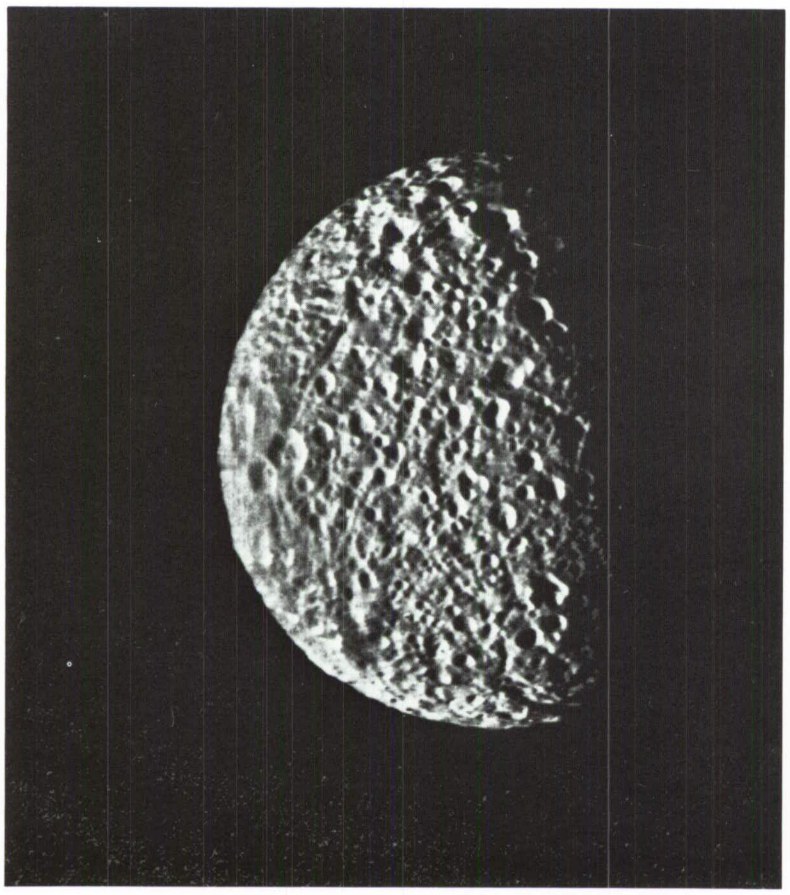

(b)

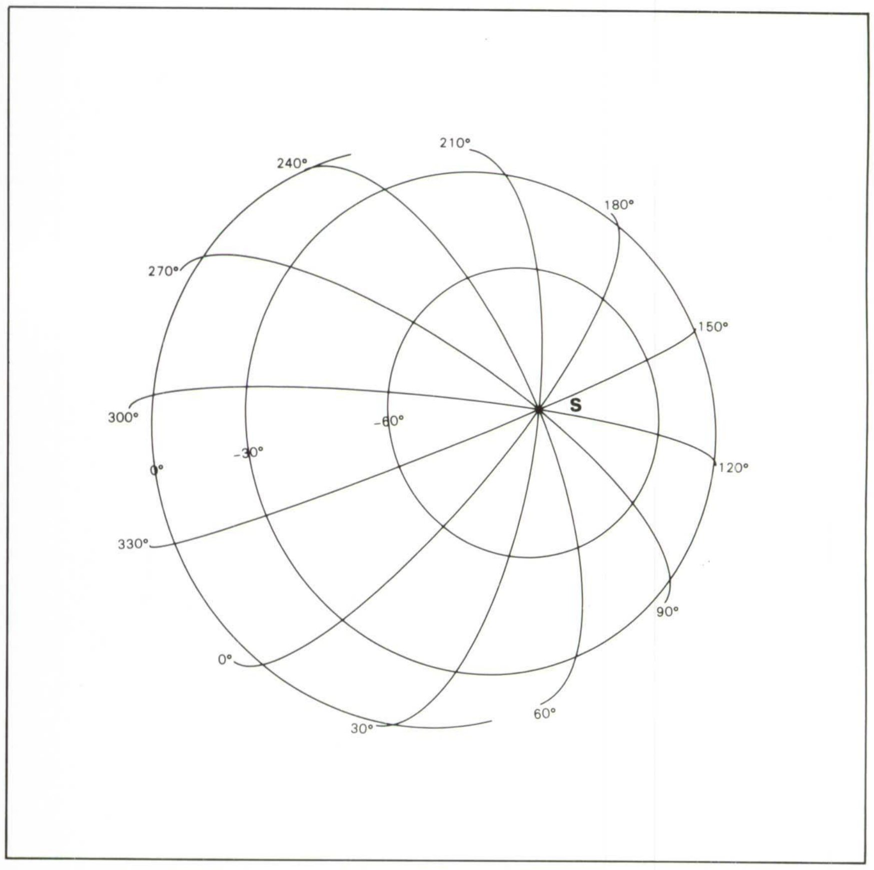

(c)

Picno	0025S1+000
FDS	34944.21
Range, km	127 341
Subspacecraft latitude/longitude, degrees	−66/321
Subsolar latitude/longitude, degrees	5/329
Resolution, km/pixel	1
Filter size, pixels	51 × 51
Filter size, km	60
Scale	1:5 000 000

Figure 1–14. Picno 0025S1+000. (*a*) Unfiltered image. (*b*) High-pass filtered image. (*c*) Perspective grid.

Page intentionally left blank

PART 2

Enceladus

Diameter	502 km (312 miles)
Density	1.1
Albedo	1.0
Distance from Saturn	240 192 km (149 250 miles)
Orbital period	33 hr, 21 min, 22 sec
Voyager 1 closest approach	202 040 km (125 542 miles)
Voyager 1 pictures used in mapping	0
Voyager 2 closest approach	87 140 km (54 146 miles)
Voyager 2 pictures used in mapping	19

Only slightly larger than Mimas, Enceladus is about one-tenth as massive as the next larger pair of satellites, Tethys and Dione. Enceladus appears to be much smoother than the other satellites of Saturn and may be source of Ring E material. Although the north polar region is heavily cratered, Voyager 2 pictures of northern intermediate and equatorial latitudes display sinuous striations reminiscent of patterns on Jupiter's moon Ganymede. On Ganymede, these structures have been interpreted as being the result of the shifting of floating slabs of ice.

	Resolution, km/pixel	Area, km^2	Percent of total
	0.5 to 2	83 000	10.6
	2 to 5	309 000	39.3
	5 to 20	177 000	22.5
	20 to 40	61 000	7.8
	>40	155 000	19.8

Figure 2–1. Resolution of Voyager pictures of Enceladus in terms of aerial coverage.

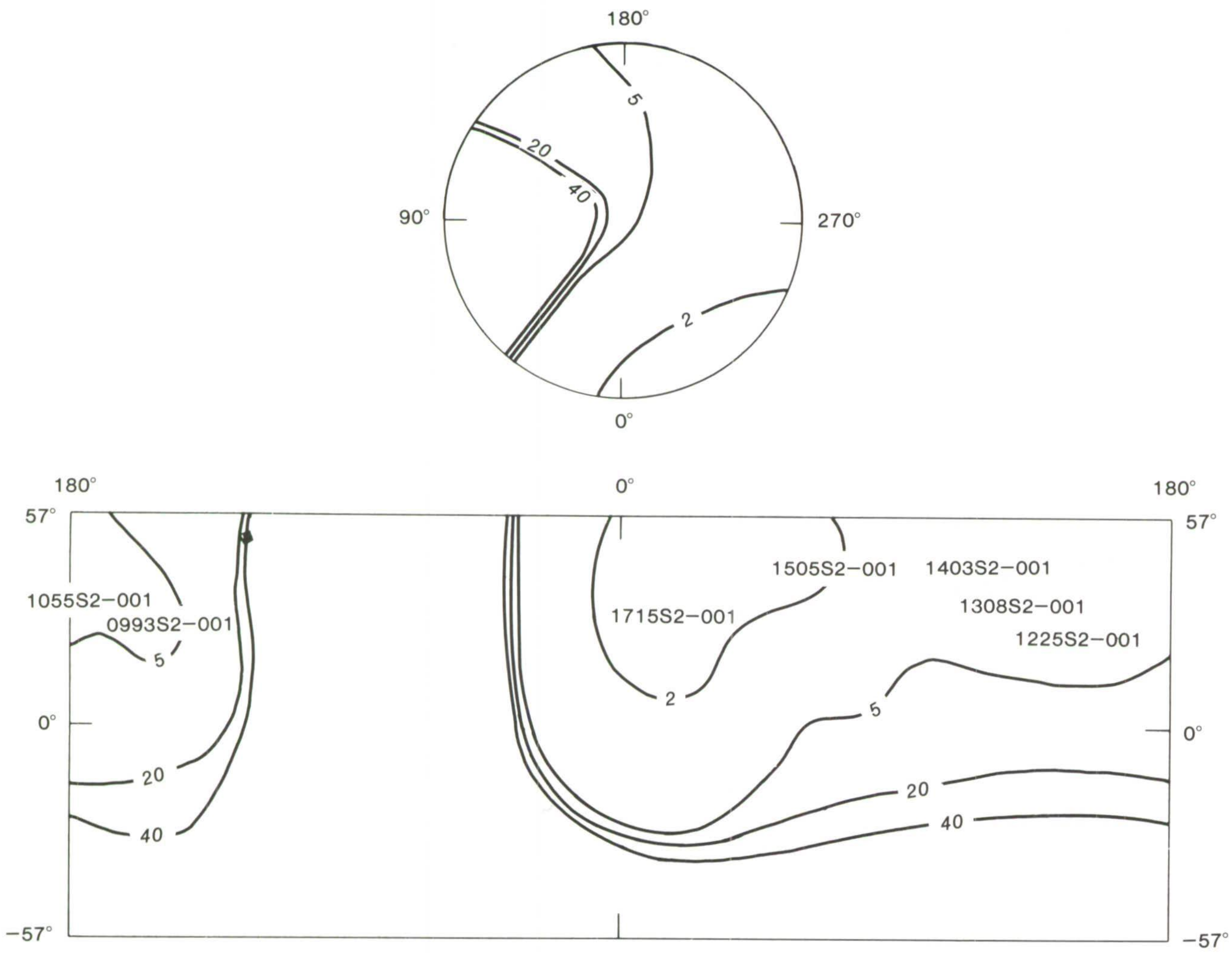

Figure 2–2. Index of Voyager 1 and 2 pictures used to compile the maps of Enceladus. Picture numbers indicate the subspacecraft point at the time the pictures were taken. Contour lines indicate the approximate resolution of available images in kilometers per picture element. (See also fig. 2–1.)

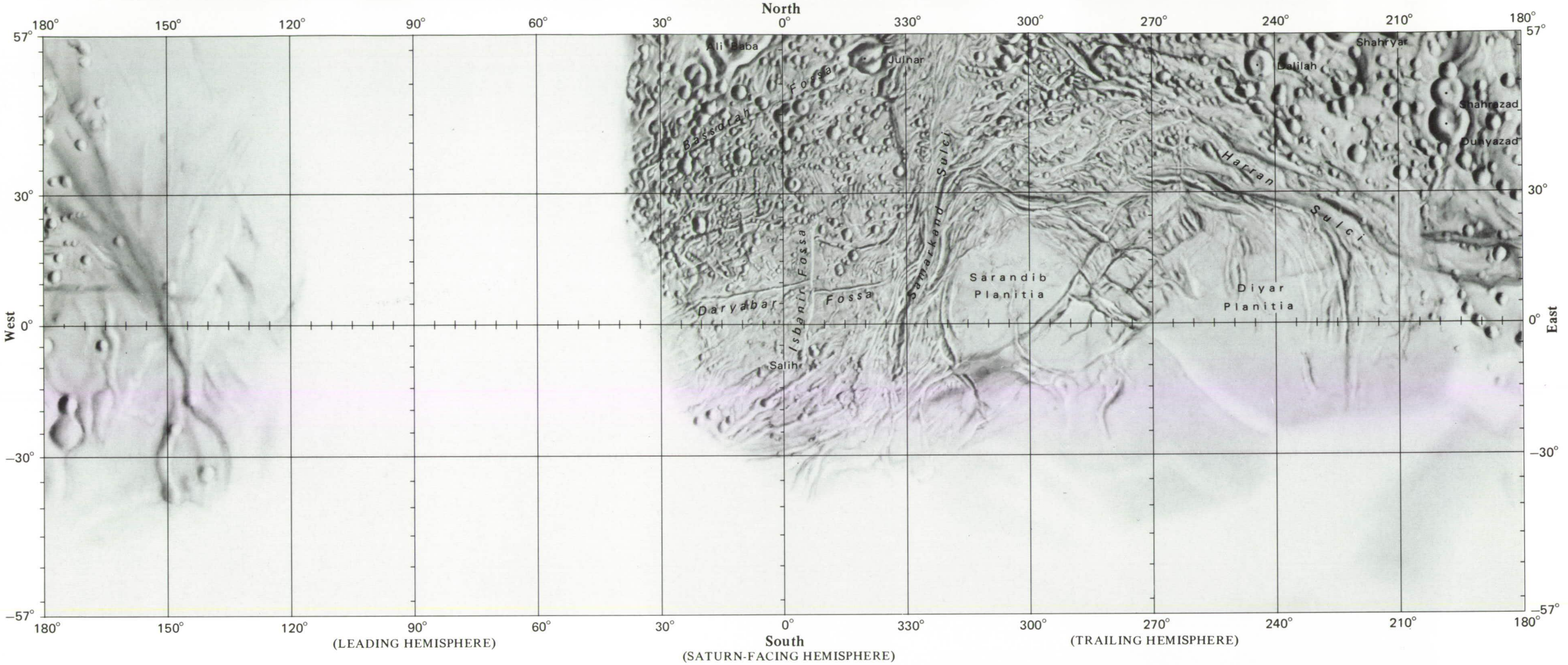

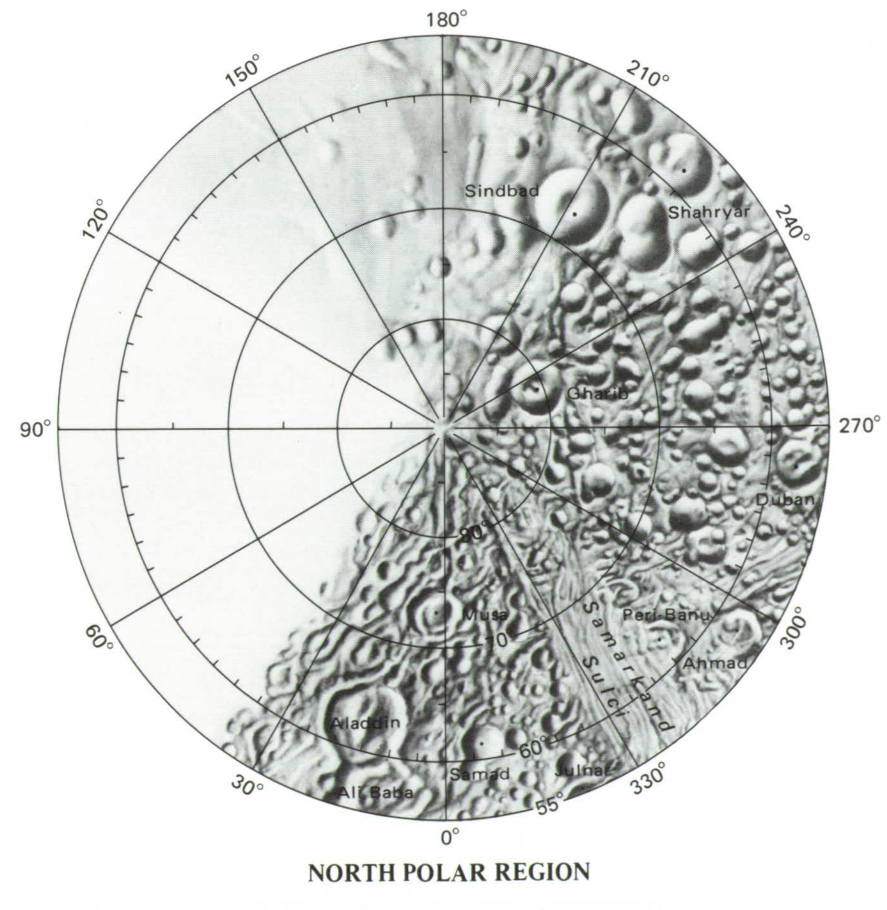

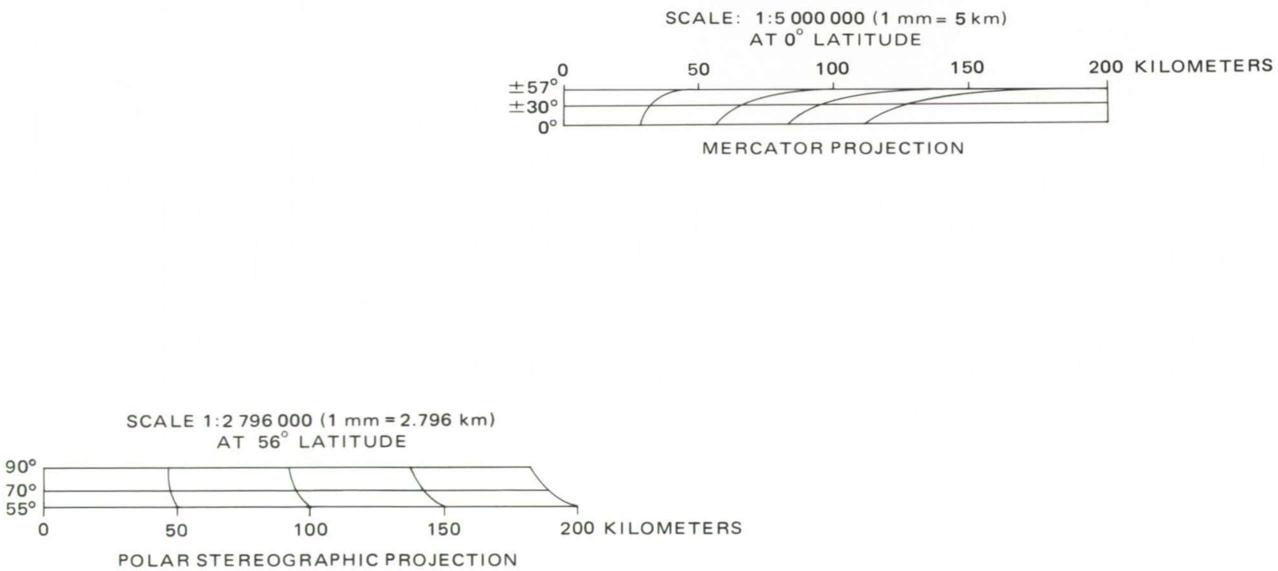

Figure 2–3. Maps of Enceladus on conformal projections (map I–1485).

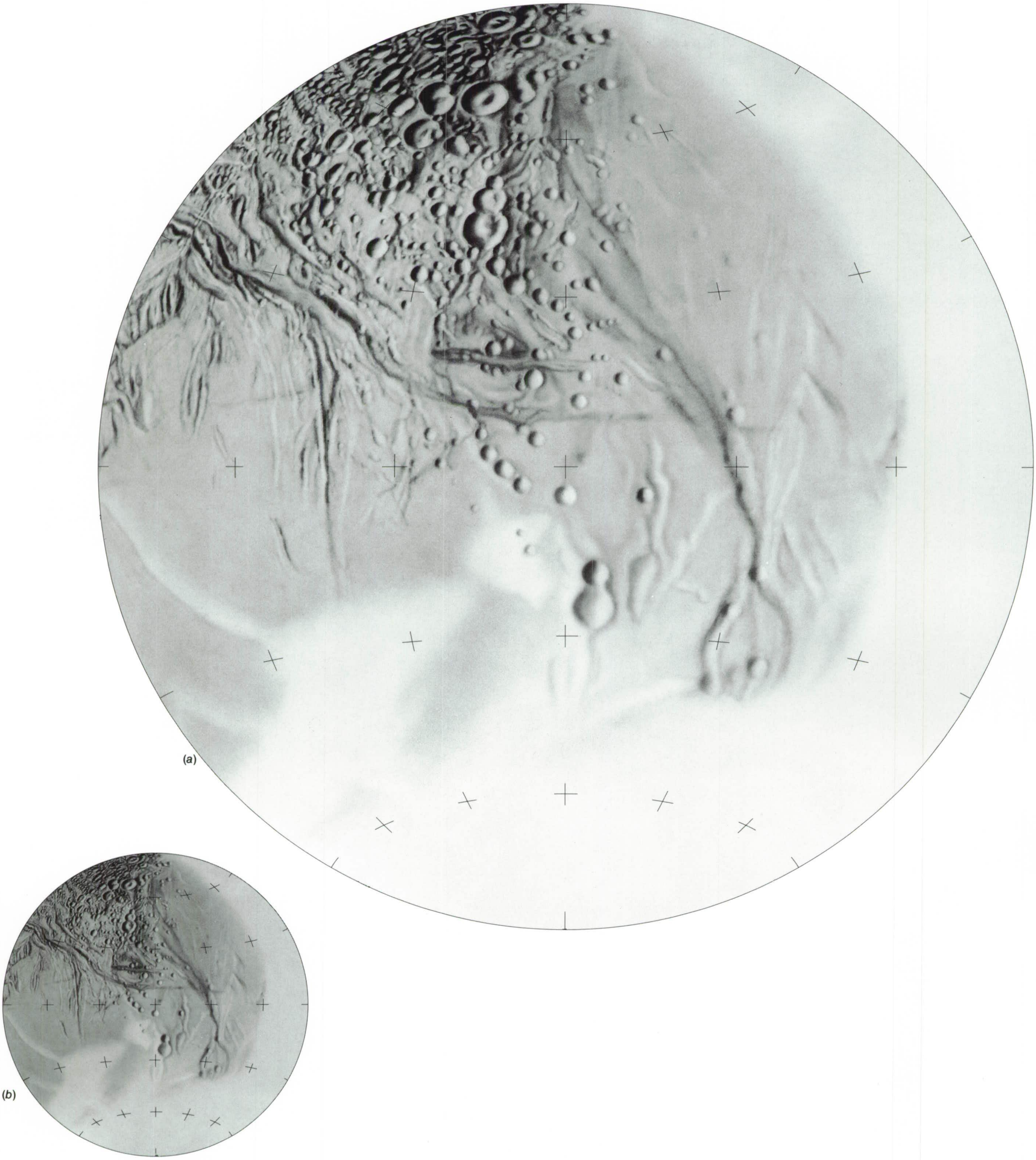

(a)

(b)

Figure 2–4. Maps of the anti-Saturn-facing hemisphere of Enceladus on a Lambert azimuthal equal-area projection. Nomenclature is not shown, to avoid obscuring detail. (*a*) Scale 1:3 285 000 (1 mm^2 = 10.79 km^2; 1 in^2 = ~2688 mi^2). (*b*) Scale 1:10 000 000 (1 mm^2 = 100 km^2; 1 in^2 = ~25 000 mi^2).

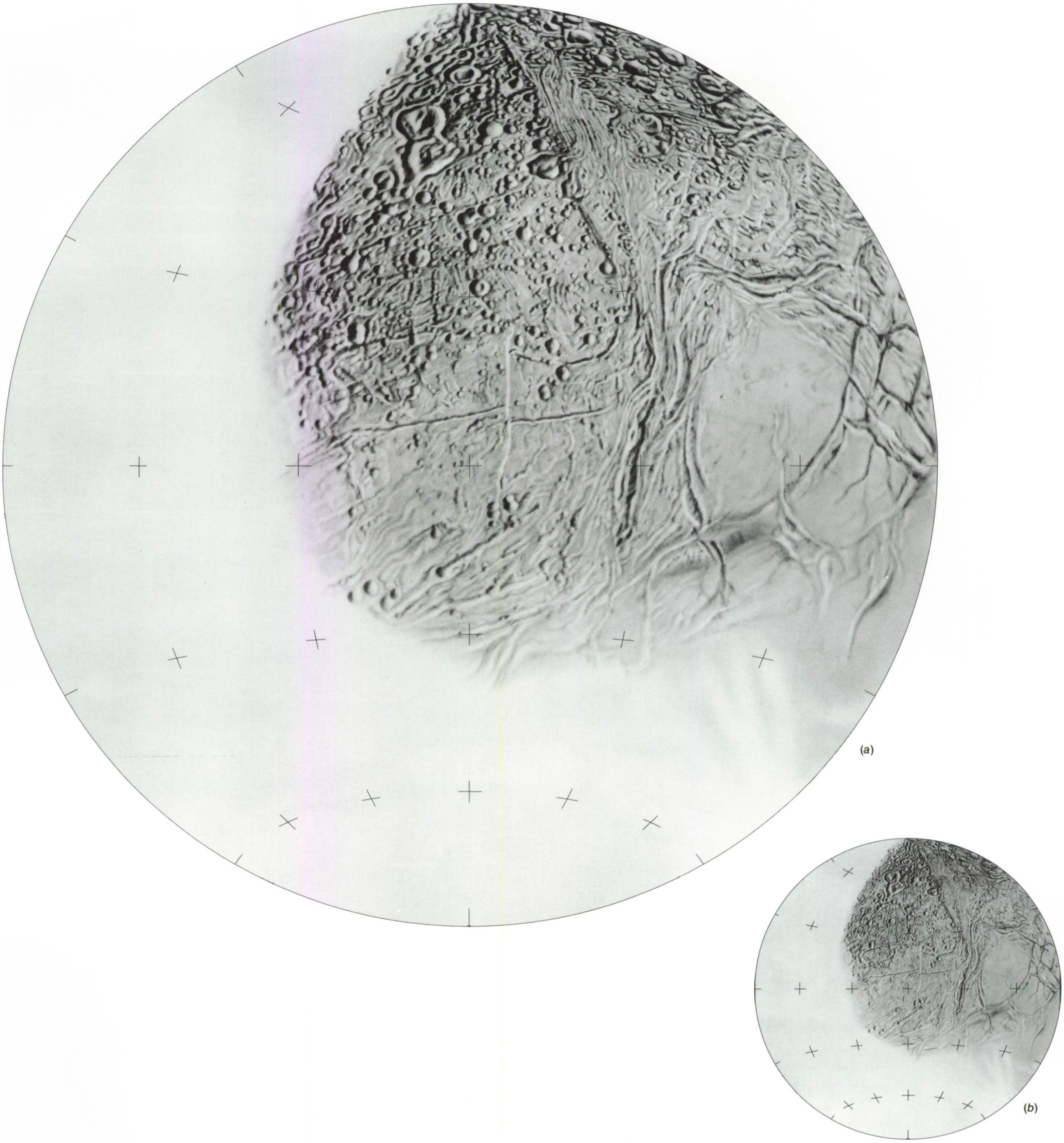

Figure 2–5. Maps of the Saturn-facing hemisphere of Enceladus on a Lambert azimuthal equal-area projection. Nomenclature is not shown, to avoid obscuring detail. (*a*) Scale 1:3 285 000 (1 mm^2 = 10.79 km^2; 1 in^2 = ~2688 mi^2). (*b*) Scale 1:10 000 000 (1 mm^2 = 100 km^2; 1 in^2 = ~25 000 mi^2).

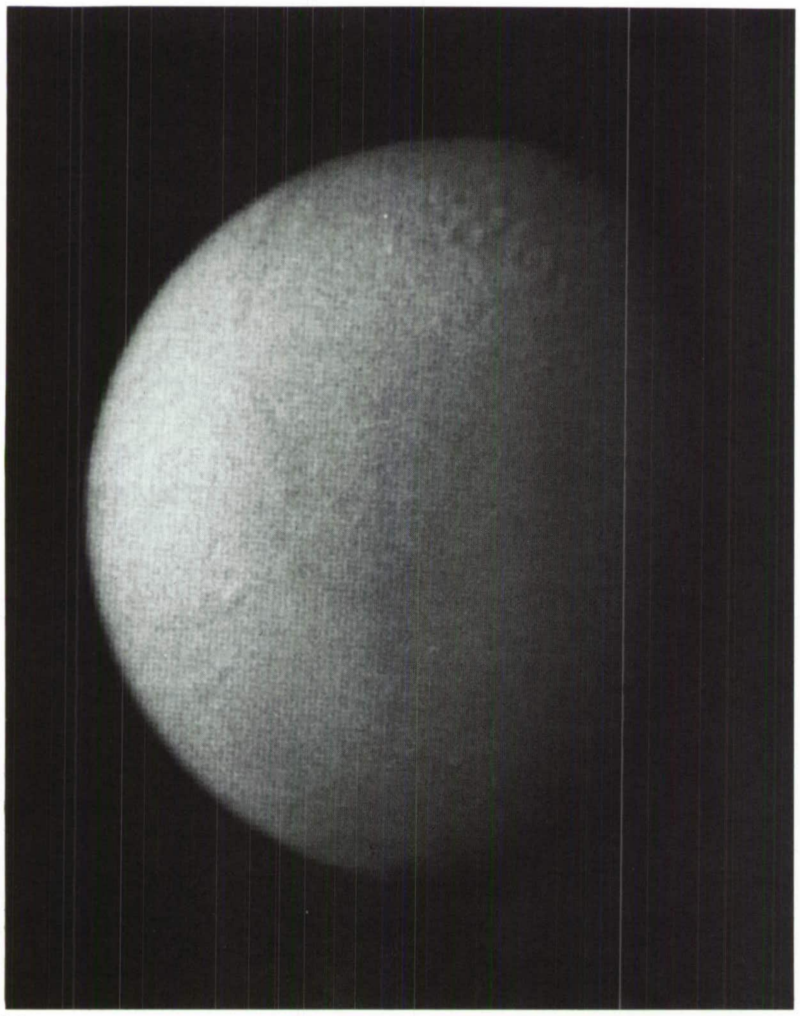

(a)

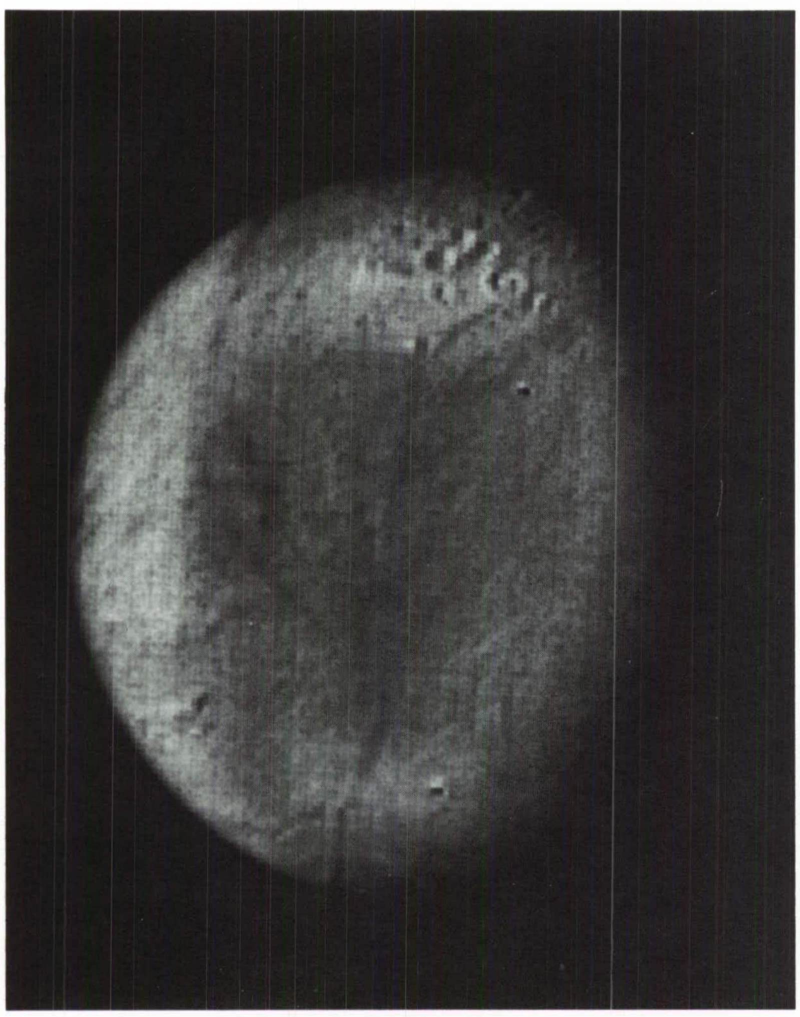

(b)

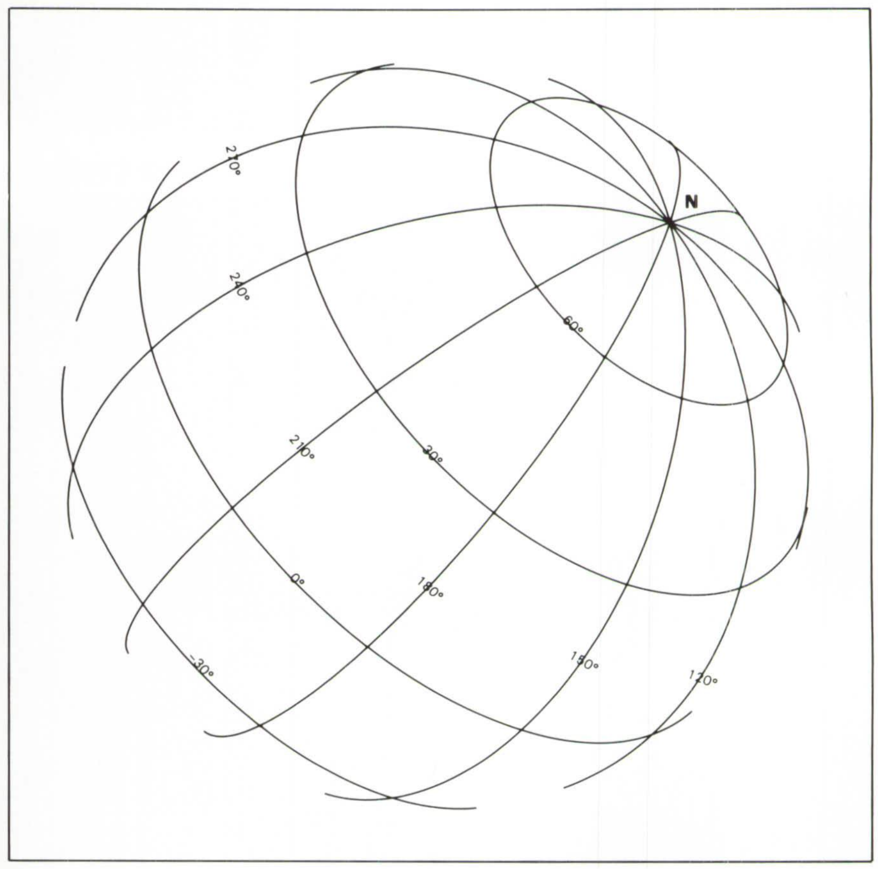

(c)

Picno	0993S2–001
FDS	43992.10
Range, km	441 895
Subspacecraft latitude/longitude, degrees	32/163
Subsolar latitude/longitude, degrees	8/201
Resolution, km/pixel	4
Filter size, pixels	41 × 41
Filter size, km	167
Scale	1:5 000 000

Figure 2–6. Picno 0993S2–001. (*a*) Unfiltered image. (*b*) High-pass filtered image. (*c*) Perspective grid.

(a)

(b)

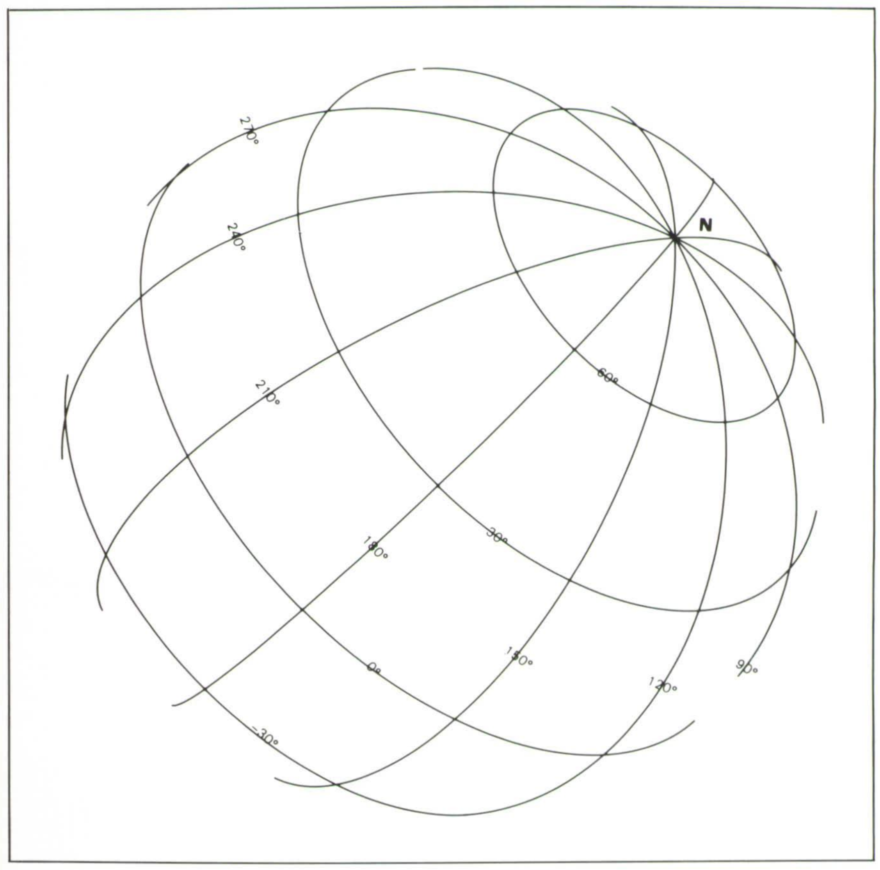

(c)

Picno	1055S2−001
FDS	43993.12
Range, km	397 738
Subspacecraft latitude/longitude, degrees	35/175
Subsolar latitude/longitude, degrees	8/210
Resolution, km/pixel	3
Filter size, pixels	41 × 41
Filter size, km	151
Scale	1:5 000 000

Figure 2–7. Picno 1055S2−001. (*a*) Unfiltered image. (*b*) High-pass filtered image. (*c*) Perspective grid.

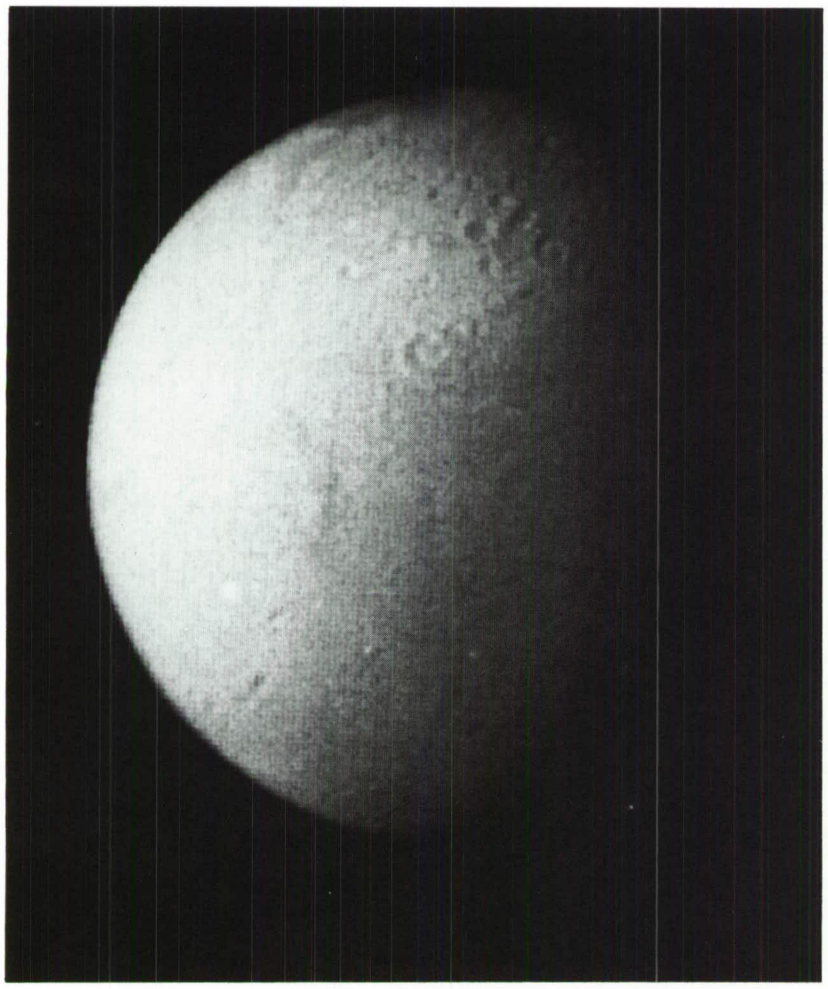

(a)

(b)

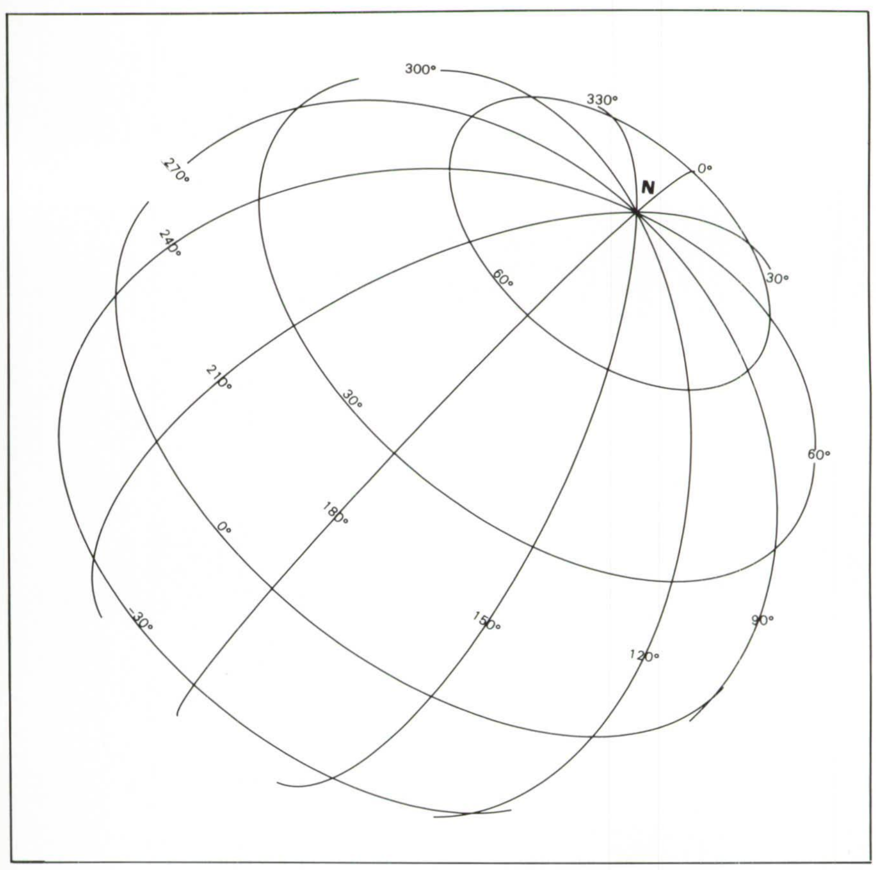

(c)

Picno	1059S2—001
FDS	43993.16
Range, km	395 076
Subspacecraft latitude/longitude, degrees	35/176
Subsolar latitude/longitude, degrees	8/210
Resolution, km/pixel	3
Filter size, pixels	37 × 37
Filter size, km	135
Scale	1:5 000 000

Figure 2–8. Picno 1059S2—001. (*a*) Unfiltered image. (*b*) High-pass filtered image. (*c*) Perspective grid.

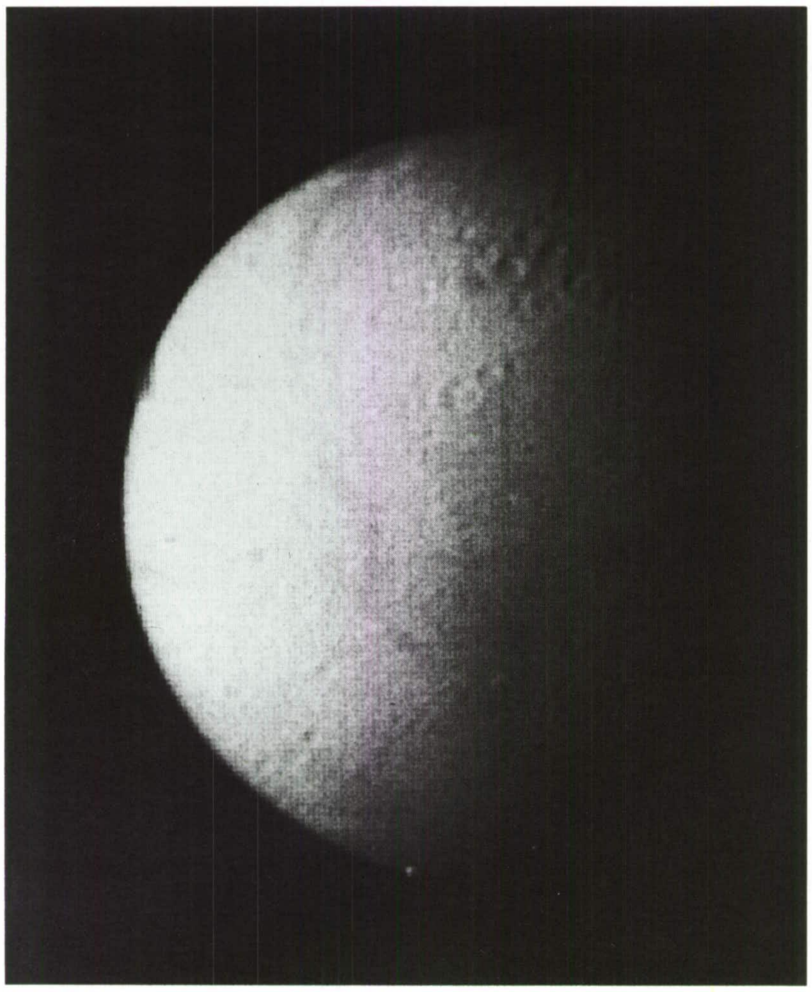

(*a*)

(*b*)

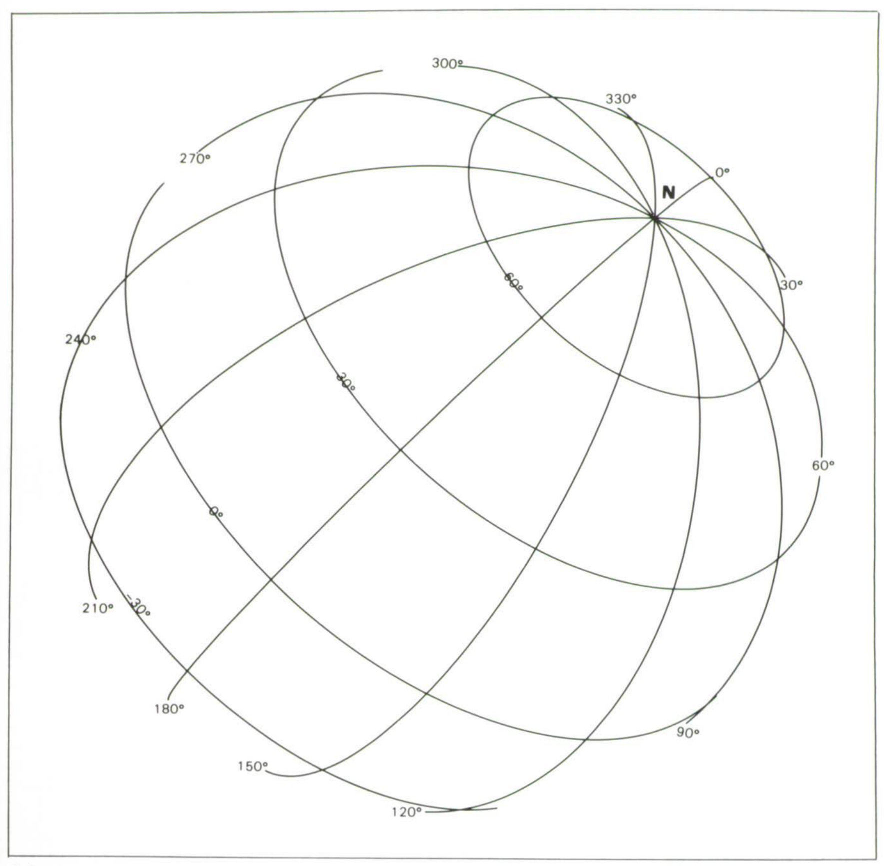

(*c*)

Picno	1063S2–001
FDS	43993.20
Range, km	392 437
Subspacecraft latitude/longitude, degrees	35/177
Subsolar latitude/longitude, degrees	8/211
Resolution, km/pixel	3
Filter size, pixels	25 × 25
Filter size, km	90
Scale	1:5 000 000

Figure 2–9. Picno 1063S2—001. (*a*) Unfiltered image. (*b*) High-pass filtered image. (*c*) Perspective grid.

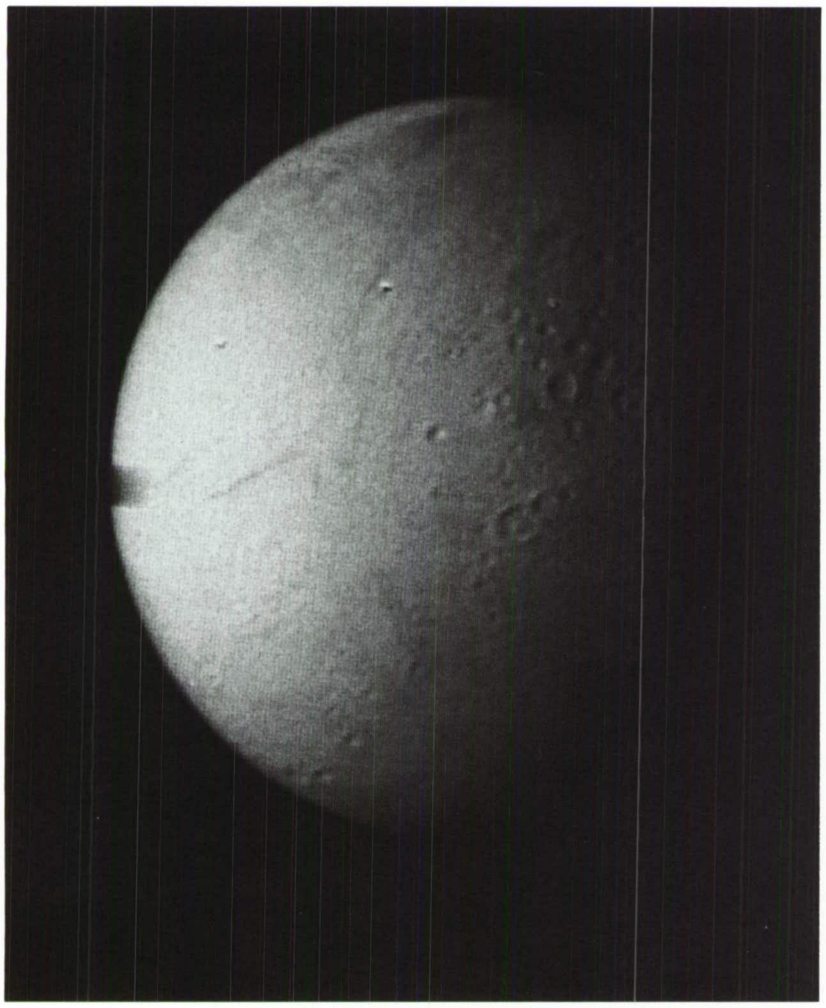

(a)

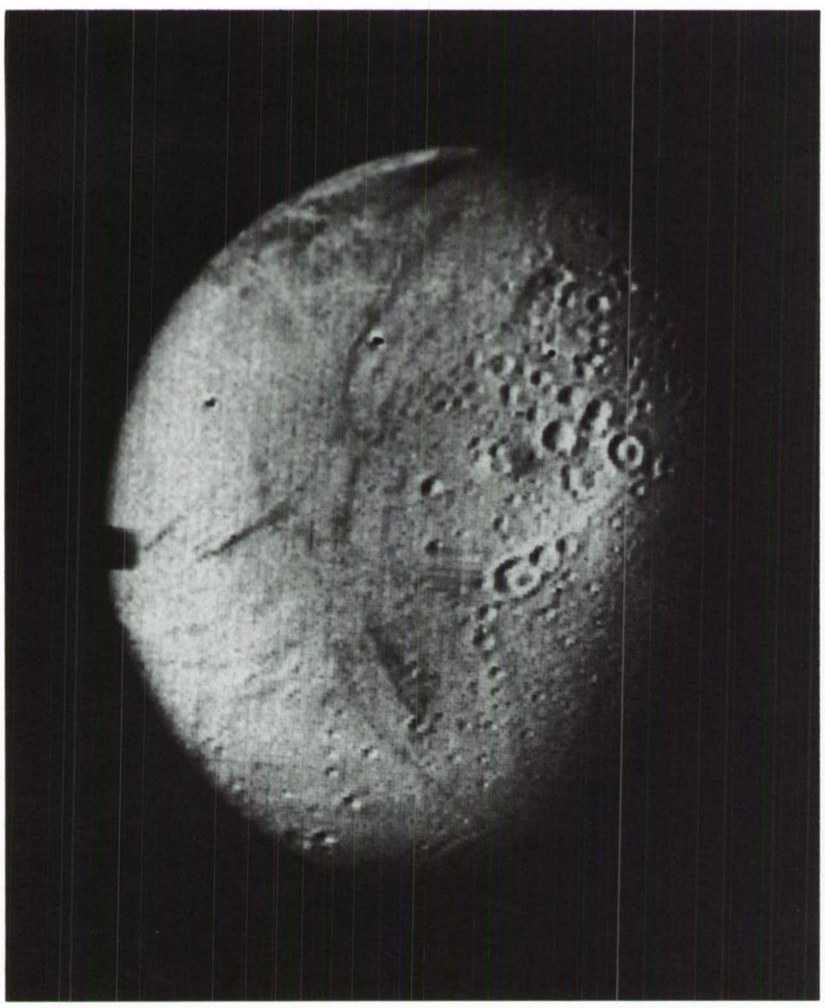

(b)

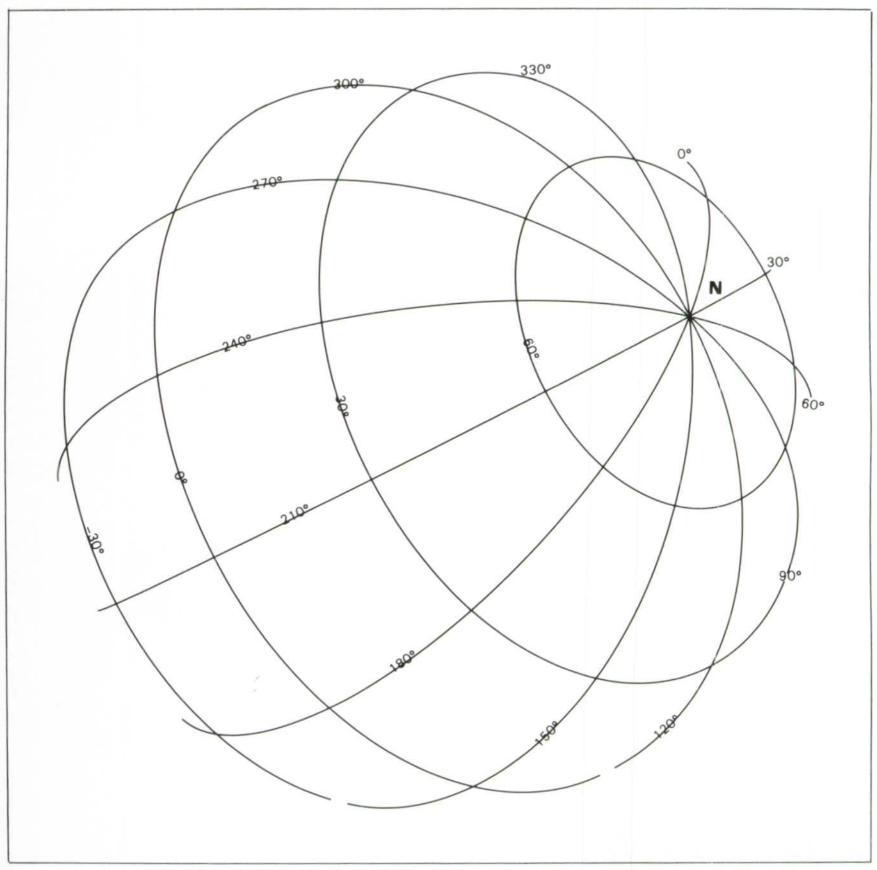

(c)

Picno	1225S2–001
FDS	43996.02
Range, km	304 160
Subspacecraft latitude/longitude, degrees	41/212
Subsolar latitude/longitude, degrees	8/234
Resolution, km/pixel	3
Filter size, pixels	69 × 69
Filter size, km	194
Scale	1:5 000 000

Figure 2–10. Picno 1225S2–001. (*a*) Unfiltered image. (*b*) High-pass filtered image. (*c*) Perspective grid.

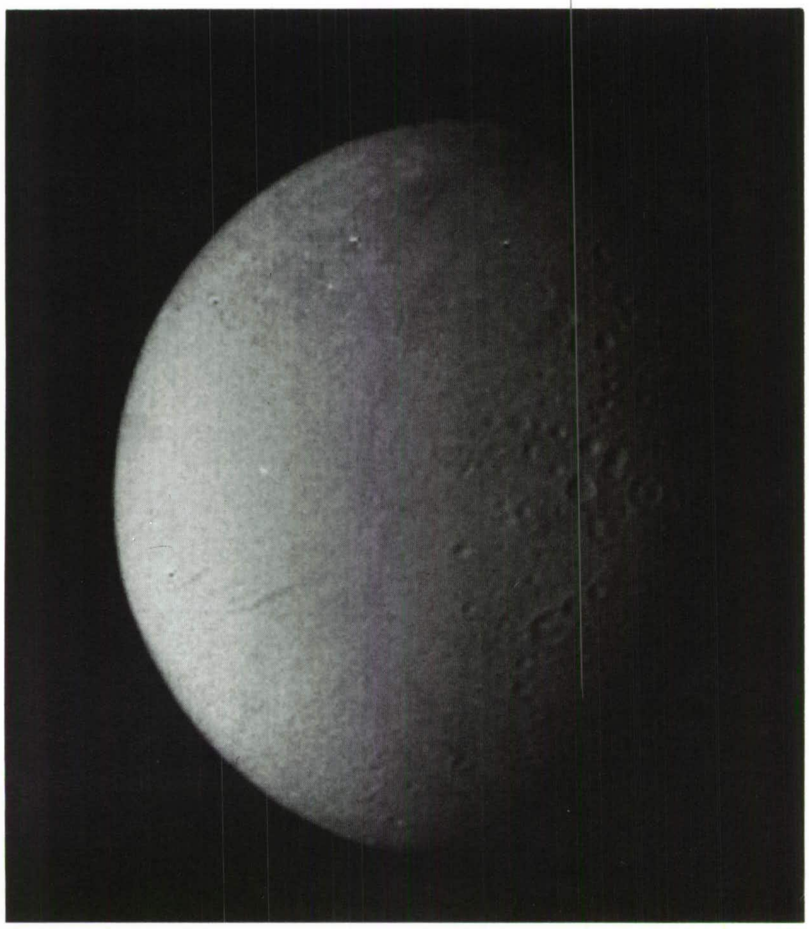

(*a*)

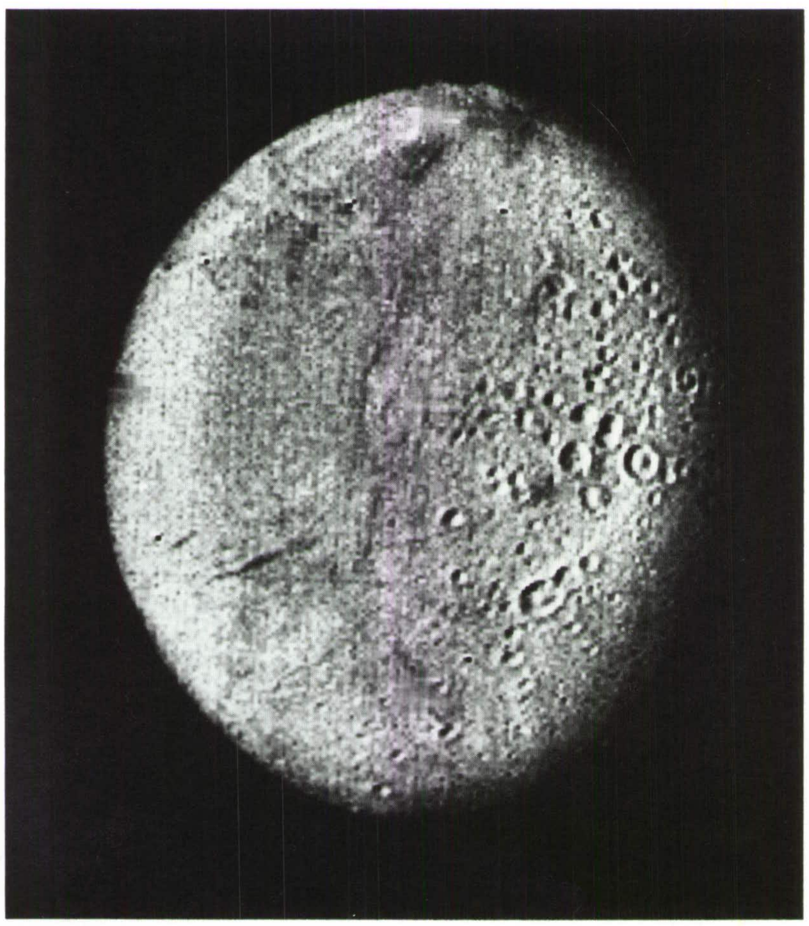

(*b*)

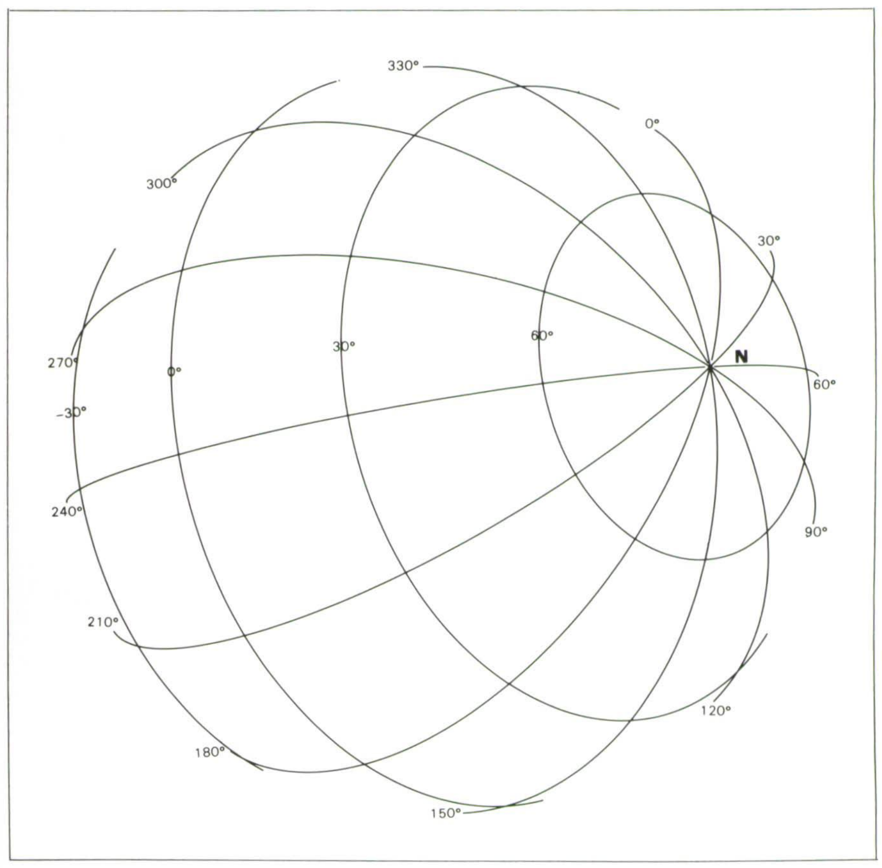

(*c*)

Picno	1308S2–001
FDS	43997.25
Range, km	271 124
Subspacecraft latitude/longitude, degrees	43/232
Subsolar latitude/longitude, degrees	8/247
Resolution, km/pixel	2
Filter size, pixels	51 × 51
Filter size, km	128
Scale	1:5 000 000

Figure 2–11. Picno 1308S2–001. (*a*) Unfiltered image. (*b*) High-pass filtered image. (*c*) Perspective grid.

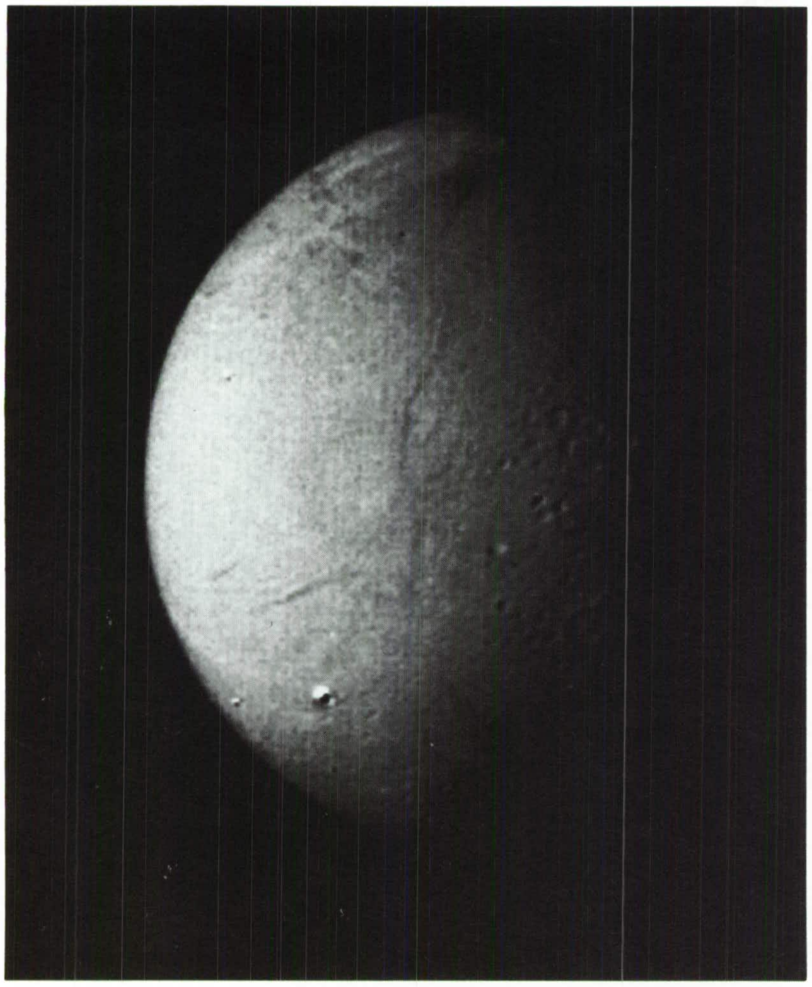

(a)

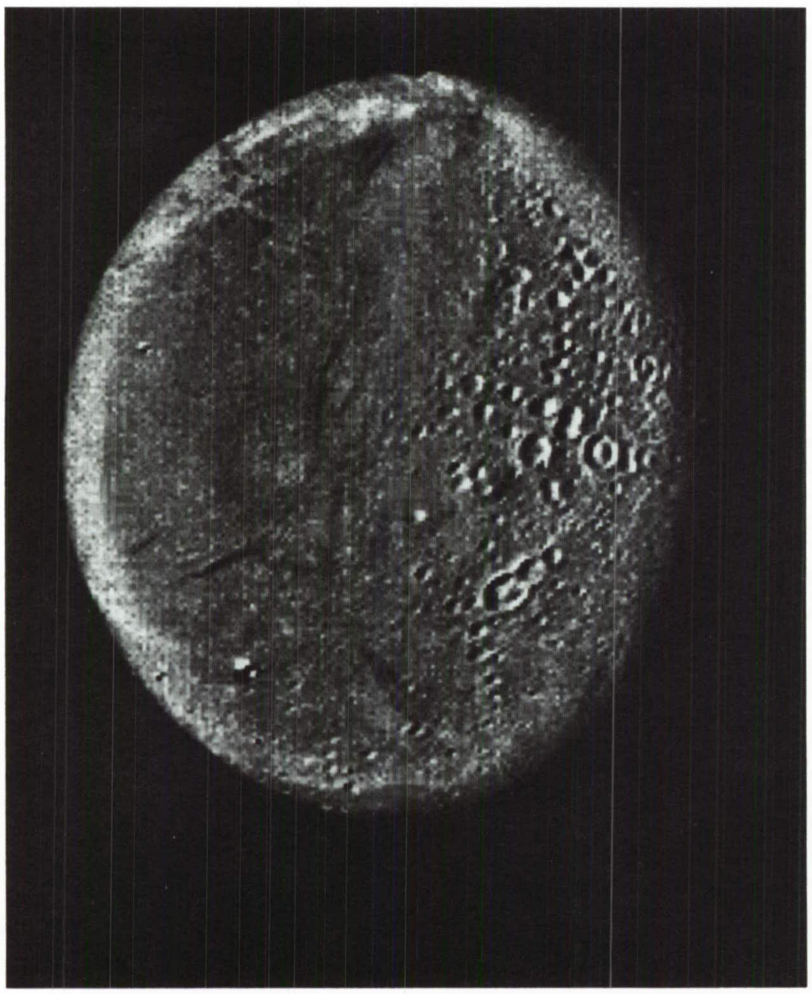

(b)

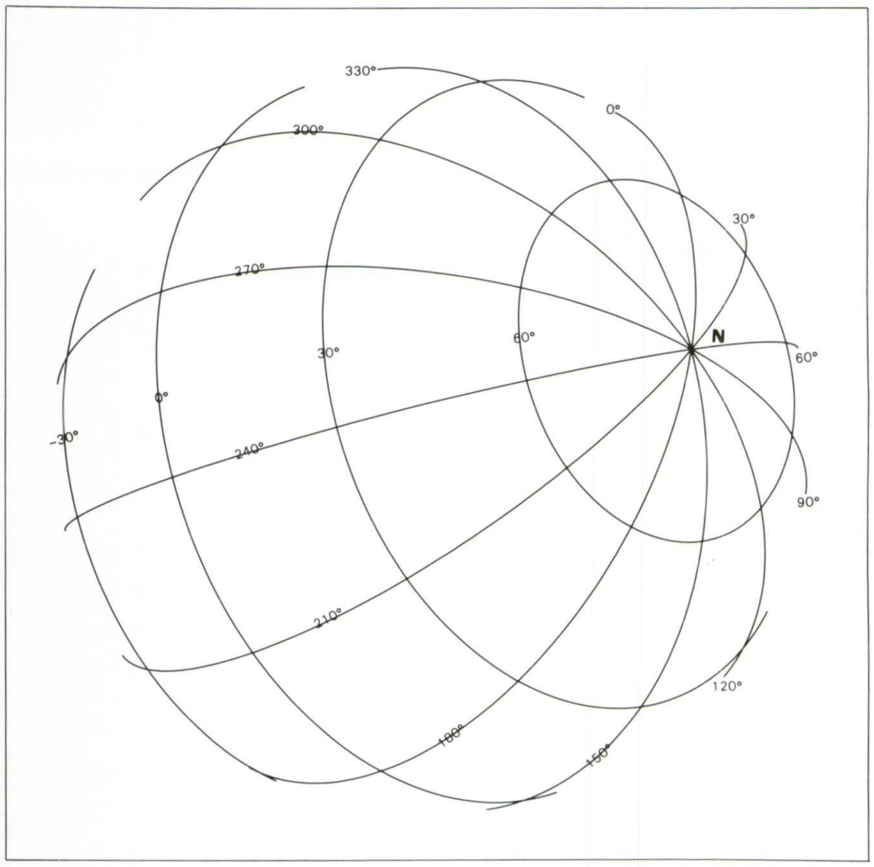

(c)

Picno	1312S2−001
FDS	43997.29
Range, km	269 684
Subspacecraft latitude/longitude, degrees	43/233
Subsolar latitude/longitude, degrees	8/247
Resolution, km/pixel	2
Filter size, pixels	25 × 25
Filter size, km	62
Scale	1:5 000 000

Figure 2–12. Picno 1312S2−001. (*a*) Unfiltered image. (*b*) High-pass filtered image. (*c*) Perspective grid.

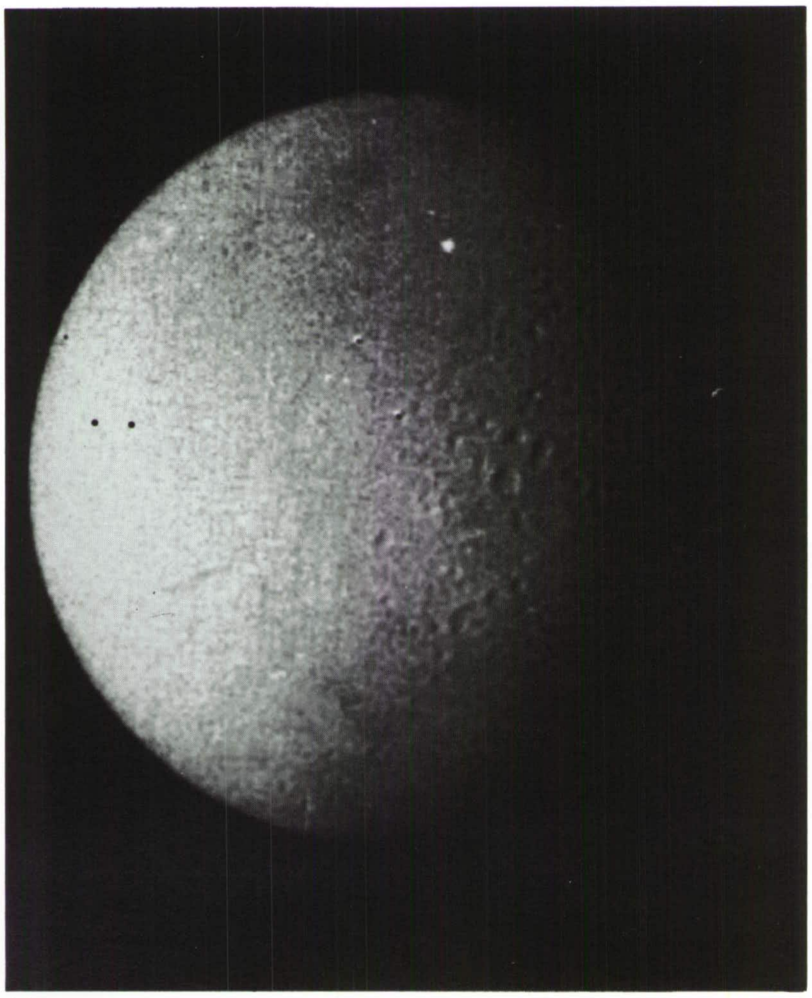

(a)

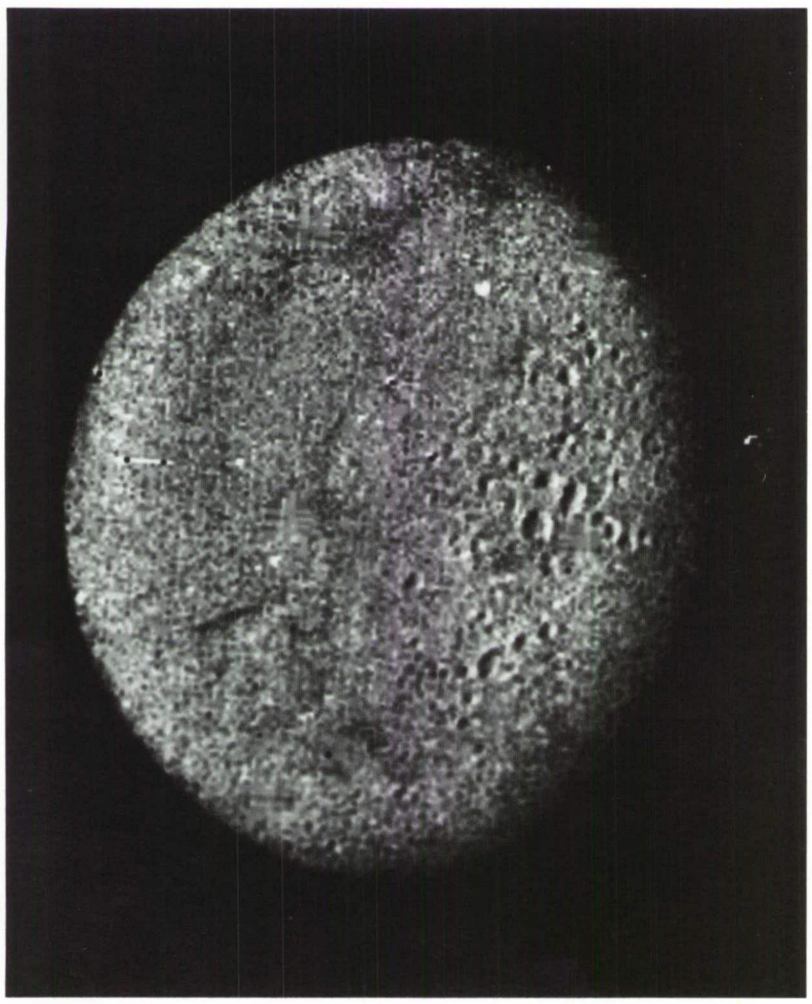

(b)

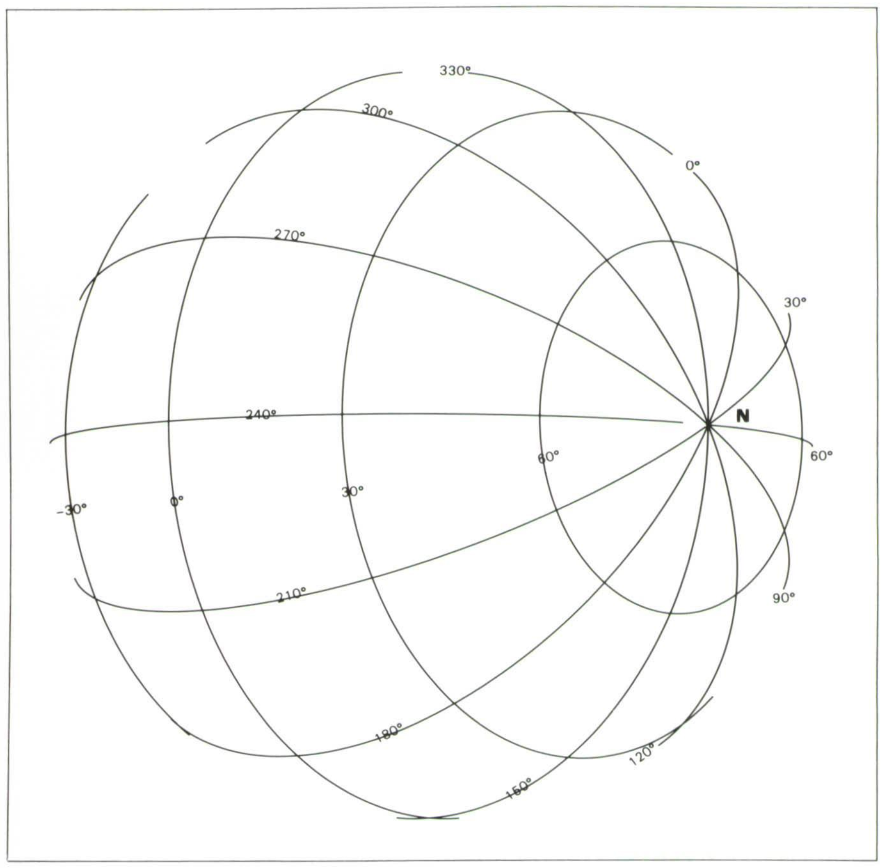

(c)

Picno	1316S2—001
FDS	43997.33
Range, km	268 258
Subspacecraft latitude/longitude, degrees	43/234
Subsolar latitude/longitude, degrees	8/248
Resolution, km/pixel	2
Filter size, pixels	41 × 41
Filter size, km	102
Scale	1:5 000 000

Figure 2–13. Picno 1316S2—001. (*a*) Unfiltered image. (*b*) High-pass filtered image. (*c*) Perspective grid.

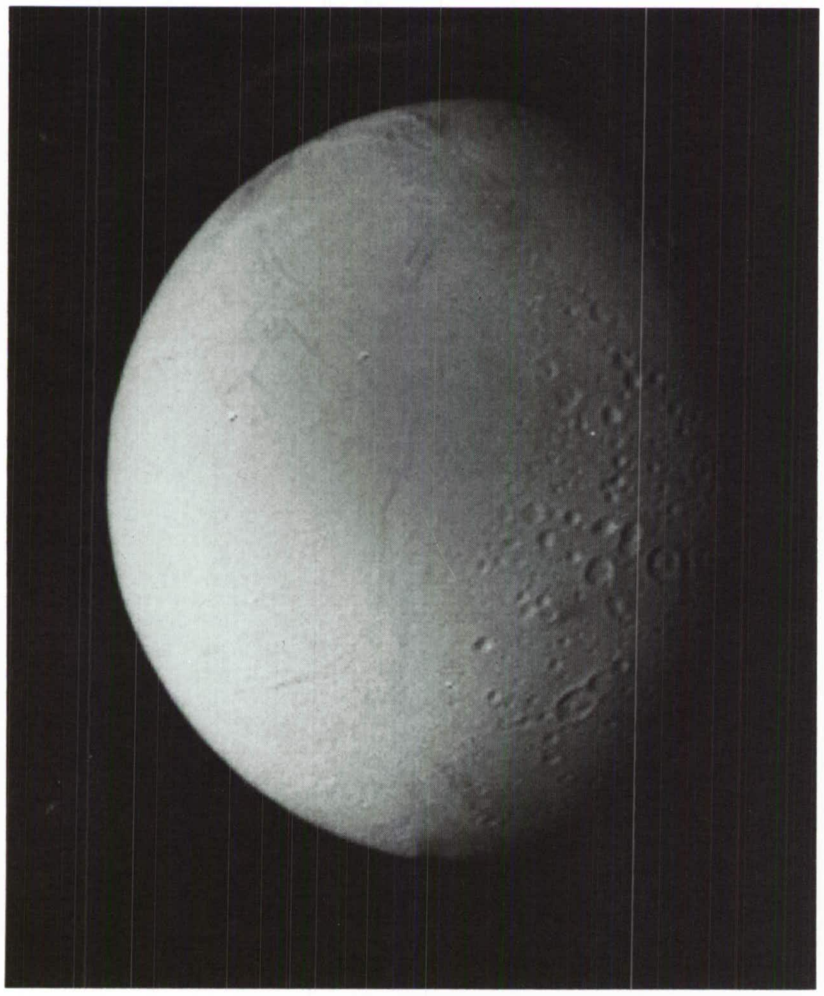

(*a*)

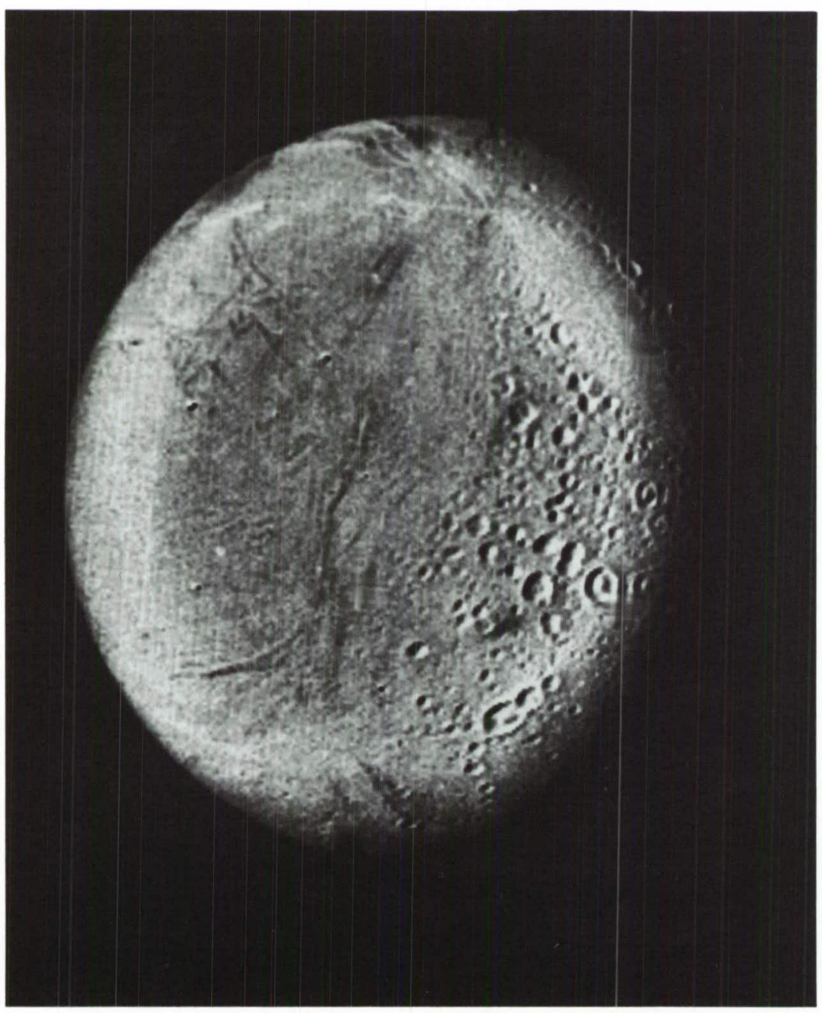

(*b*)

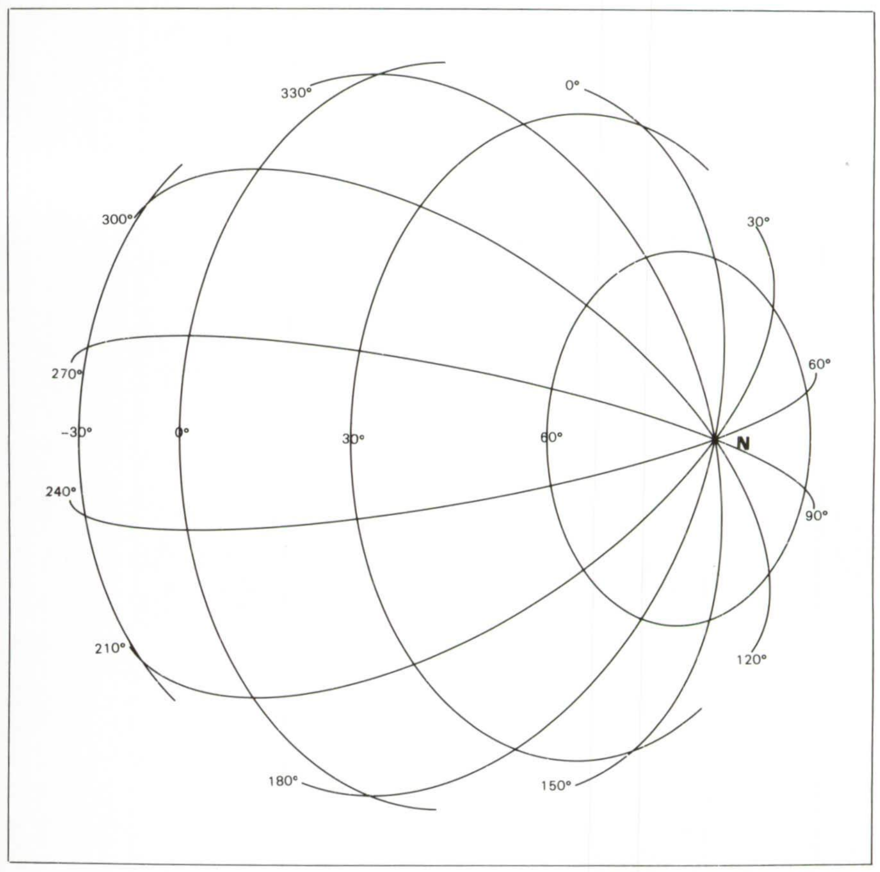

(*c*)

Picno	1403S2—001
FDS	43999.00
Range, km	239 199
Subspacecraft latitude/longitude, degrees	44/255
Subsolar latitude/longitude, degrees	8/260
Resolution, km/pixel	2
Filter size, pixels	61 × 61
Filter size, km	135
Scale	1:5 000 000

Figure 2–14. Picno 1403S2—001. (*a*) Unfiltered image. (*b*) High-pass filtered image. (*c*) Perspective grid.

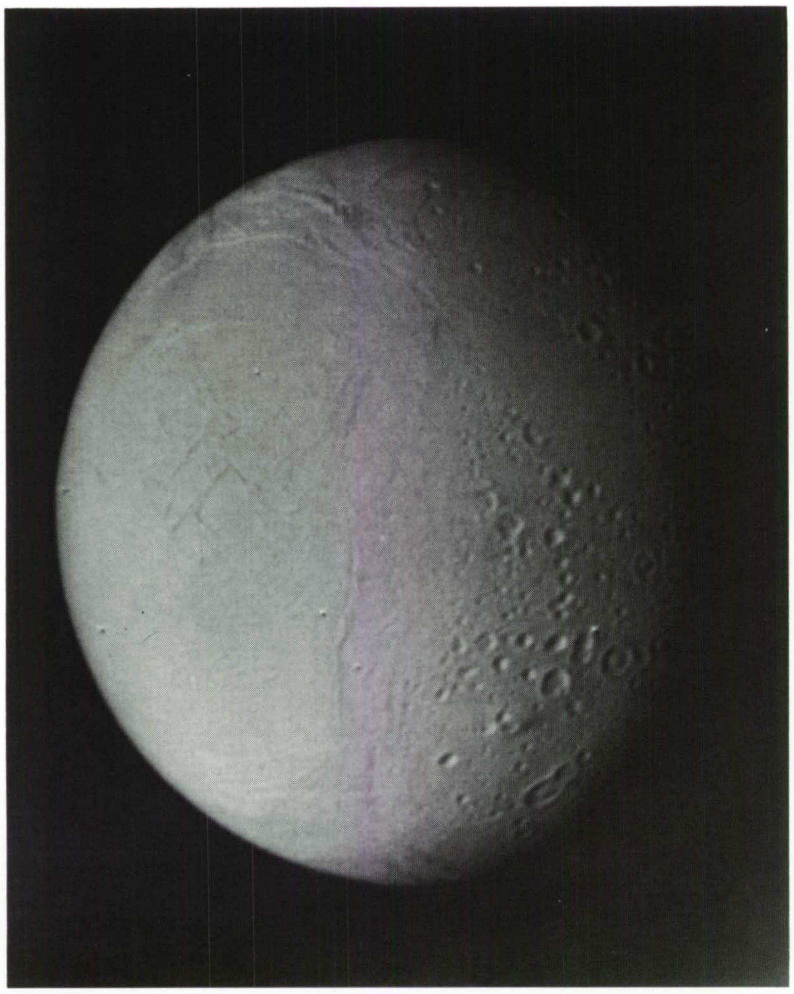

(a)

(b)

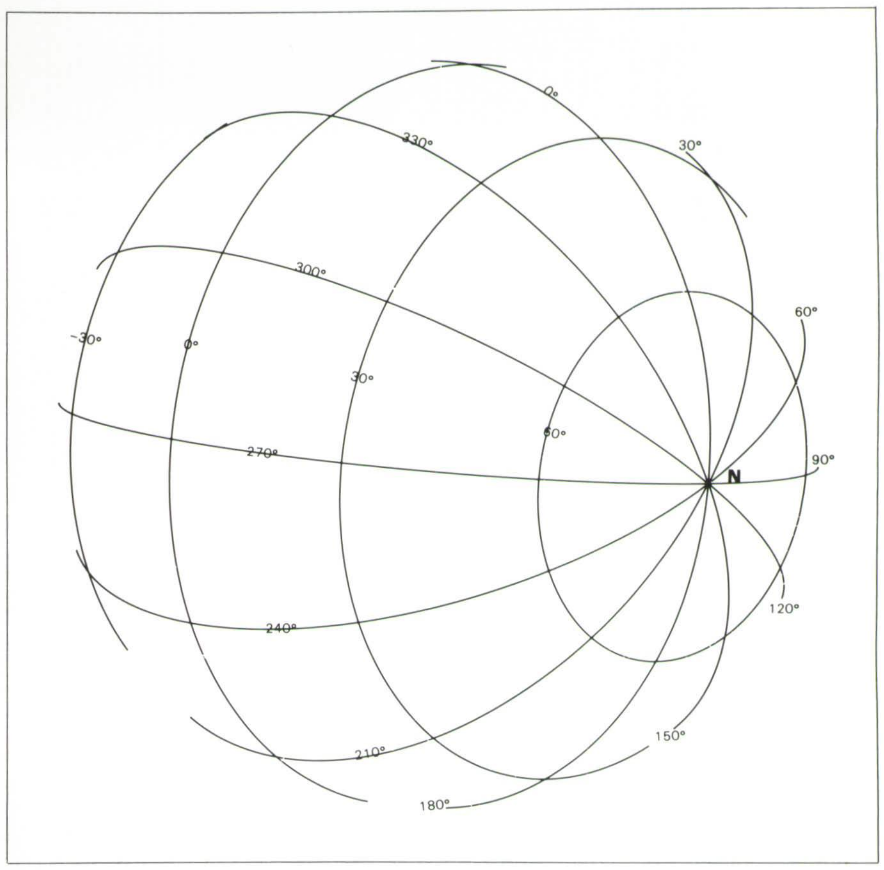

(c)

Picno	1505S2—001
FDS	44000.42
Range, km	206 000
Subspacecraft latitude/longitude, degrees	44/278
Subsolar latitude/longitude, degrees	8/275
Resolution, km/pixel	2
Filter size, pixels	65 × 65
Filter size, km	124
Scale	1:5 000 000

Figure 2–15. Picno 1505S2—001. (*a*) Unfiltered image. (*b*) High-pass filtered image. (*c*) Perspective grid.

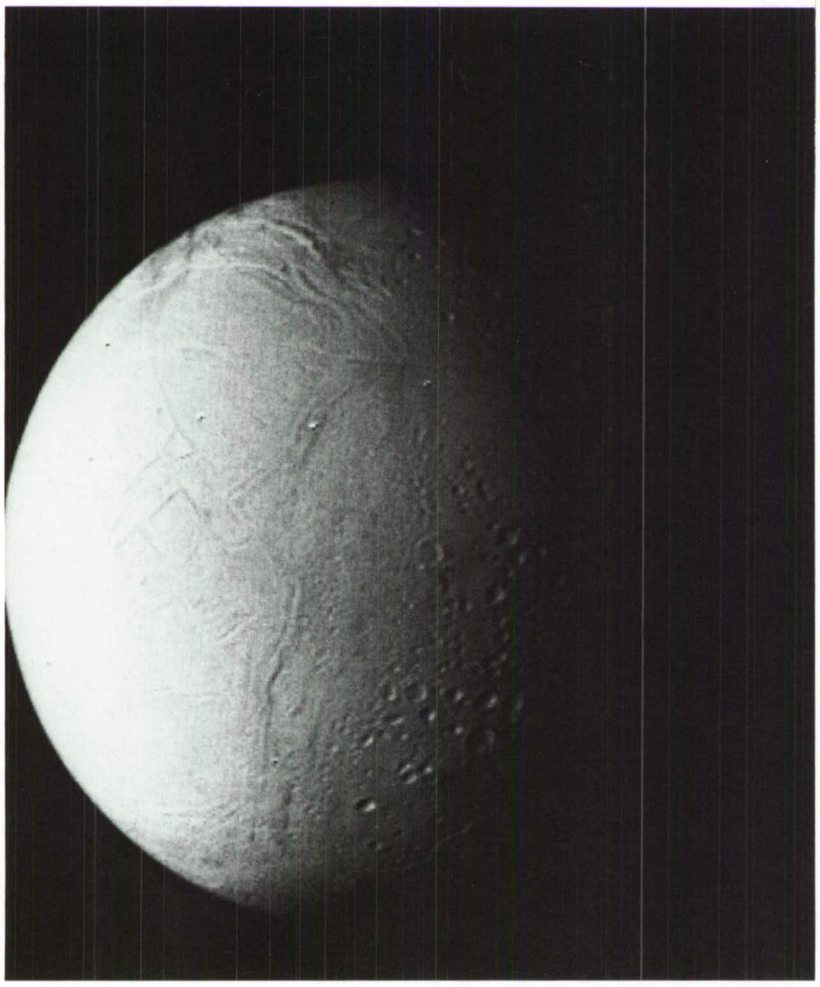

(a)

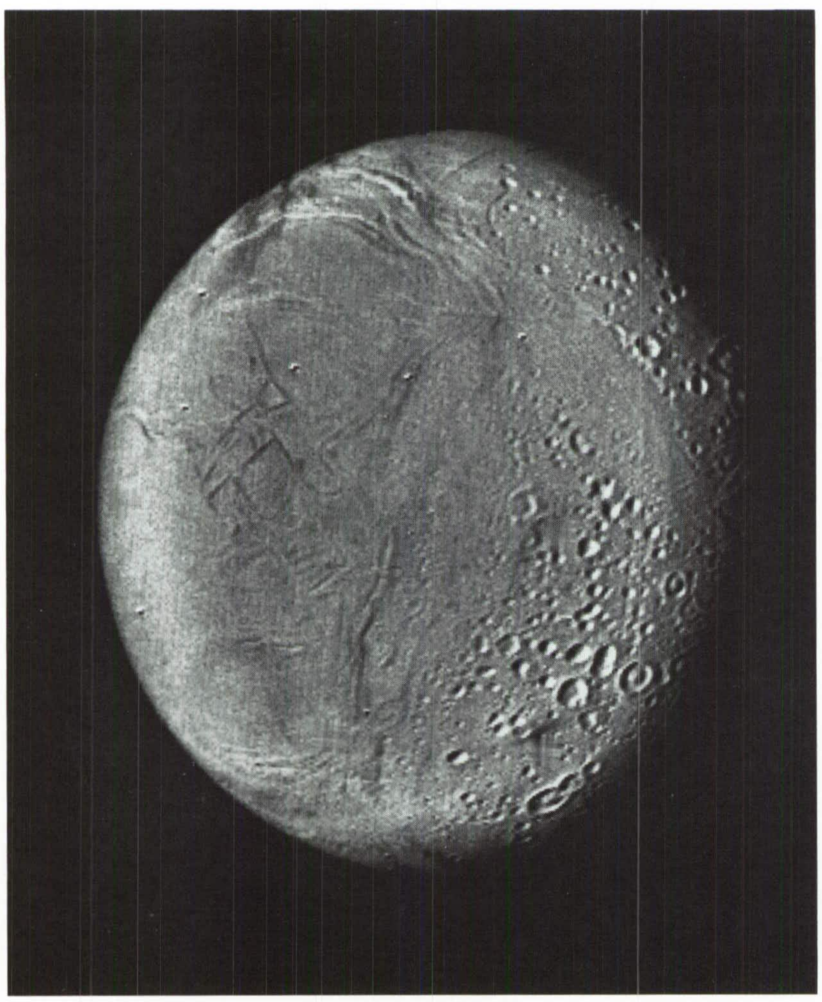

(b)

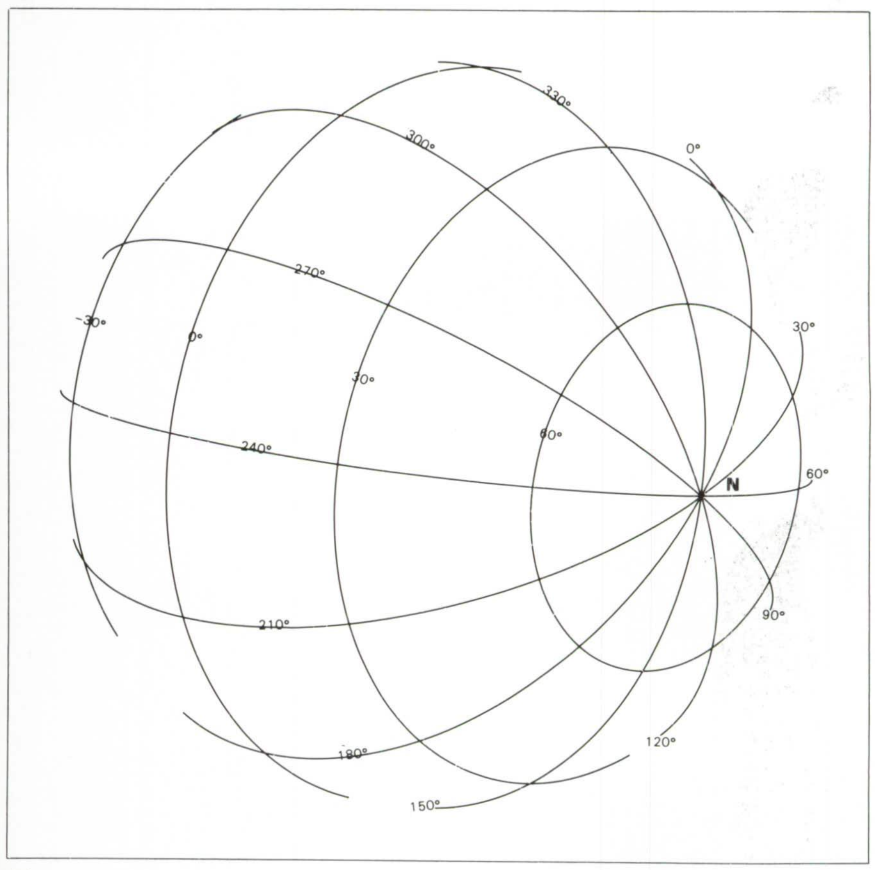

(c)

Picno	1507S2−001
FDS	44000.44
Range, km	205 316
Subspacecraft latitude/longitude, degrees	44/279
Subsolar latitude/longitude, degrees	8/276
Resolution, km/pixel	2
Filter size, pixels	57 × 57
Filter size, km	108
Scale	1:5 000 000

Figure 2–16. Picno 1507S2−001. (*a*) Unfiltered image. (*b*) High-pass filtered image. (*c*) Perspective grid.

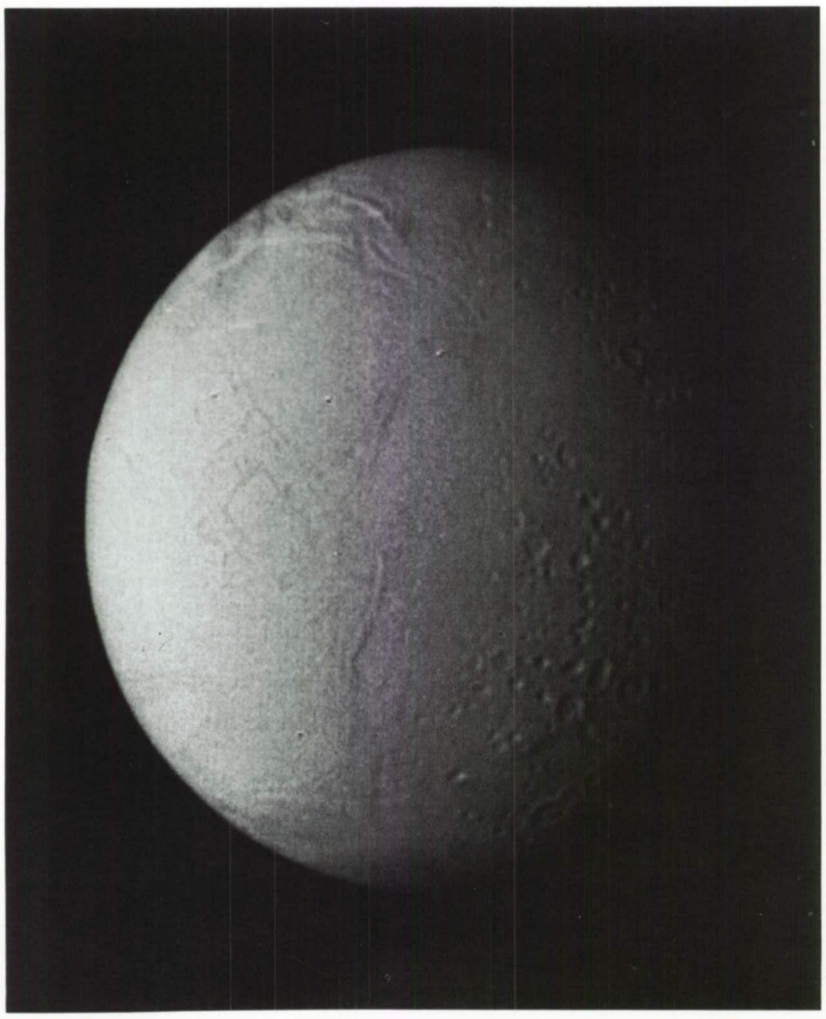

(a)

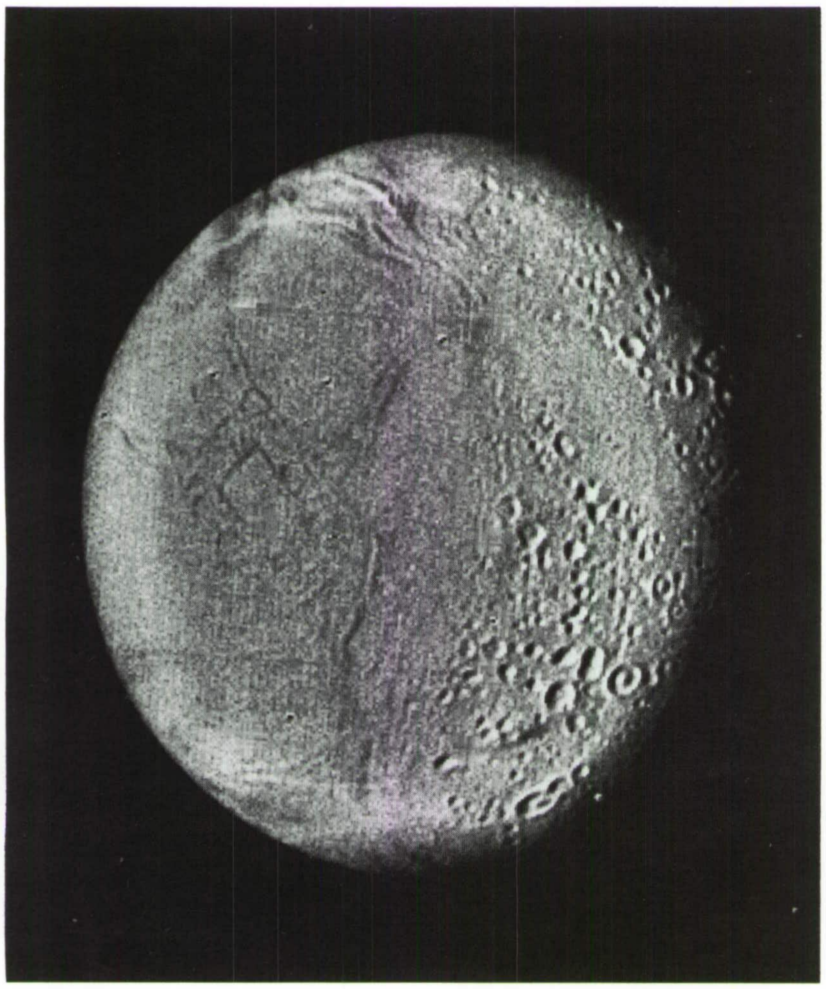

(b)

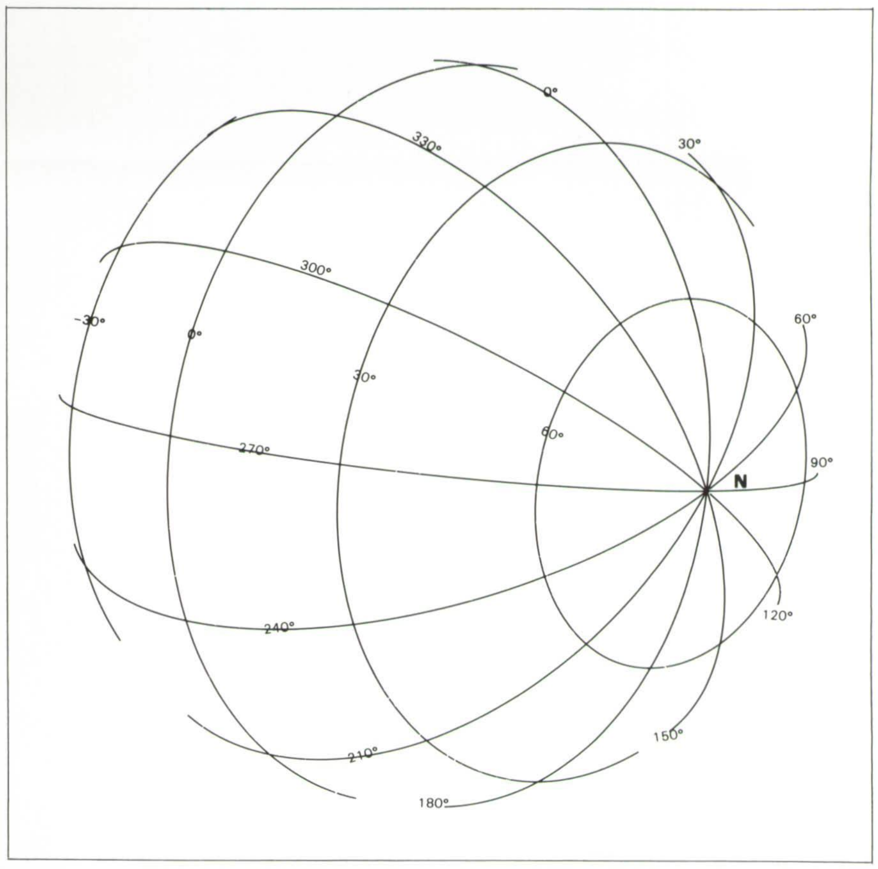

(c)

Picno	1509S2–001
FDS	44000.46
Range, km	204 630
Subspacecraft latitude/longitude, degrees	44/279
Subsolar latitude/longitude, degrees	8/276
Resolution, km/pixel	2
Filter size, pixels	57 × 57
Filter size, km	108
Scale	1:5 000 000

Figure 2–17. Picno 1509S2–001. (*a*) Unfiltered image. (*b*) High-pass filtered image. (*c*) Perspective grid.

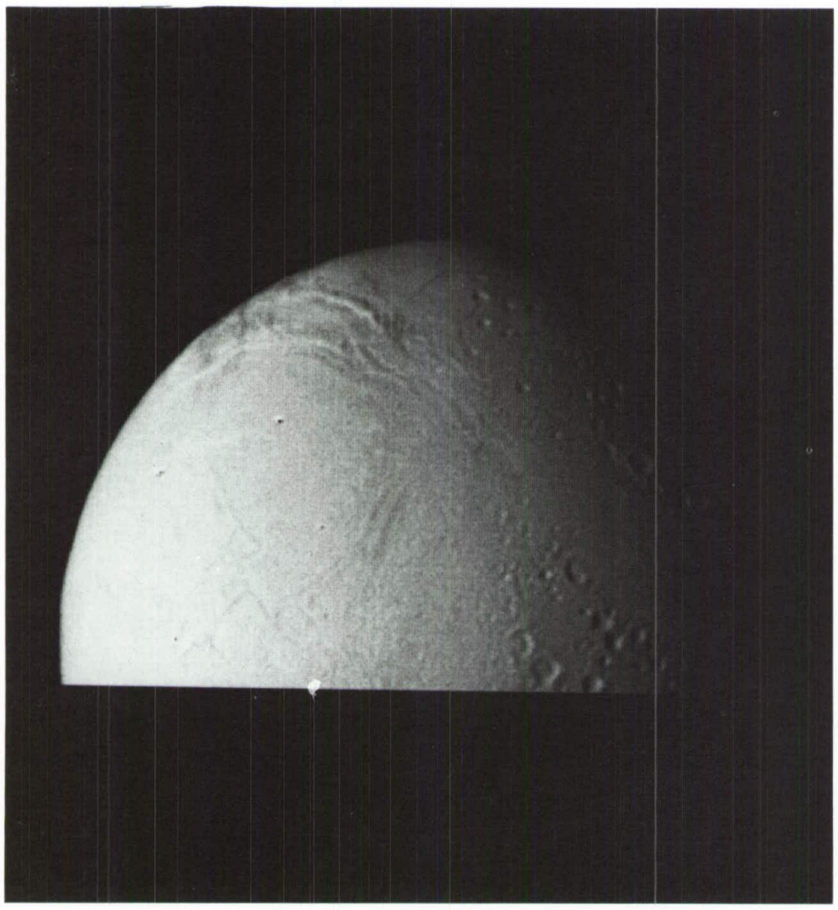

(a)

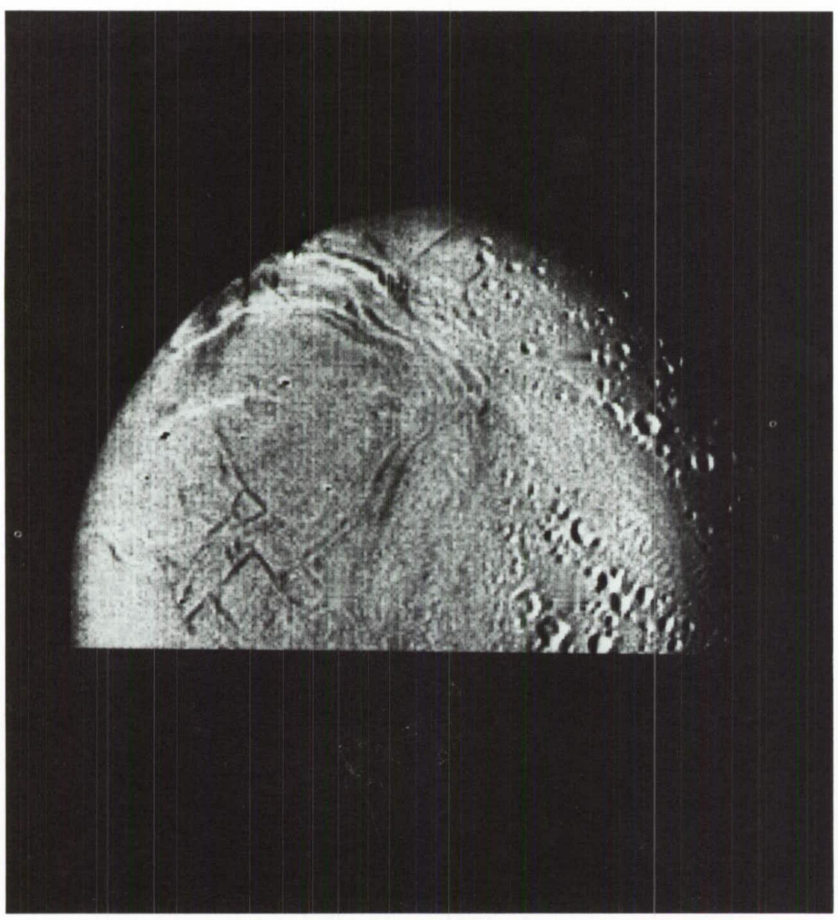

(b)

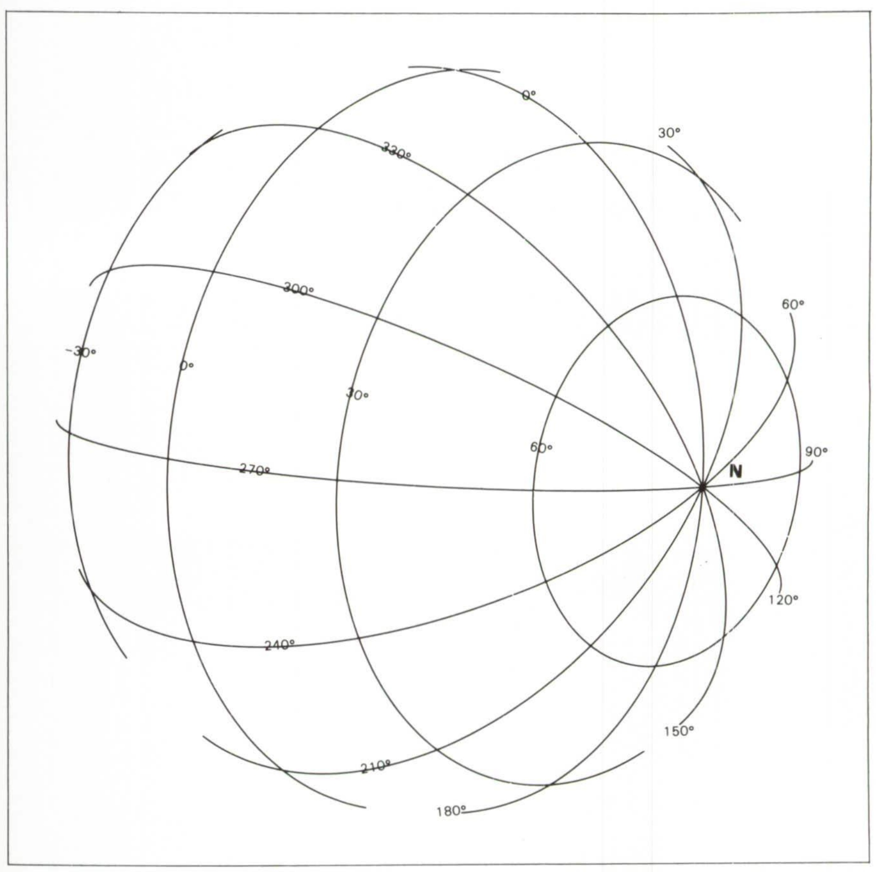

(c)

Picno	1511S2−001
FDS	44000.48
Range, km	203 940
Subspacecraft latitude/longitude, degrees	44/280
Subsolar latitude/longitude, degrees	8/276
Resolution, km/pixel	2
Filter size, pixels	59 × 59
Filter size, km	111
Scale	1:5 000 000

Figure 2–18. Picno 1511S2−001. (*a*) Unfiltered image. (*b*) High-pass filtered image. (*c*) Perspective grid.

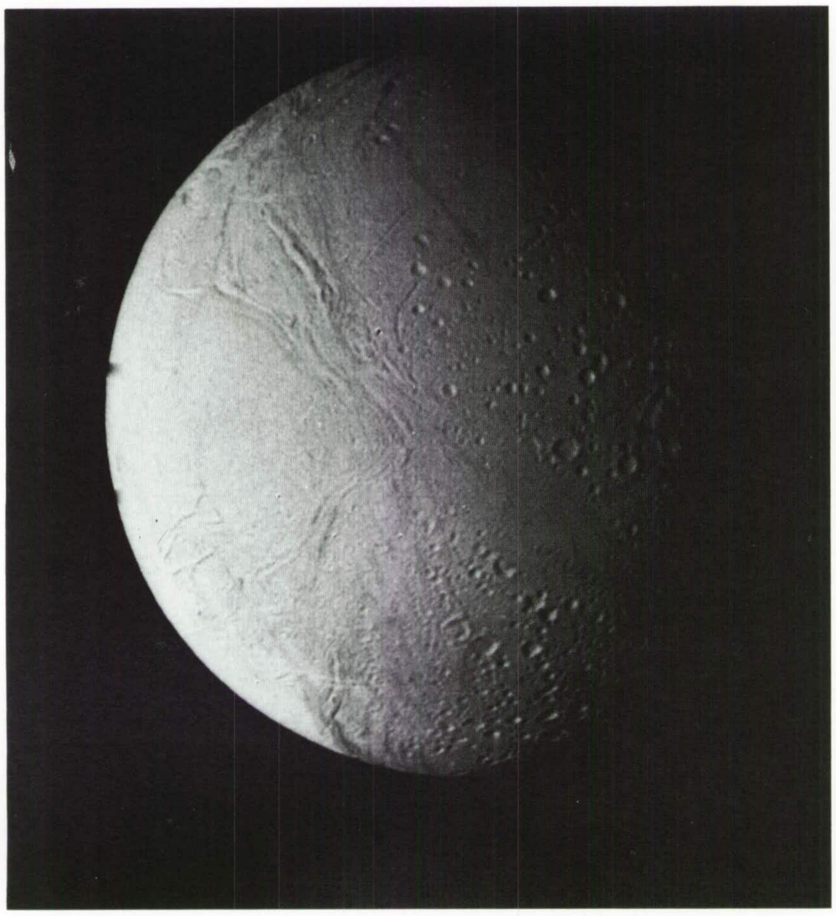

(a)

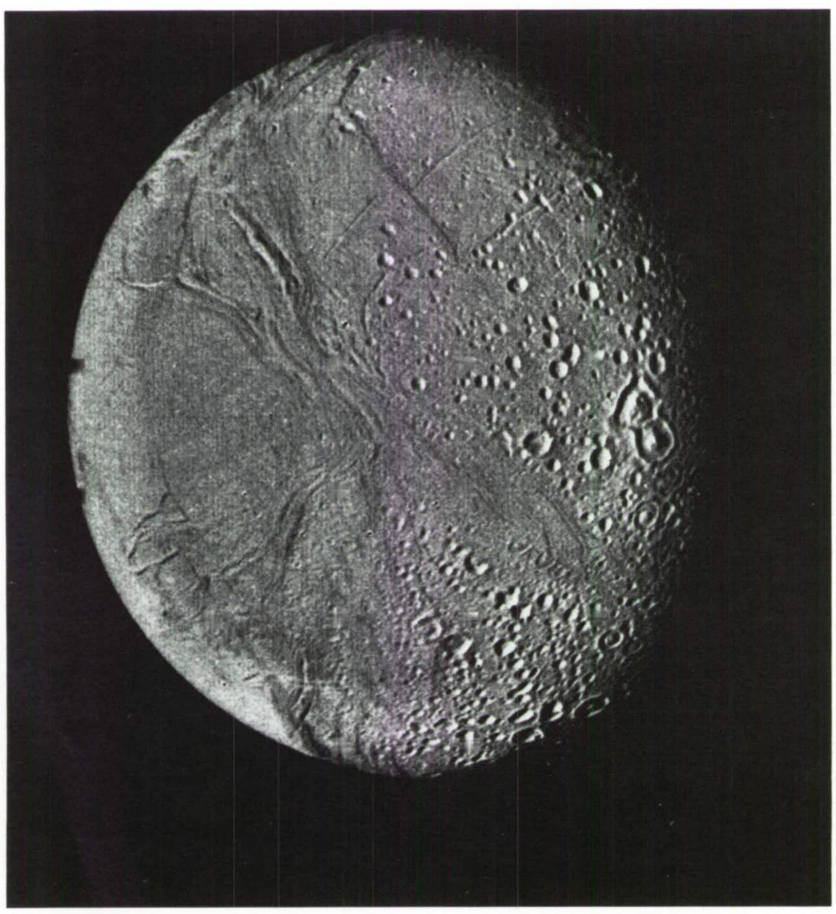

(b)

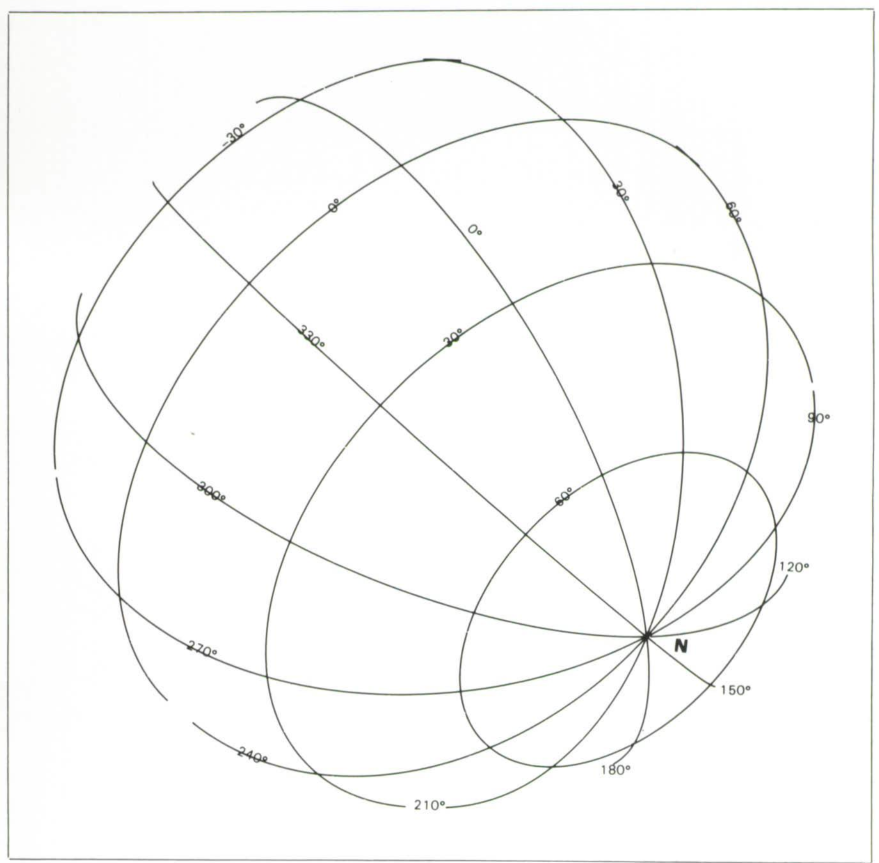

(c)

Picno	1715S2−001
FDS	44004.12
Range, km	118 931
Subspacecraft latitude/longitude, degrees	39/333
Subsolar latitude/longitude, degrees	8/306
Resolution, km/pixel	1
Filter size, pixels	89 × 89
Filter size, km	98
Scale	1:5 000 000

Figure 2–19. Picno 1715S2−001. (*a*) Unfiltered image. (*b*) High-pass filtered image. (*c*) Perspective grid.

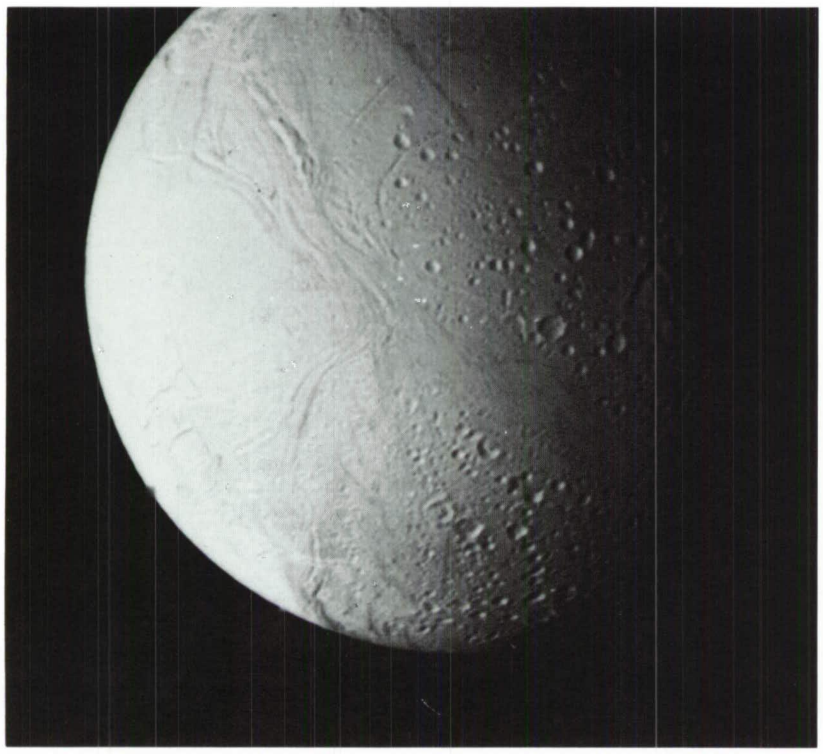

(a)

(b)

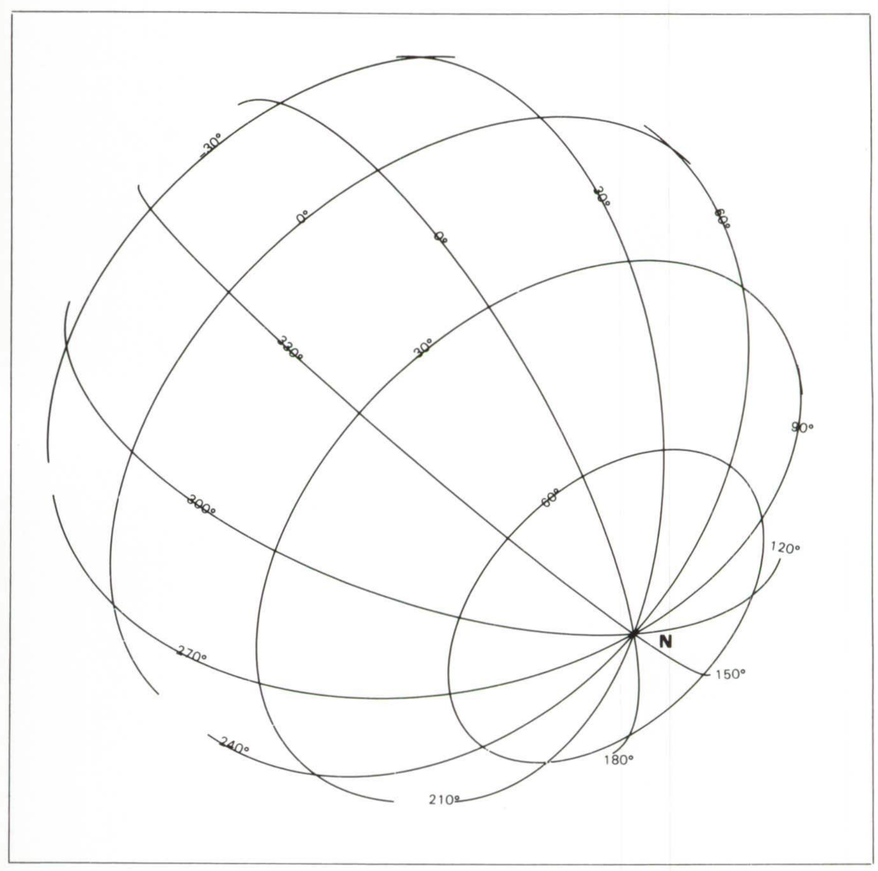

(c)

Picno	1723S2–001
FDS	44004.20
Range, km	115 338
Subspacecraft latitude/longitude, degrees	39/336
Subsolar latitude/longitude, degrees	8/307
Resolution, km/pixel	1
Filter size, pixels	83 × 83
Filter size, km	88
Scale	1:5 000 000

Figure 2–20. Picno 1713S2–001. (*a*) Unfiltered image. (*b*) High-pass filtered image. (*c*) Perspective grid.

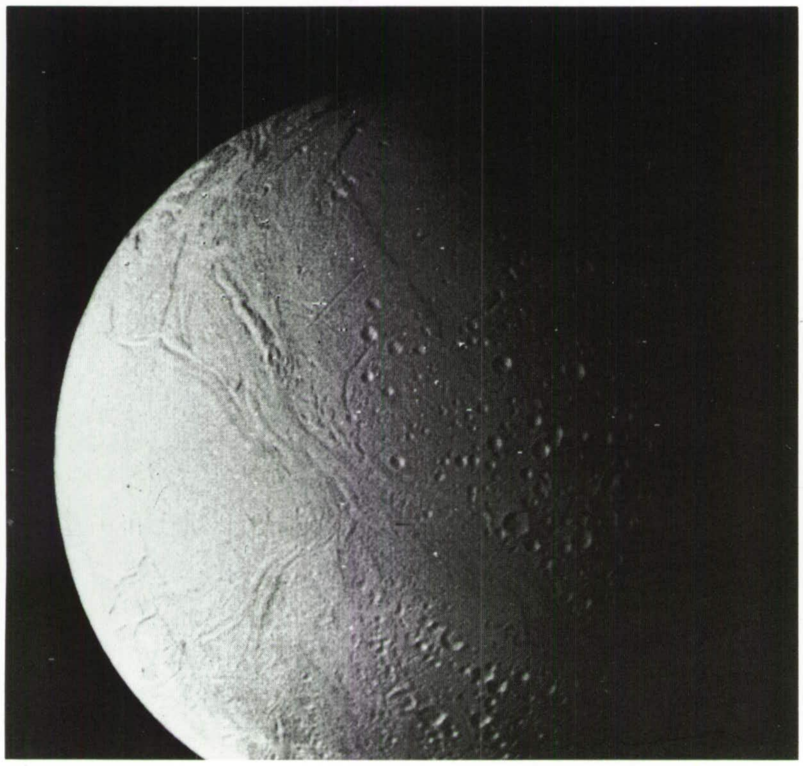

(a)

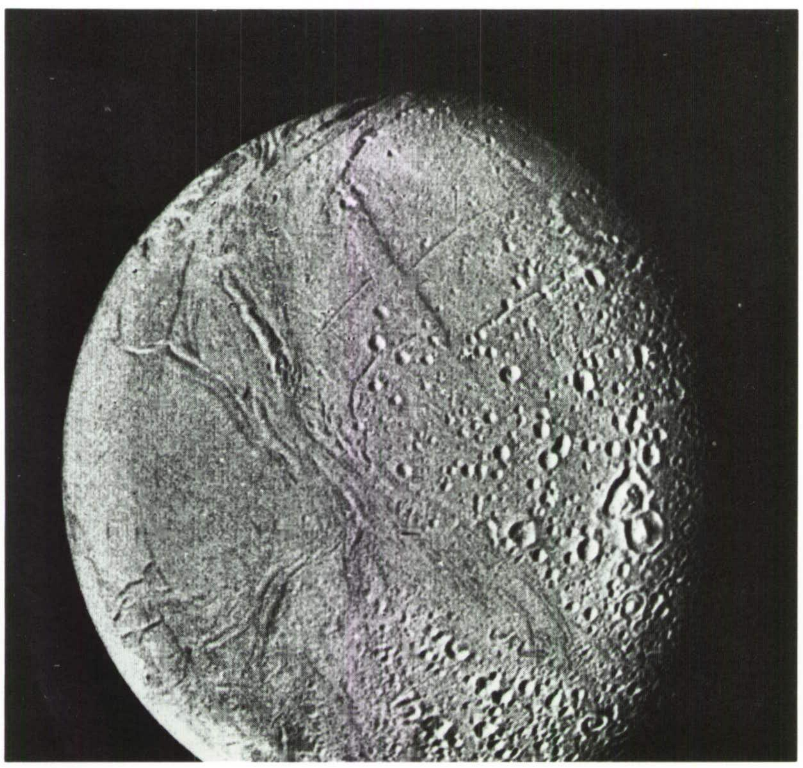

(b)

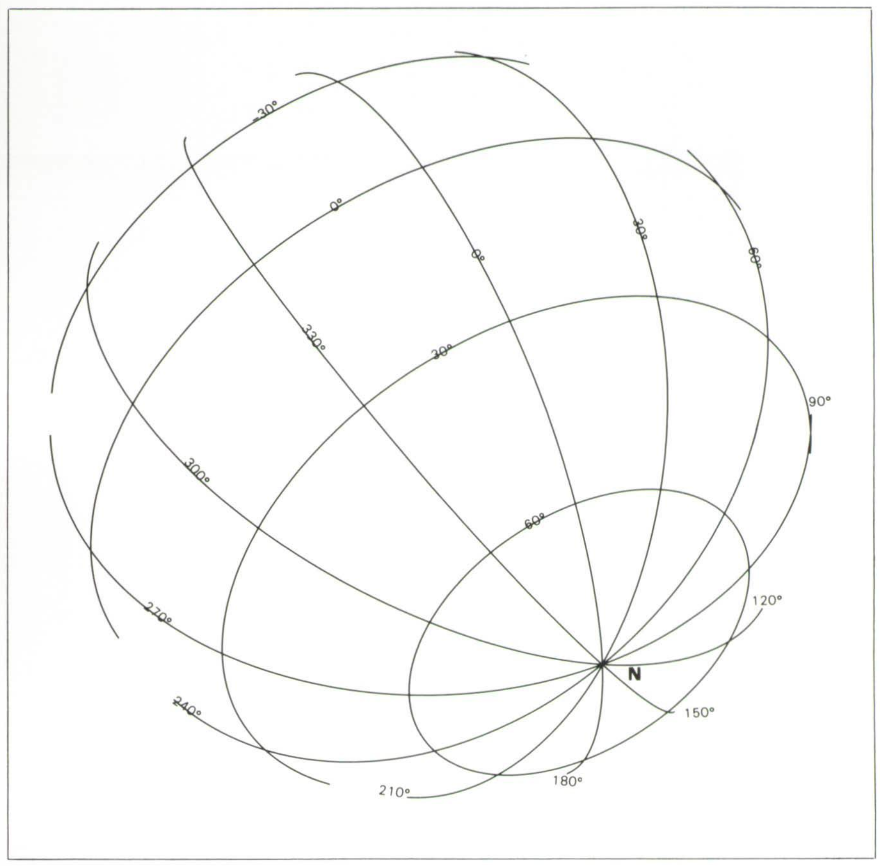

(c)

Picno	1727S2–001
FDS	44004.24
Range, km	113 571
Subspacecraft latitude/longitude, degrees	38/338
Subsolar latitude/longitude, degrees	8/308
Resolution, km/pixel	1
Filter size, pixels	95 × 95
Filter size, km	100
Scale	1:5 000 000

Figure 2–21. Picno 1727S2–001. (*a*) Unfiltered image. (*b*) High-pass filtered image. (*c*) Perspective grid.

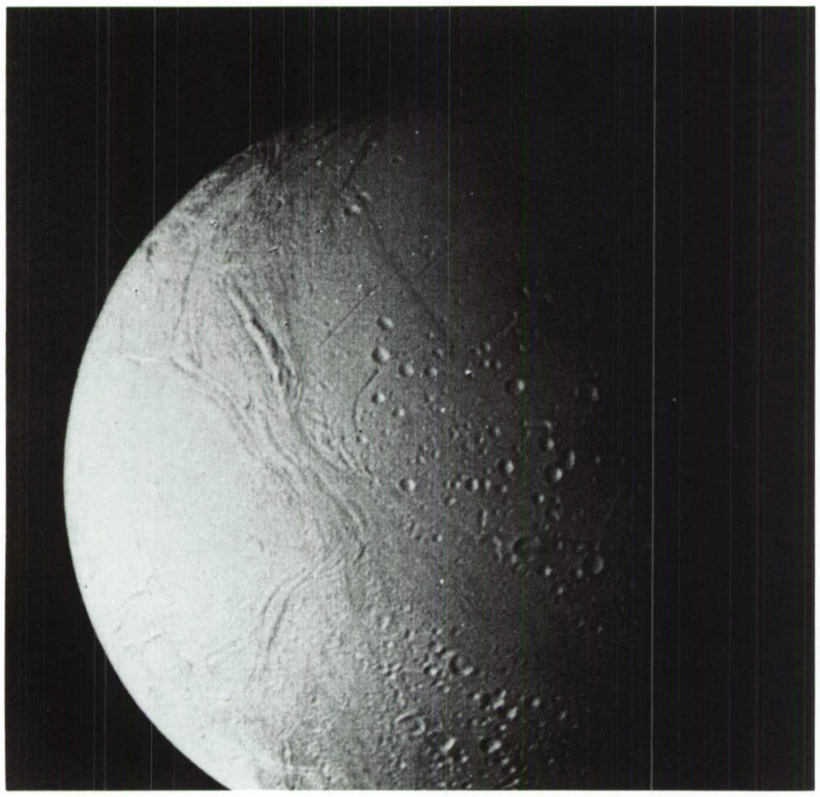

(a)

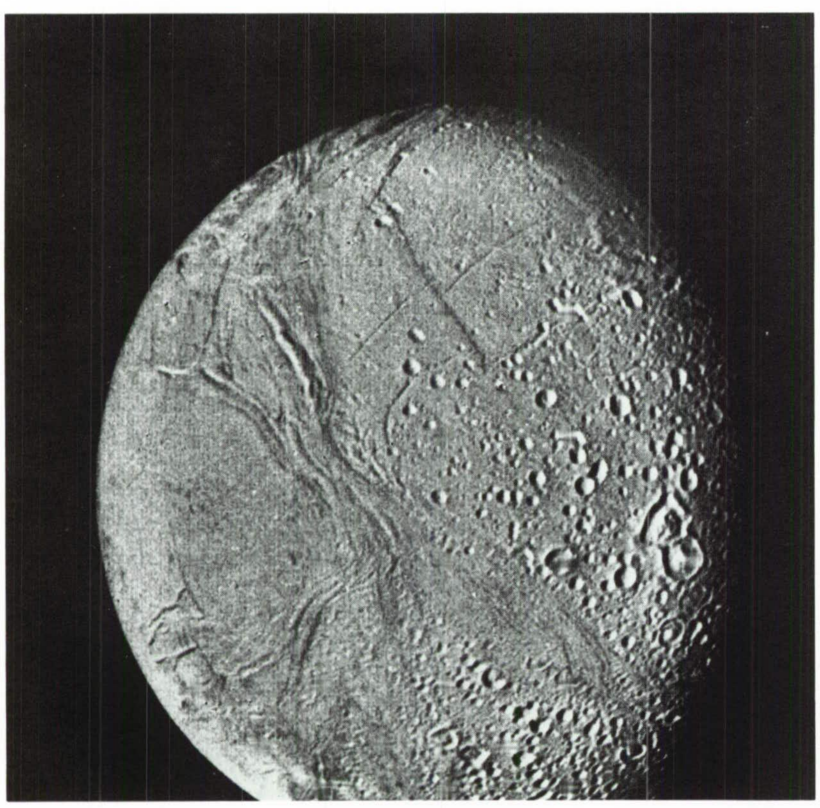

(b)

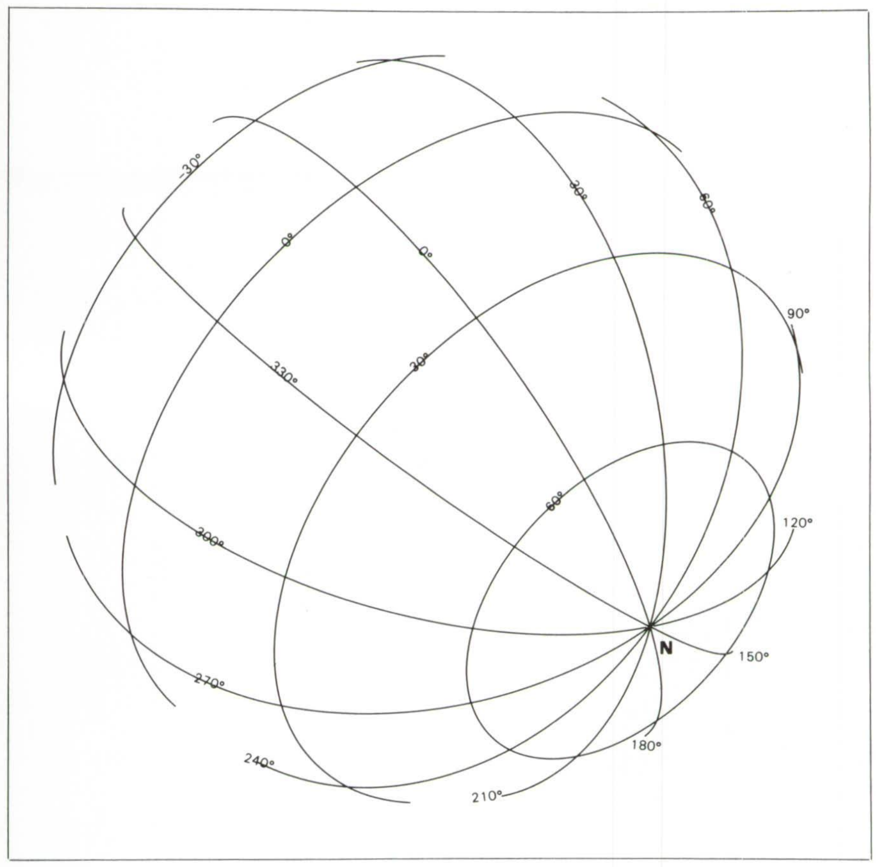

(c)

Picno	1731S2–001
FDS	44004.28
Range, km	111 827
Subspacecraft latitude/longitude, degrees	38/340
Subsolar latitude/longitude, degrees	8/308
Resolution, km/pixel	1
Filter size, pixels	95 × 95
Filter size, km	98
Scale	1:5 000 000

Figure 2–22. Picno 1731S2–001. (*a*) Unfiltered image. (*b*) High-pass filtered image. (*c*) Perspective grid.

(a)

(b)

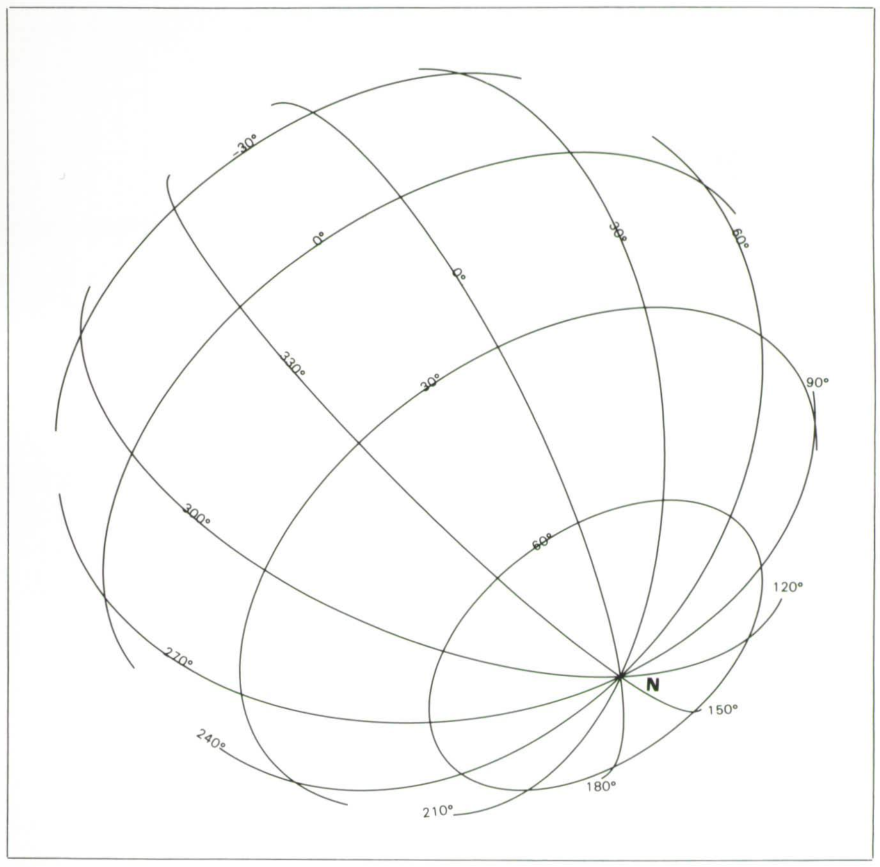

(c)

Picno	1735S2–001
FDS	44004.32
Range, km	110 109
Subspacecraft latitude/longitude, degrees	37/341
Subsolar latitude/longitude, degrees	8/309
Resolution, km/pixel	1
Filter size, pixels	95 × 95
Filter size, km	97
Scale	1:5 000 000

Figure 2–23. Picno 1735S2–001. (*a*) Unfiltered image. (*b*) High-pass filtered image. (*c*) Perspective grid.

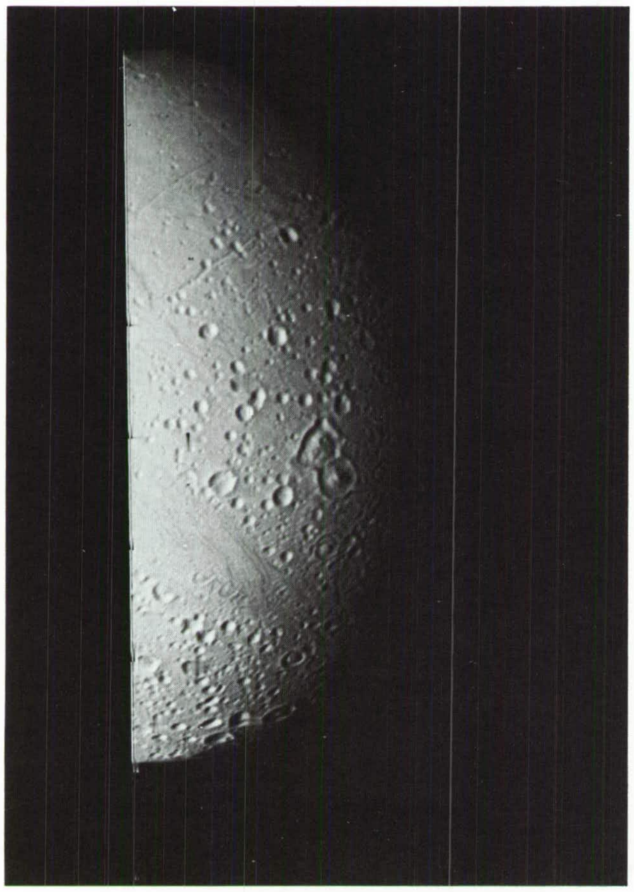

(a)

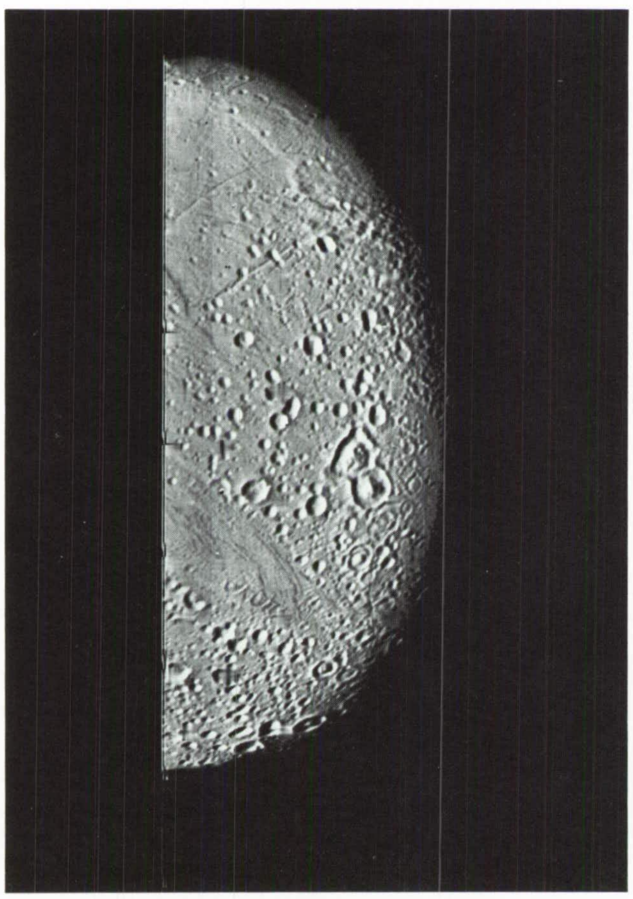

(b)

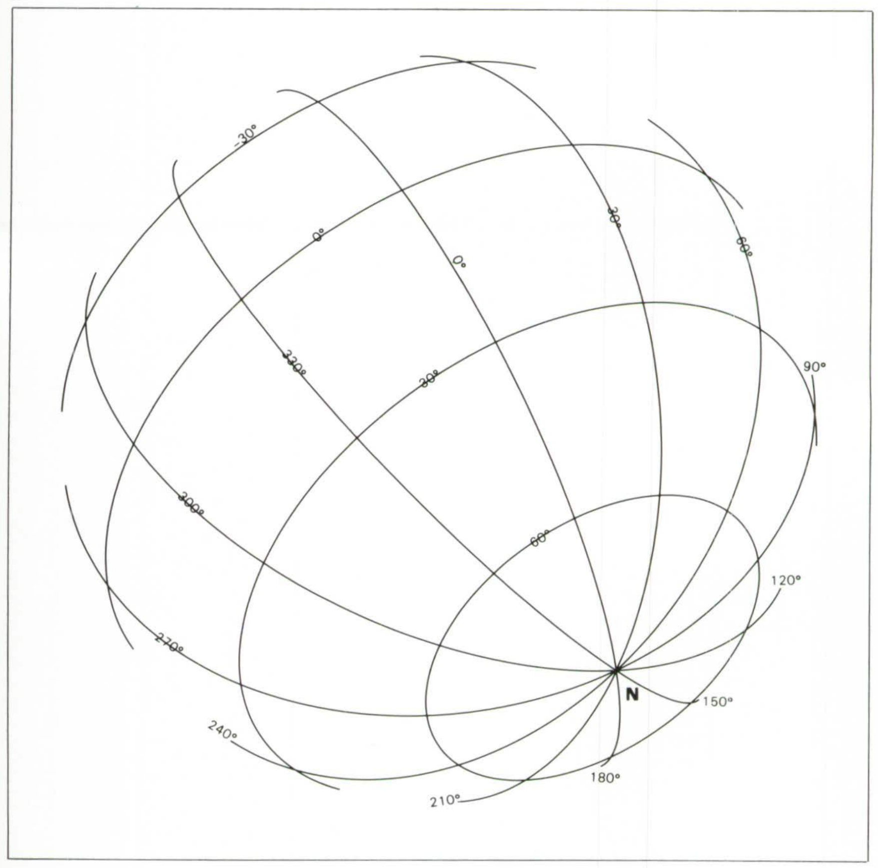

(c)

Picno	1739S2−001
FDS	44004.36
Range, km	108 421
Subspacecraft latitude/longitude, degrees	37/343
Subsolar latitude/longitude, degrees	8/309
Resolution, km/pixel	1
Filter size, pixels	69 × 69
Filter size, km	69
Scale	1:5 000 000

Figure 2–24. Picno 1739S2−001. (*a*) Unfiltered image. (*b*) High-pass filtered image. (*c*) Perspective grid.

PAGE MISSING FROM AVAILABLE VERSION

PART 3

Tethys

Diameter	1048 km (651 miles)
Density	1.0
Albedo	0.8
Distance from Saturn	296 563 km (184 275 miles)
Orbital period	45 hr, 45 min, 43 sec
Voyager 1 closest approach	415 670 km (258 285 miles)
Voyager 1 pictures used in mapping	6
Voyager 2 closest approach	93 000 km (57 787 miles)
Voyager 2 pictures used in mapping	10

The most distinctive feature visible in Voyager pictures of Tethys is a very large valley 50 to 100 km wide that extends nearly two-thirds of the way around the satellite. A huge crater is also visible at 30° N latitude and 130° W longitude. This crater is about 500 km in diameter (about half the diameter of Tethys).

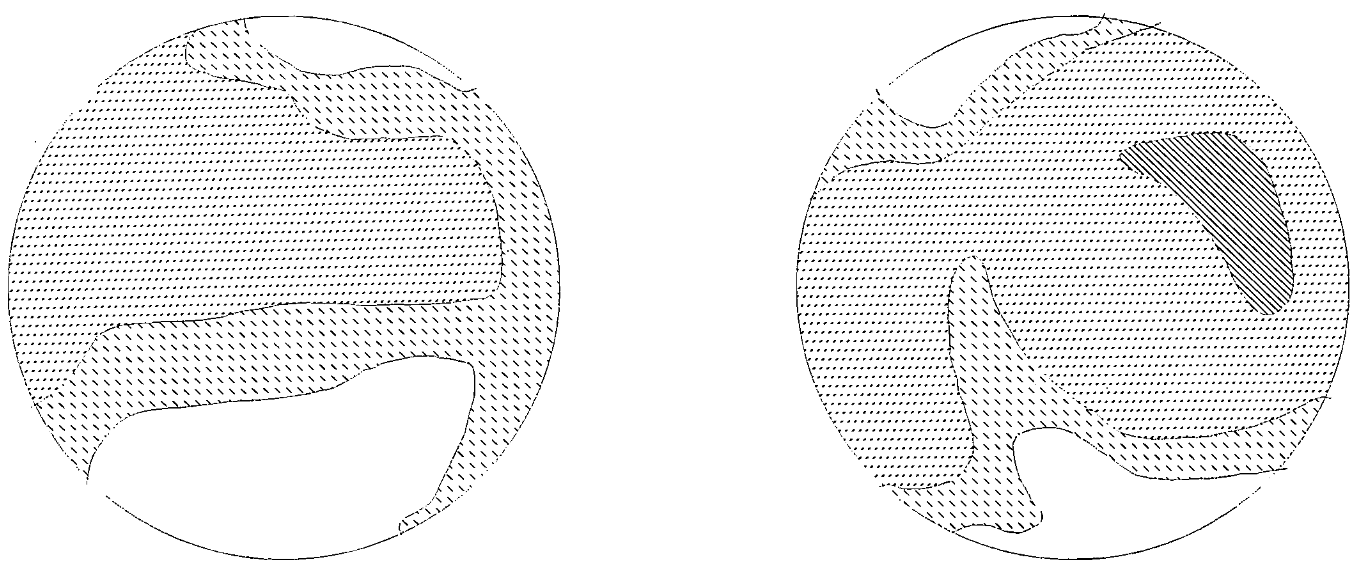

Resolution, km/pixel	Area, km²	Percent of total
0.5 to 2	—	—
2 to 5	116 000	3.3
5 to 20	1 888 000	53.5
20 to 40	854 000	24.2
>40	671 000	19.0

Figure 3–1. Resolution of Voyager pictures of Tethys in terms of aerial coverage.

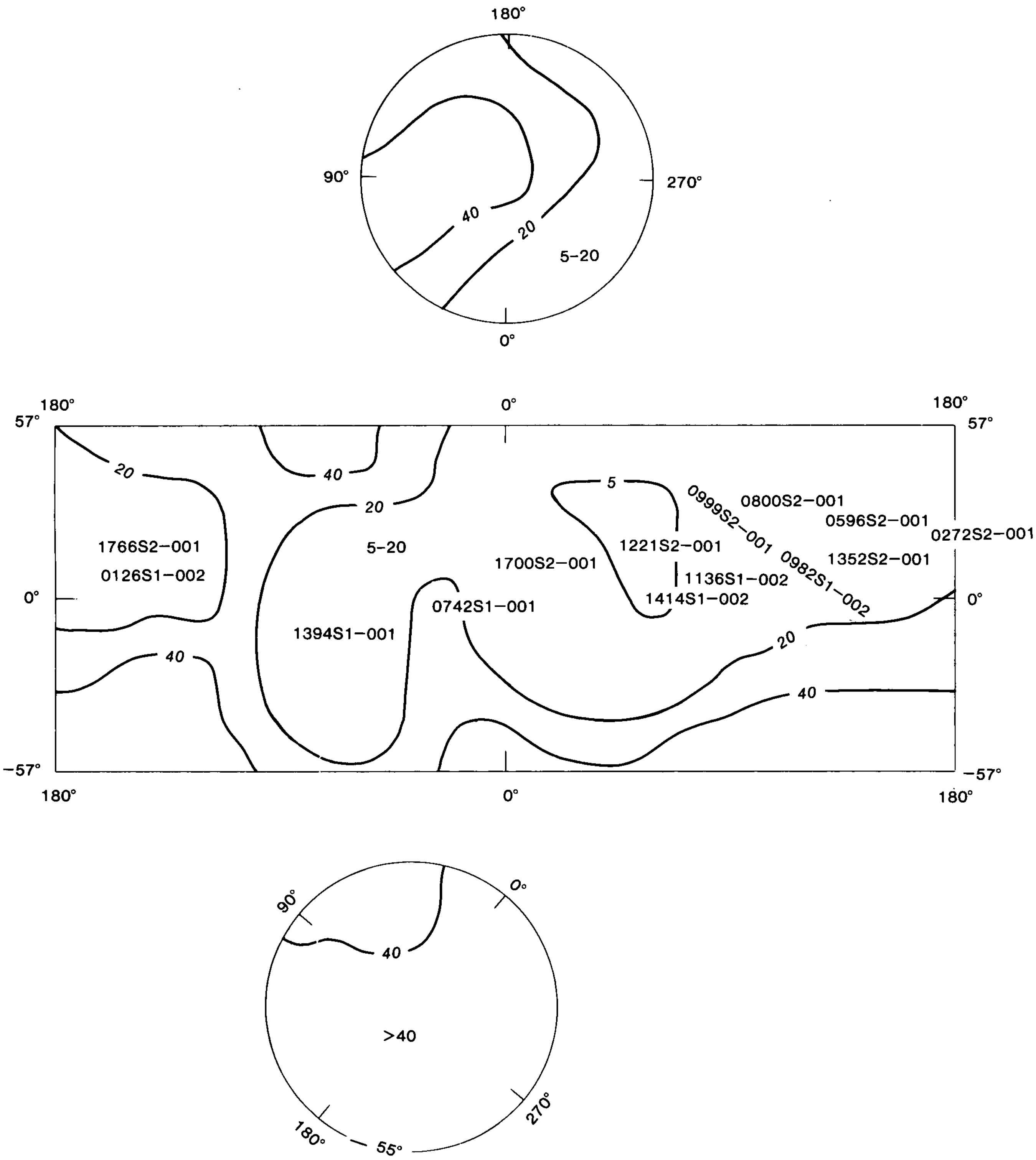

Figure 3–2. Index of Voyager 1 and 2 pictures used to compile the maps of Tethys. Picture numbers indicate the subspacecraft point at the time the pictures were taken. Contour lines indicate the approximate resolution of available images in kilometers per picture element. (See also fig. 3–1.)

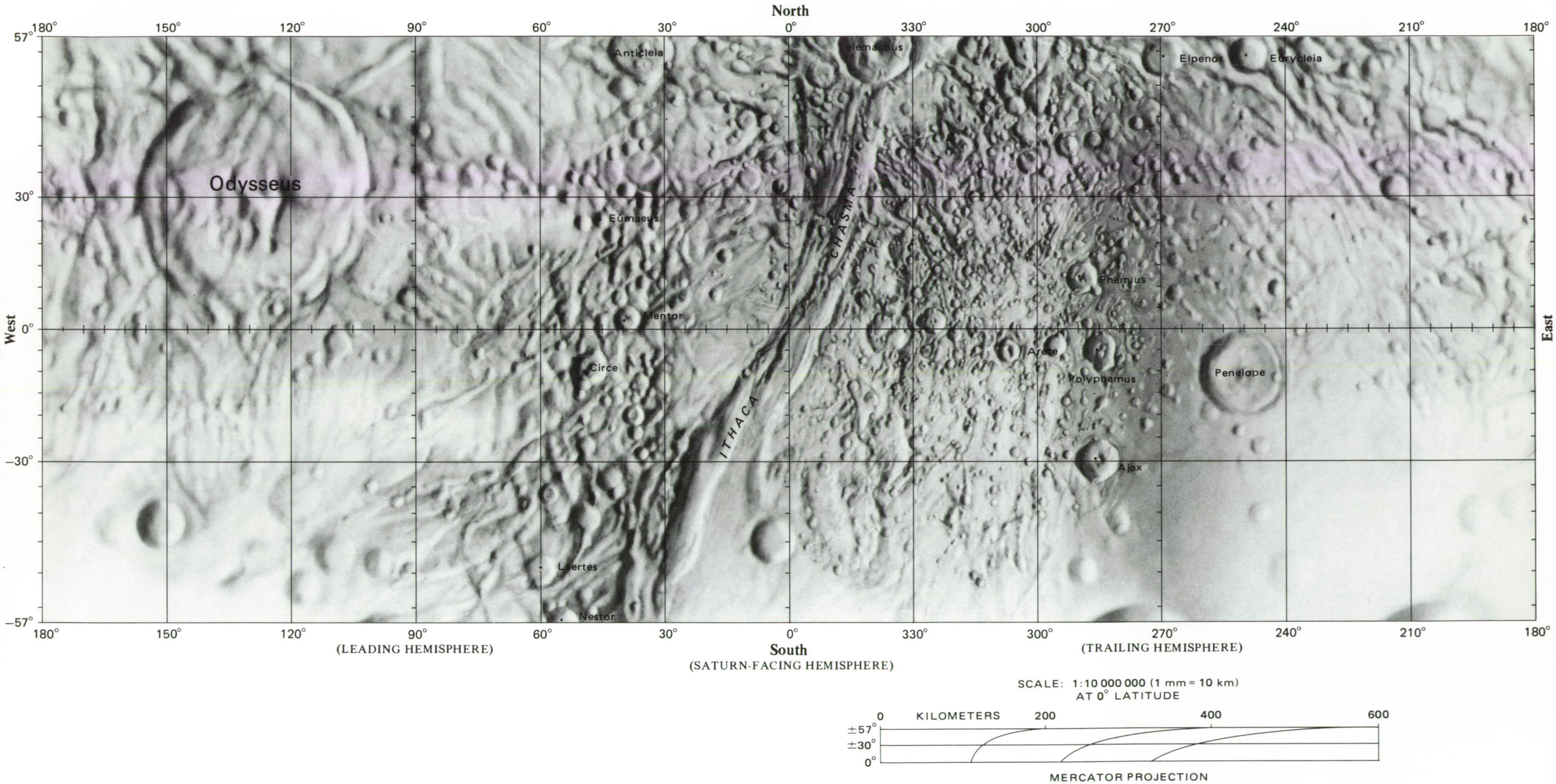

Figure 3–3. Map of the equatorial region of Tethys on a Mercator projection (part of map I–1487).

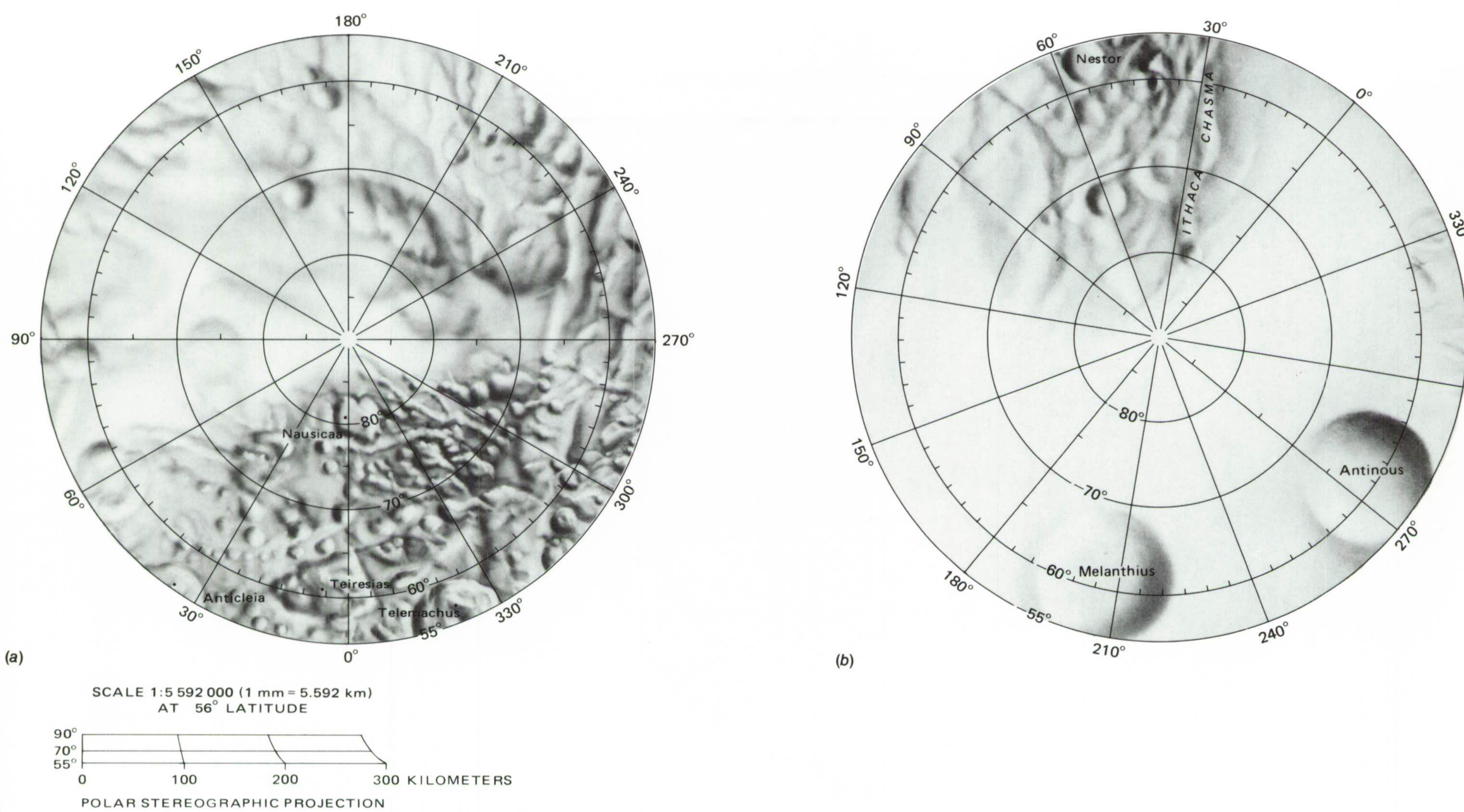

Figure 3–4. Maps of the polar regions of Tethys on polar stereographic projections (part of map I–1487). (*a*) North polar region. (*b*) South polar region.

Figure 3–5. Maps of Tethys on Lambert azimuthal equal-area projections. Nomenclature is not shown, to avoid obscuring detail. Scale 1:10 000 000 (1 $mm^2 = 100$ km^2; 1 $in^2 =$ ~25 000 mi^2). (*a*) Anti-Saturn-facing hemisphere. (*b*) Saturn-facing hemisphere.

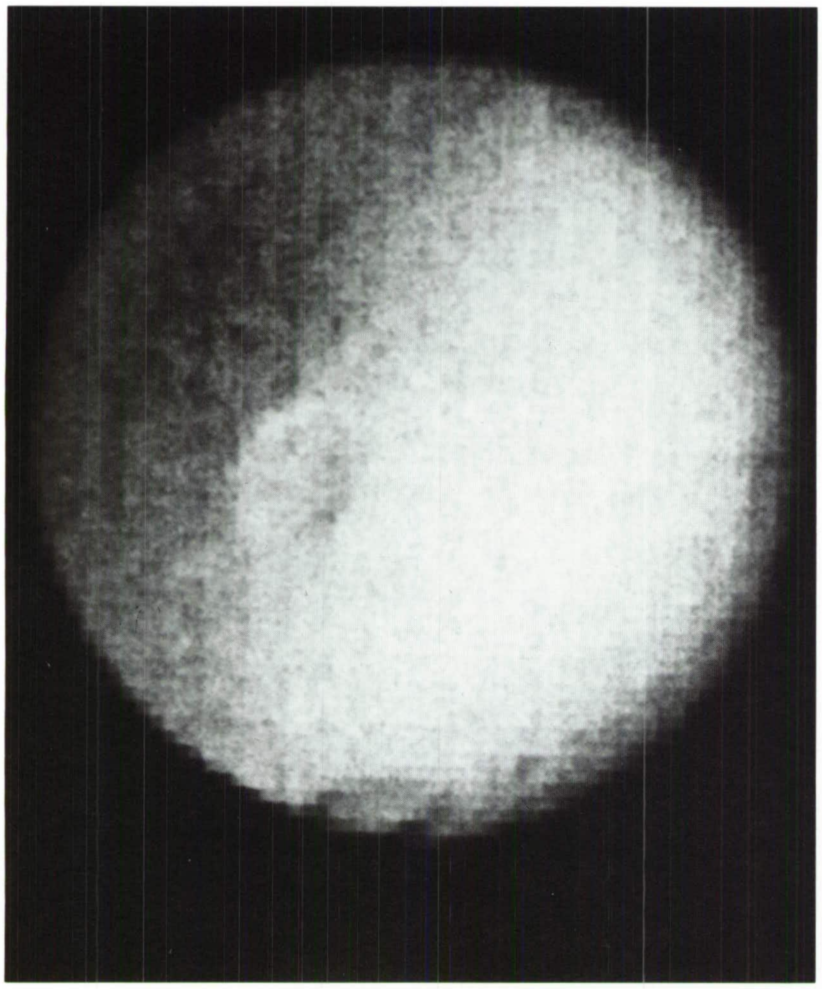

(a)

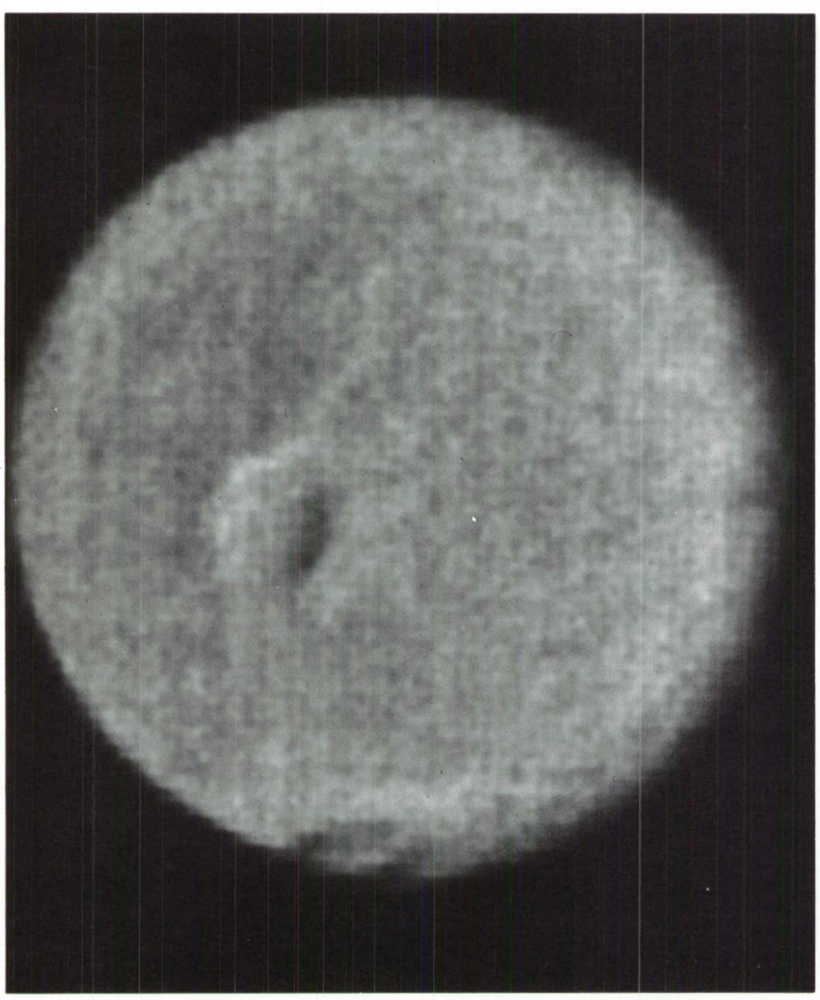

(b)

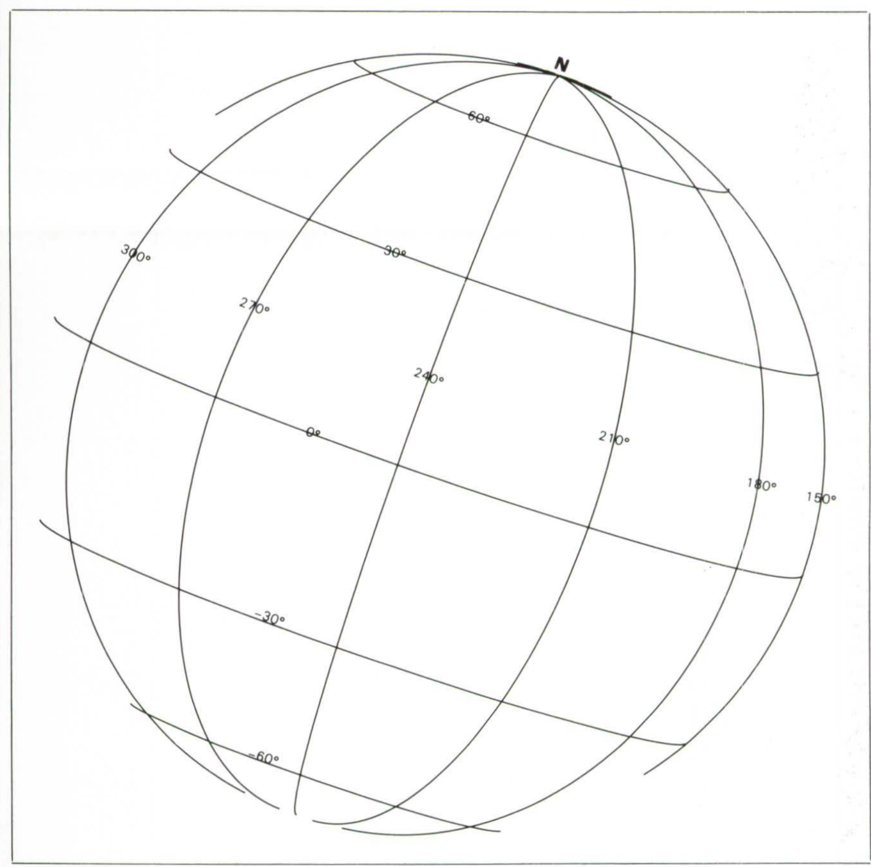

(c)

Picno	1002S1−002
FDS	34900.38
Range, km	1 993 641
Subspacecraft latitude/longitude, degrees	4/237
Subsolar latitude/longitude, degrees	4/248
Resolution, km/pixel	18
Filter size, pixels	13 × 13
Filter size, km	239
Scale	1:10 000 000

Figure 3–6. Picno 1002S1−002. (*a*) Unfiltered image. (*b*) High-pass filtered image. (*c*) Perspective grid.

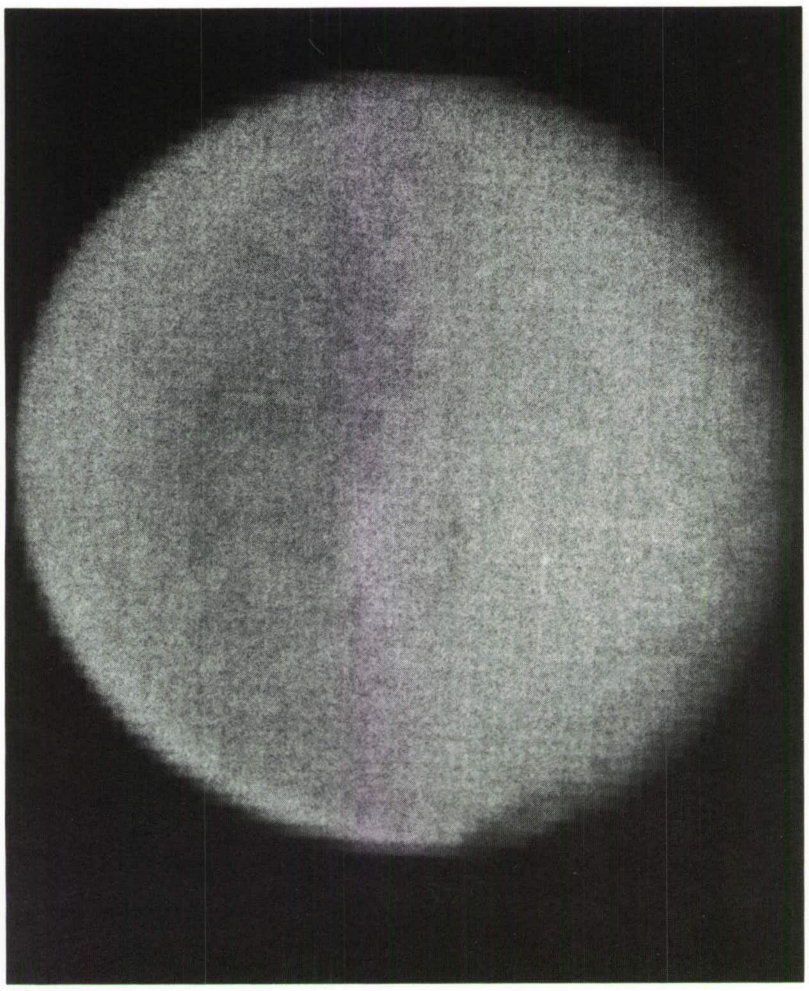

(a)

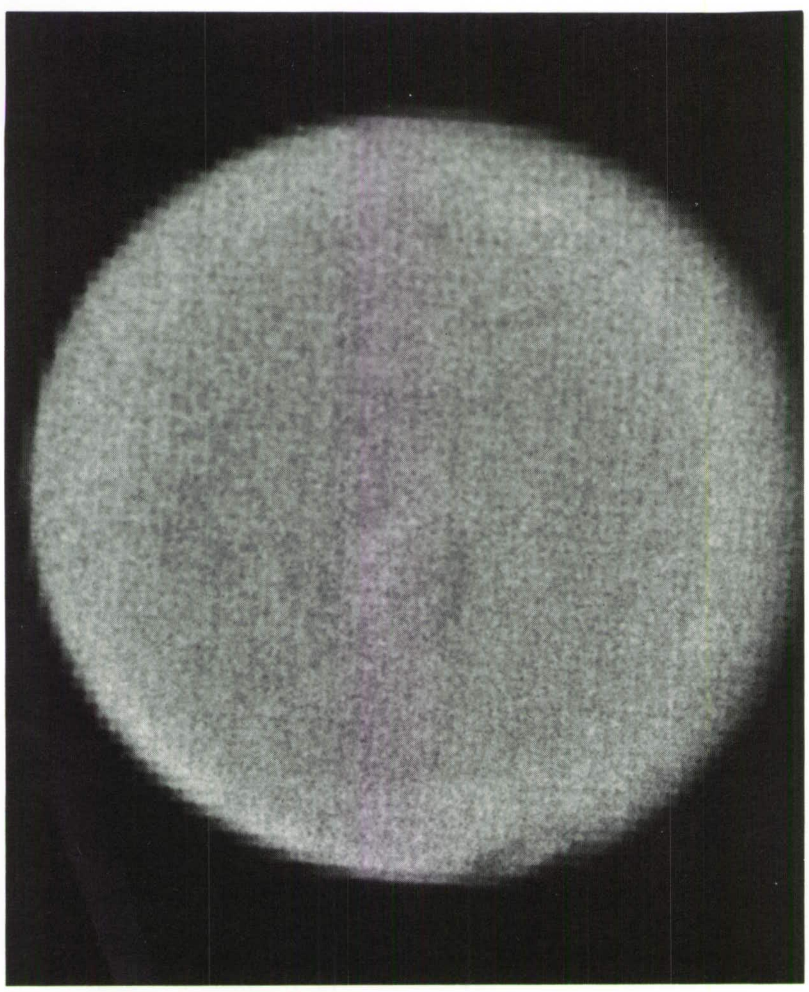

(b)

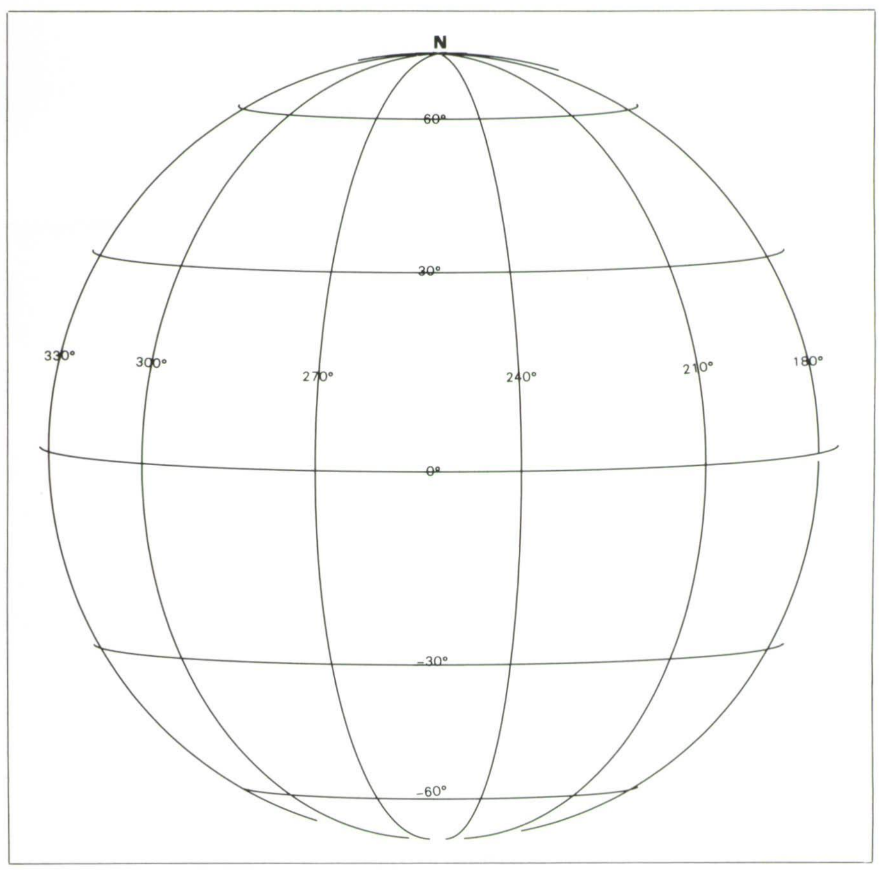

(c)

Picno	1136S1−002
FDS	34902.52
Range, km	1 953 077
Subspacecraft latitude/longitude, degrees	4/252
Subsolar latitude/longitude, degrees	4/262
Resolution, km/pixel	18
Filter size, pixels	15 × 15
Filter size, km	271
Scale	1:10 000 000

Figure 3–7. Picno 1136S1−002. (*a*) Unfiltered image. (*b*) High-pass filtered image. (*c*) Perspective grid.

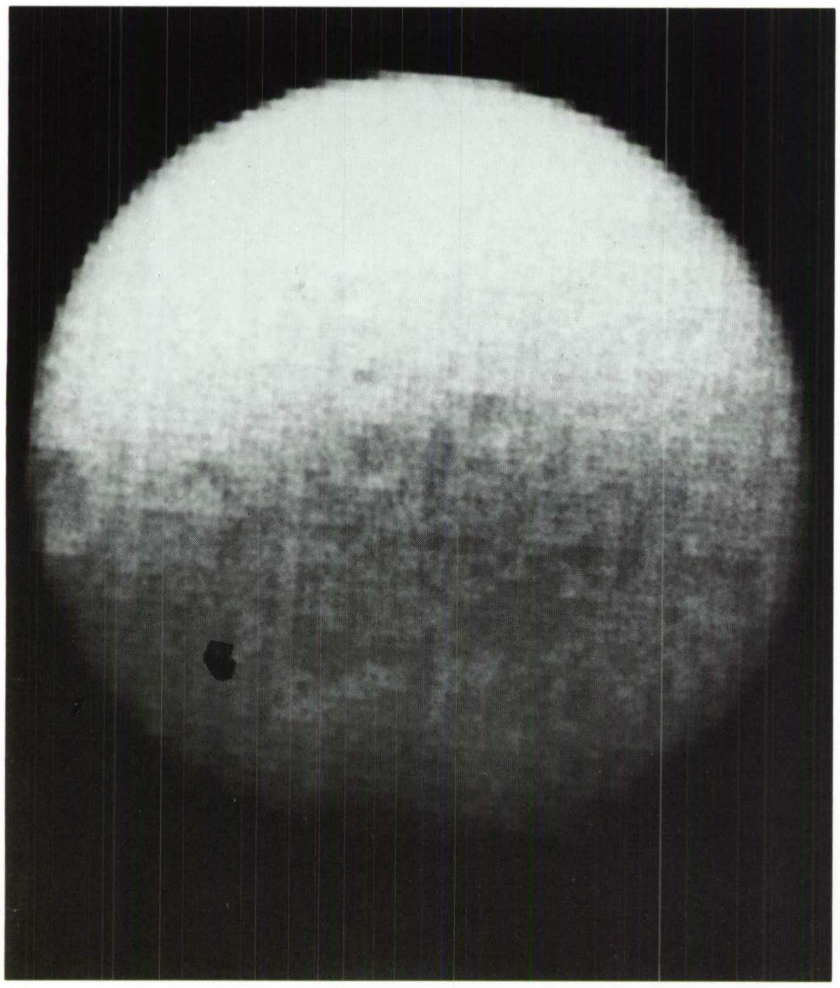

(a)

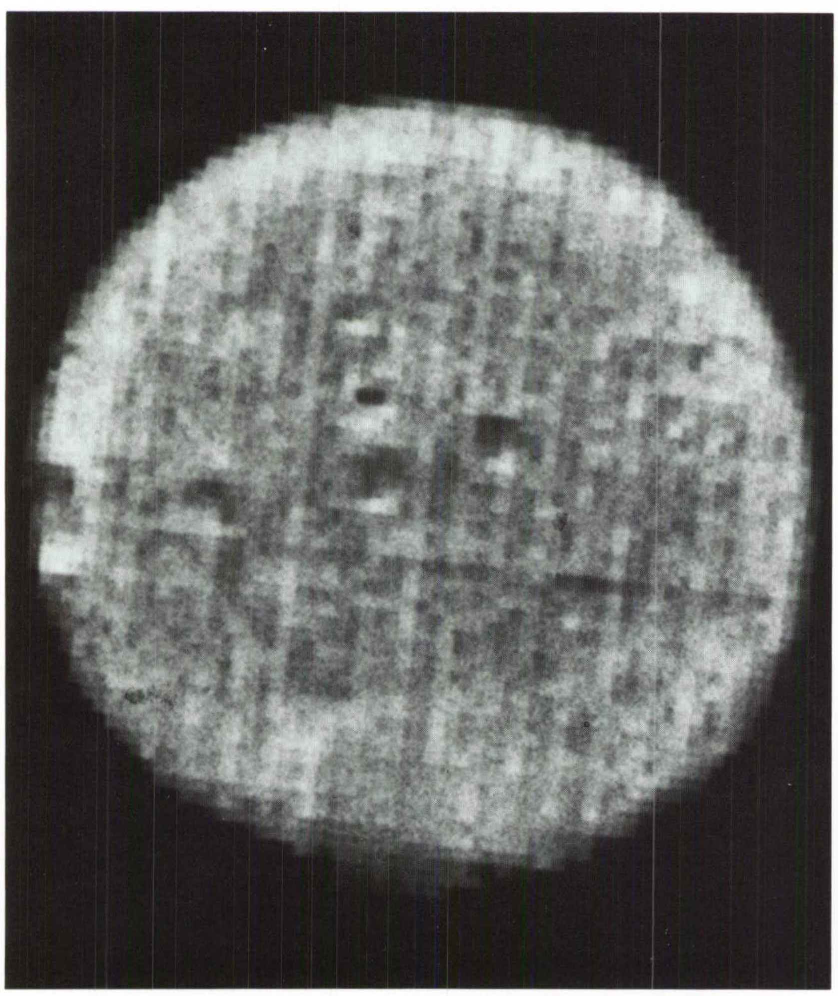

(b)

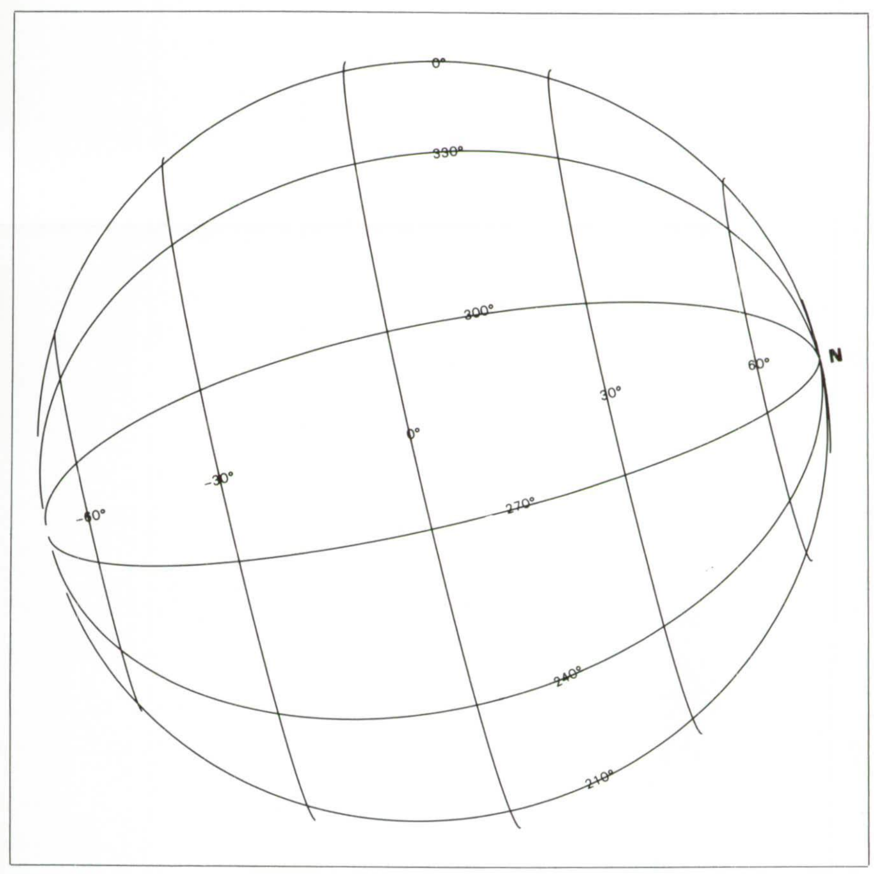

(c)

Picno	1414S1–002
FDS	34907.30
Range, km	1 884 331
Subspacecraft latitude/longitude, degrees	3/282
Subsolar latitude/longitude, degrees	4/292
Resolution, km/pixel	17
Filter size, pixels	11 × 11
Filter size, km	191
Scale	1:10 000 000

Figure 3–8. Picno 1414S1–002. (*a*) Unfiltered image. (*b*) High-pass filtered image. (*c*) Perspective grid.

(a)

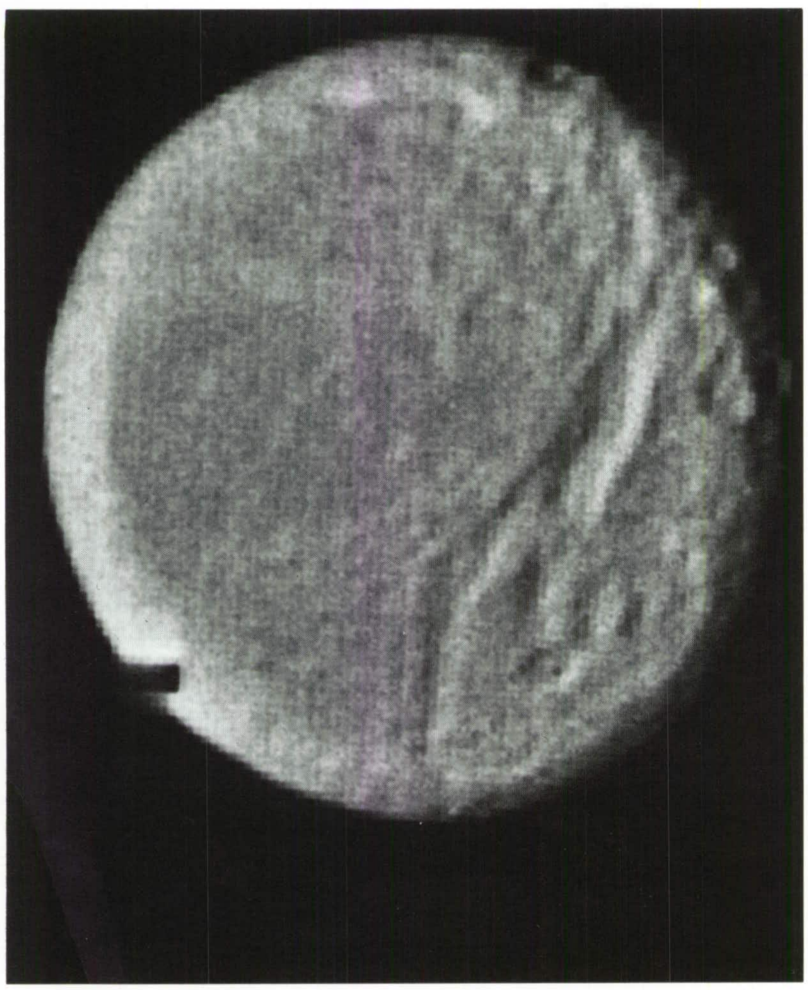

(b)

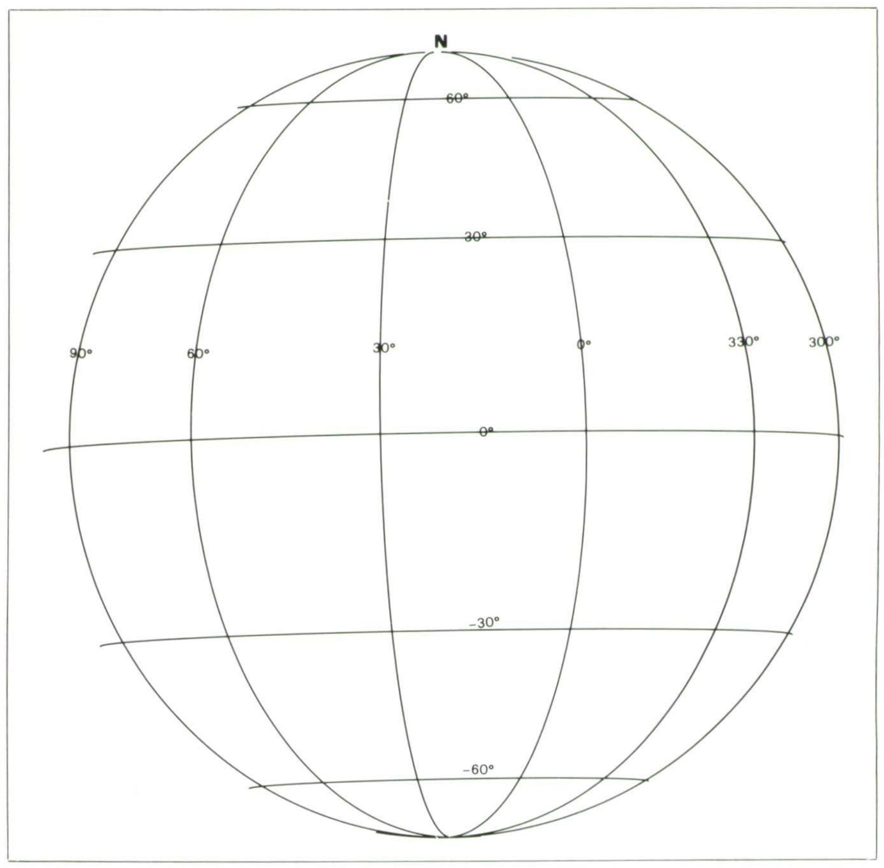

(c)

Picno	0742S1−001
FDS	34926.18
Range, km	1 241 268
Subspacecraft latitude/longitude, degrees	−1/21
Subsolar latitude/longitude, degrees	4/51
Resolution, km/pixel	11
Filter size, pixels	17 × 17
Filter size, km	195
Scale	1:10 000 000

Figure 3–9. Picno 0742S1−001. (*a*) Unfiltered image. (*b*) High-pass filtered image. (*c*) Perspective grid.

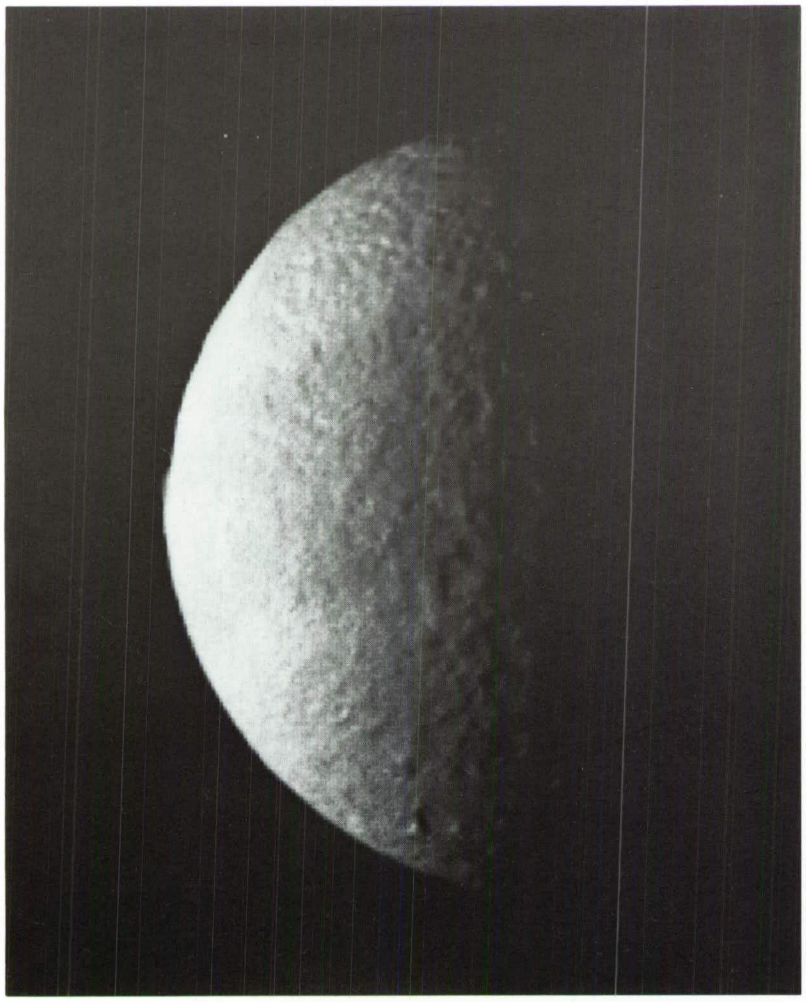

(a)

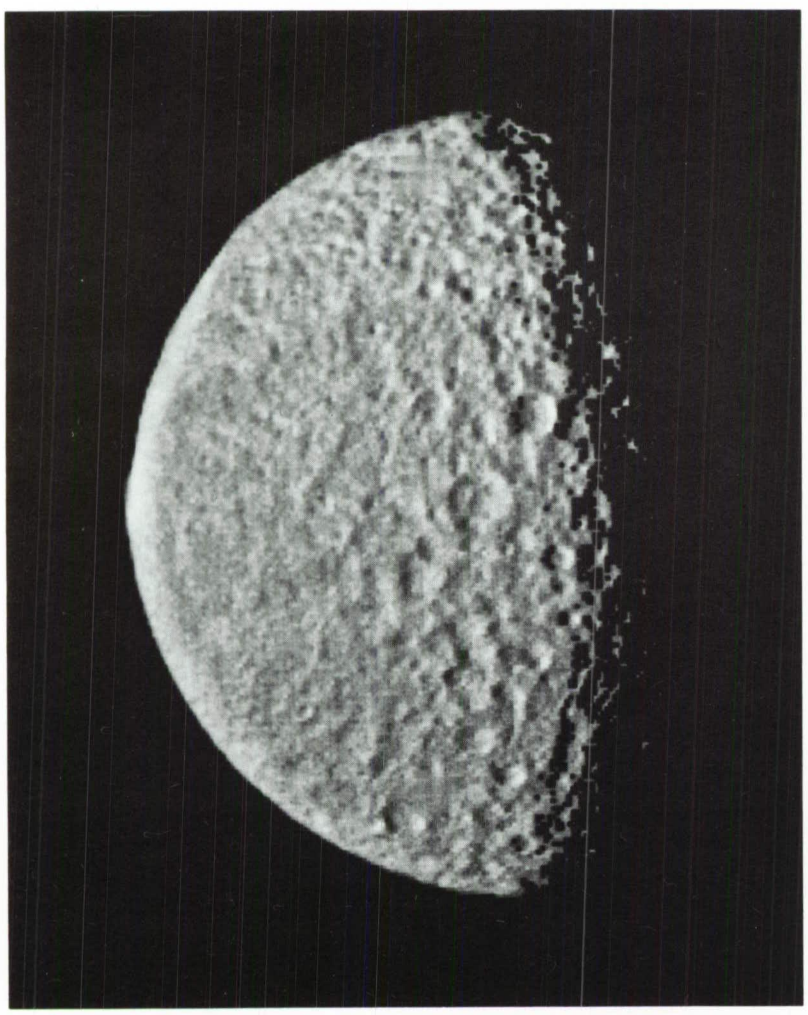

(b)

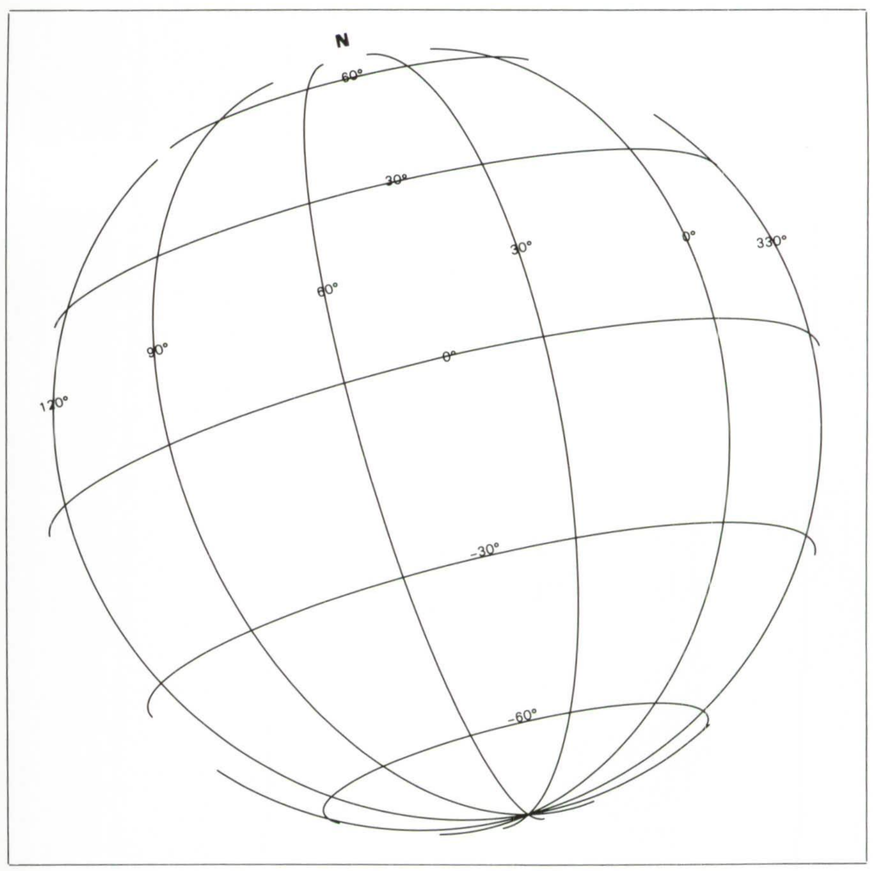

(c)

Picno	1390S1–001
FDS	34937.06
Range, km	576 130
Subspacecraft latitude/longitude, degrees	–11/50
Subsolar latitude/longitude, degrees	4/120
Resolution, km/pixel	5
Filter size, pixels	17 × 17
Filter size, km	90
Scale	1:10 000 000

Figure 3–10. Picno 1390S1–001. (*a*) Unfiltered image. (*b*) High-pass filtered image. (*c*) Perspective grid.

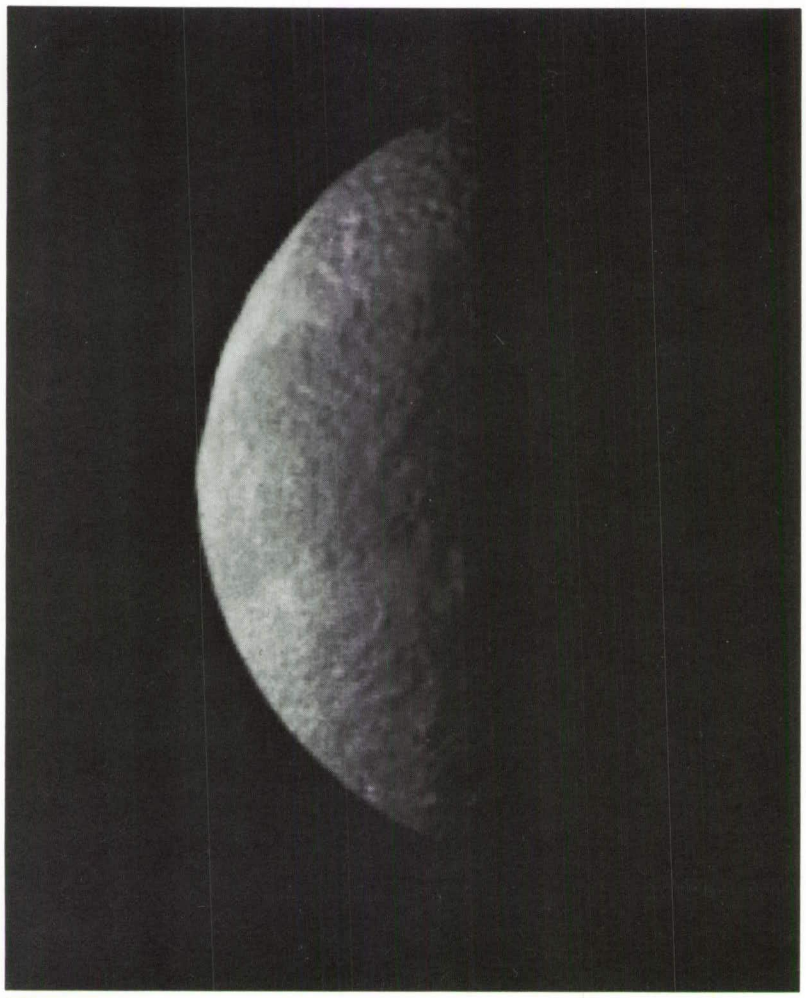
(a)

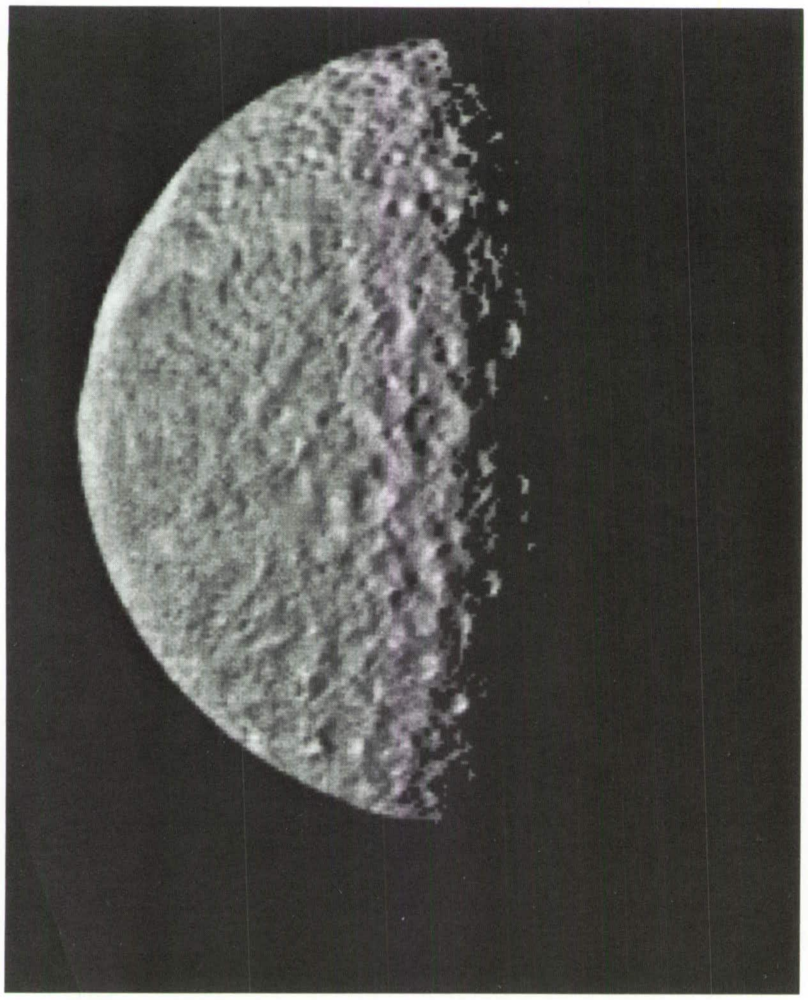
(b)

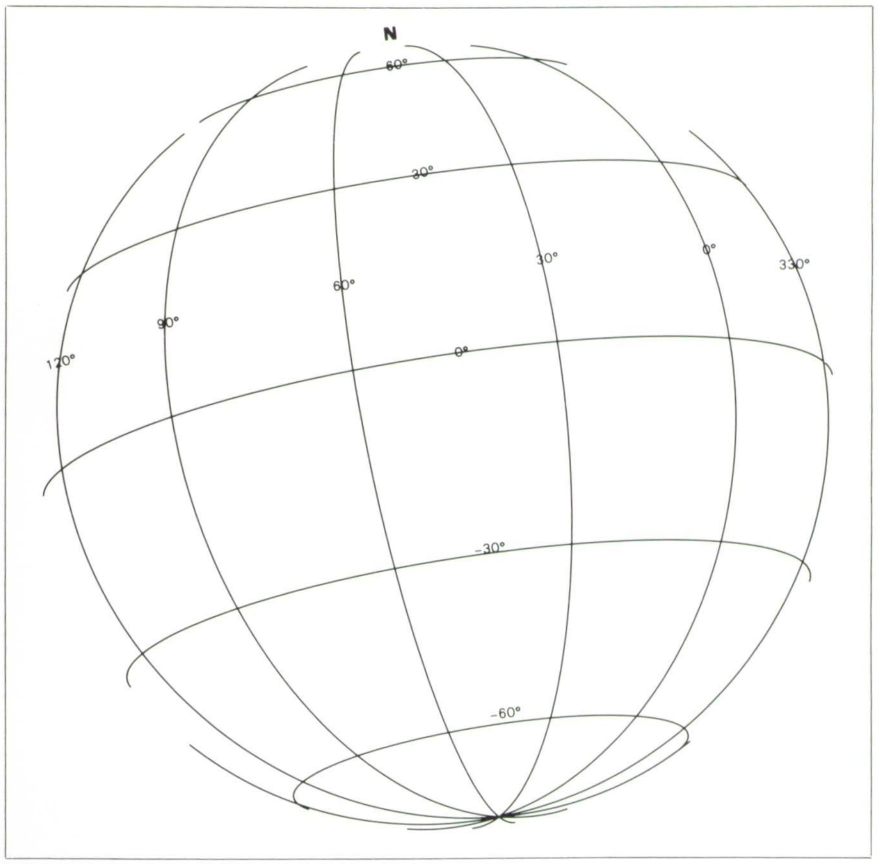

(c)

Picno	1394S1−001
FDS	34937.10
Range, km	572 526
Subspacecraft latitude/longitude, degrees	−12/50
Subsolar latitude/longitude, degrees	4/120
Resolution, km/pixel	5
Filter size, pixels	17 × 17
Filter size, km	90
Scale	1:10 000 000

Figure 3–11. Picno 1394S1−001. (*a*) Unfiltered image. (*b*) High-pass filtered image. (*c*) Perspective grid.

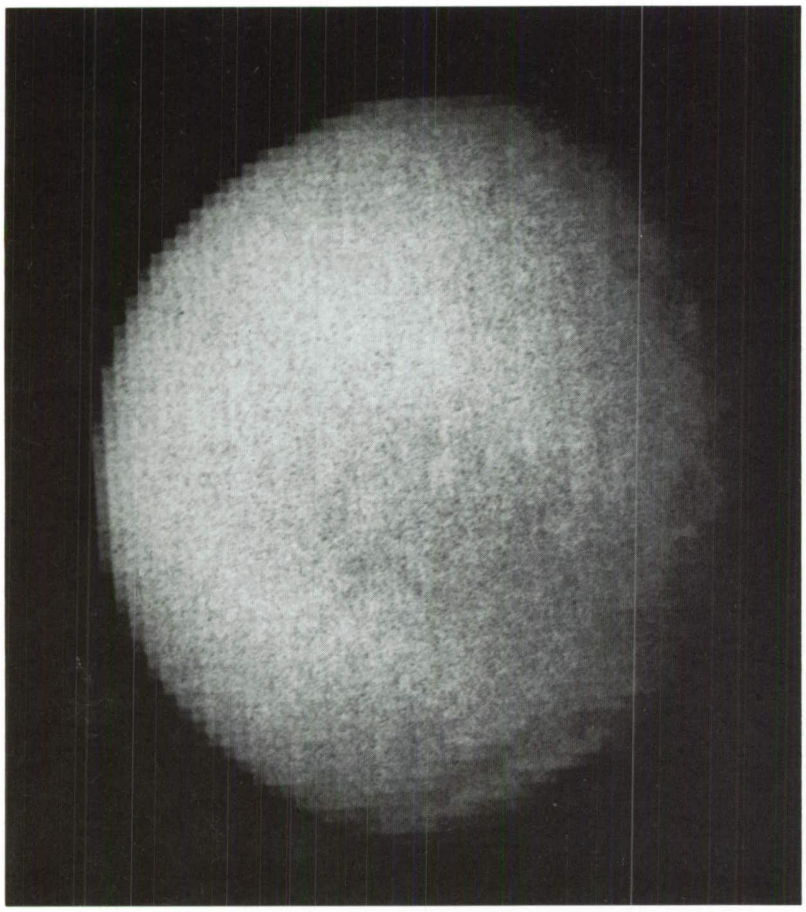

(a)

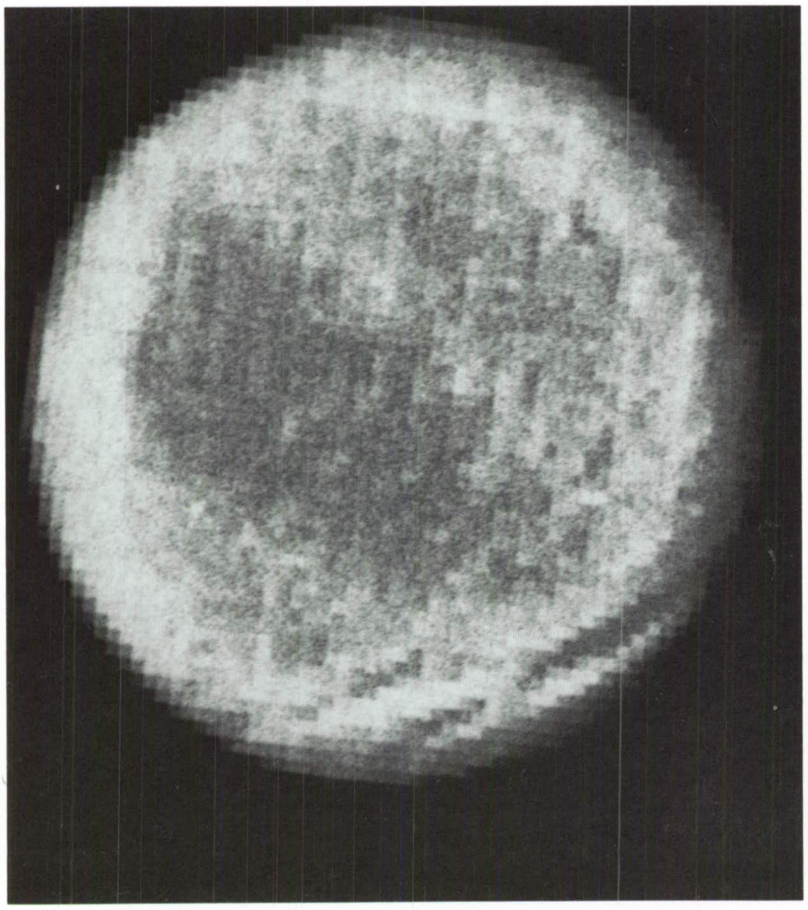

(b)

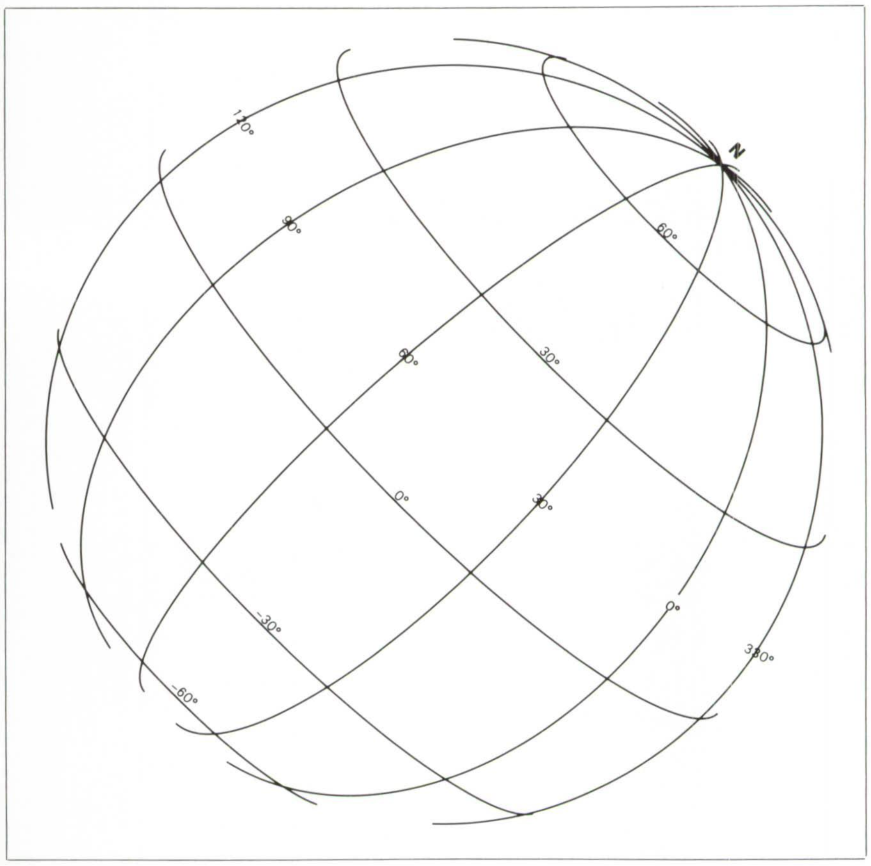

(c)

Picno	0824S2−002
FDS	43959.21
Range, km	2 059 181
Subspacecraft latitude/longitude, degrees	12/48
Subsolar latitude/longitude, degrees	7/69
Resolution, km/pixel	19
Filter size, pixels	15 × 15
Filter size, km	286
Scale	1:10 000 000

Figure 3–12. Picno 0824S2−002. (*a*) Unfiltered image. (*b*) High-pass filtered image. (*c*) Perspective grid.

(a)

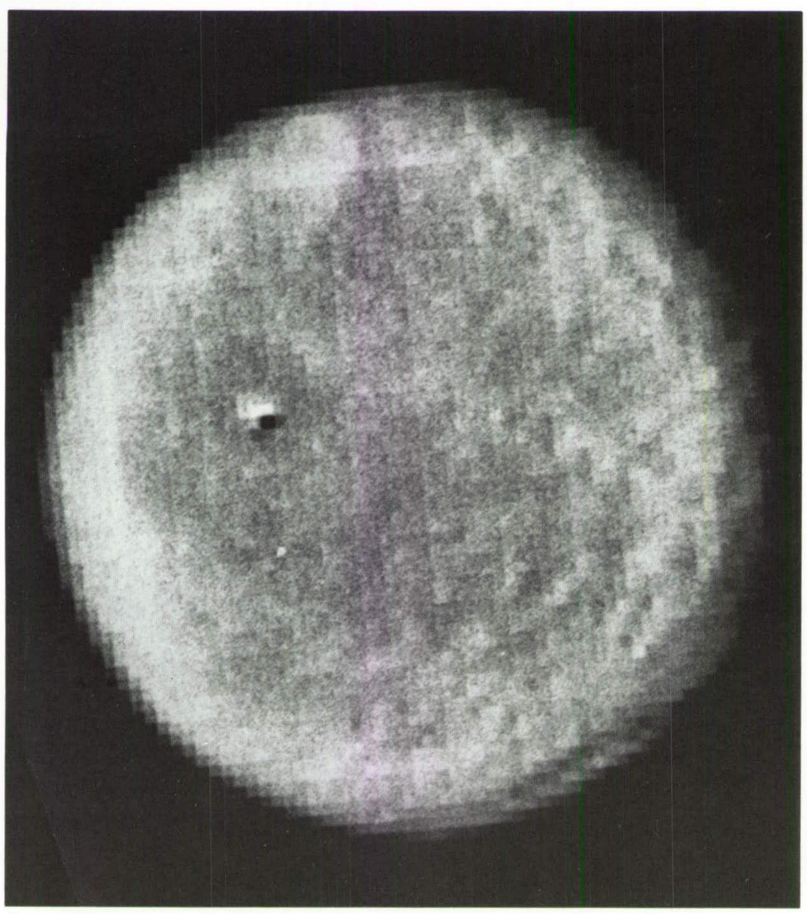

(b)

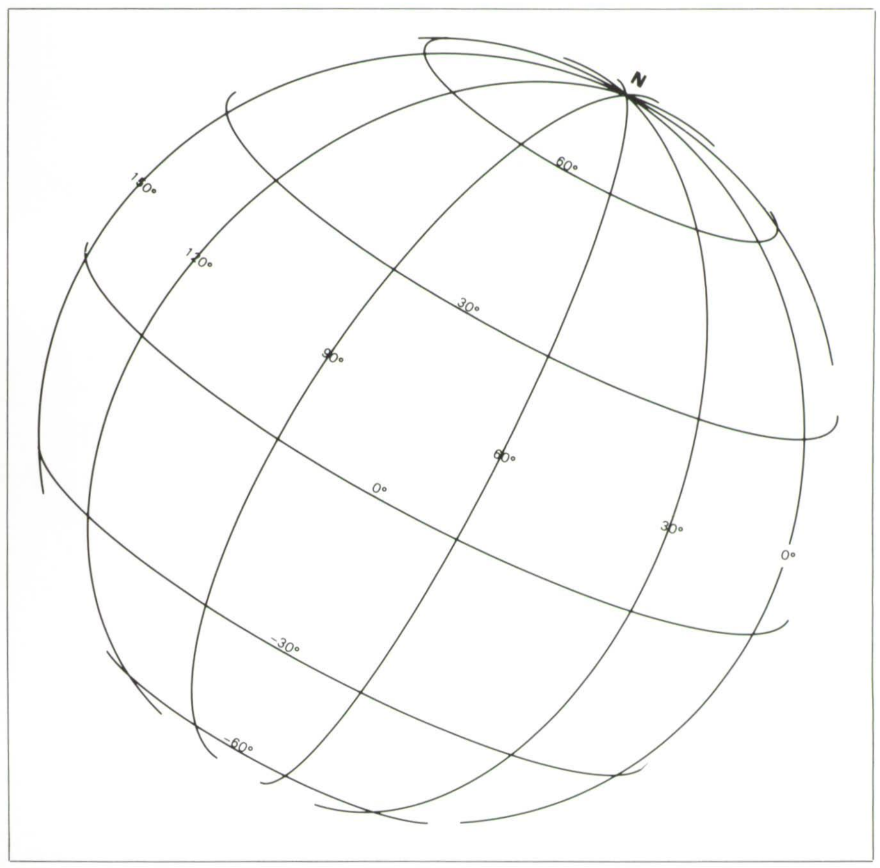

(c)

Picno	1060S2−002
FDS	43963.17
Range, km	1 820 441
Subspacecraft latitude/longitude, degrees	13/70
Subsolar latitude/longitude, degrees	7/94
Resolution, km/pixel	17
Filter size, pixels	15 × 15
Filter size, km	253
Scale	1:10 000 000

Figure 3–13. Picno 1060S2−002. (*a*) Unfiltered image. (*b*) High-pass filtered image. (*c*) Perspective grid.

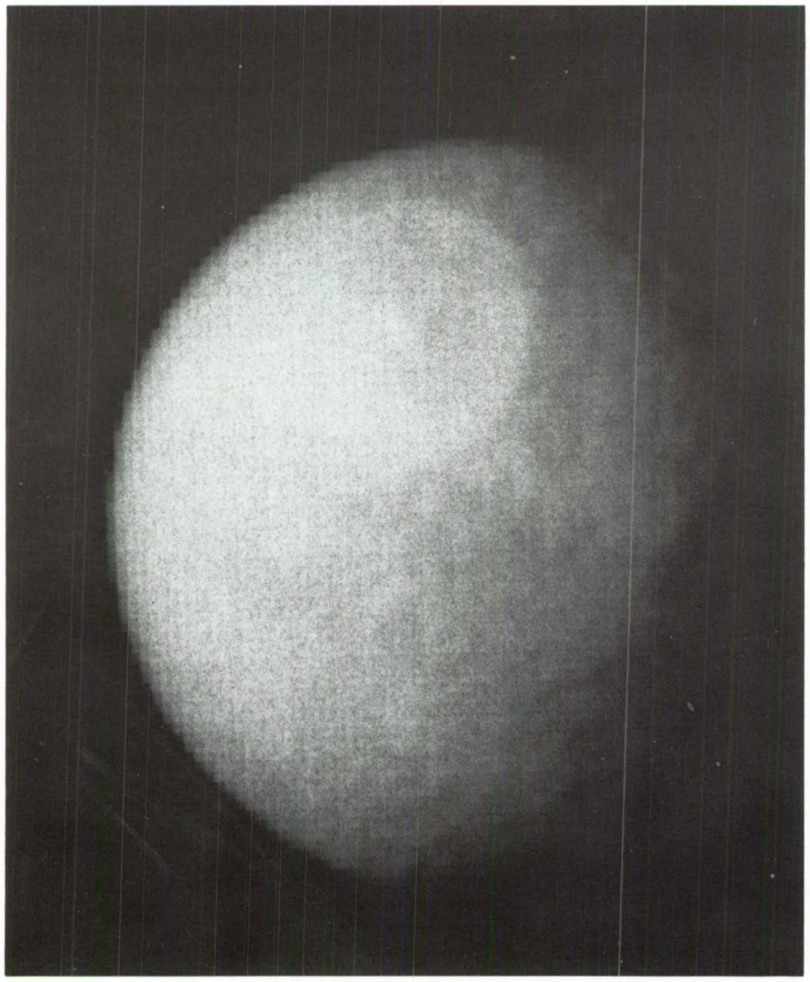

(a)

(b)

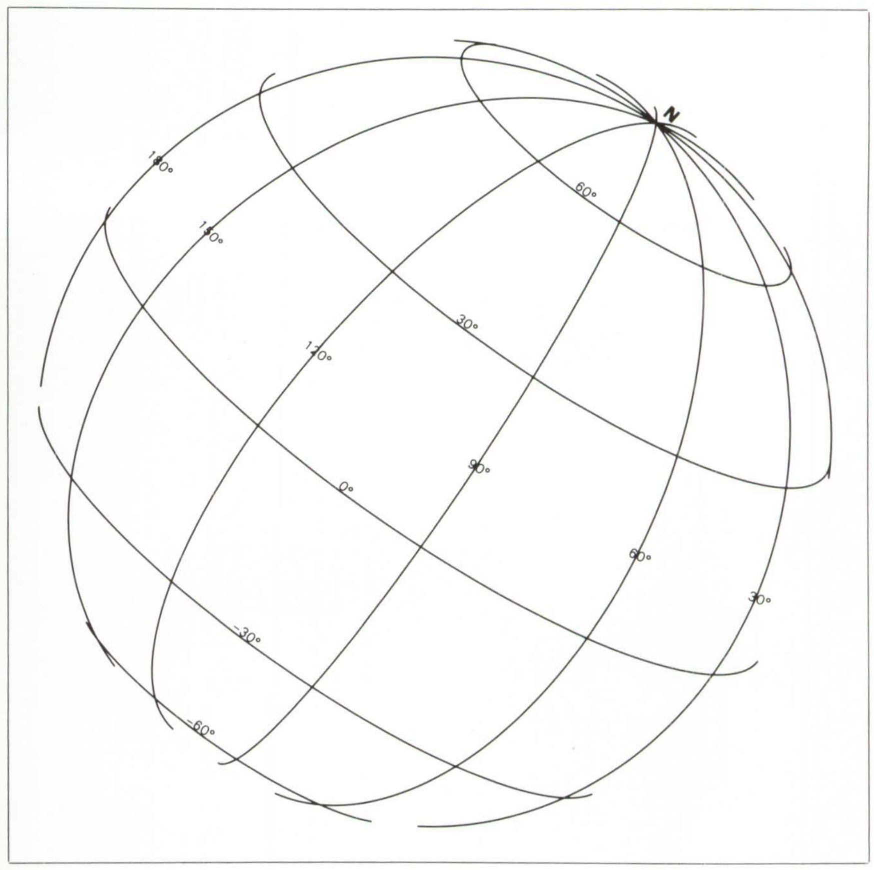

(c)

Picno	1352S2−002
FDS	43968.09
Range, km	1 503 463
Subspacecraft latitude/longitude, degrees	15/98
Subsolar latitude/longitude, degrees	7/125
Resolution, km/pixel	14
Filter size, pixels	25 × 25
Filter size, km	348
Scale	1:10 000 000

Figure 3–14. Picno 1352S2−002. (*a*) Unfiltered image. (*b*) High-pass filtered image. (*c*) Perspective grid.

(a)

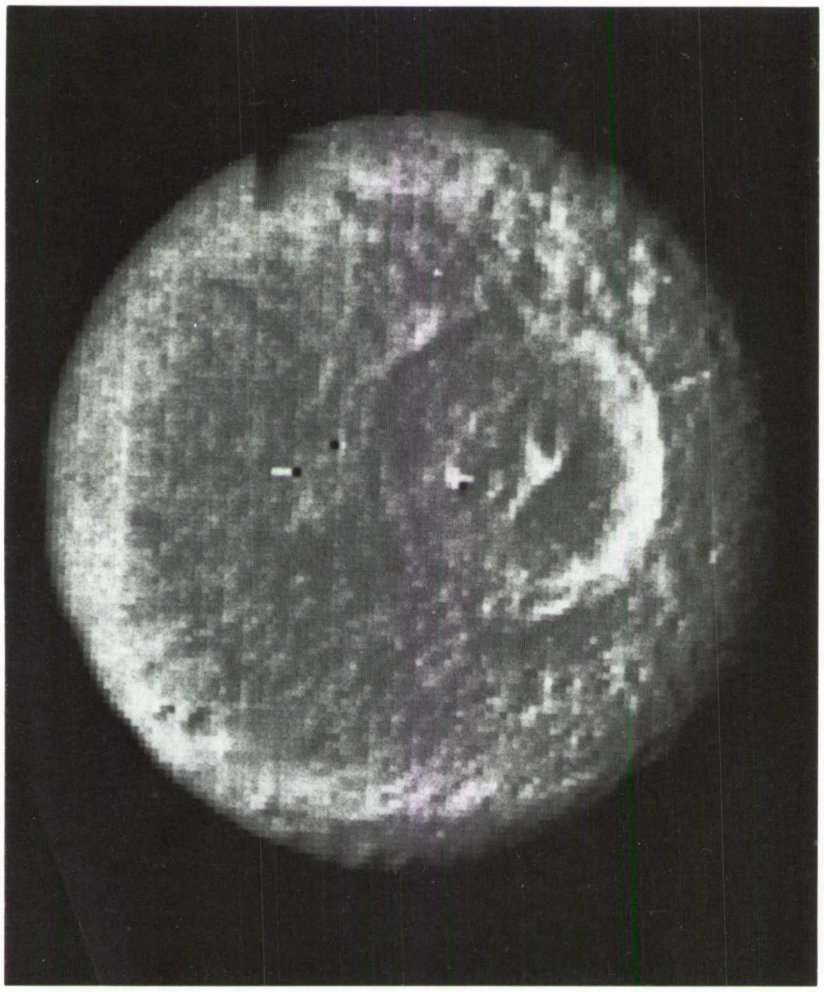

(b)

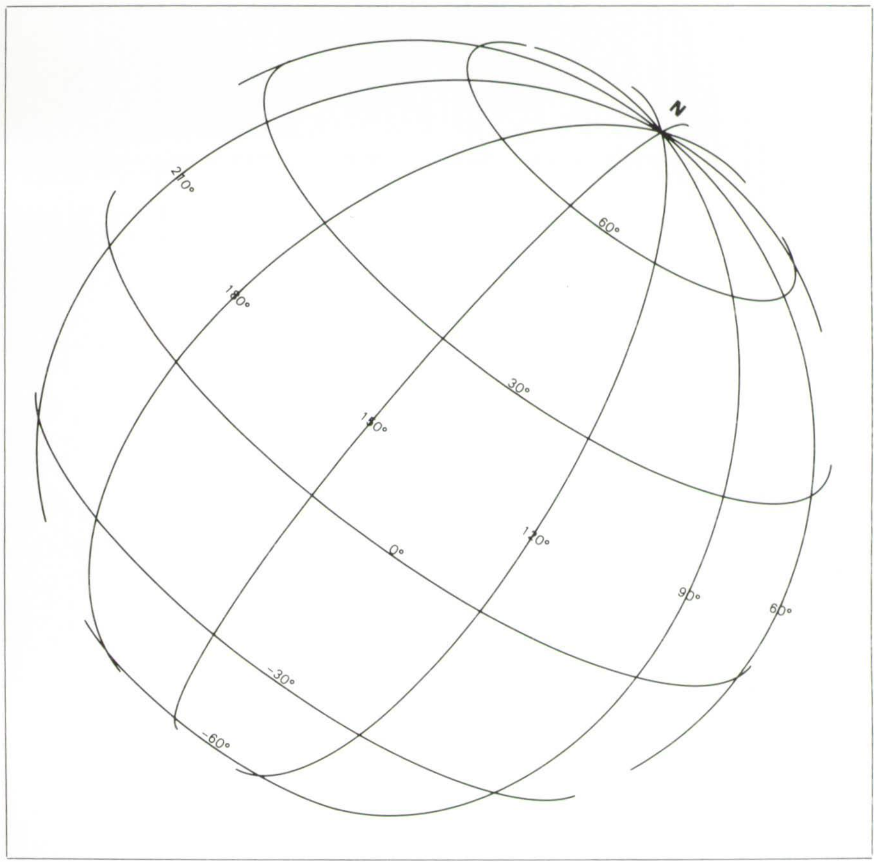

(c)

Picno	1770S2−002
FDS	43975.07
Range, km	1 073 890
Subspacecraft latitude/longitude, degrees	19/142
Subsolar latitude/longitude, degrees	7/169
Resolution, km/pixel	10
Filter size, pixels	25 × 25
Filter size, km	248
Scale	1:10 000 000

Figure 3–15. Picno 1770S2−002. (*a*) Unfiltered image. (*b*) High-pass filtered image. (*c*) Perspective grid.

(a)

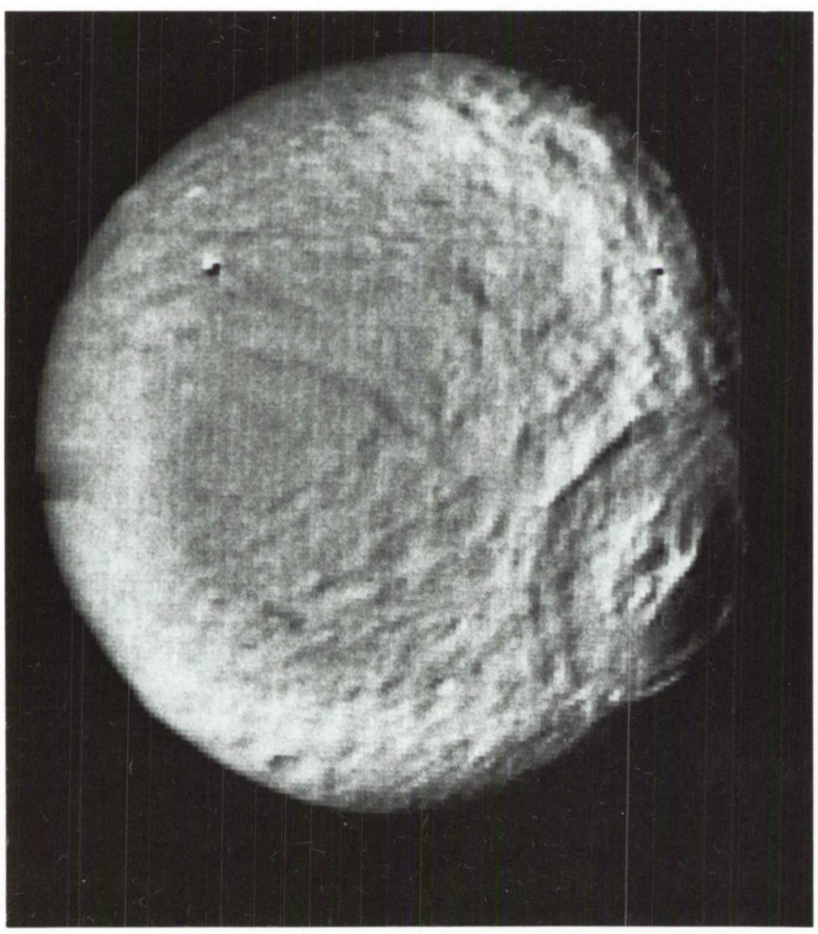

(b)

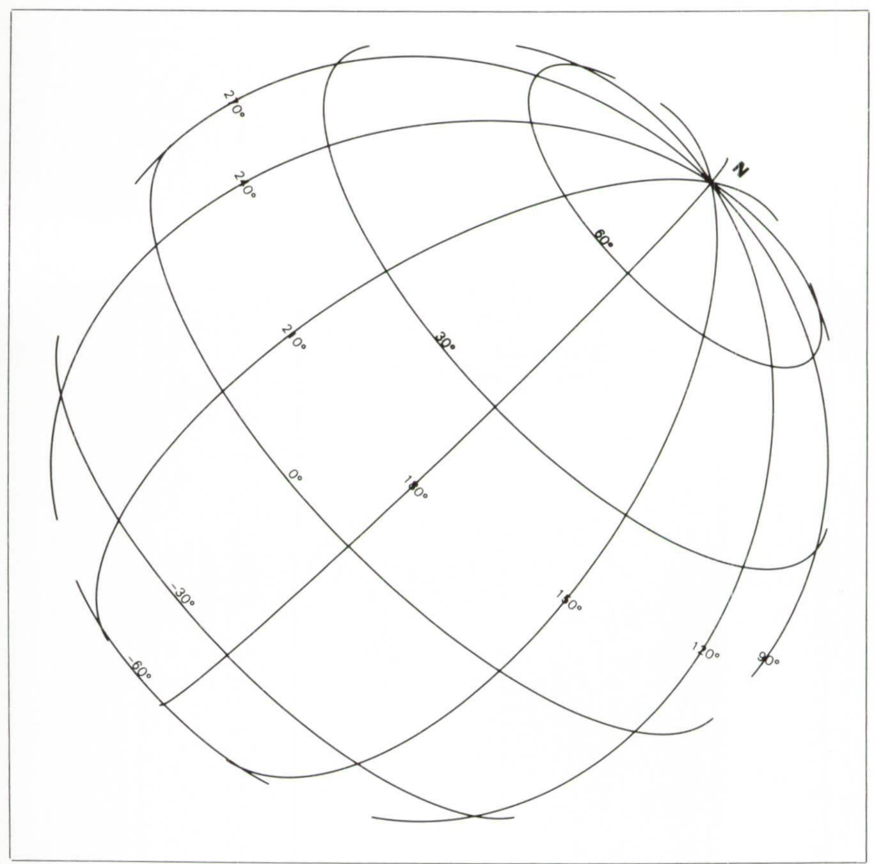

(c)

Picno	0290S2−001
FDS	43980.27
Range, km	825 955
Subspacecraft latitude/longitude, degrees	22/183
Subsolar latitude/longitude, degrees	7/203
Resolution, km/pixel	8
Filter size, pixels	41 × 41
Filter size, km	313
Scale	1:10 000 000

Figure 3–16. Picno 0290S2−001. (*a*) Unfiltered image. (*b*) High-pass filtered image. (*c*) Perspective grid.

(a)

(b)

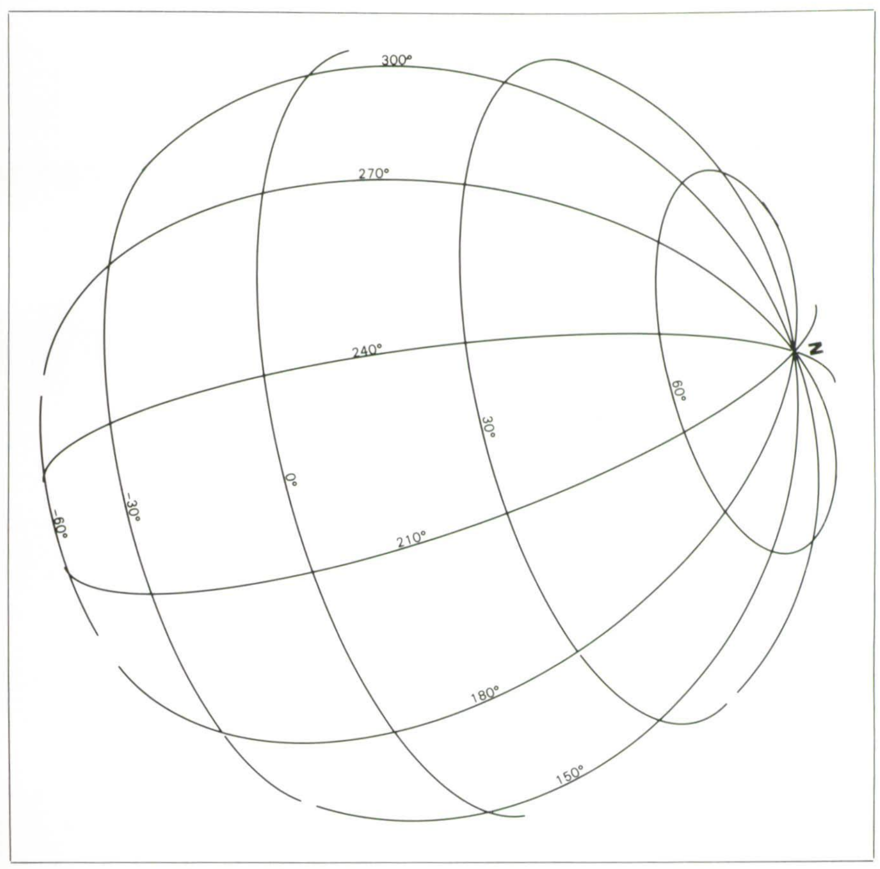

(c)

Picno	0604S2–001
FDS	43985.41
Range, km	683 286
Subspacecraft latitude/longitude, degrees	24/226
Subsolar latitude/longitude, degrees	7/236
Resolution, km/pixel	6
Filter size, pixels	51 × 51
Filter size, km	322
Scale	1:10 000 000

Figure 3–17. Picno 0604S2–001. (*a*) Unfiltered image. (*b*) High-pass filtered image. (*c*) Perspective grid.

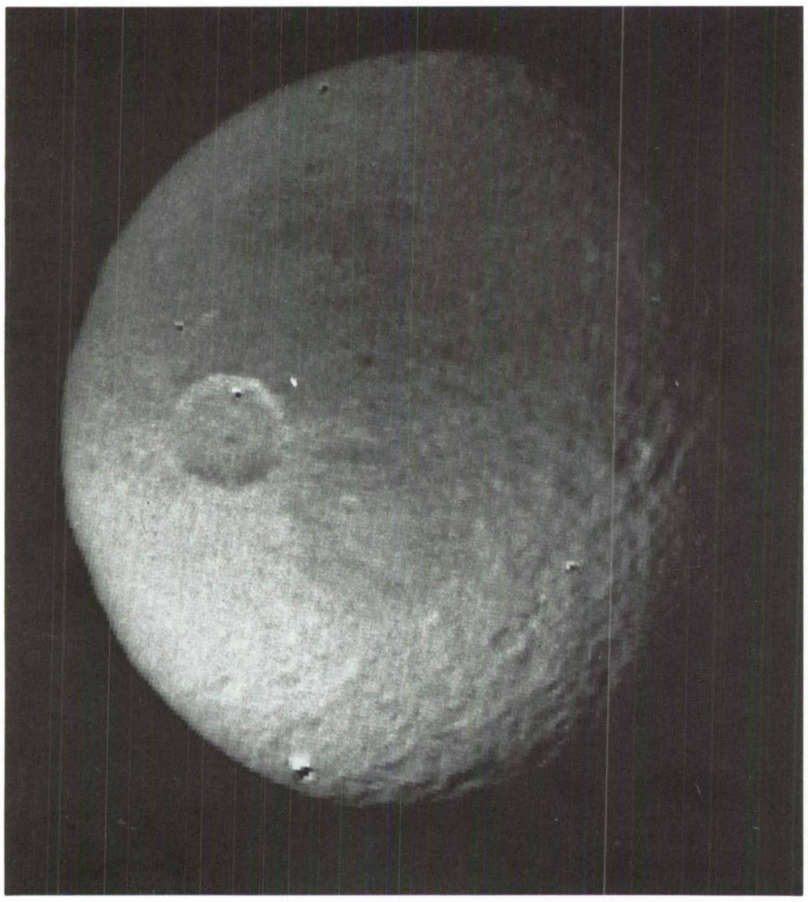

(a)

(b)

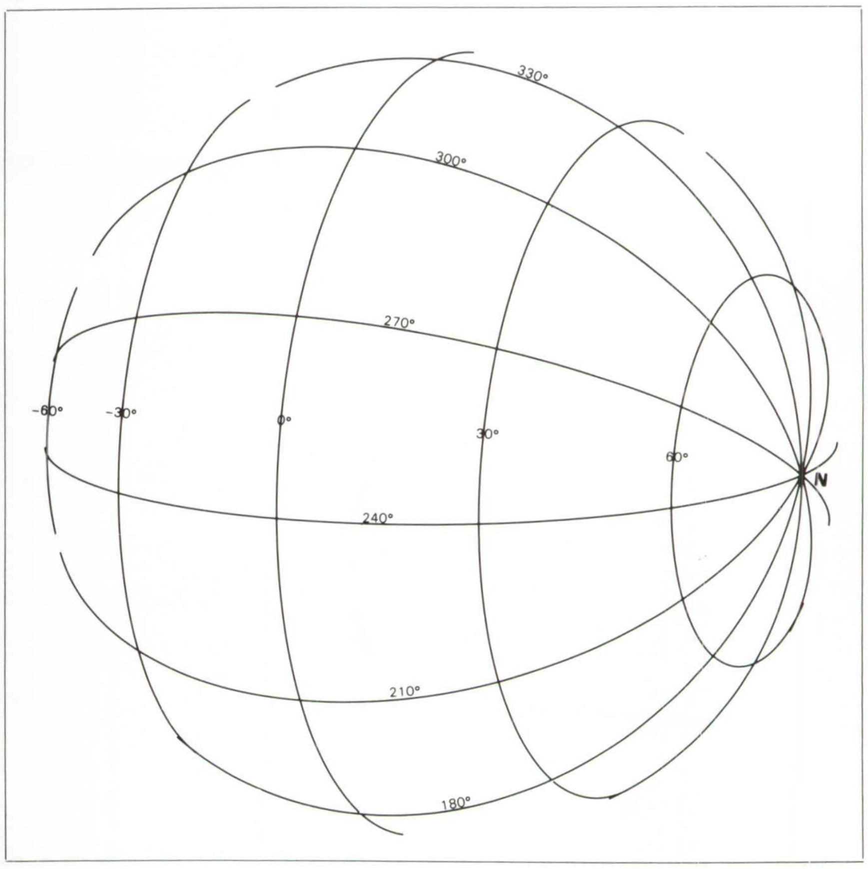

(c)

Picno	0800S2−001
FDS	43988.57
Range, km	633 985
Subspacecraft latitude/longitude, degrees	24/253
Subsolar latitude/longitude, degrees	7/257
Resolution, km/pixel	6
Filter size, pixels	51 × 51
Filter size, km	299
Scale	1:10 000 000

Figure 3–18. Picno 0800S2−001. (*a*) Unfiltered image. (*b*) High-pass filtered image. (*c*) Perspective grid.

(*a*)

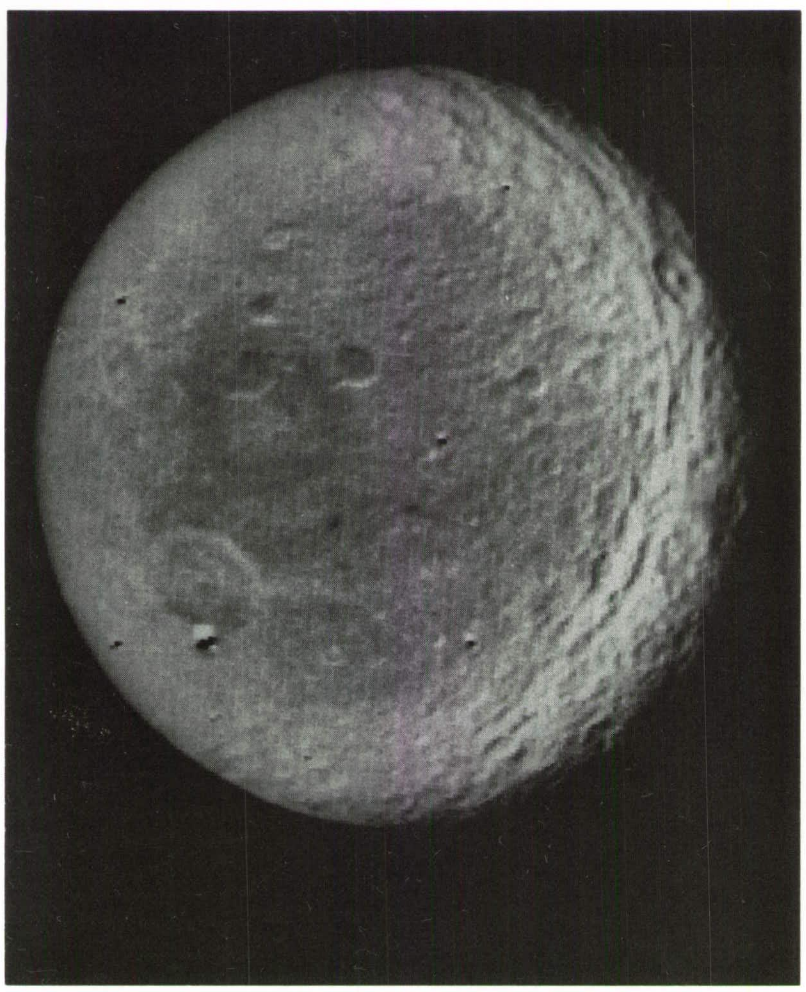

(*b*)

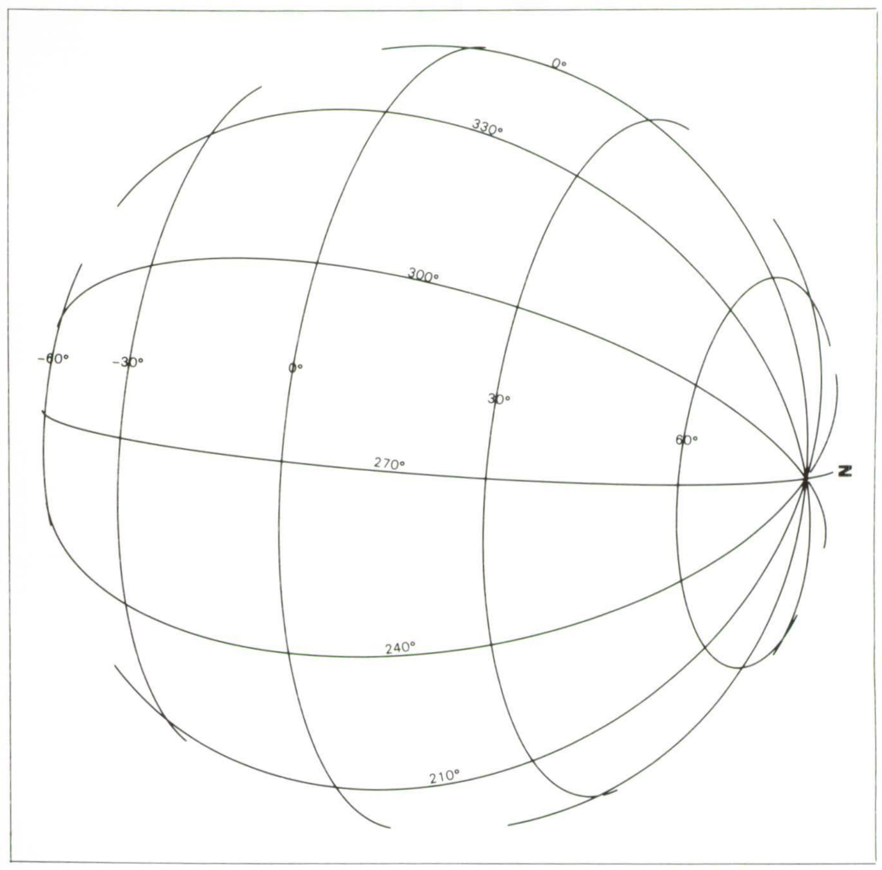

(*c*)

Picno	0999S2–001
FDS	43992.16
Range, km	594 153
Subspacecraft latitude/longitude, degrees	23/276
Subsolar latitude/longitude, degrees	7/278
Resolution, km/pixel	5
Filter size, pixels	61 × 61
Filter size, km	335
Scale	1:10 000 000

Figure 3–19. Picno 0999S2–001. (*a*) Unfiltered image. (*b*) High-pass filtered image. (*c*) Perspective grid.

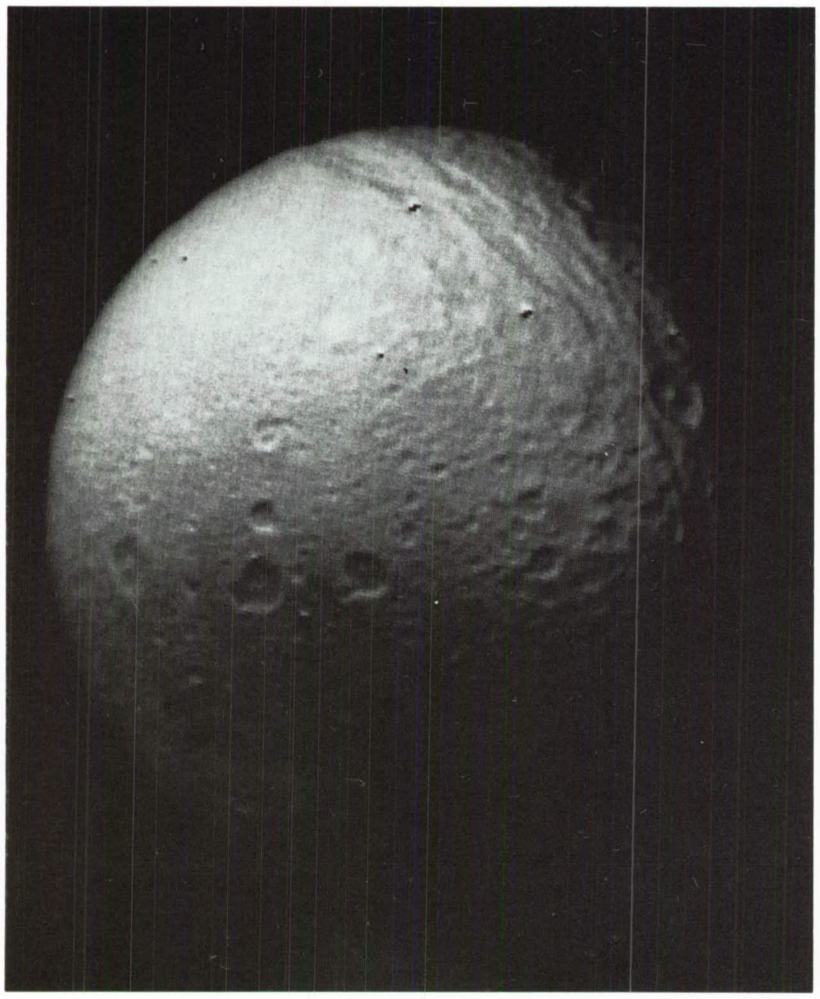

(a)

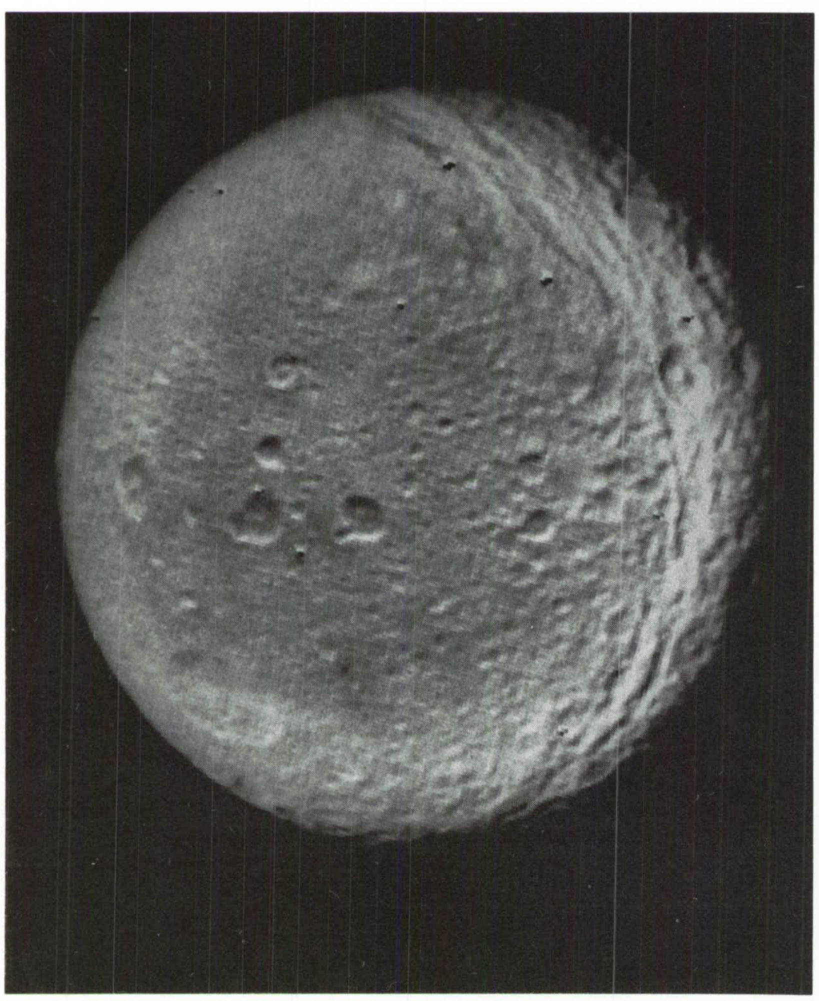

(b)

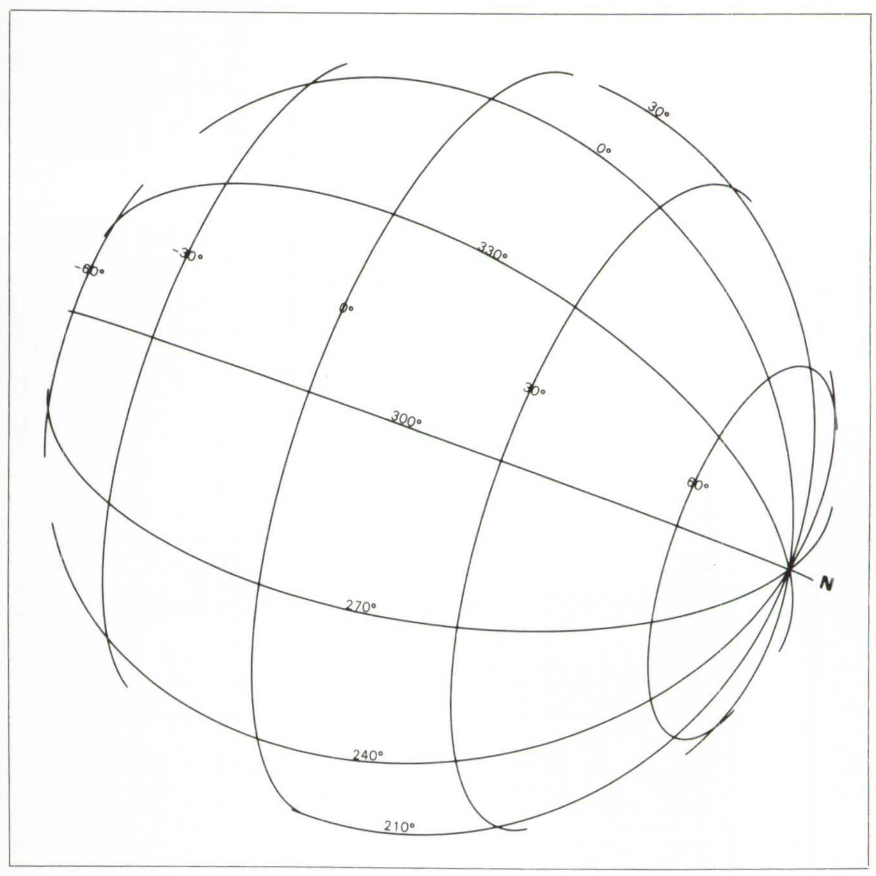

(c)

Picno	1221S2–001
FDS	43995.58
Range, km	538 200
Subspacecraft latitude/longitude, degrees	21/299
Subsolar latitude/longitude, degrees	7/302
Resolution, km/pixel	5
Filter size, pixels	61 × 61
Filter size, km	304
Scale	1:10 000 000

Figure 3–20. Picno 1221S2–001. (*a*) Unfiltered image. (*b*) High-pass filtered image. (*c*) Perspective grid.

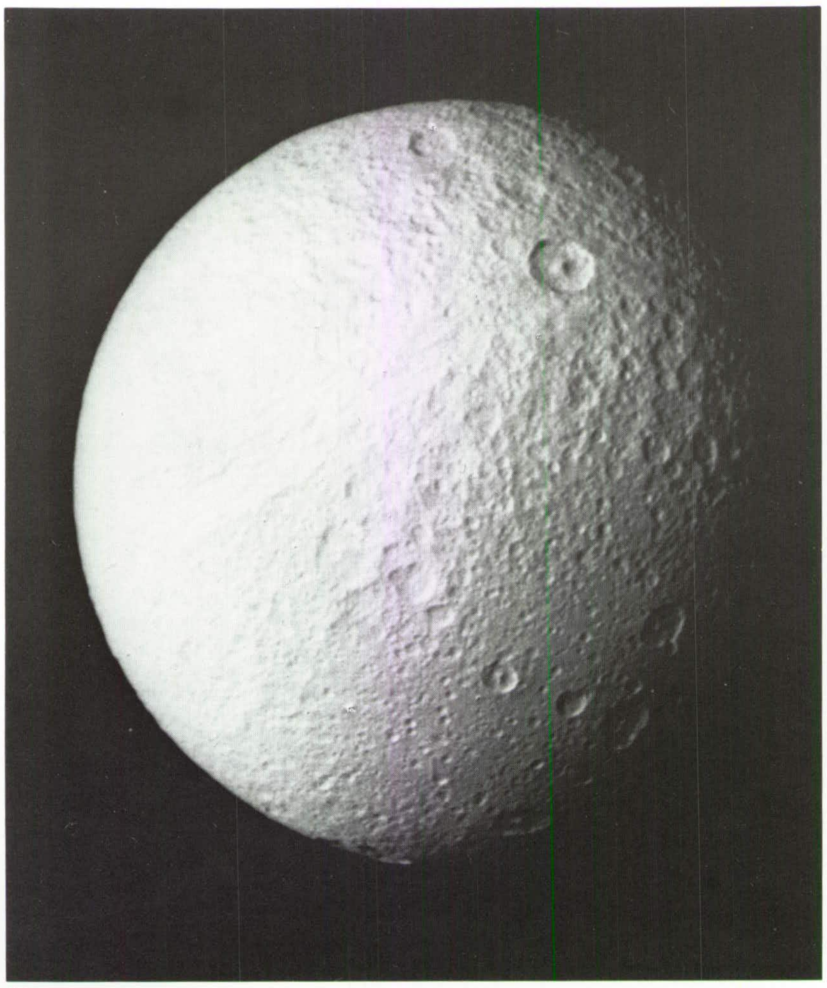

(a)

(b)

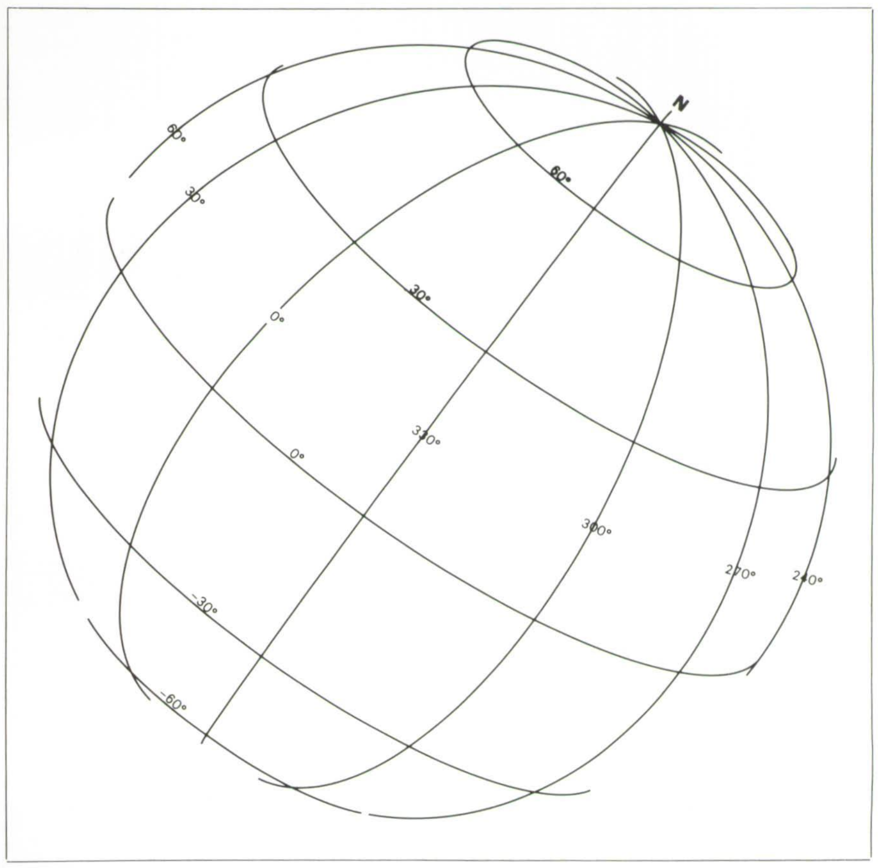

(c)

Picno	1700S2–001
FDS	44003.57
Range, km	282 615
Subspacecraft latitude/longitude, degrees	17/329
Subsolar latitude/longitude, degrees	7/352
Resolution, km/pixel	3
Filter size, pixels	101 × 101
Filter size, km	264
Scale	1:10 000 000

Figure 3–21. Picno 1700S2–001. (*a*) Unfiltered image. (*b*) High-pass filtered image. (*c*) Perspective grid.

(a)

(b)

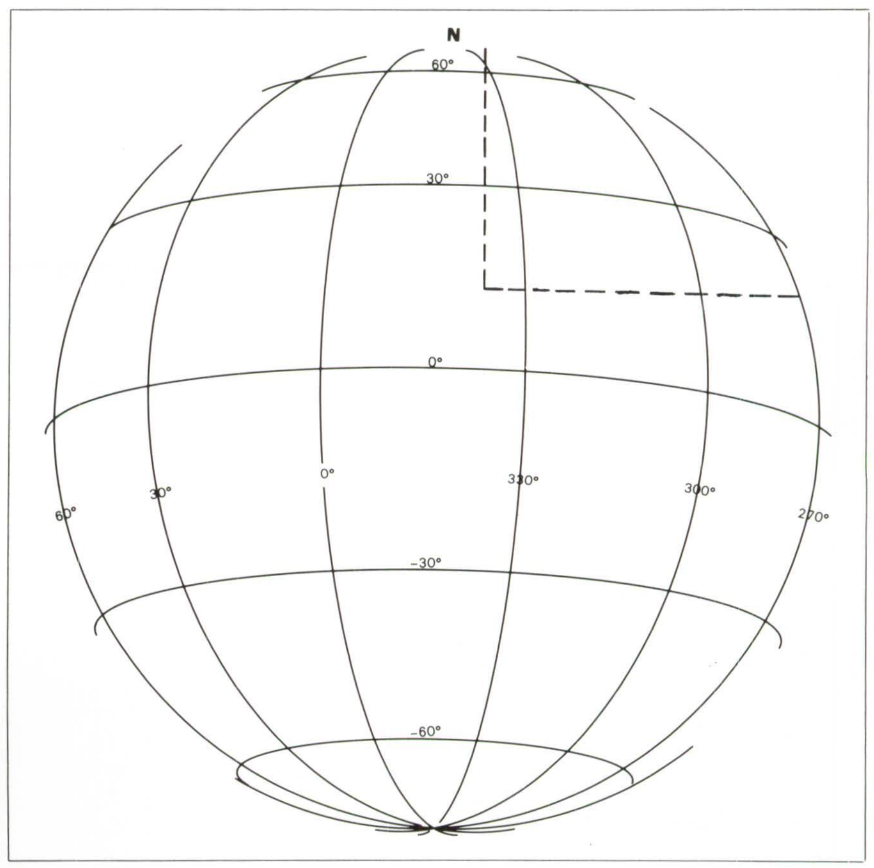

(c)

Picno	0115S2+000
FDS	44007.32
Range, km	119 066
Subspacecraft latitude/longitude, degrees	−11/342
Subsolar latitude/longitude, degrees	7/15
Resolution, km/pixel	1
Filter size, pixels	31 × 31
Filter size, km	34
Scale	1:10 000 000

Figure 3–22. Picno 0115S2+000. This picture of Tethys was one of a series that was not completed because of a malfunction in the spacecraft camera-pointing mechanism. Its location on Tethys has not been verified and it was not used in the preliminary mapping. (*a*) Unfiltered image. (*b*) High-pass filtered image. (*c*) Perspective grid.

PAGE MISSING FROM AVAILABLE VERSION

PART 4

Dione

Diameter	1118 km (695 miles)
Density	1.4
Albedo:	
Brightest	0.6
Darkest	0.3
Distance from Saturn	379 074 km (235 545 miles)
Orbital period	66 hr, 7 min, 59 sec
Voyager 1 closest approach	161 520 km (100 364 miles)
Voyager 1 pictures used in mapping	9
Voyager 2 closest approach	502 250 km (312 083 miles)
Voyager 2 pictures used in mapping	0

Although it is only slightly larger than Tethys, Dione has a distinctly higher density. It exhibits albedo contrast second only in the Saturnian system to Iapetus. A complex network of bright wispy markings divides the dark trailing hemisphere into polygons, whereas the cratered leading hemisphere has an albedo intermediate between the wispy material and the dark polygons.

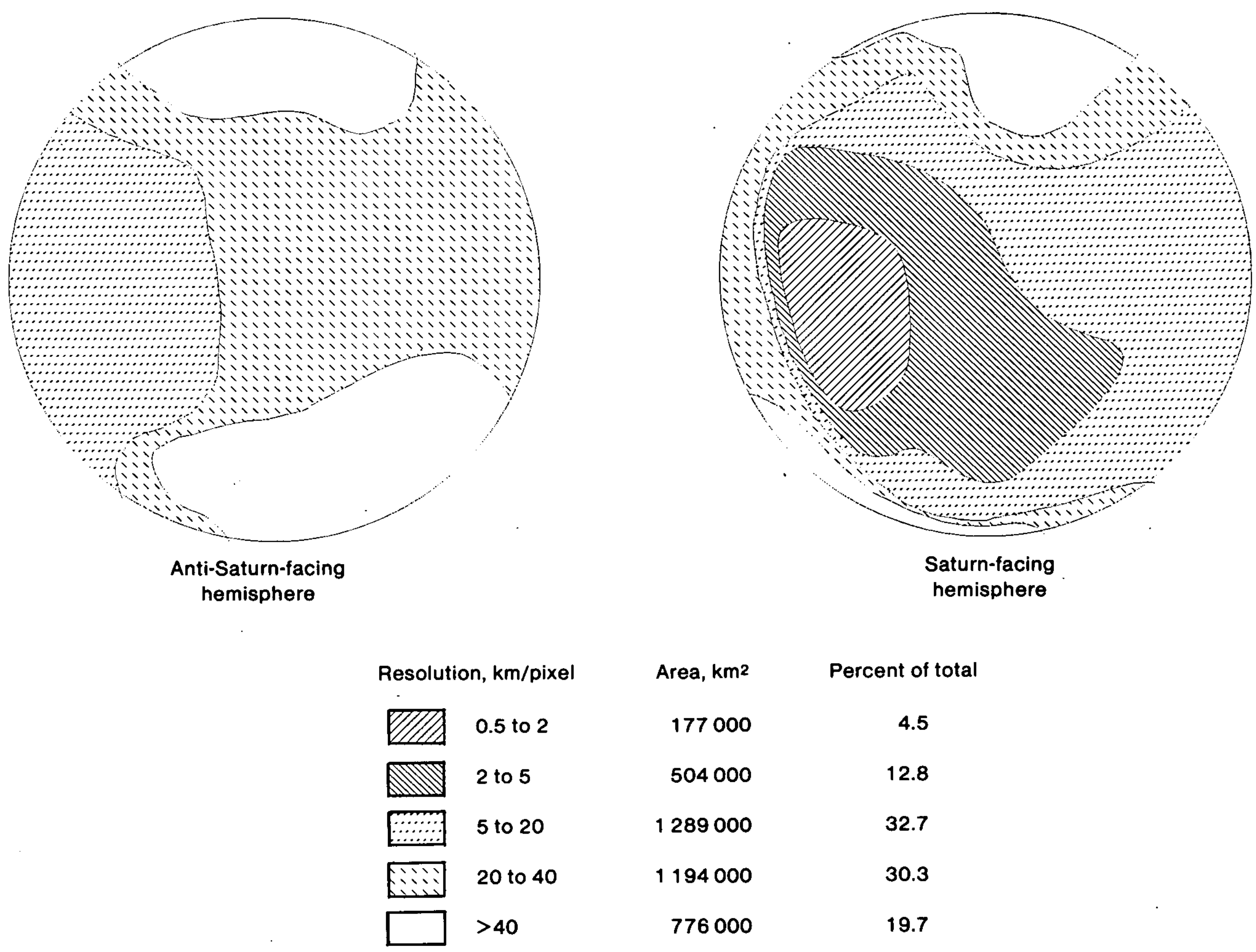

Resolution, km/pixel	Area, km²	Percent of total
0.5 to 2	177 000	4.5
2 to 5	504 000	12.8
5 to 20	1 289 000	32.7
20 to 40	1 194 000	30.3
>40	776 000	19.7

Figure 4–1. Resolution of Voyager pictures of Dione in terms of aerial coverage.

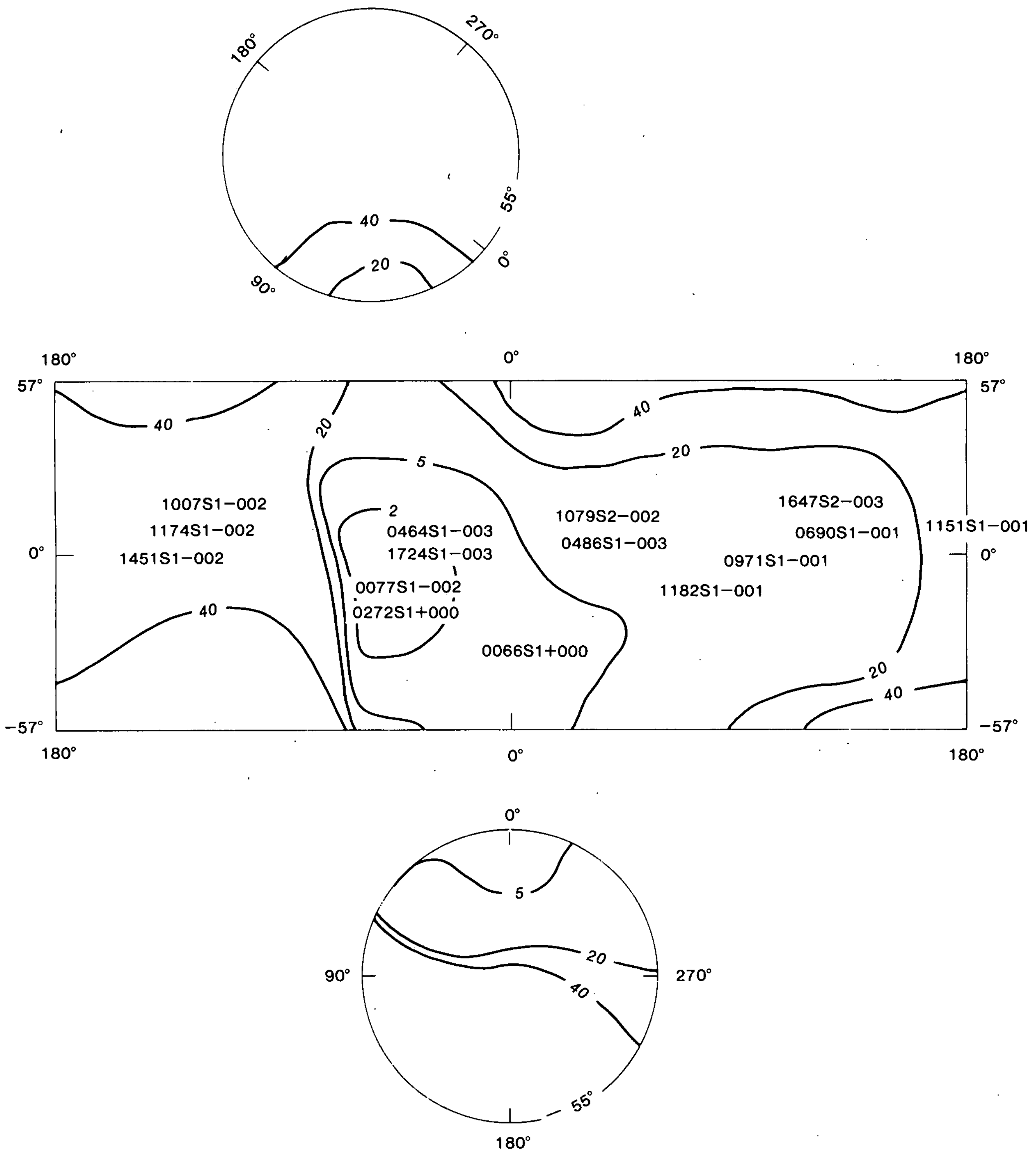

Figure 4–2. Index of Voyager 1 and 2 pictures used to compile the maps of Dione. Picture numbers indicate the subspacecraft point at the time the pictures were taken. Contour lines indicate the approximate resolution of available images in kilometers per picture element. (See also fig. 4–1.)

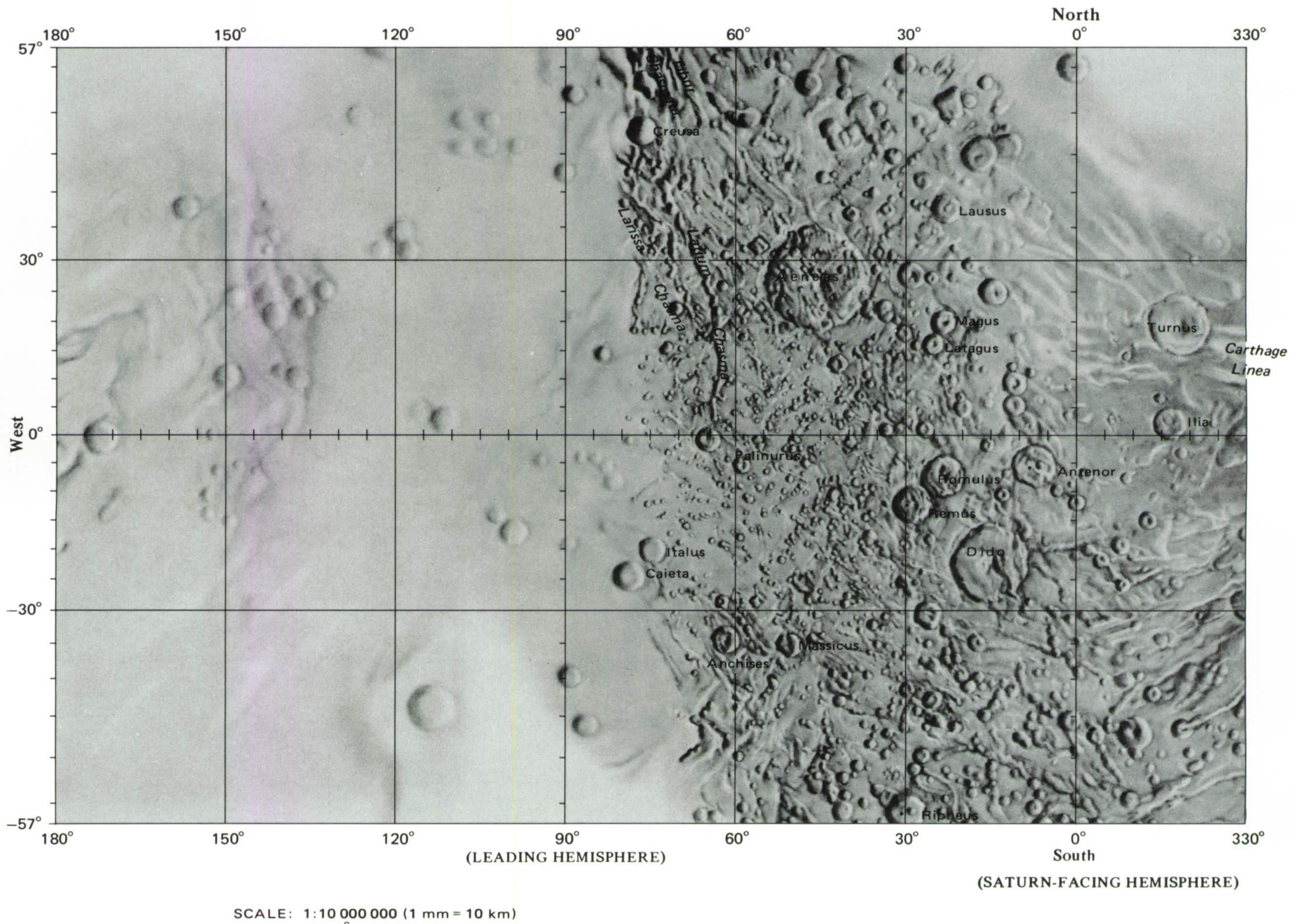

North
180°
150°
120°
90°
60°
30°
0°
330°
57°
30°
0°
−30°
−57°
West
South
(LEADING HEMISPHERE)
(SATURN-FACING HEMISPHERE)
Creusa
Larissa
Latium
Chasma
Chasma
Aeneas
Lausus
Magus
Catagus
Turnus
Carthage
Linea
Ilia
Palinurus
Romulus
Antenor
Remus
Dido
Italus
Caieta
Massicus
Anchises
Ripheus

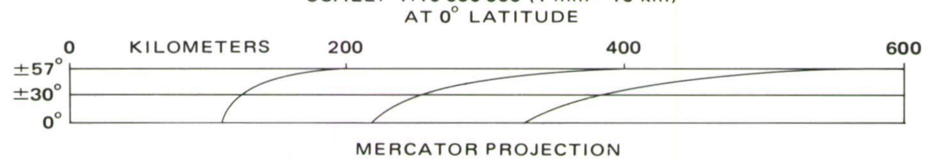

SCALE: 1:10 000 000 (1 mm = 10 km)
AT 0° LATITUDE
0
KILOMETERS
200
400
600
±57°
±30°
0°
MERCATOR PROJECTION

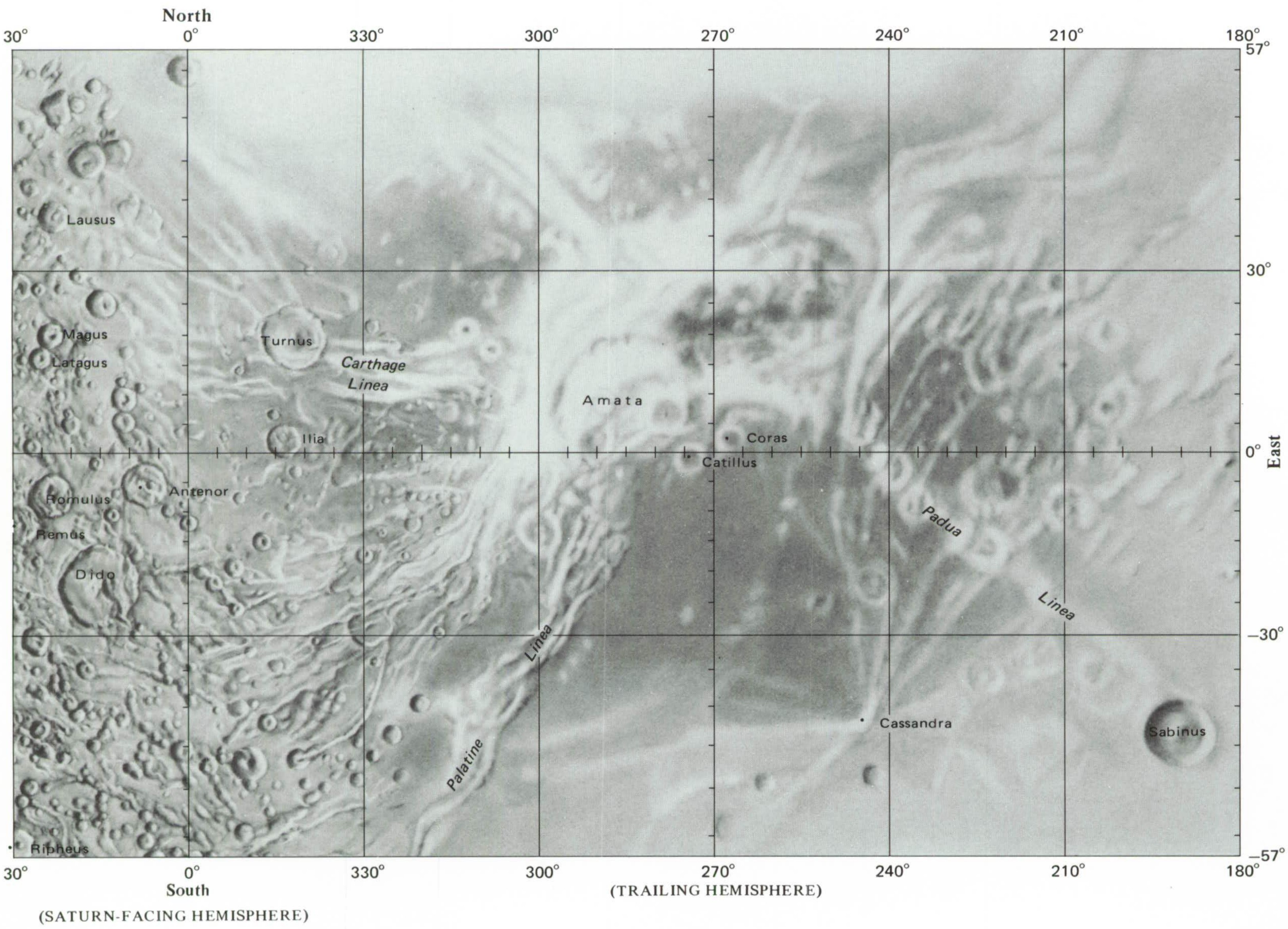

Figure 4–3. Map of the equatorial region of Dione on a Mercator projection (part of map I–1488).

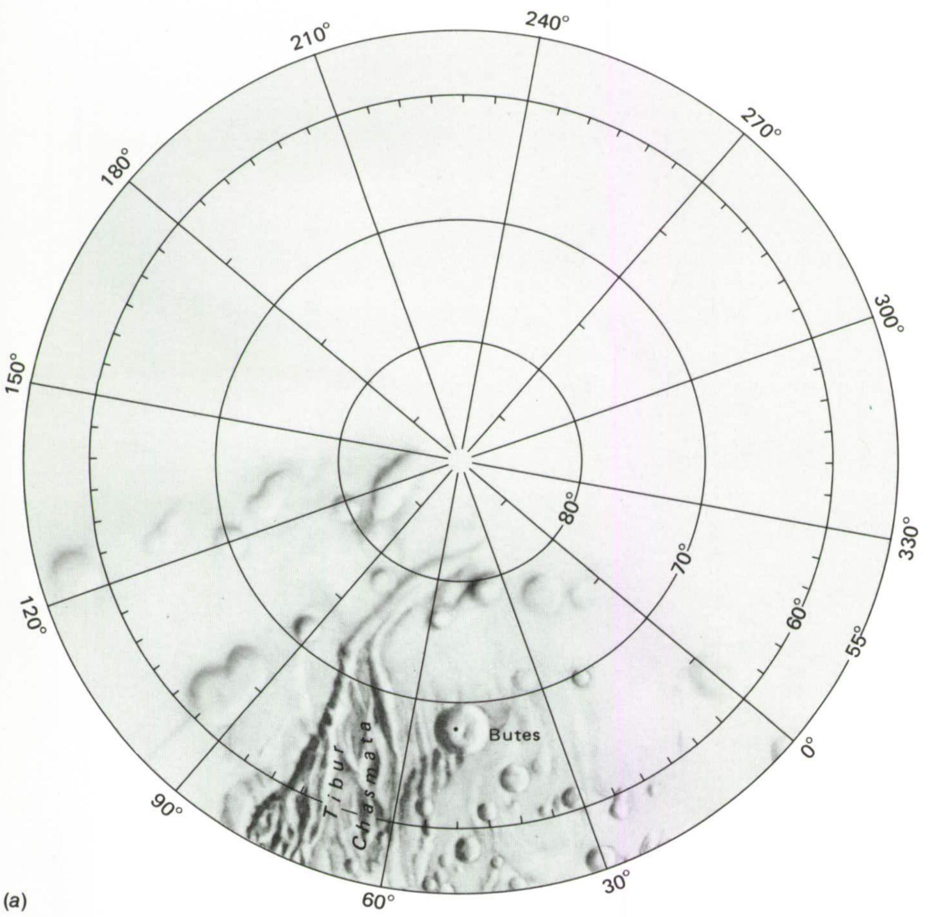

(a)

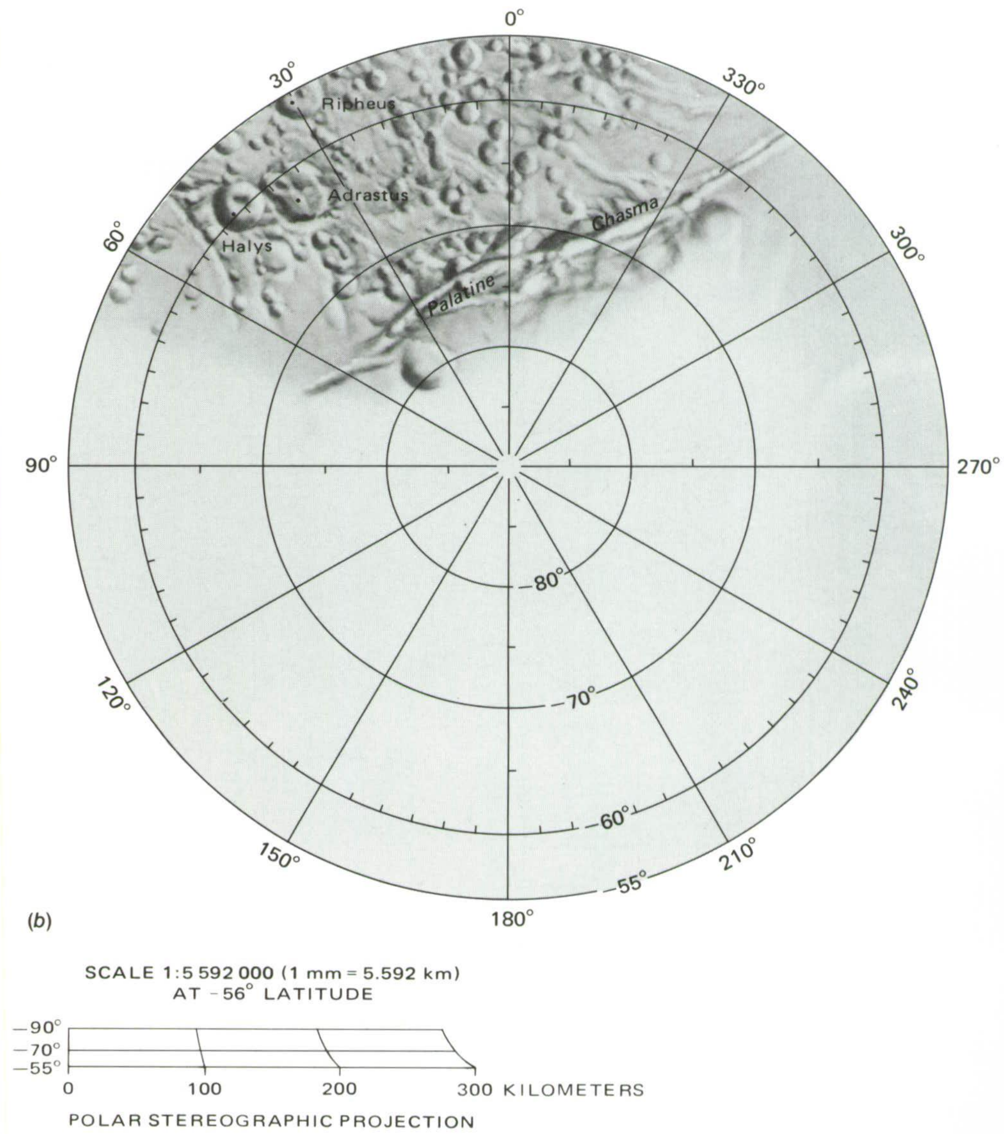

(b)

Figure 4–4. Maps of the polar regions of Dione on polar stereographic projections (part of map I–1488). (*a*) North polar region. (*b*) South polar region.

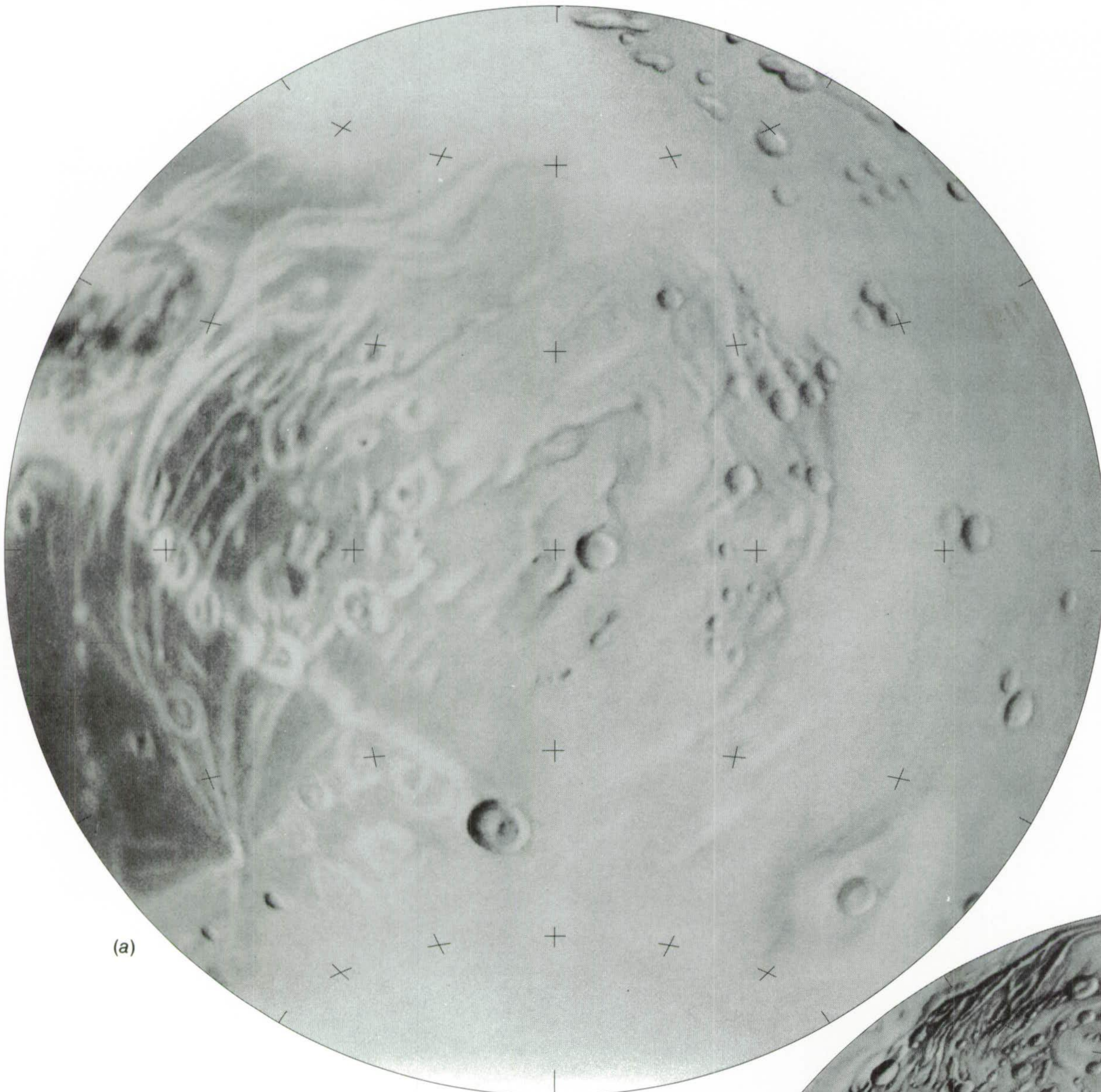

(a)

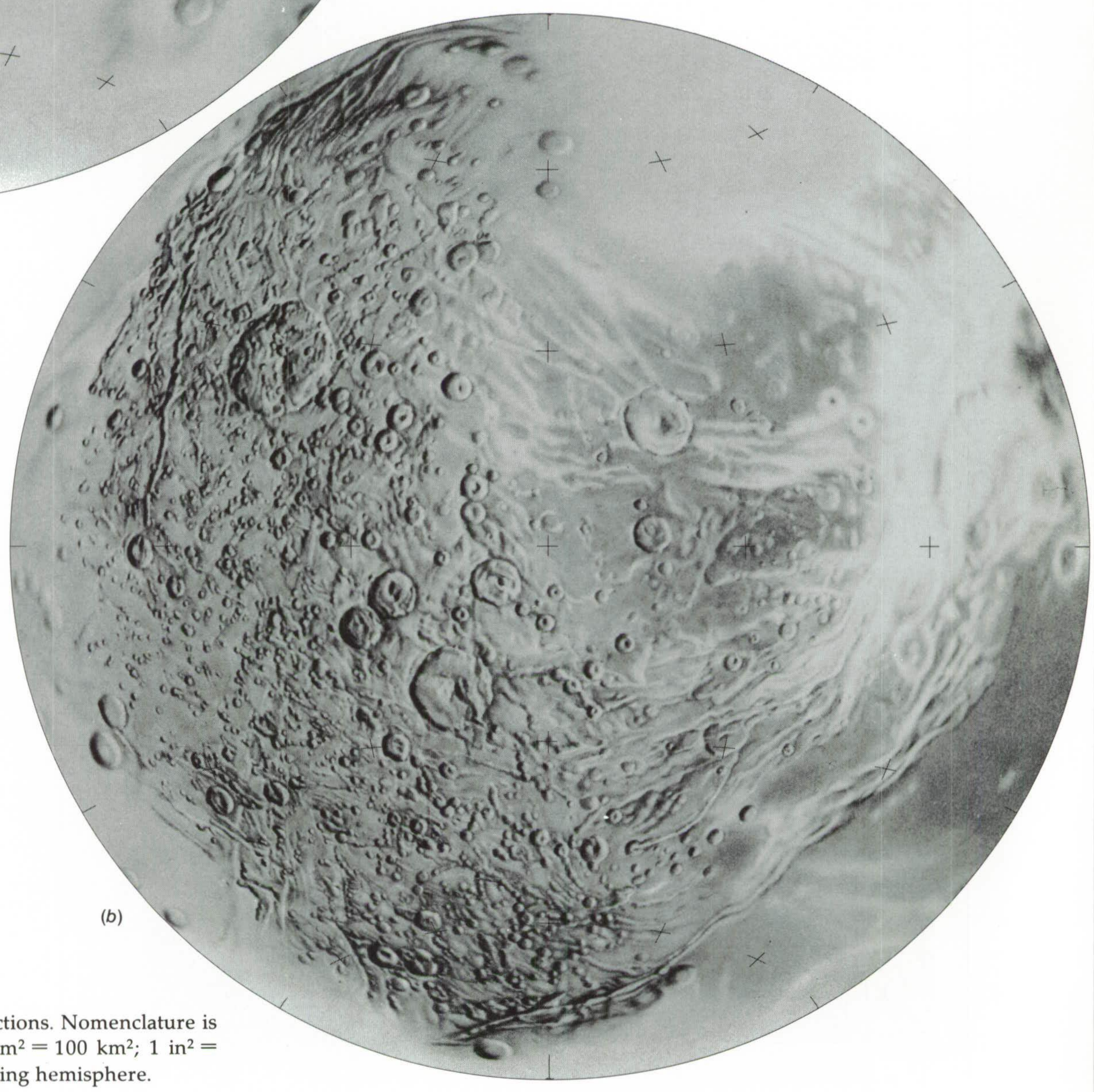

(b)

Figure 4–5. Maps of Dione on Lambert azimuthal equal-area projections. Nomenclature is not shown, to avoid obscuring detail. Scale 1:10 000 000 (1 mm^2 = 100 km^2; 1 in^2 = ~25 000 mi^2). (*a*) Anti-Saturn-facing hemisphere. (*b*) Saturn-facing hemisphere.

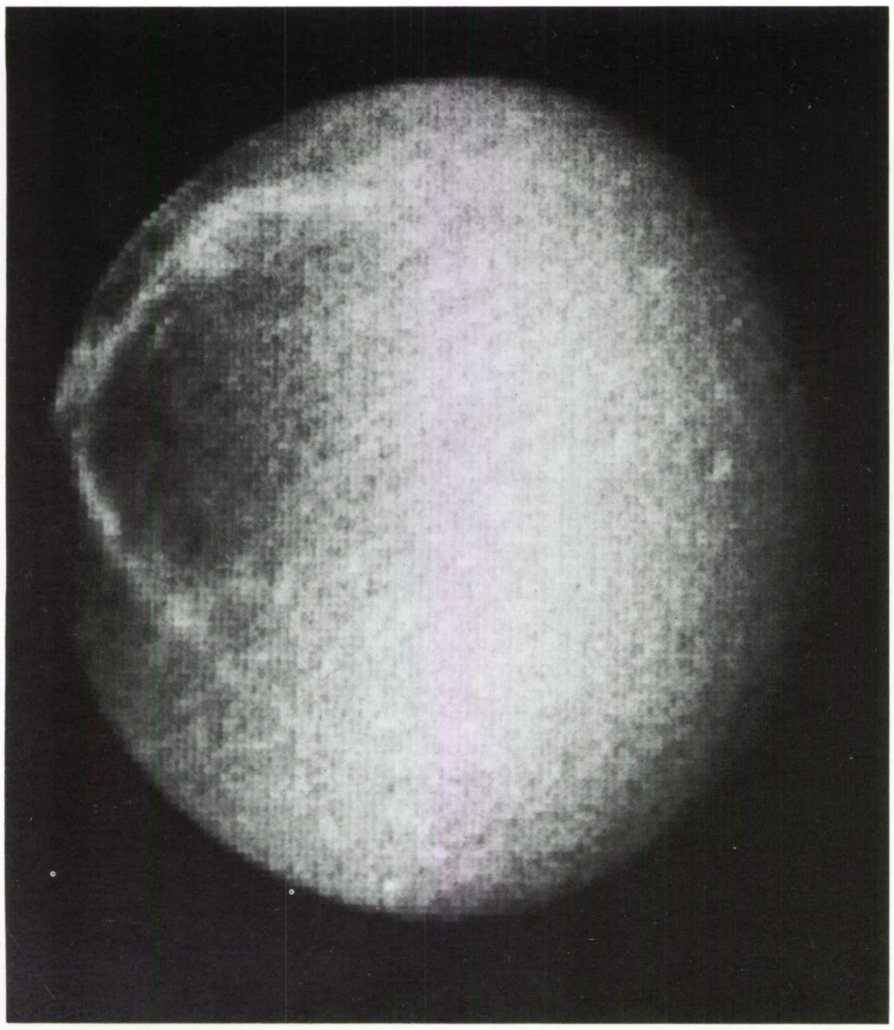

(a)

(b)

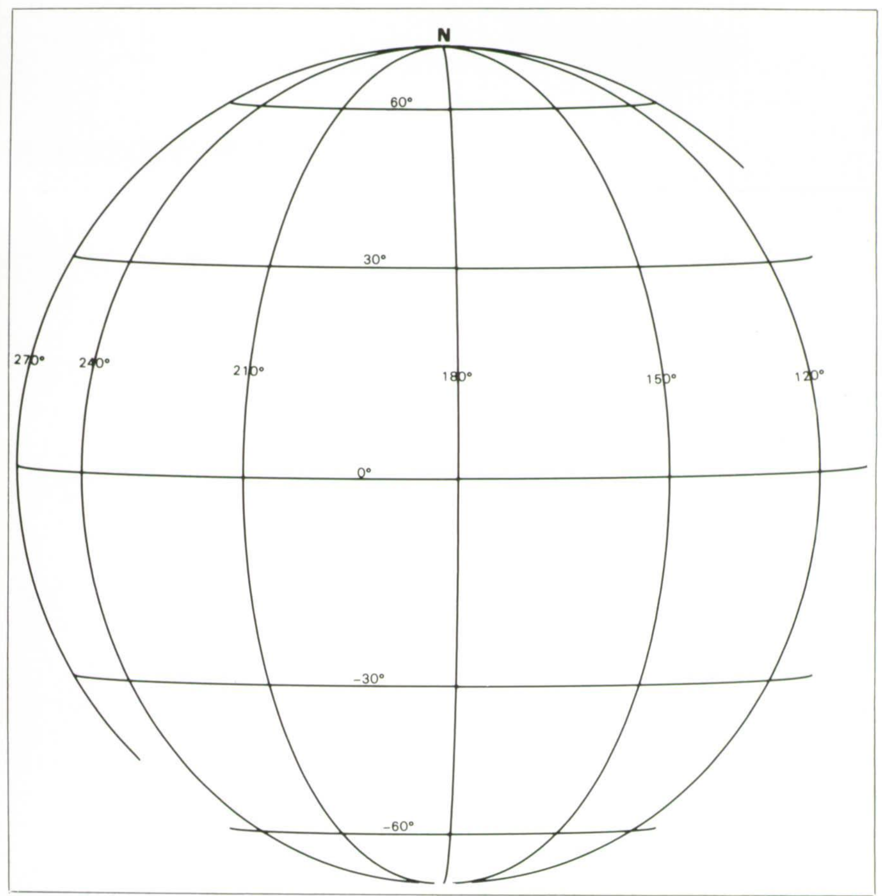

(c)

Picno	0011S1–001
FDS	34914.07
Range, km	1 171 769
Subspacecraft latitude/longitude, degrees	2/182
Subsolar latitude/longitude, degrees	4/201
Resolution, km/pixel	11
Filter size, pixels	101 × 101
Filter size, km	1094
Scale	1:10 000 000

Figure 4–6. Picno 0011S1–001. (*a*) Unfiltered image. (*b*) High-pass filtered image. (*c*) Perspective grid.

(a)

(b)

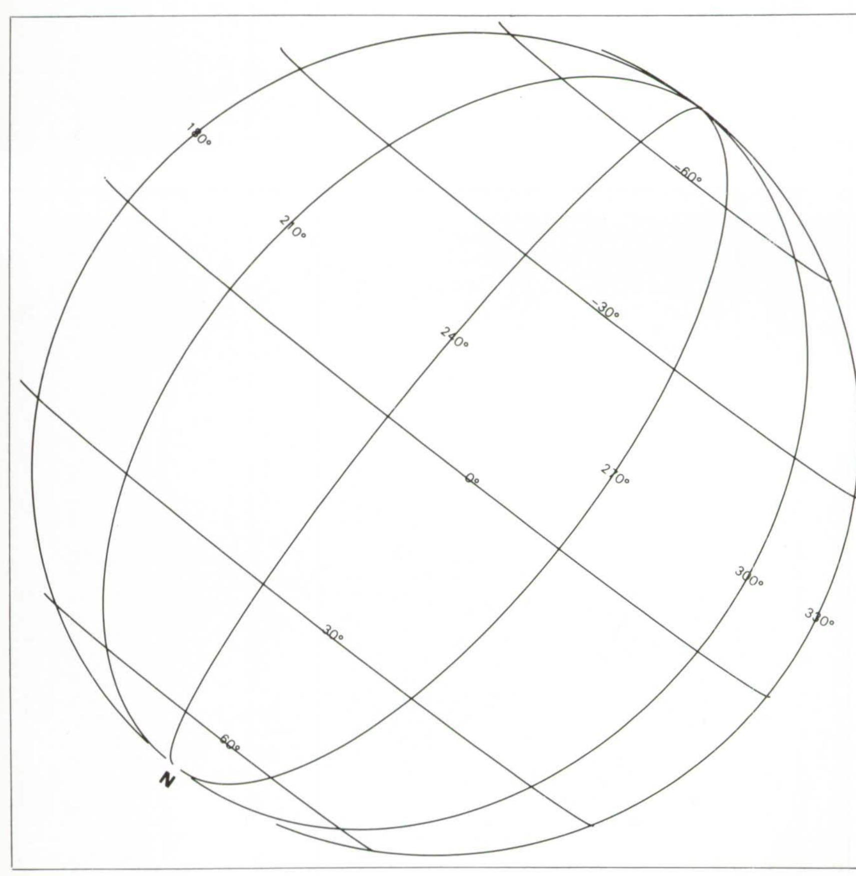

(c)

Picno	0690S1−001
FDS	34925.26
Range, km	794 254
Subspacecraft latitude/longitude, degrees	−2/246
Subsolar latitude/longitude, degrees	4/250
Resolution, km/pixel	7
Filter size, pixels	101 × 101
Filter size, km	742
Scale	1:10 000 000

Figure 4–7. Picno 0690S1−001. (*a*) Unfiltered image. (*b*) High-pass filtered image. (*c*) Perspective grid.

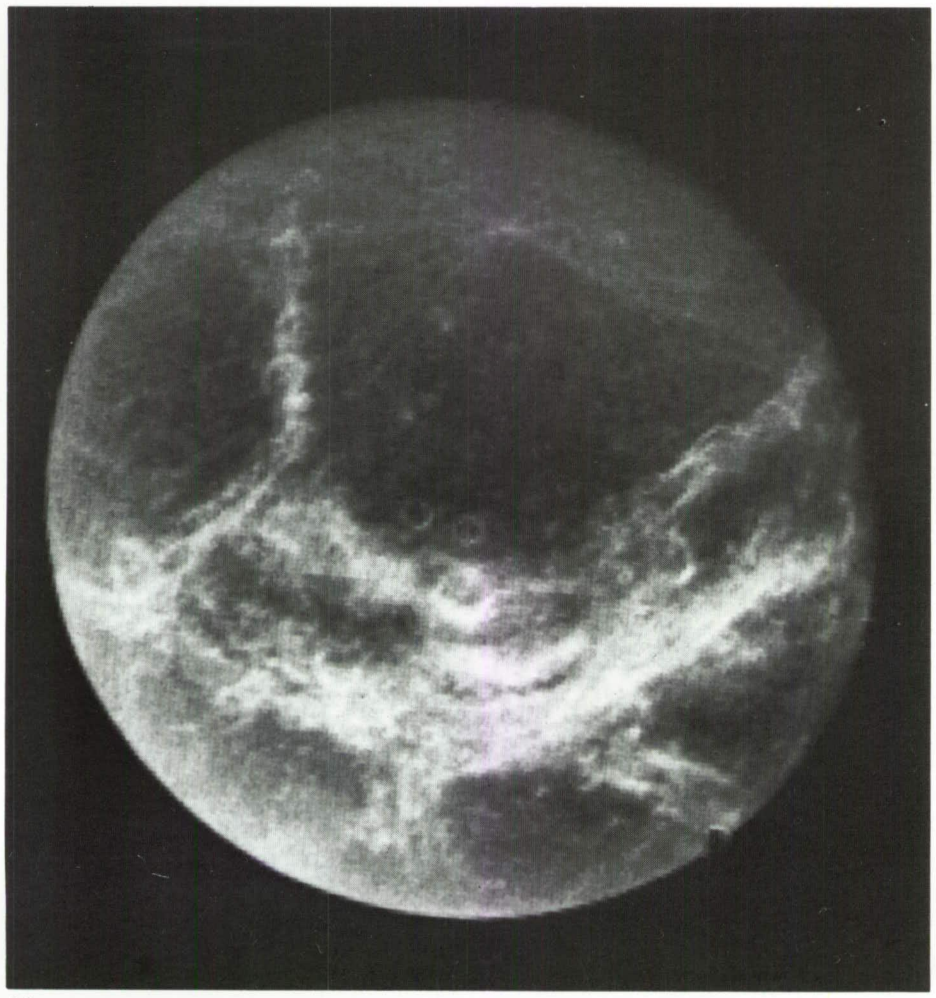

(*a*)

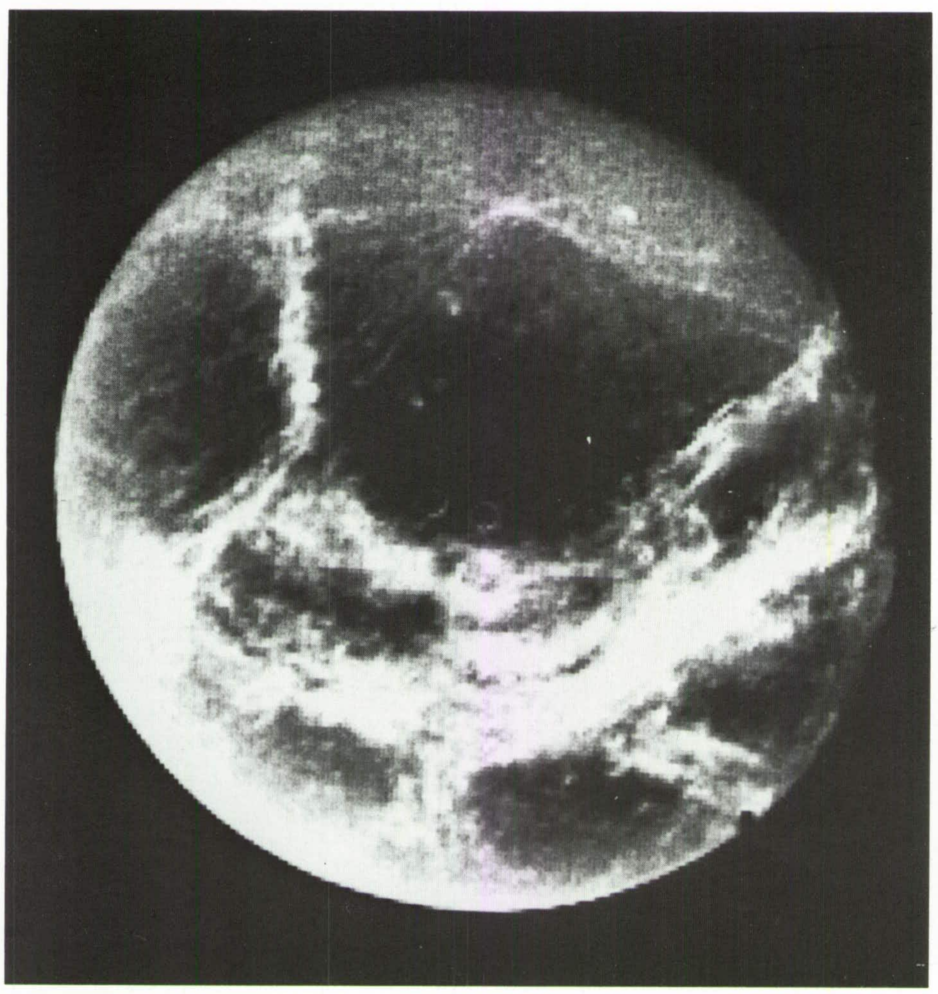

(*b*)

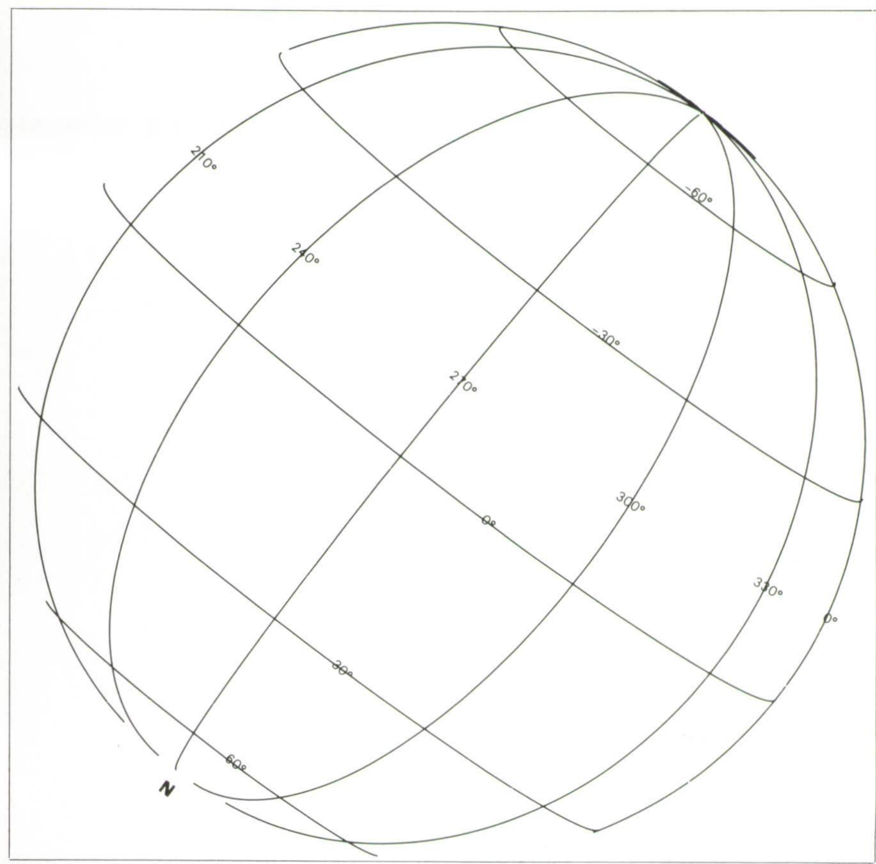

(*c*)

Picno	0971S1−001
FDS	34930.07
Range, km	697 095
Subspacecraft latitude/longitude, degrees	−5/272
Subsolar latitude/longitude, degrees	4/271
Resolution, km/pixel	6
Filter size, pixels	101 × 101
Filter size, km	651
Scale	1:10 000 000

Figure 4–8. Picno 0971S1−001. (*a*) Unfiltered image. (*b*) High-pass filtered image. (*c*) Perspective grid.

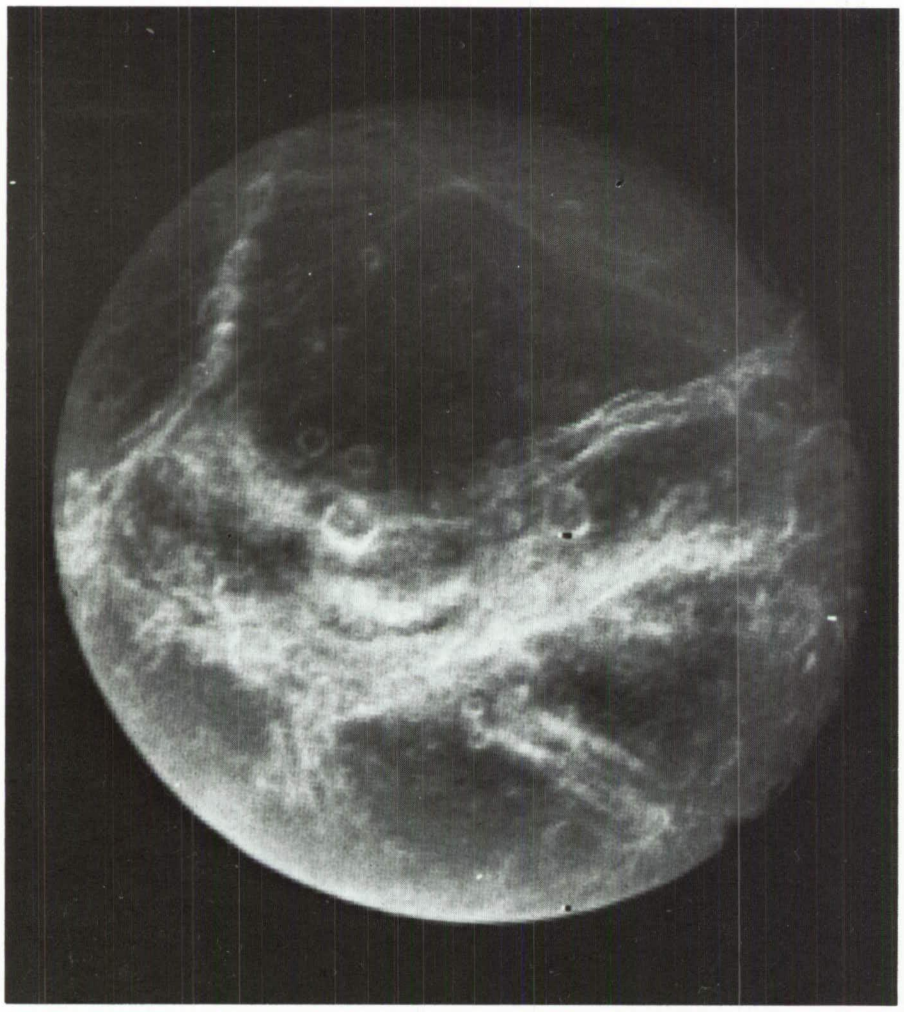

(a)

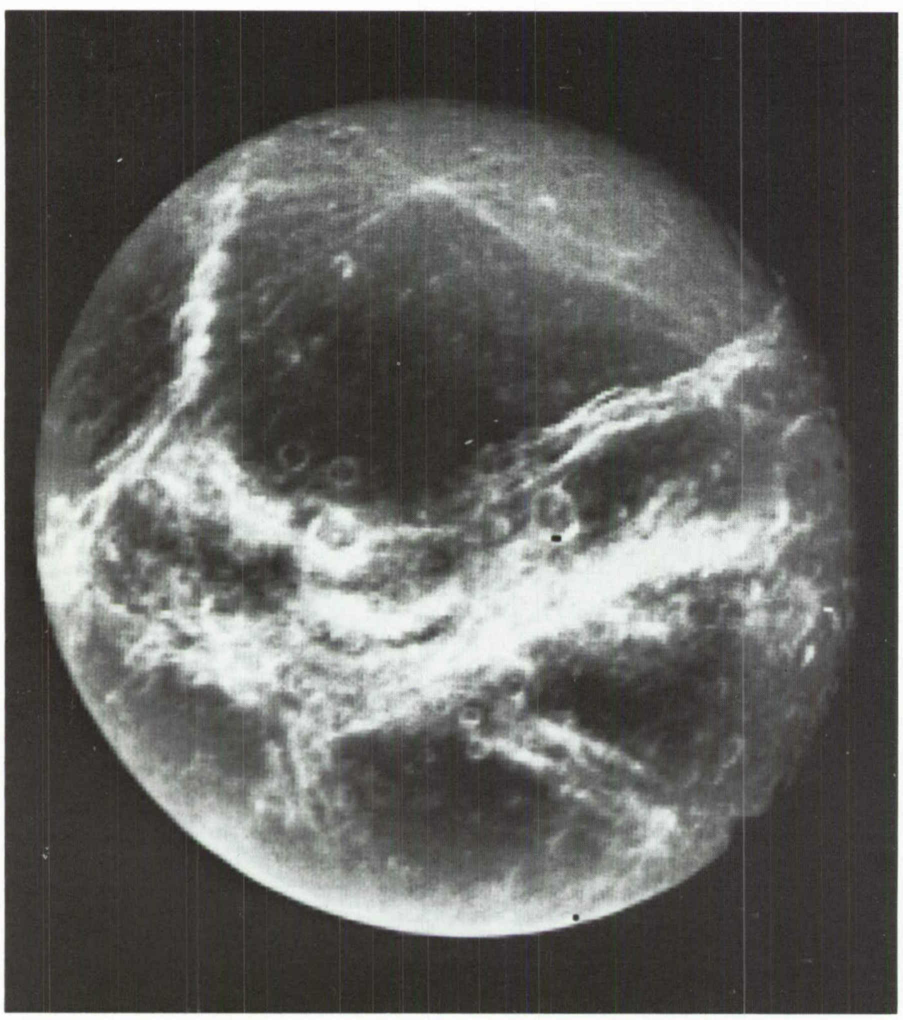

(b)

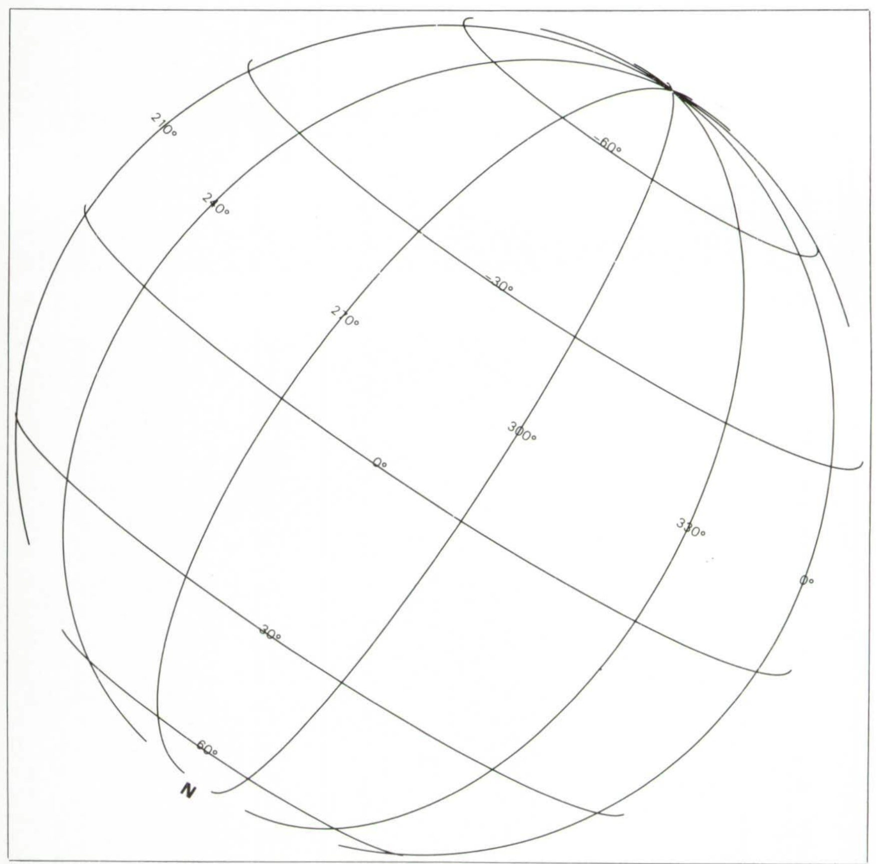

(c)

Picno	1182S1−001
FDS	34933.38
Range, km	622 631
Subspacecraft latitude/longitude, degrees	−8/291
Subsolar latitude/longitude, degrees	4/287
Resolution, km/pixel	5
Filter size, pixels	101 × 101
Filter size, km	581
Scale	1:10 000 000

Figure 4–9. Picno 1182S1−001. (*a*) Unfiltered image. (*b*) High-pass filtered image. (*c*) Perspective grid.

(a)

(b)

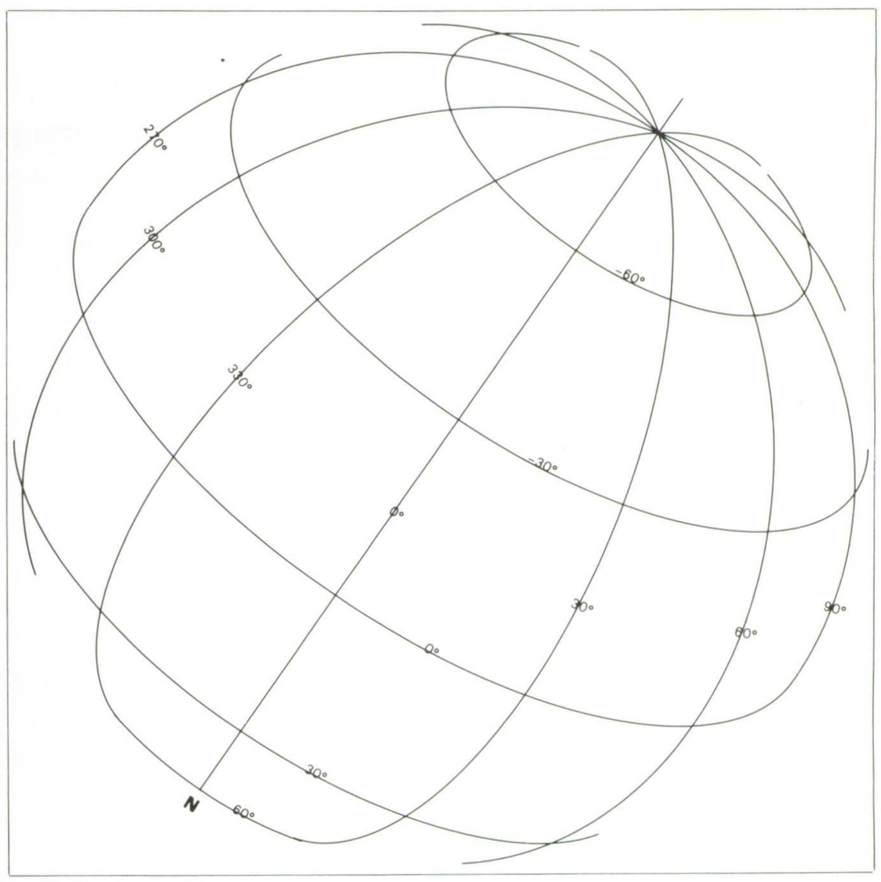

(c)

Picno	0062S1+000
FDS	34944.58
Range, km	237 809
Subspacecraft latitude/longitude, degrees	−26/360
Subsolar latitude/longitude, degrees	4/336
Resolution, km/pixel	2
Filter size, pixels	101 × 101
Filter size, km	222
Scale	1:10 000 000

Figure 4–10. Picno 0062S1+000. (*a*) Unfiltered image. (*b*) High-pass filtered image. (*c*) Perspective grid.

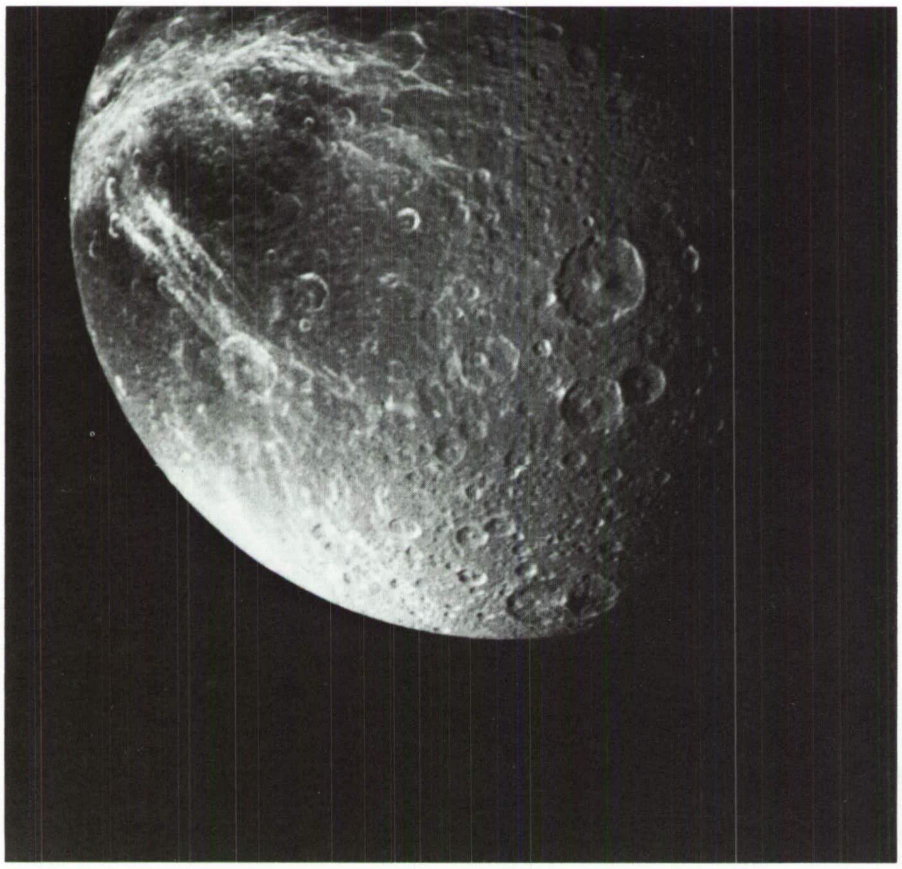

(a)

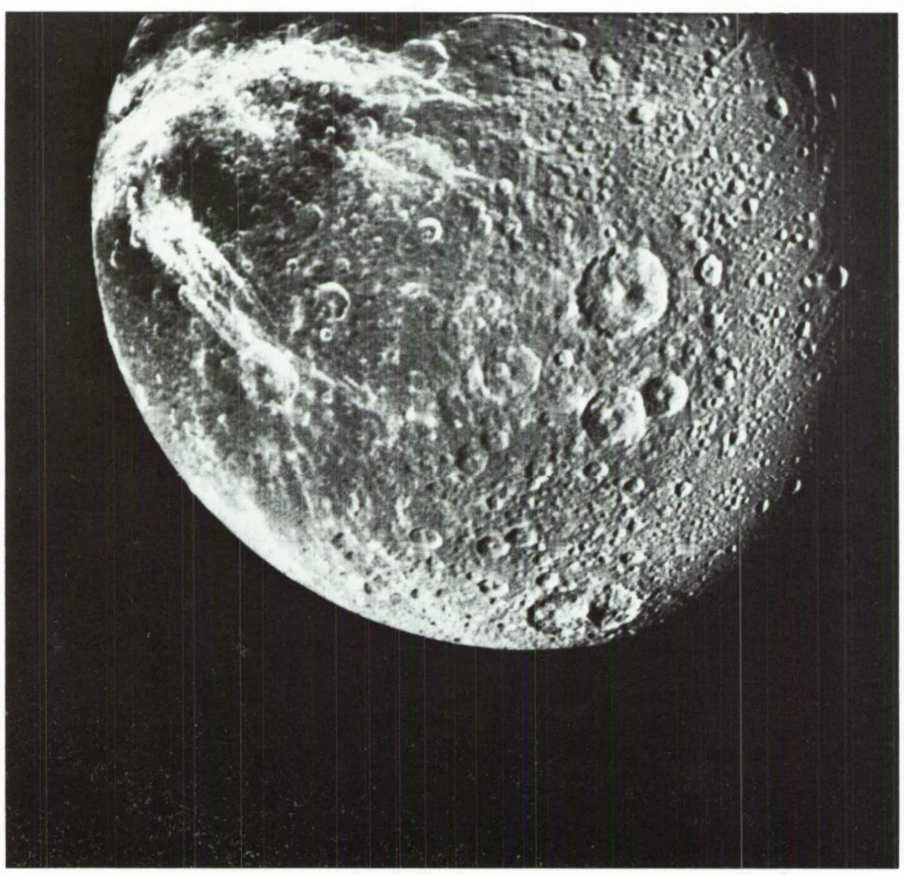

(b)

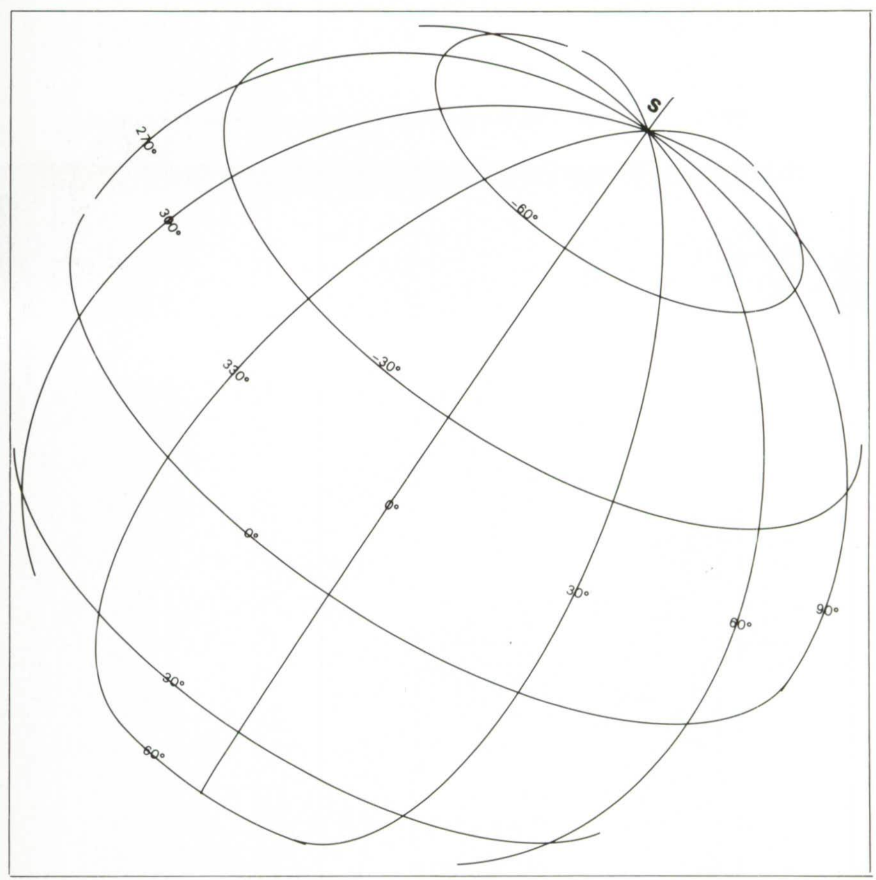

(c)

Picno	0066S1+000
FDS	34945.02
Range, km	235 367
Subspacecraft latitude/longitude, degrees	−26/1
Subsolar latitude/longitude, degrees	4/336
Resolution, km/pixel	2
Filter size, pixels	101 × 101
Filter size, km	220
Scale	1:10 000 000

Figure 4–11. Picno 0066S1+000. (*a*) Unfiltered image. (*b*) High-pass filtered image. (*c*) Perspective grid.

(*a*)

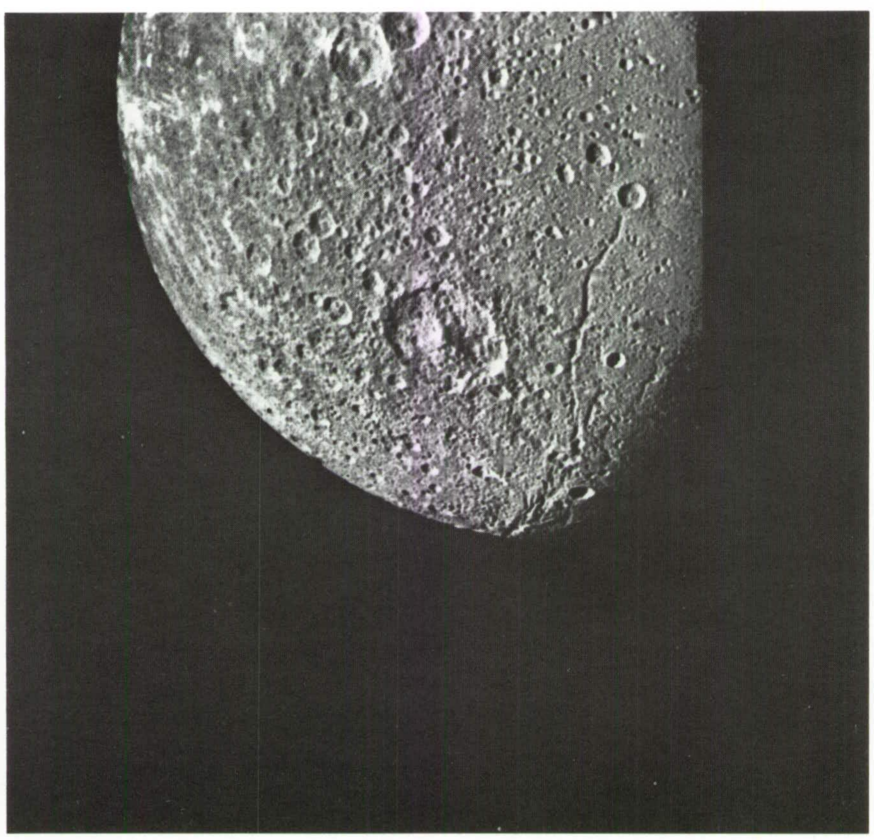

(*b*)

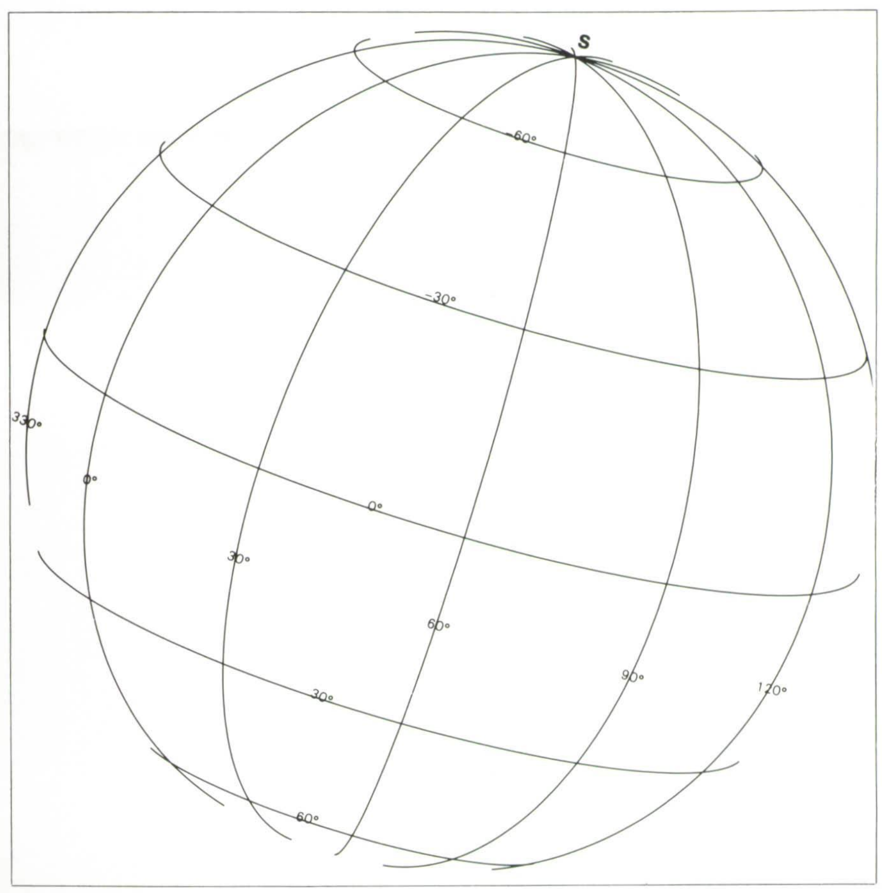

(*c*)

Picno	0266S1+000
FDS	34948.22
Range, km	162 832
Subspacecraft latitude/longitude, degrees	−11/55
Subsolar latitude/longitude, degrees	4/351
Resolution, km/pixel	1
Filter size, pixels	101 × 101
Filter size, km	152
Scale	1:10 000 000

Figure 4–12. Picno 0266S1+000. (*a*) Unfiltered image. (*b*) High-pass filtered image. (*c*) Perspective grid.

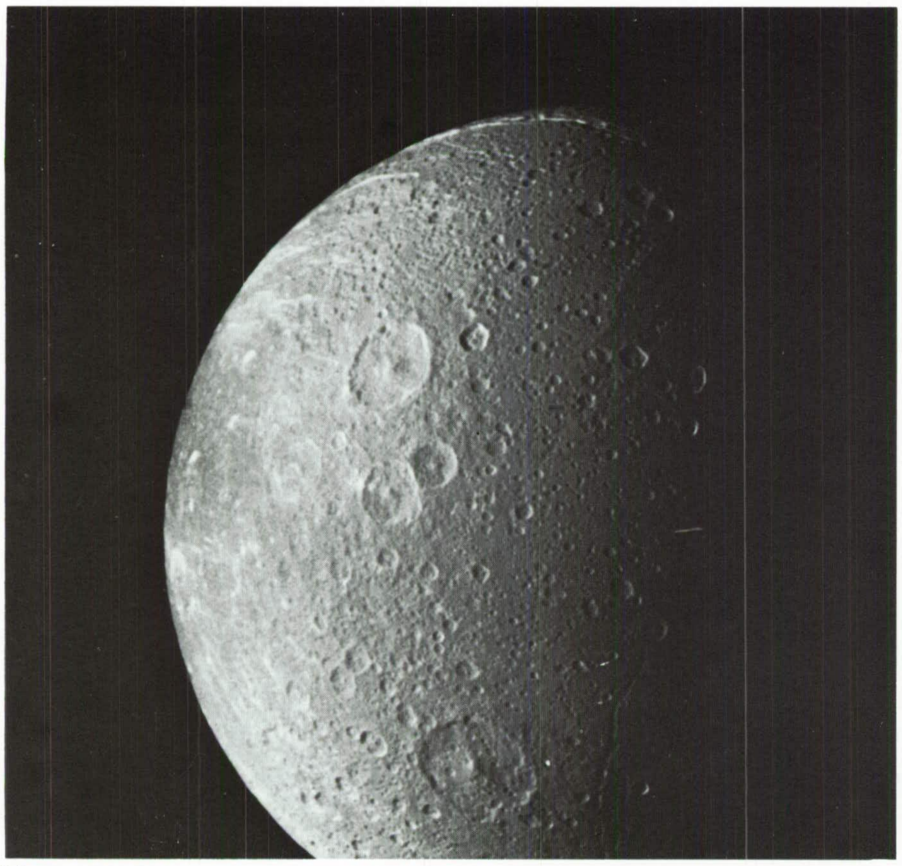

(a)

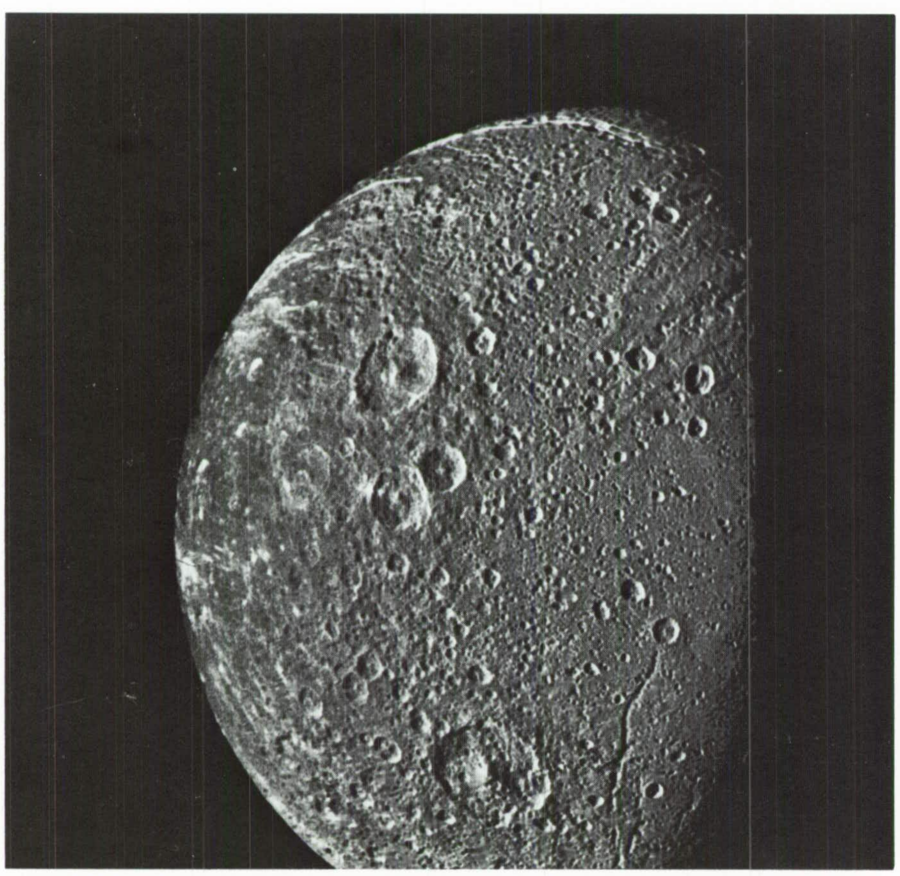

(b)

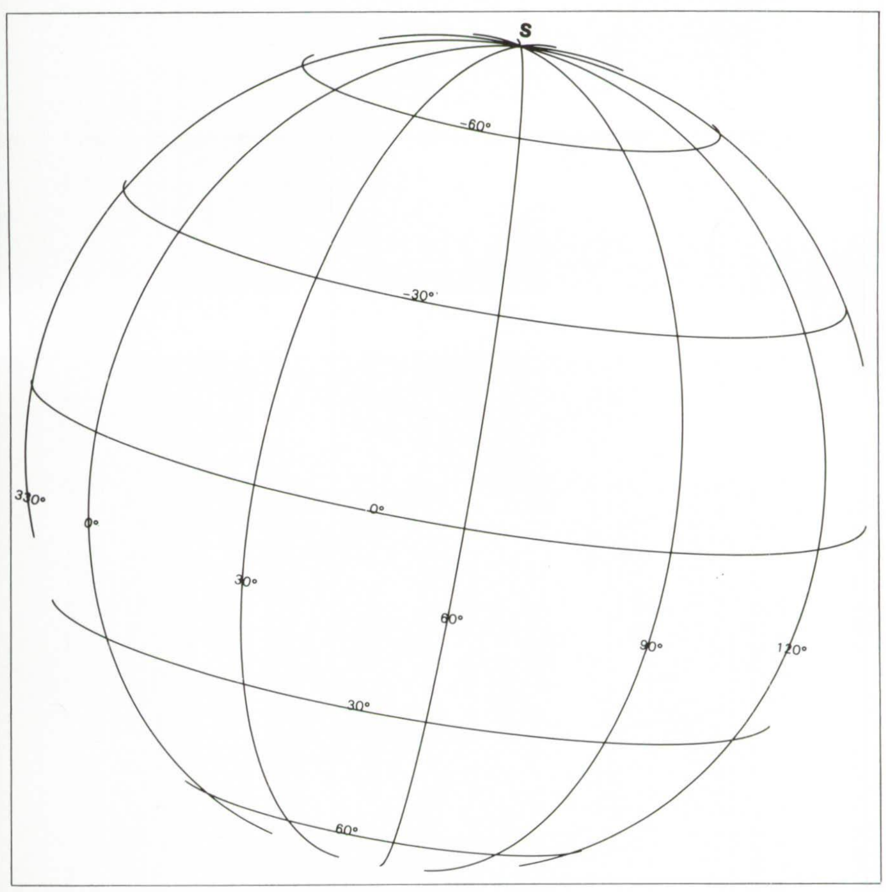

(c)

Picno	0272S1+000
FDS	34948.28
Range, km	162 363
Subspacecraft latitude/longitude, degrees	−10/56
Subsolar latitude/longitude, degrees	4/351
Resolution, km/pixel	1
Filter size, pixels	101 × 101
Filter size, km	152
Scale	1:10 000 000

Figure 4–13. Picno 0272S1+000. (*a*) Unfiltered image. (*b*) High-pass filtered image. (*c*) Perspective grid.

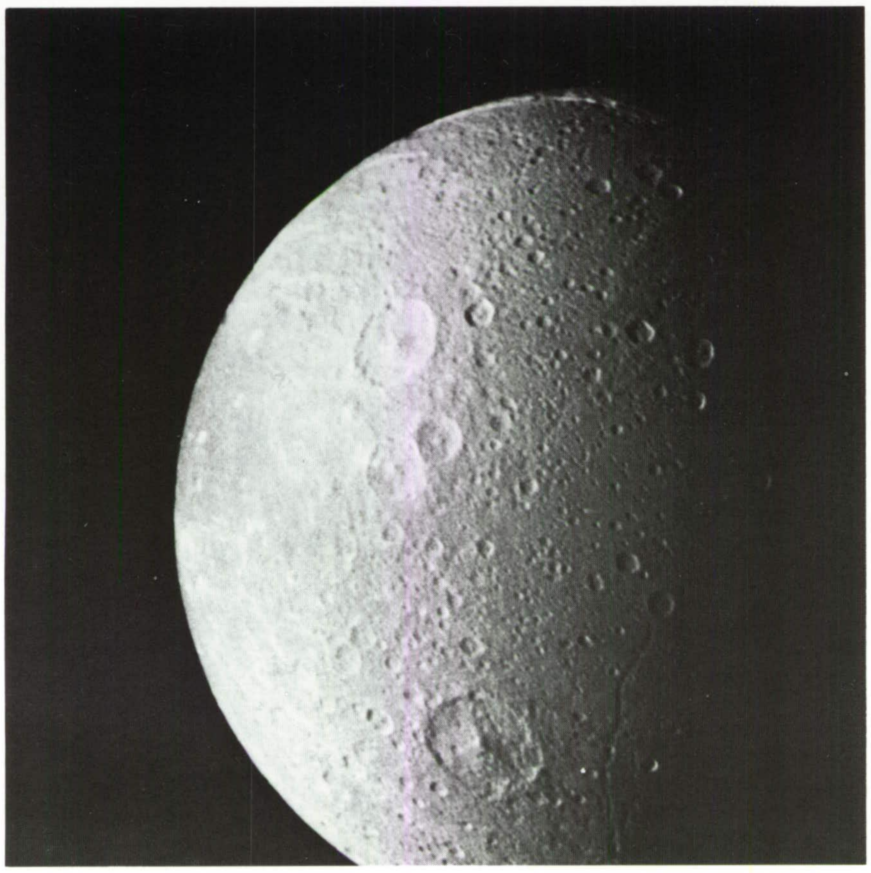

(a)

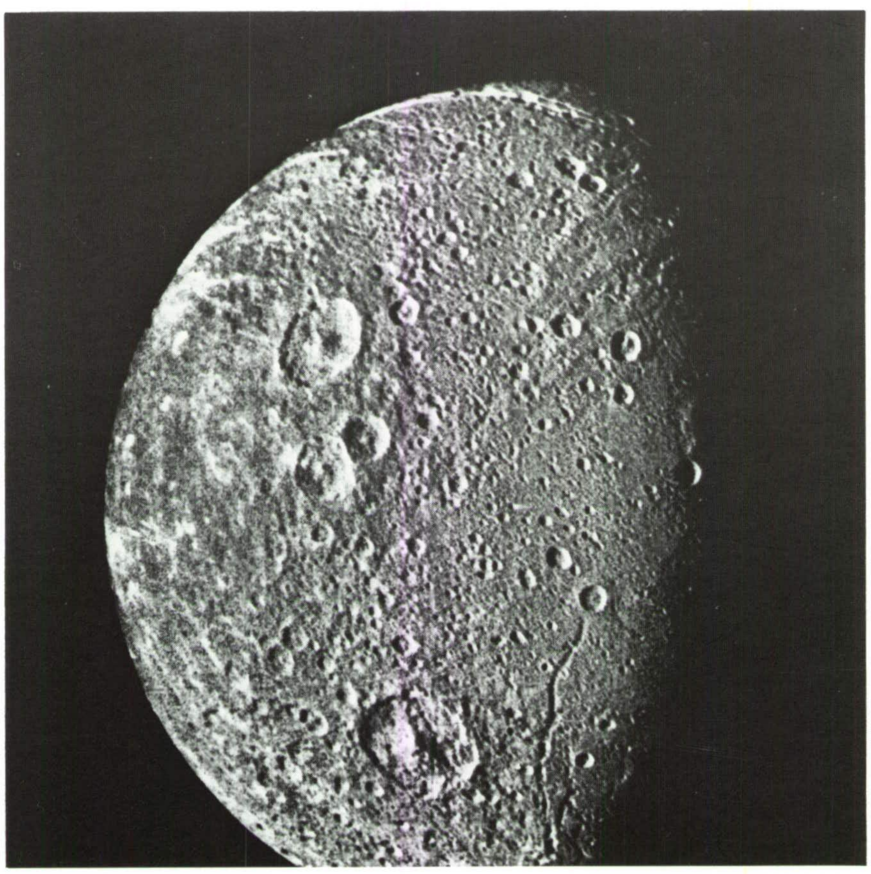

(b)

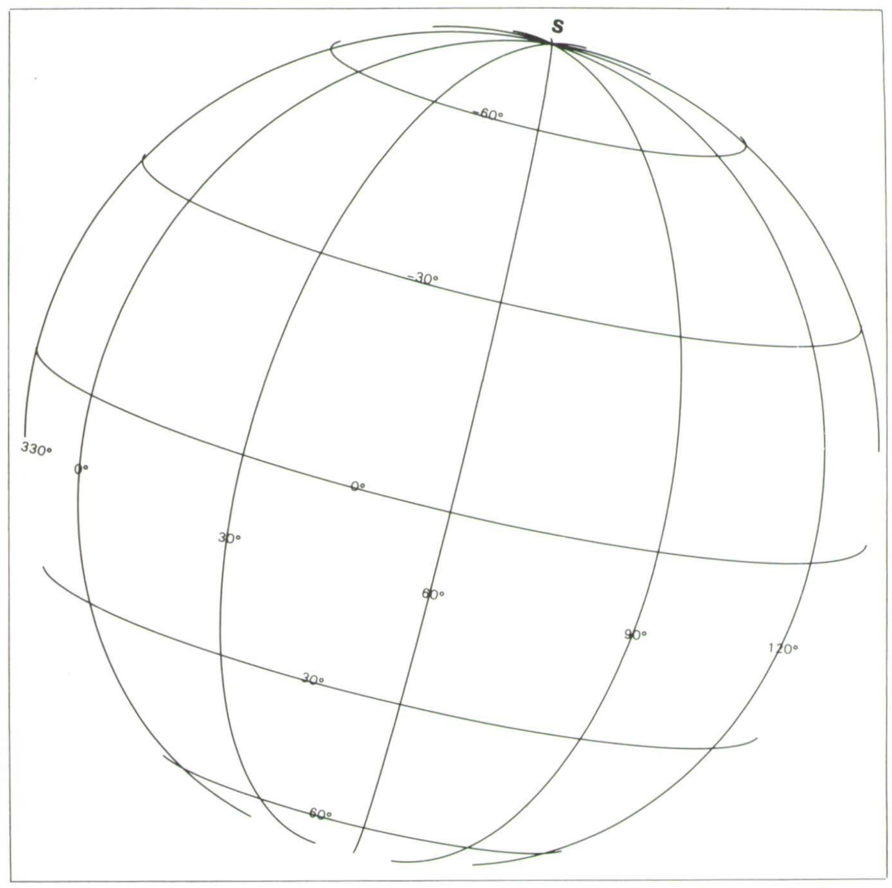

(c)

Picno	0276S1+000
FDS	34948.32
Range, km	162 108
Subspacecraft latitude/longitude, degrees	−9/58
Subsolar latitude/longitude, degrees	4/352
Resolution, km/pixel	1
Filter size, pixels	101 × 101
Filter size, km	151
Scale	1:10 000 000

Figure 4–14. Picno 0276S1+000. (*a*) Unfiltered image. (*b*) High-pass filtered image. (*c*) Perspective grid.

PART 5

Rhea

Diameter	1528 km (949 miles)
Density	1.2
Albedo	0.6
Distance from Saturn	527 828 km (327 976 miles)
Orbital period	108 hr, 39 min, 36 sec
Voyager 1 closest approach	73 980 km (45 969 miles)
Voyager 1 pictures used in mapping	25
Voyager 2 closest approach	645 280 km (400 958 miles)
Voyager 2 pictures used in mapping	0

Rhea is heavily cratered, at least on the Saturn-facing hemisphere, where the highest resolution pictures were taken. Light-colored, "wispy" markings characterize the images on the other side of Rhea. The exact nature of these wispy markings is not known, although they may be frost from water vapor escaping from cracks in the surface. These markings are similar to those found on Dione. The location of the markings with respect to the Saturn-facing hemisphere is probably coincidental.

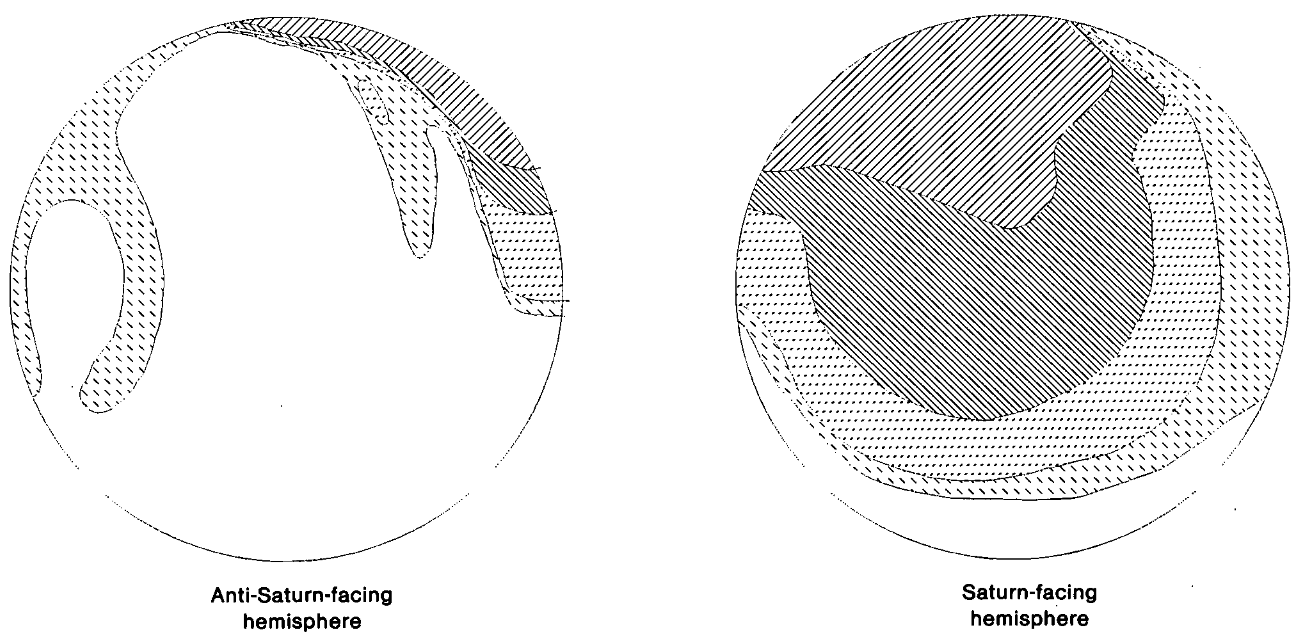

Resolution, km/pixel	Area, km^2	Percent of total
0.5 to 2	846 000	11.5
2 to 5	1 250 000	17.0
5 to 20	978 000	13.3
20 to 40	1 059 000	14.4
>40	3 221 000	43.8

Figure 5–1. Resolution of Voyager pictures of Rhea in terms of aerial coverage.

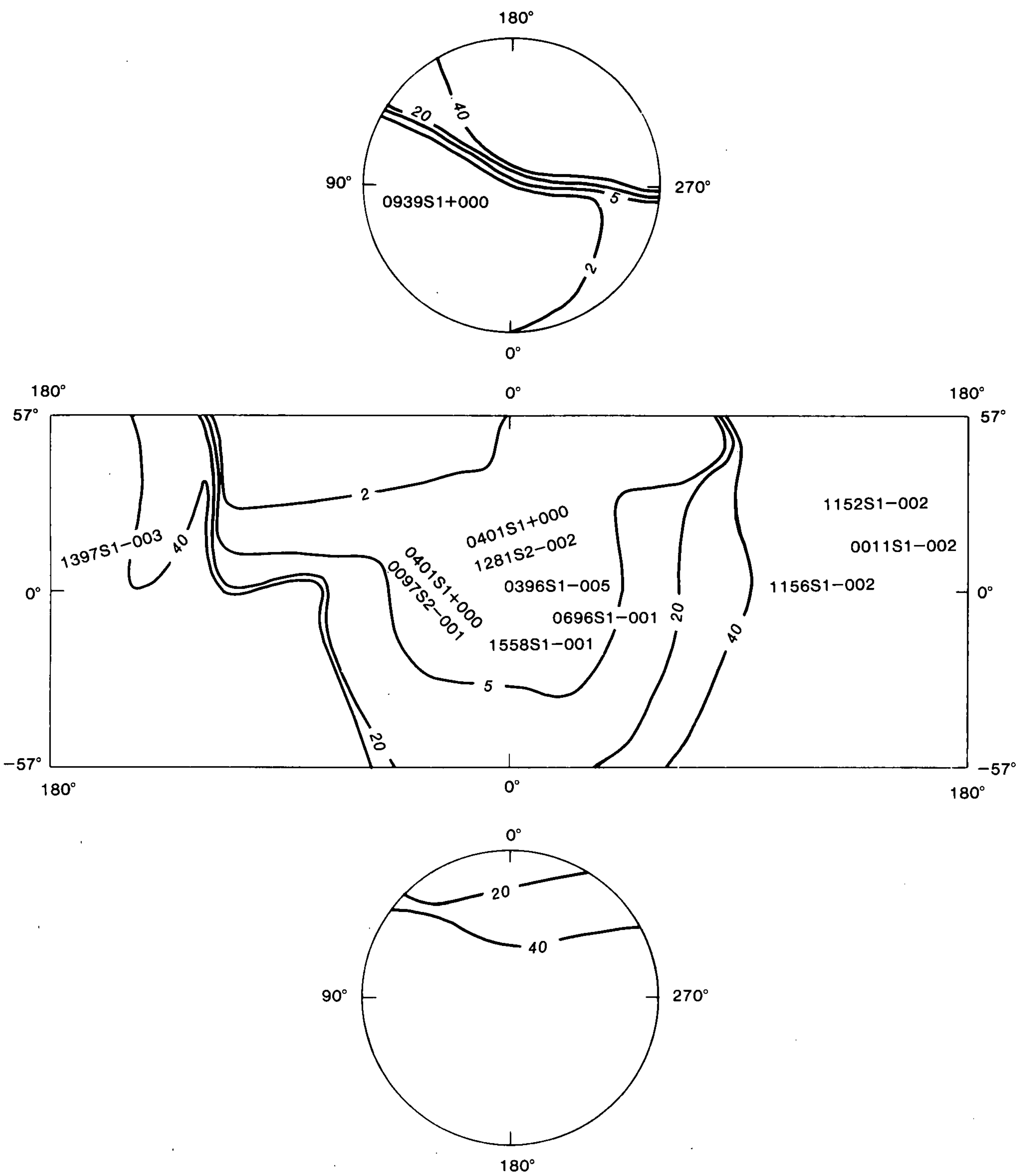

Figure 5–2. Index of Voyager 1 and 2 pictures used to compile the maps of Rhea. Picture numbers indicate the subspacecraft point at the time the pictures were taken. Contour lines indicate the approximate resolution of available images in kilometers per picture element. (See also fig. 5–1.)

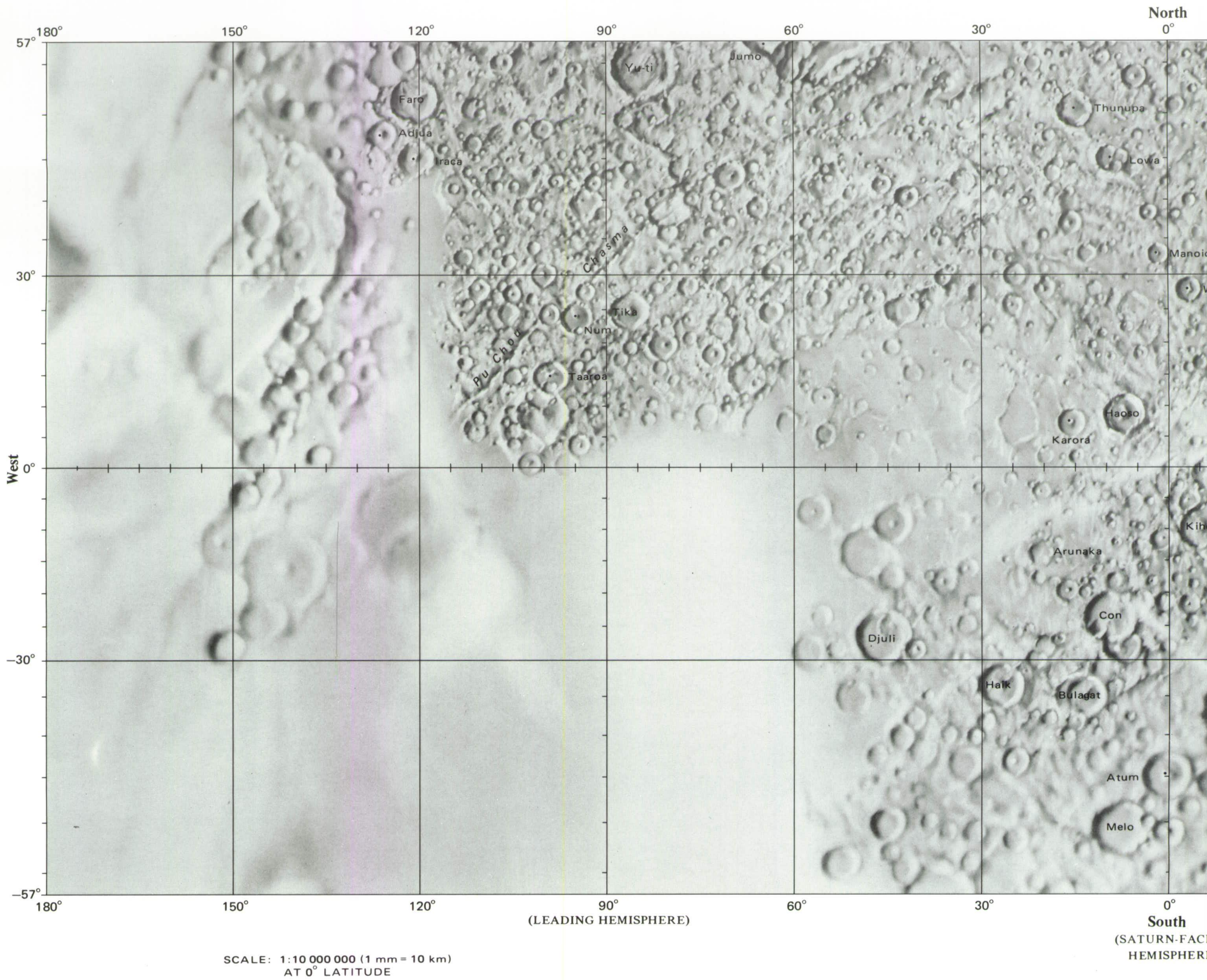
North
180°
150°
120°
90°
60°
30°
0°
57°
30°
0°
−30°
−57°
West
Yu-ti
Jumo
Faro
Adjua
Iraca
Thunupa
Lowa
Pu Chou Chasma
Tika
Num
Taaroa
Haoso
Karora
Arunaka
Con
Djuli
Haik
Bulagat
Atum
Melo
(LEADING HEMISPHERE)
South

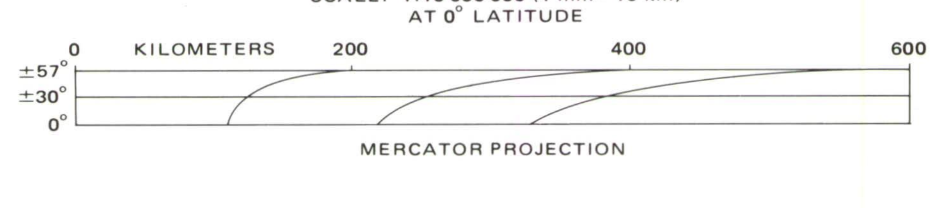
SCALE: 1:10 000 000 (1 mm = 10 km)
AT 0° LATITUDE
0
KILOMETERS
200
400
600
±57°
±30°
0°
MERCATOR PROJECTION

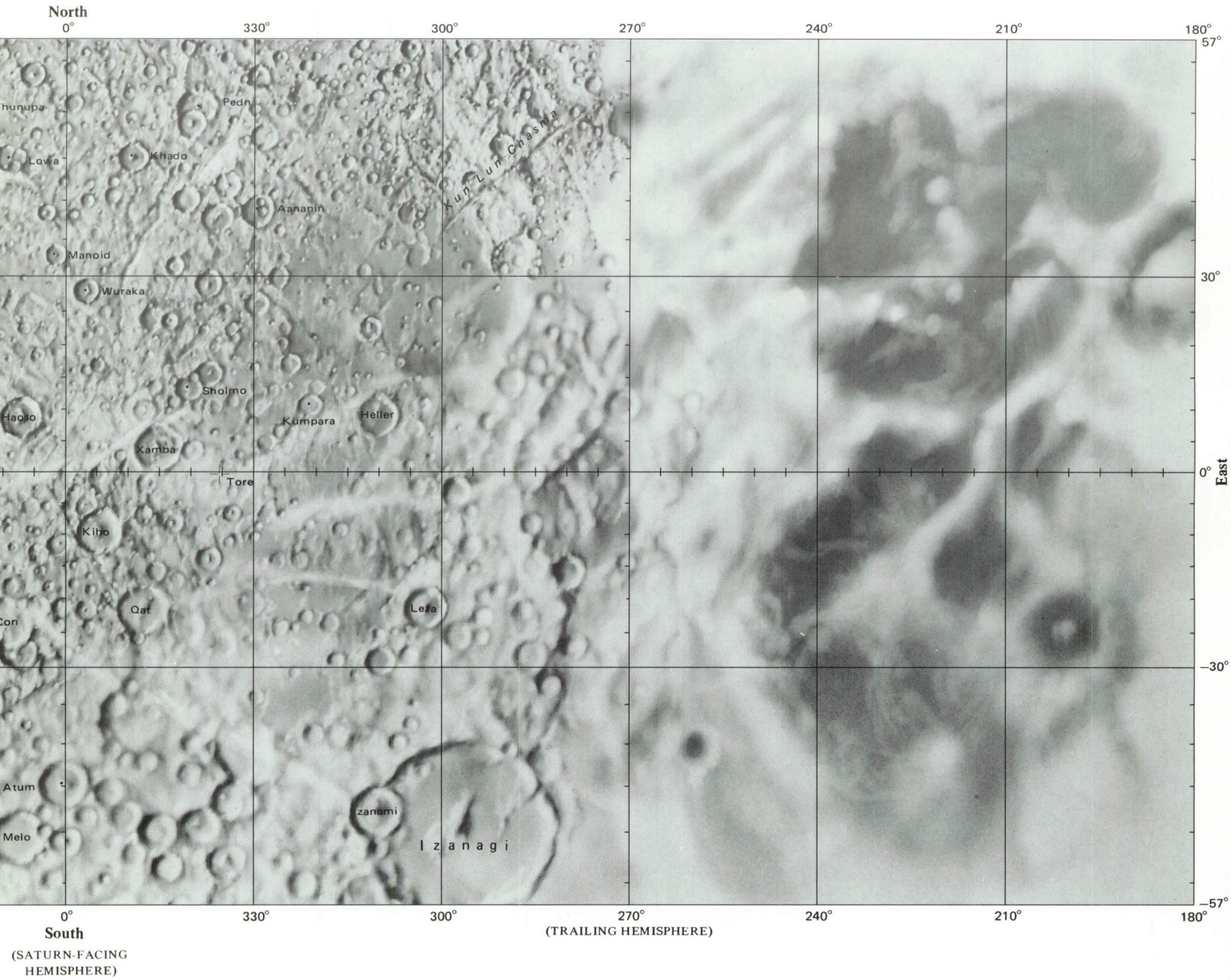

Figure 5–3. Map of the equatorial region of Rhea on a Mercator projection (part of map I–1484).

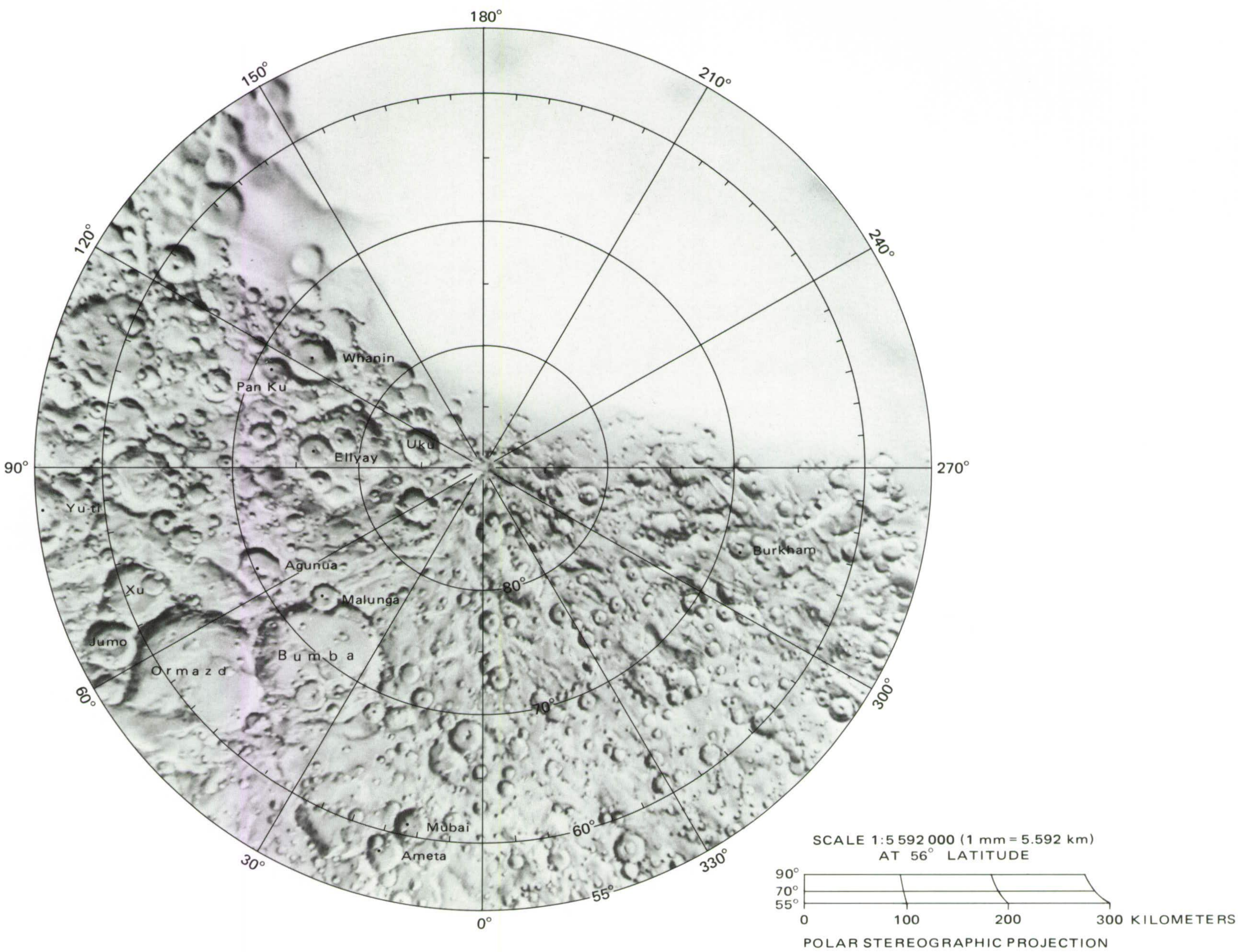

Figure 5–4. Map of the north polar regions of Rhea on a polar stereographic projection (part of map I–1484).

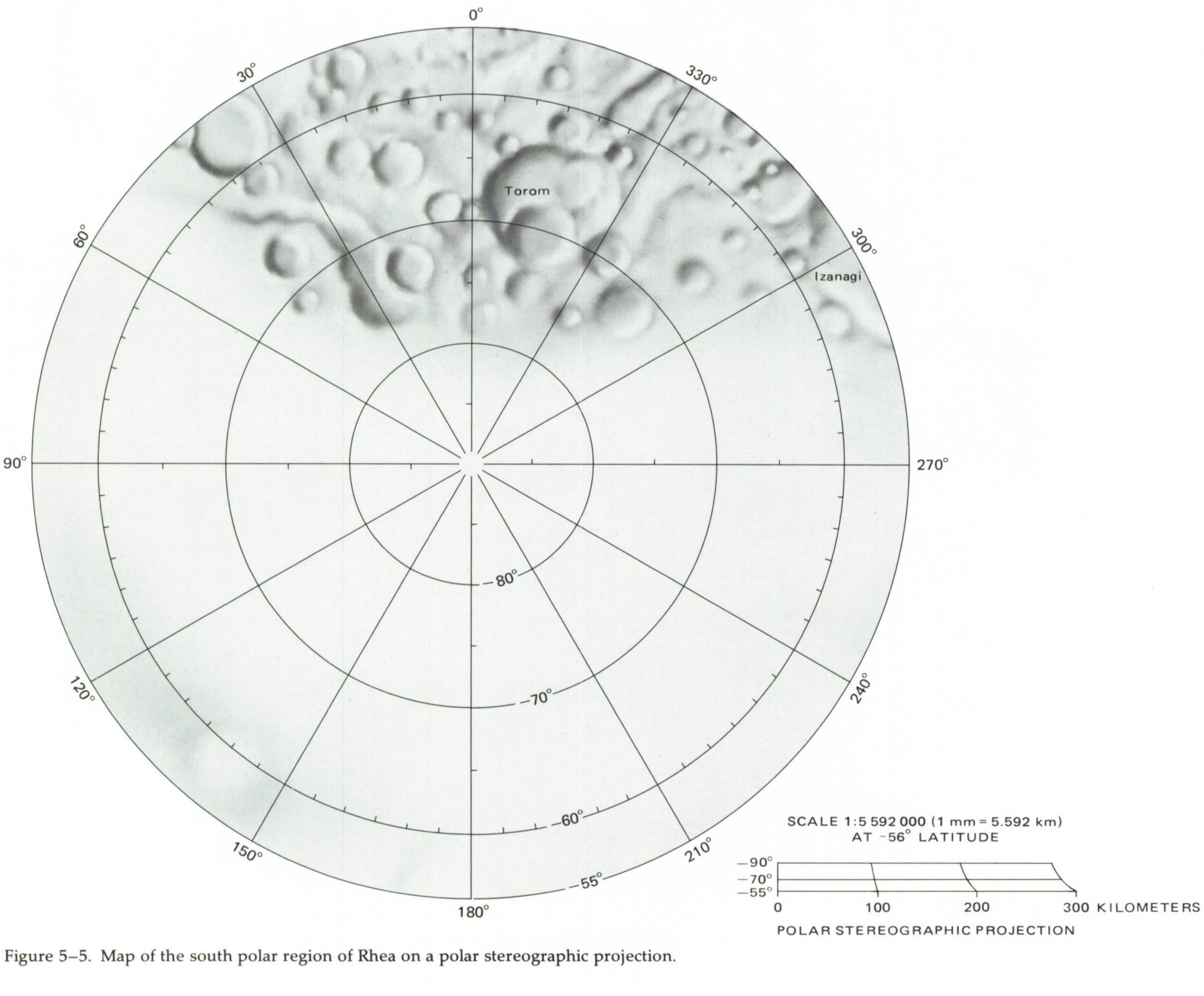

Figure 5–5. Map of the south polar region of Rhea on a polar stereographic projection.

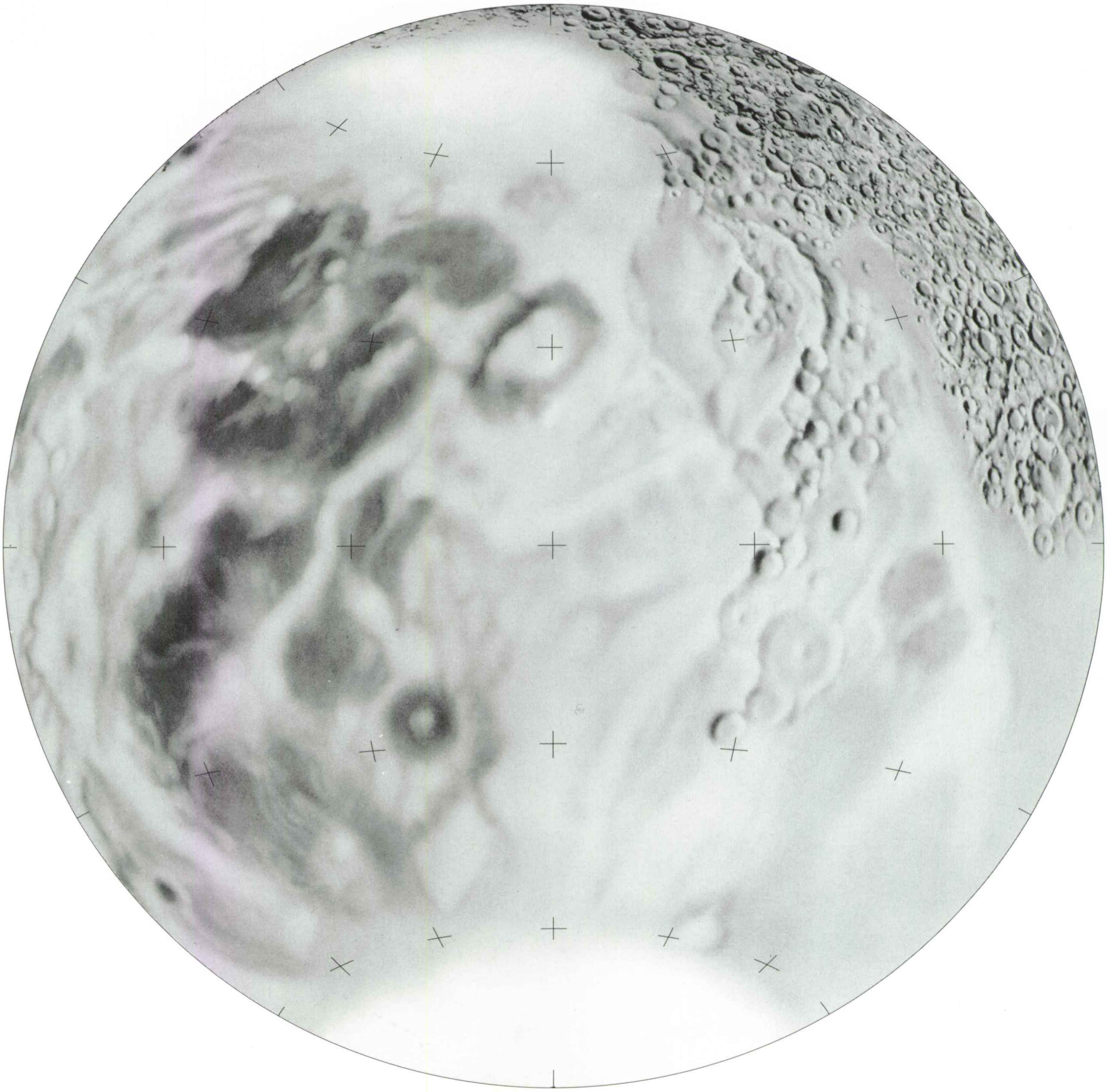

Figure 5–6. Map of the anti-Saturn-facing hemisphere of Rhea on a Lambert azimuthal equal-area projection. Nomenclature is not shown, to avoid obscuring detail. Scale 1:10 000 000 (1 mm^2 = 100 km^2; 1 in^2 = ~25 000 mi^2).

Figure 5–7. Map of the Saturn-facing hemisphere of Rhea on a Lambert azimuthal equal-area projection. Nomenclature is not shown, to avoid obscuring detail. Scale 1:10 000 000 (1 mm^2 = 100 km^2; 1 in^2 = ~25 000 mi^2).

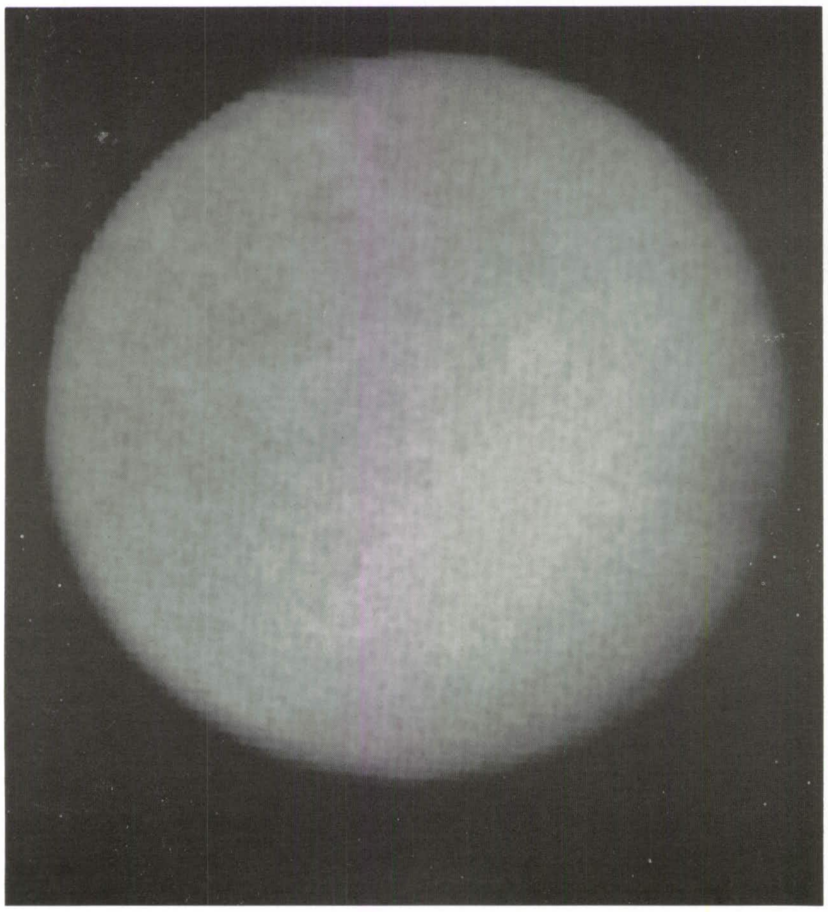

(a)

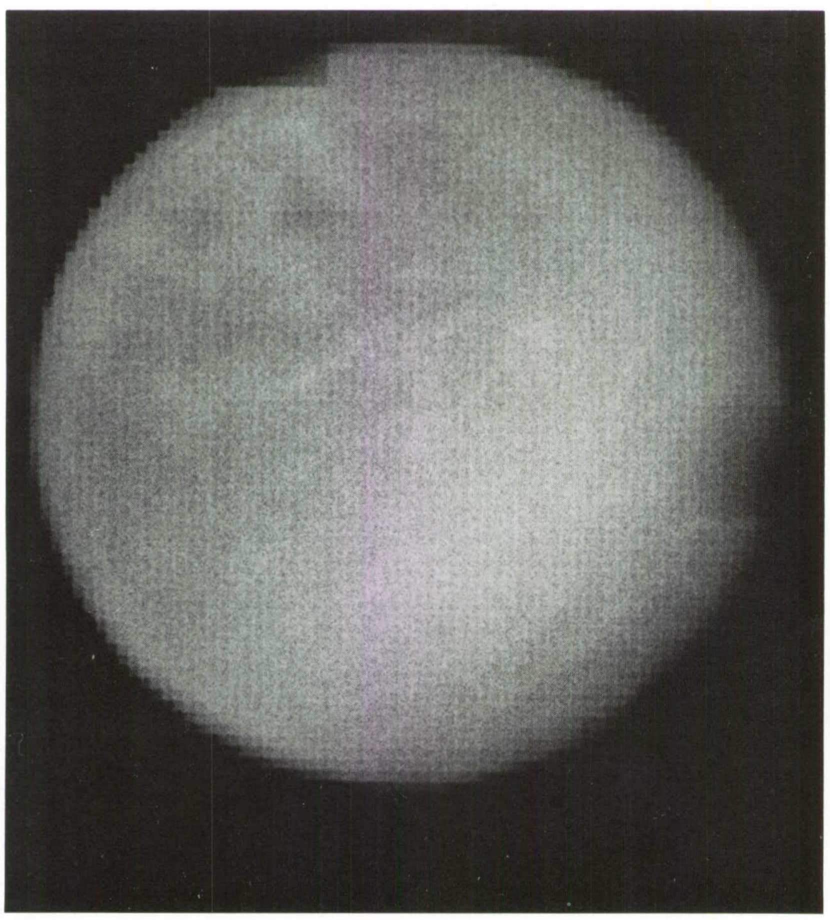

(b)

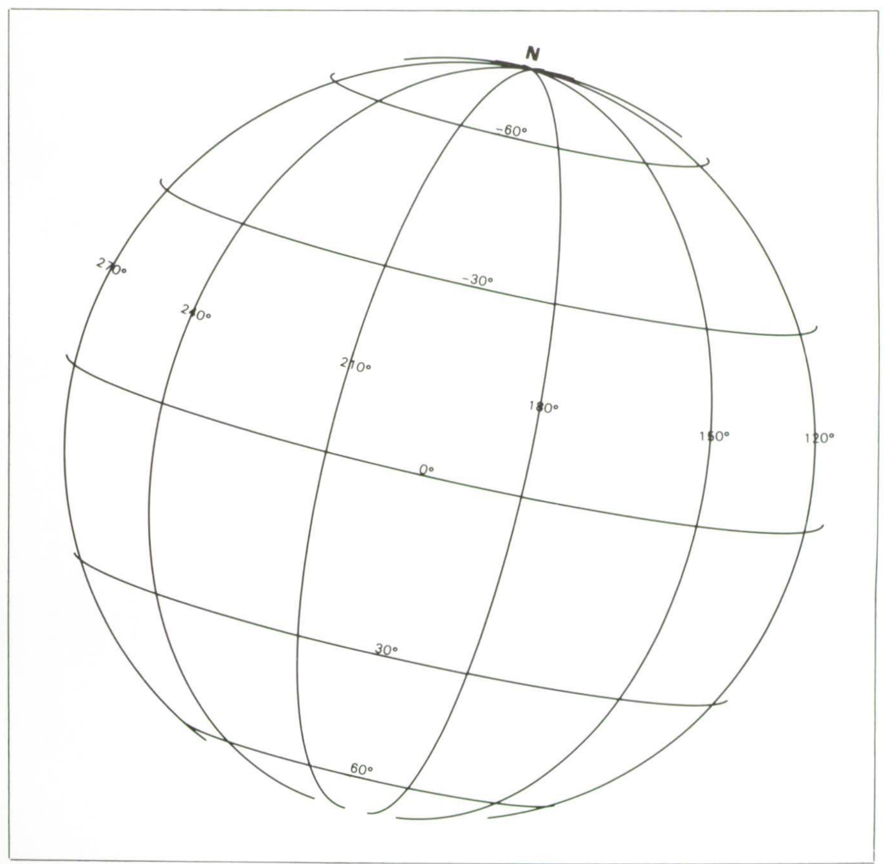

(c)

Picno	0011S1−002
FDS	34884.07
Range, km	2 428 265
Subspacecraft latitude/longitude, degrees	6/193
Subsolar latitude/longitude, degrees	3/207
Resolution, km/pixel	22
Filter size, pixels	101 × 101
Filter size, km	2268
Scale	1:15 000 000

Figure 5–8. Picno 0011S1−002. (*a*) Unfiltered image. (*b*) High-pass filtered image. (*c*) Perspective grid.

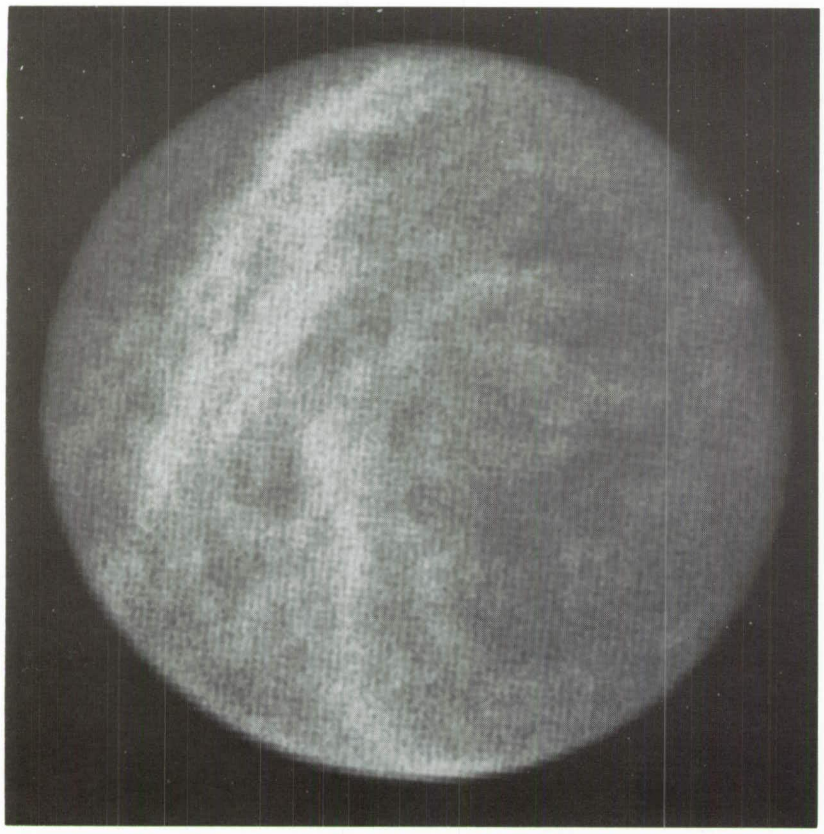

(a)

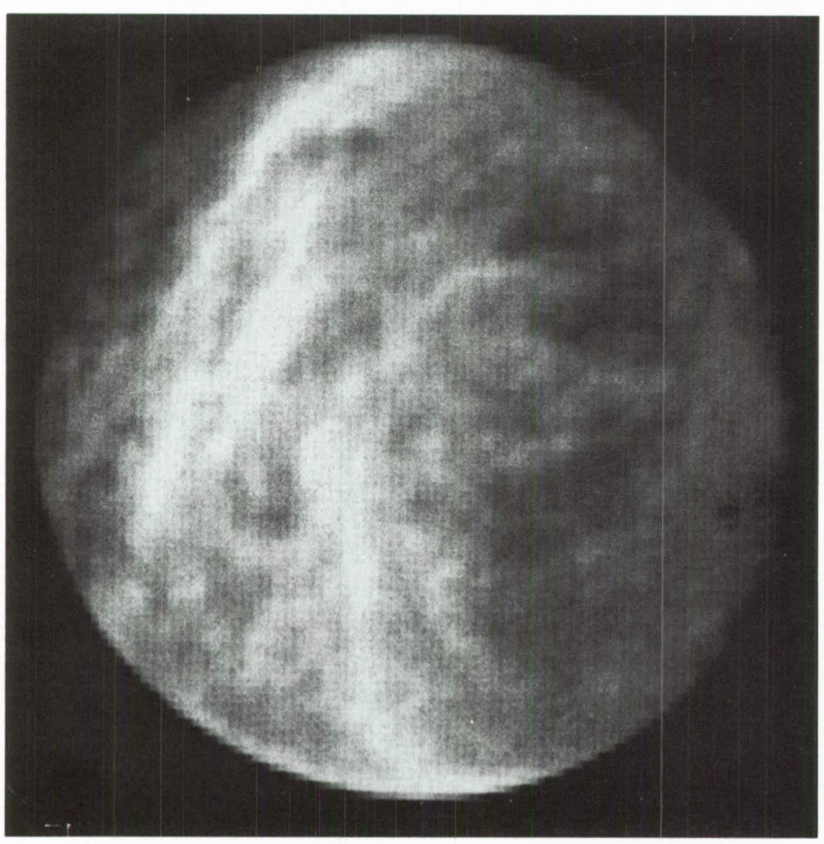

(b)

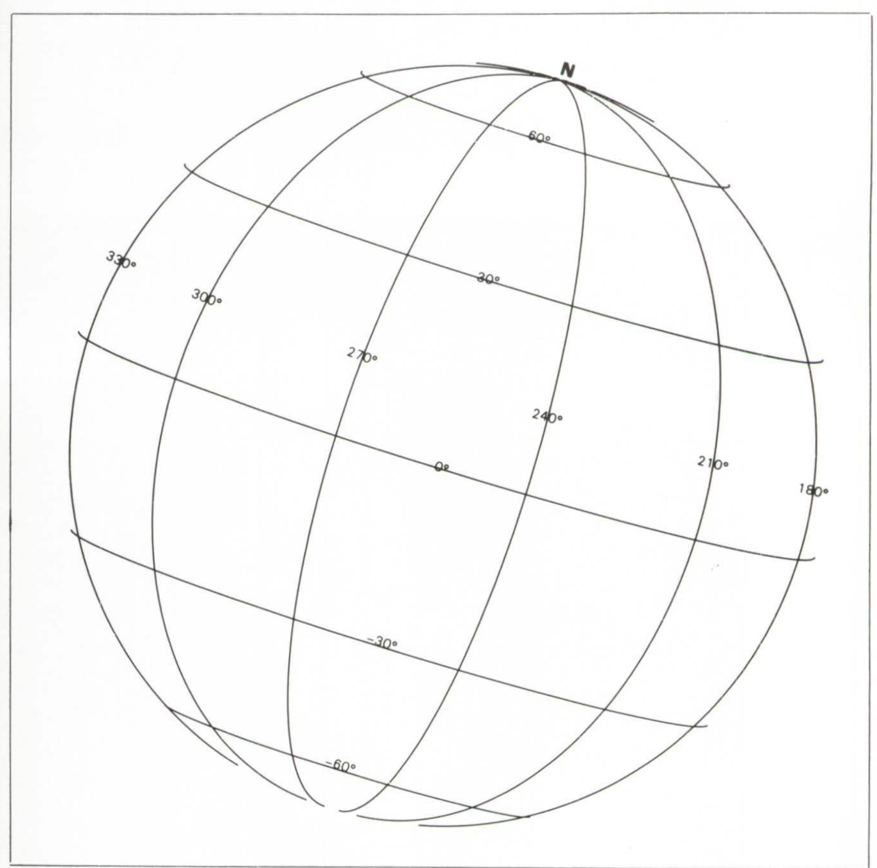

(c)

Picno	1156S1−002
FDS	34903.12
Range, km	1 849 831
Subspacecraft latitude/longitude, degrees	4/254
Subsolar latitude/longitude, degrees	3/257
Resolution, km/pixel	17
Filter size, pixels	101 × 101
Filter size, km	1728
Scale	1:15 000 000

Figure 5–9. Picno 1156S1−002. (*a*) Unfiltered image. (*b*) High-pass filtered image. (*c*) Perspective grid.

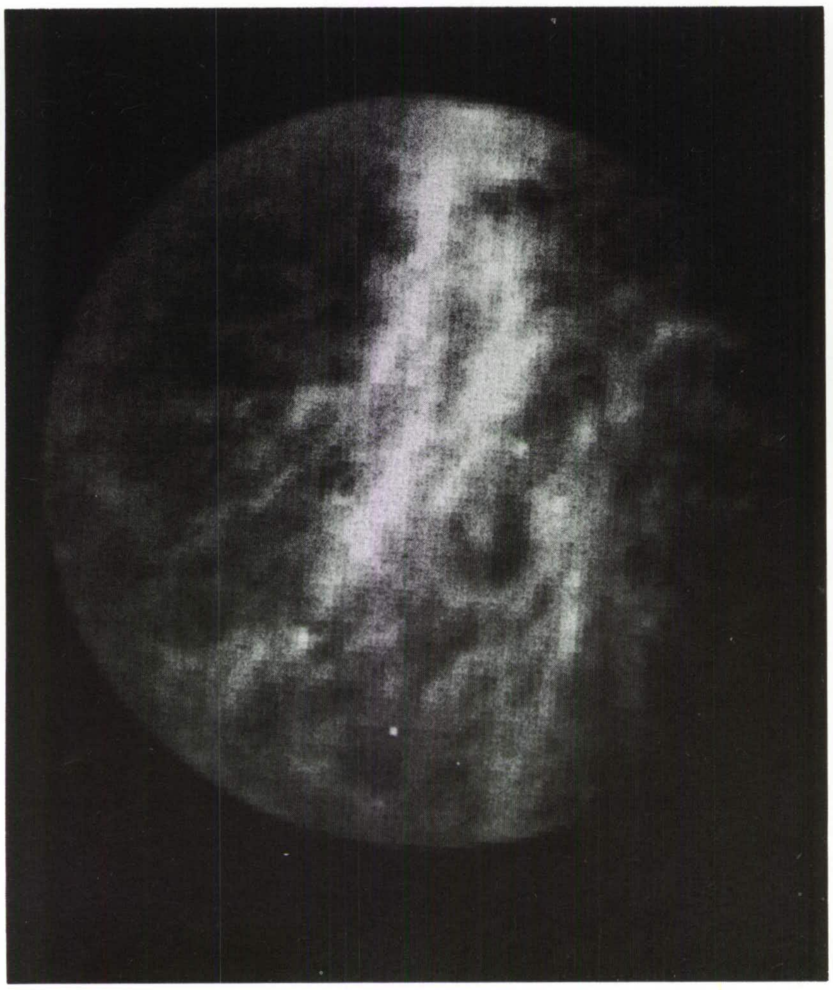

(*a*)

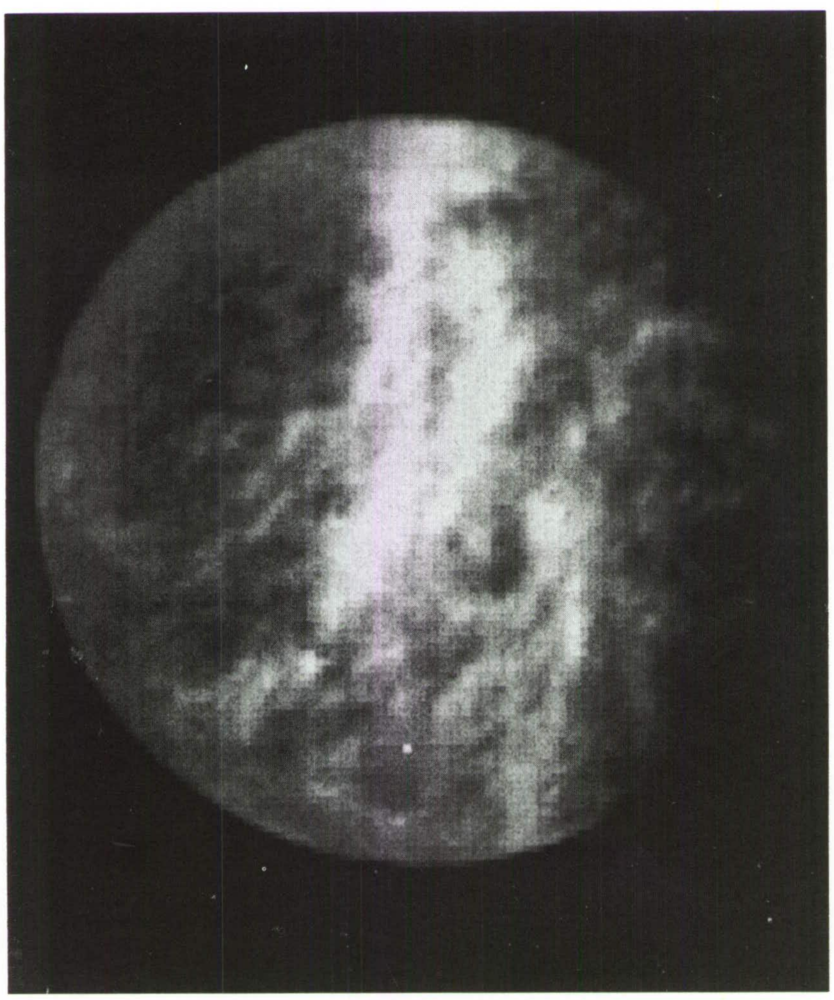

(*b*)

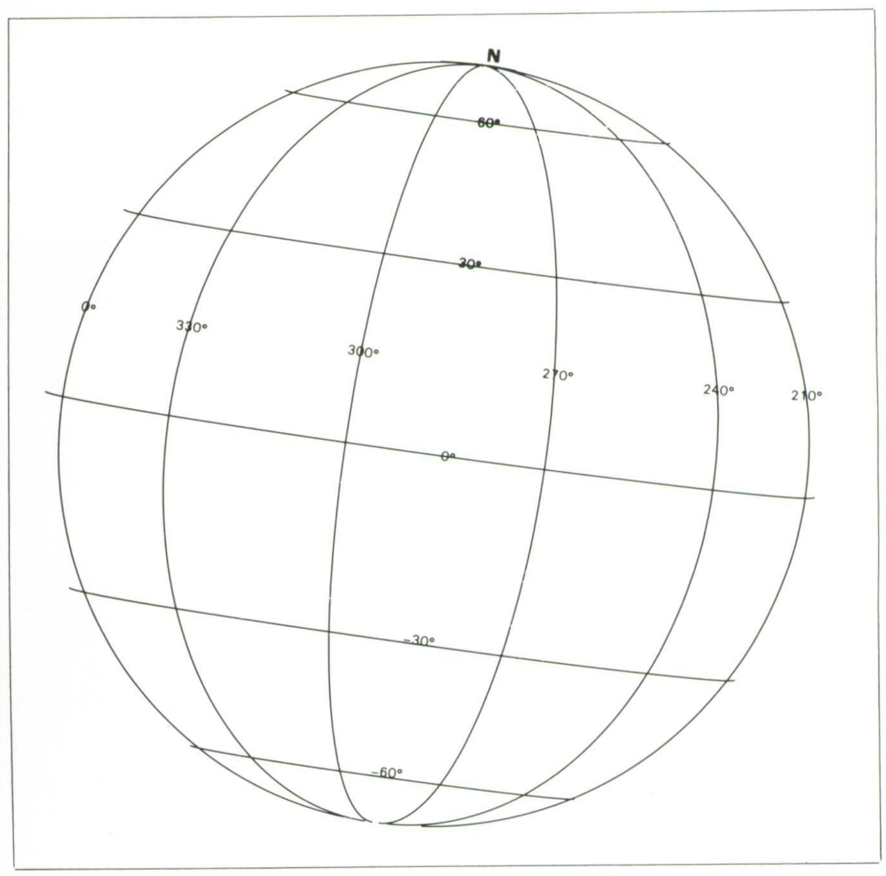

(*c*)

Picno	0055S1−001
FDS	34914.51
Range, km	1 586 518
Subspacecraft latitude/longitude, degrees	1/288
Subsolar latitude/longitude, degrees	3/288
Resolution, km/pixel	14
Filter size, pixels	101 × 101
Filter size, km	1482
Scale	1:15 000 000

Figure 5–10. Picno 0055S1−001. (*a*) Unfiltered image. (*b*) High-pass filtered image. (*c*) Perspective grid.

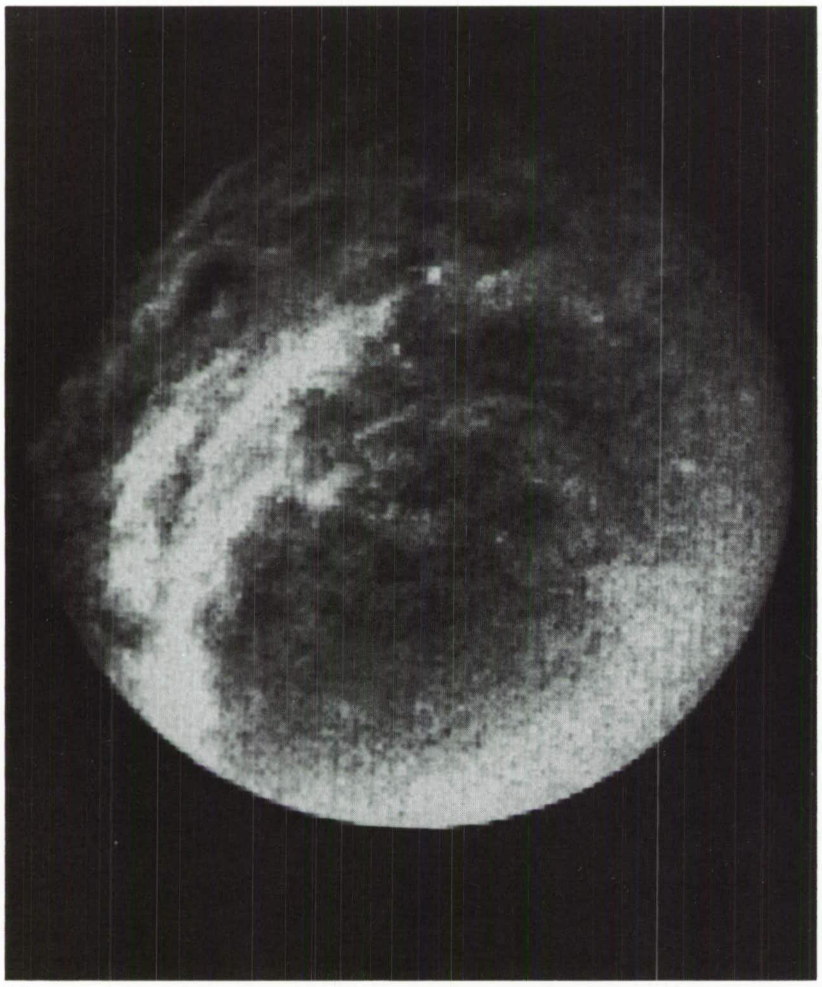

(a)

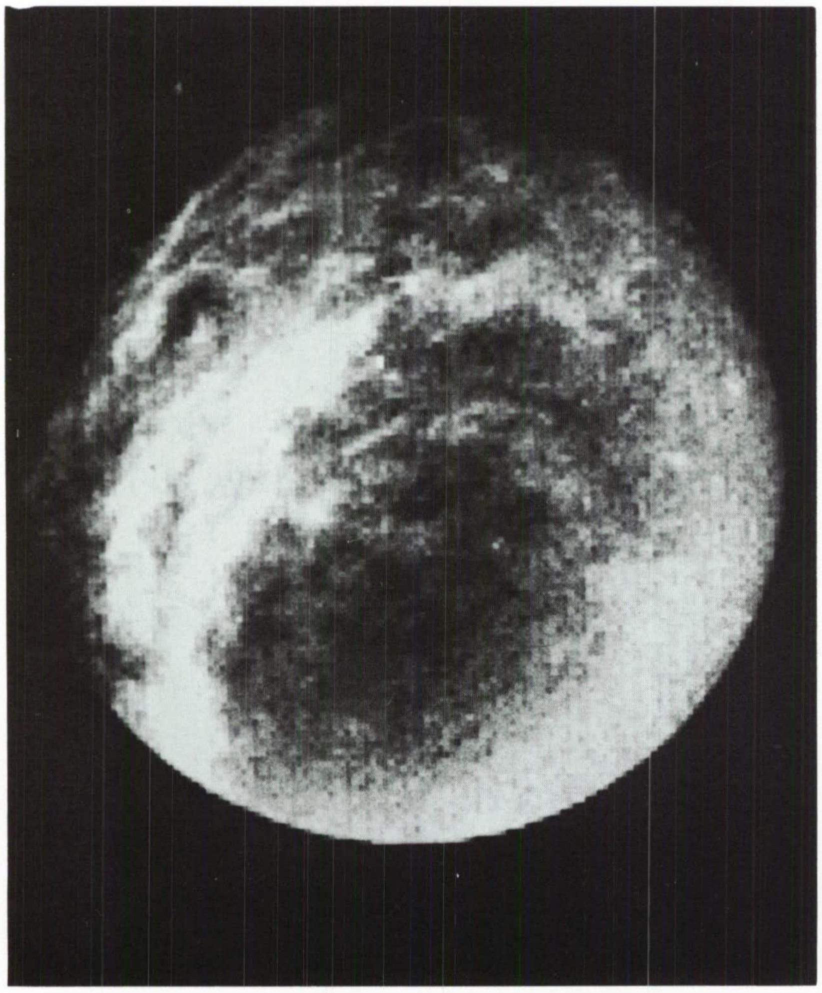

(b)

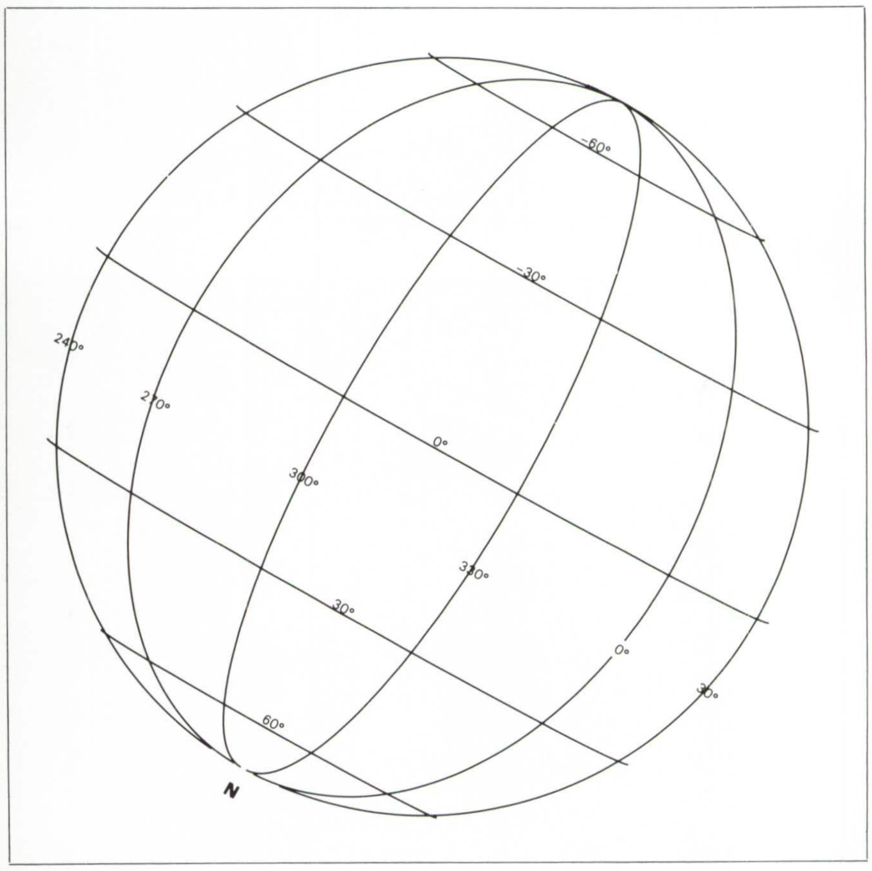

(c)

Picno	0696S1—001
FDS	34925.32
Range, km	1 297 847
Subspacecraft latitude/longitude, degrees	−1/315
Subsolar latitude/longitude, degrees	3/317
Resolution, km/pixel	12
Filter size, pixels	101 × 101
Filter size, km	1212
Scale	1:15 000 000

Figure 5–11. Picno 0696S1—001. (*a*) Unfiltered image. (*b*) High-pass filtered image. (*c*) Perspective grid.

(a)

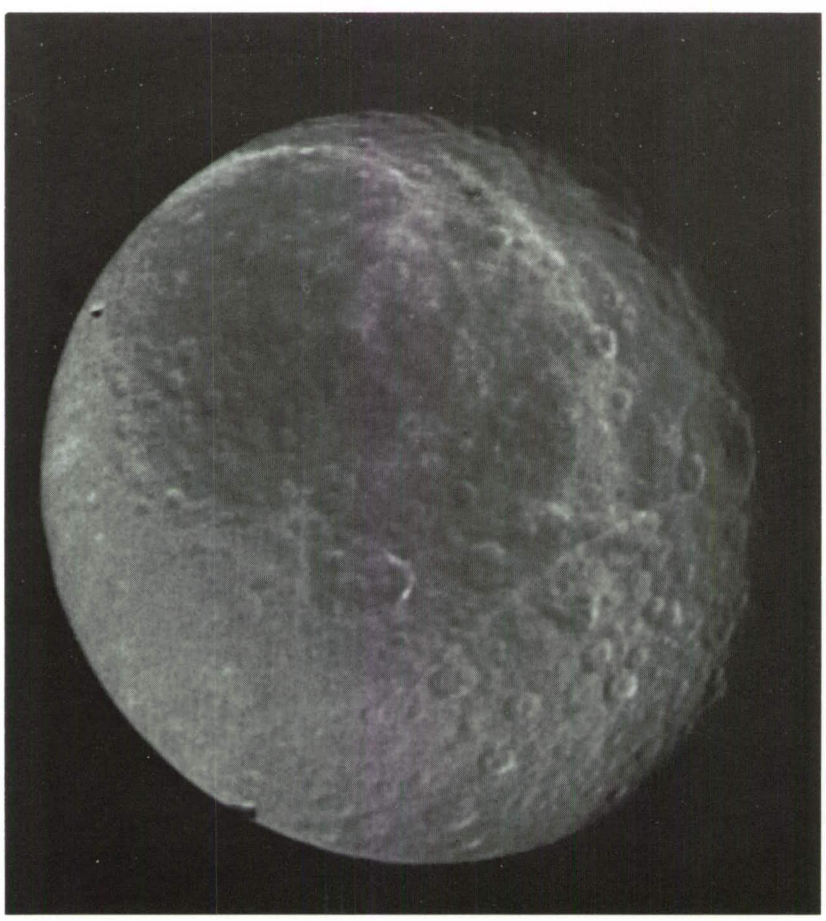

(b)

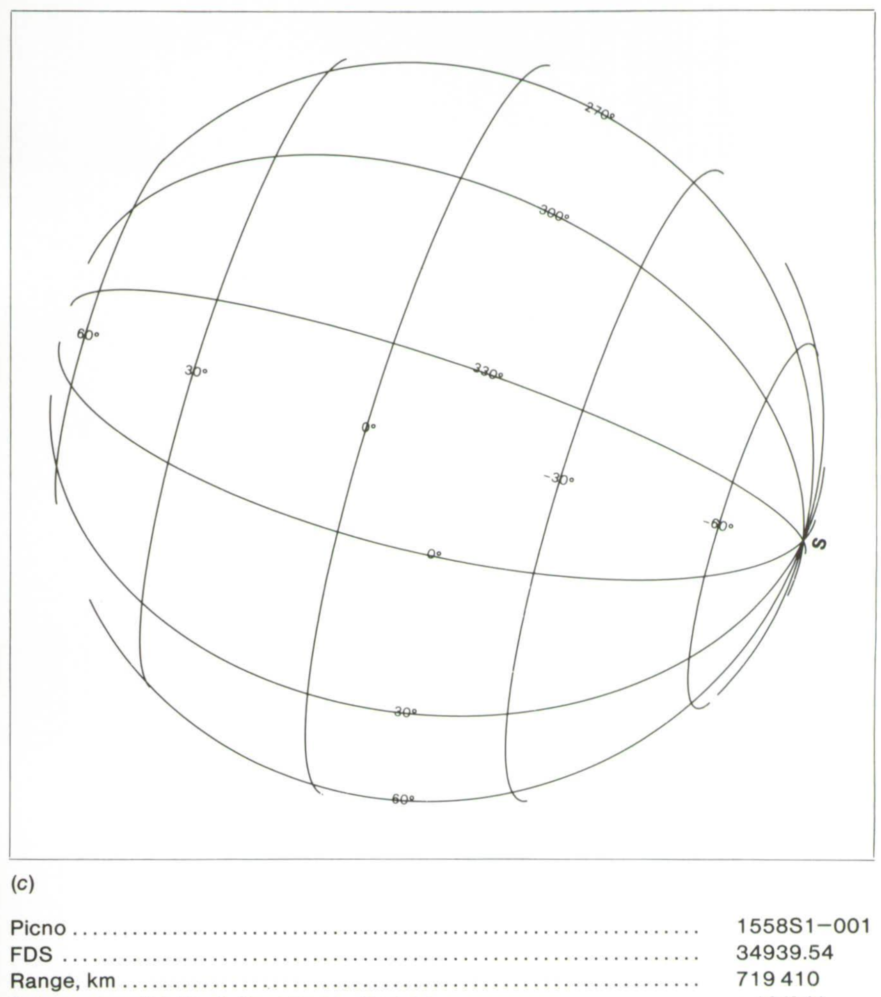

(c)

Picno	1558S1−001
FDS	34939.54
Range, km	719 410
Subspacecraft latitude/longitude, degrees	−10/341
Subsolar latitude/longitude, degrees	3/355
Resolution, km/pixel	6
Filter size, pixels	101 × 101
Filter size, km	672
Scale	1:15 000 000

Figure 5–12. Picno 1558S1−001. (*a*) Unfiltered image. (*b*) High-pass filtered image. (*c*) Perspective grid.

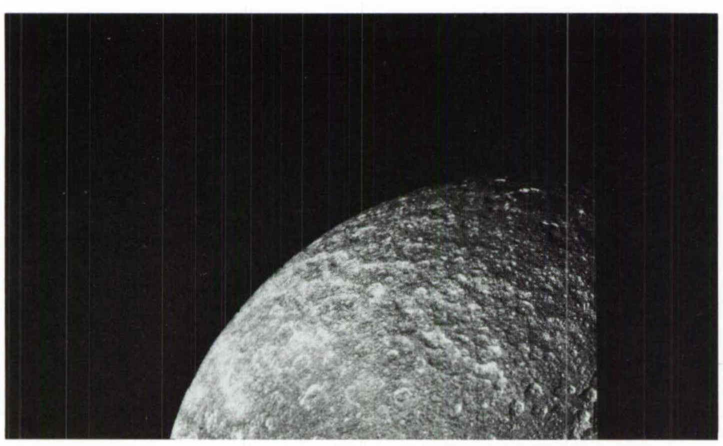

(a)

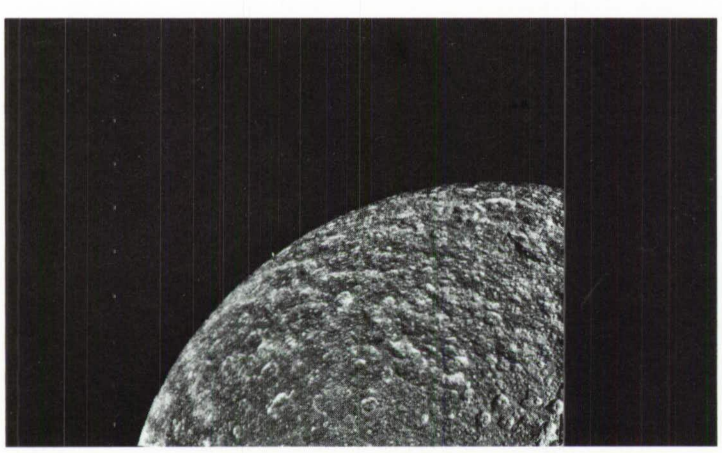

(b)

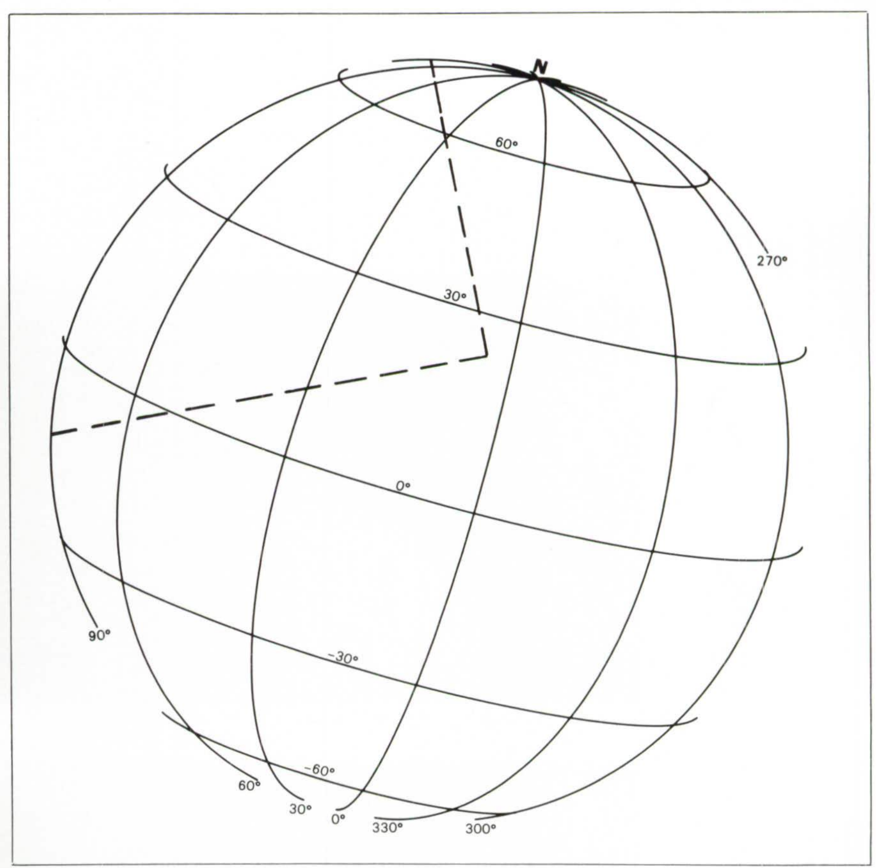

(c)

Picno	0387S1+000
FDS	34950.23
Range, km	121 017
Subspacecraft latitude/longitude, degrees	9/9
Subsolar latitude/longitude, degrees	3/22
Resolution, km/pixel	1
Filter size, pixels	101 × 101
Filter size, km	113
Scale	1:15 000 000

Figure 5–13. Picno 0387S1+000. (*a*) Unfiltered image. (*b*) High-pass filtered image. (*c*) Perspective grid.

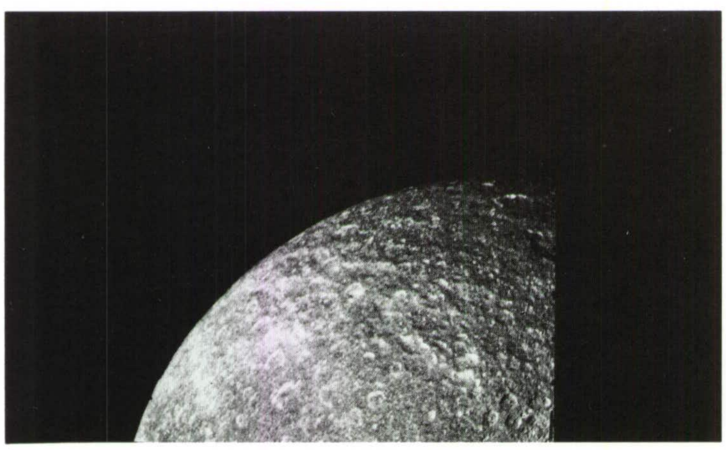

(a)

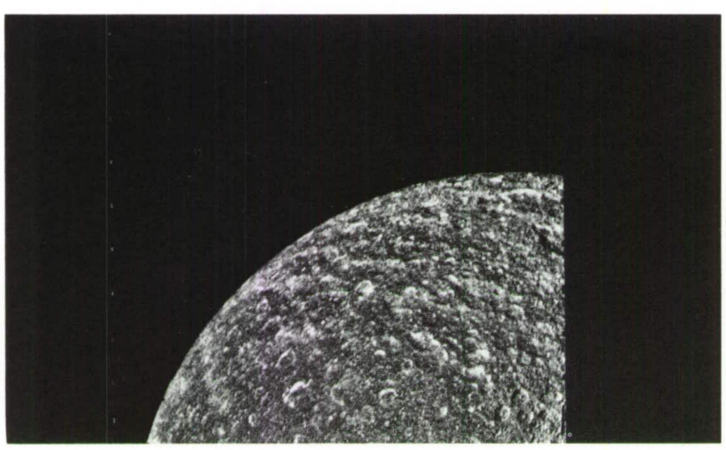

(b)

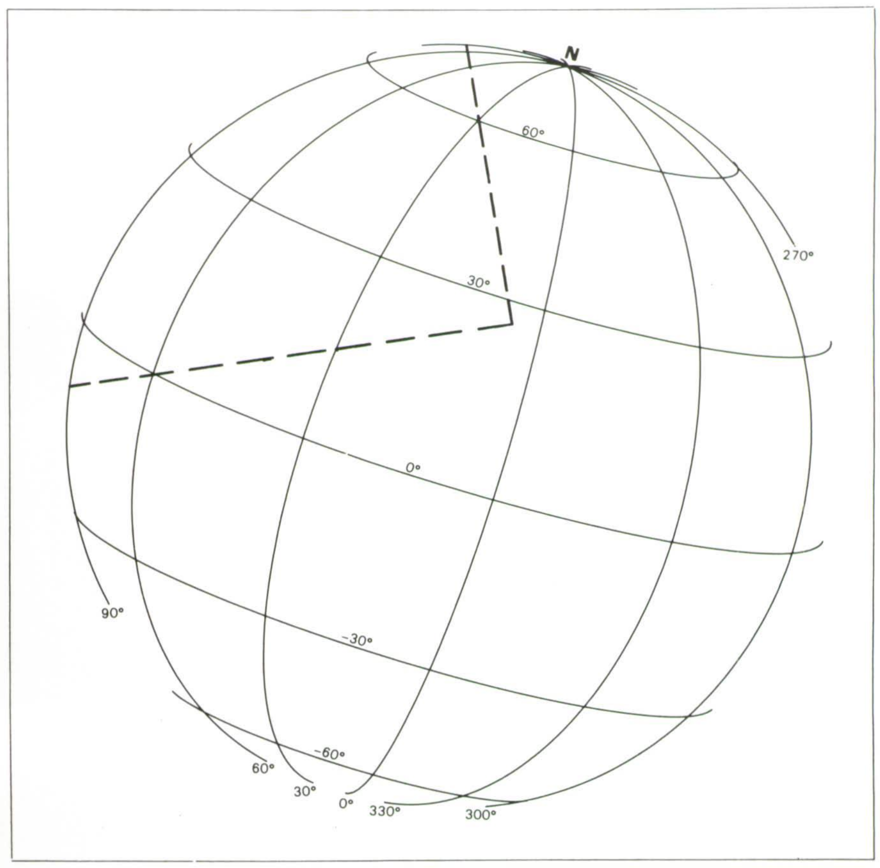

(c)

Picno	0389S1+000
FDS	34950.25
Range, km	119 645
Subspacecraft latitude/longitude, degrees	9/9
Subsolar latitude/longitude, degrees	3/22
Resolution, km/pixel	1
Filter size, pixels	101 × 101
Filter size, km	112
Scale	1:15 000 000

Figure 5–14. Picno 0389S1+000. (*a*) Unfiltered image. (*b*) High-pass filtered image. (*c*) Perspective grid.

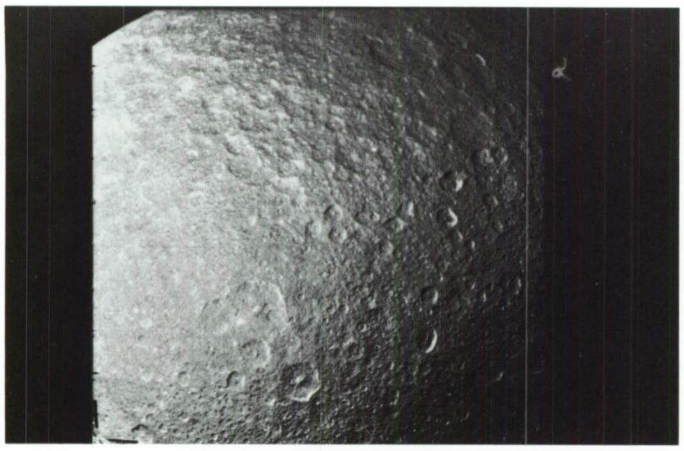

(a)

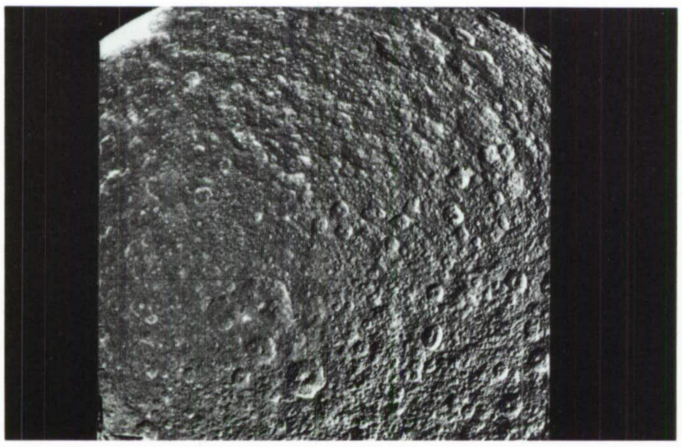

(b)

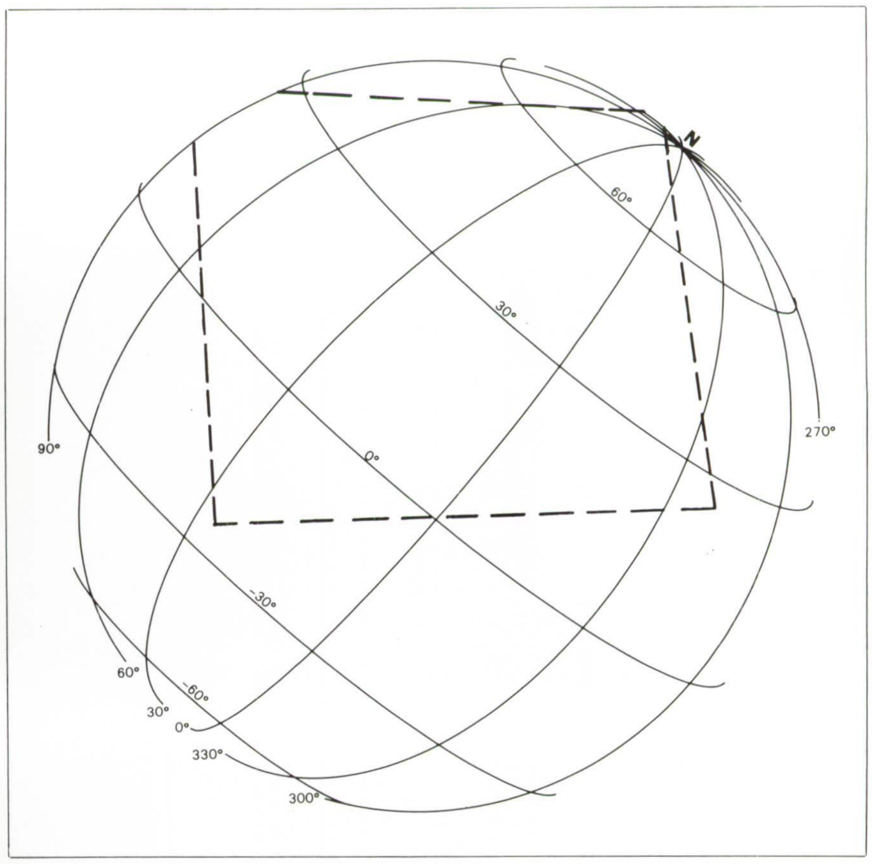

(c)

Picno	0393S1+000
FDS	34950.29
Range, km	116 928
Subspacecraft latitude/longitude, degrees	10/9
Subsolar latitude/longitude, degrees	3/22
Resolution, km/pixel	1
Filter size, pixels	101 × 101
Filter size, km	109
Scale	1:15 000 000

Figure 5–15. Picno 0393S1+000. (*a*) Unfiltered image. (*b*) High-pass filtered image. (*c*) Perspective grid.

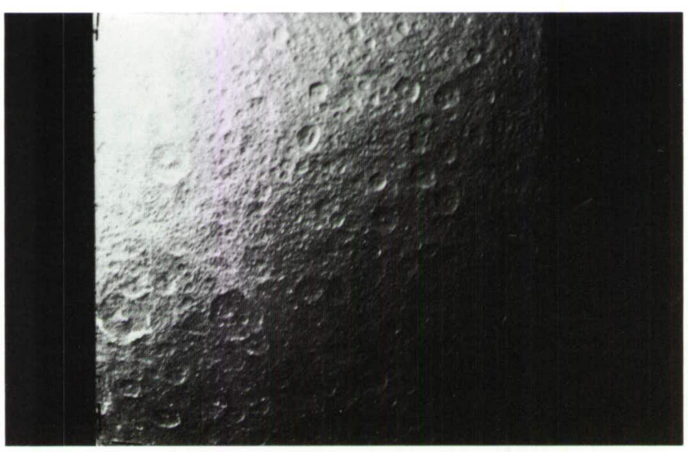

(a)

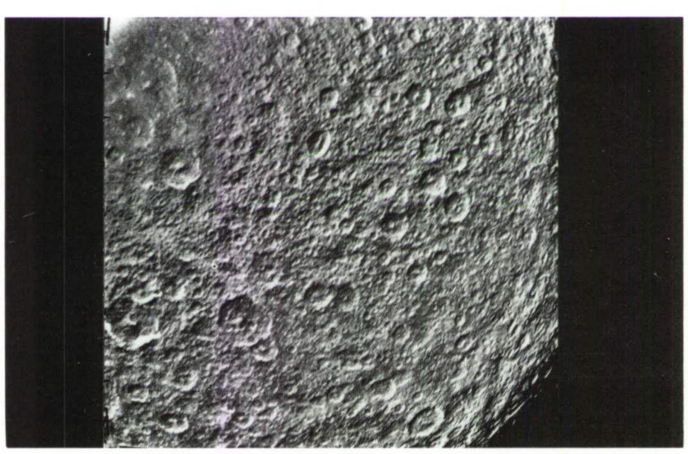

(b)

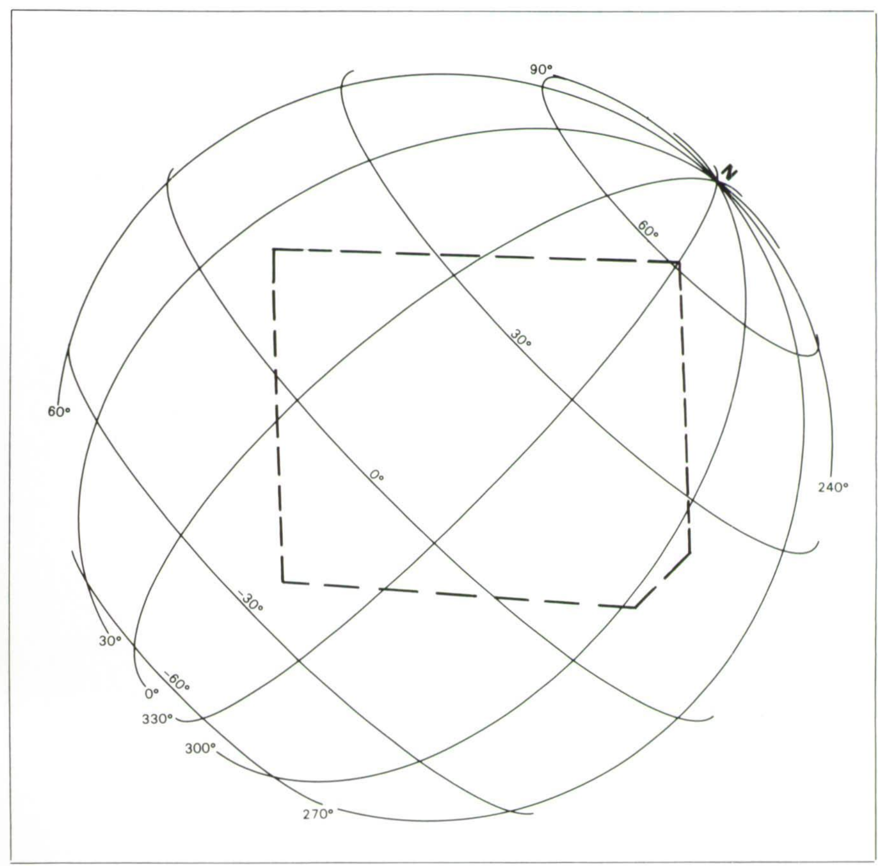

(c)

Picno	0401S1+000
FDS	34950.37
Range, km	111 633
Subspacecraft latitude/longitude, degrees	12/10
Subsolar latitude/longitude, degrees	3/23
Resolution, km/pixel	1
Filter size, pixels	101 × 101
Filter size, km	104
Scale	1:15 000 000

Figure 5–16. Picno 0401S1+000. (*a*) Unfiltered image. (*b*) High-pass filtered image. (*c*) Perspective grid.

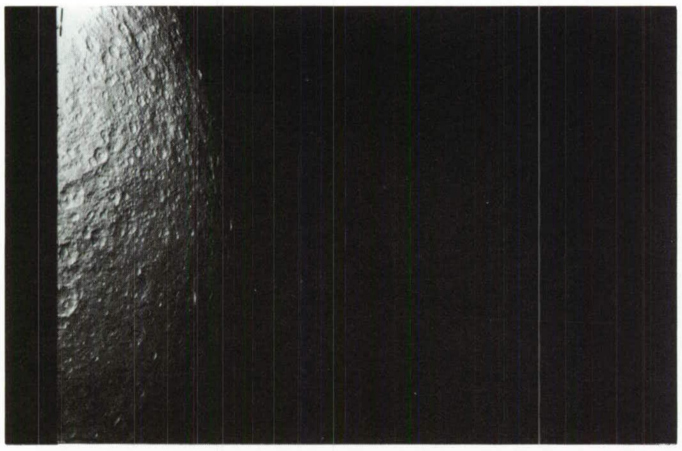

(a)

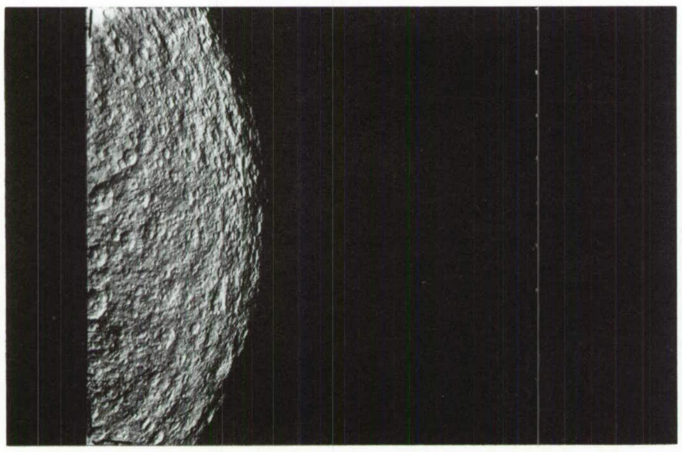

(b)

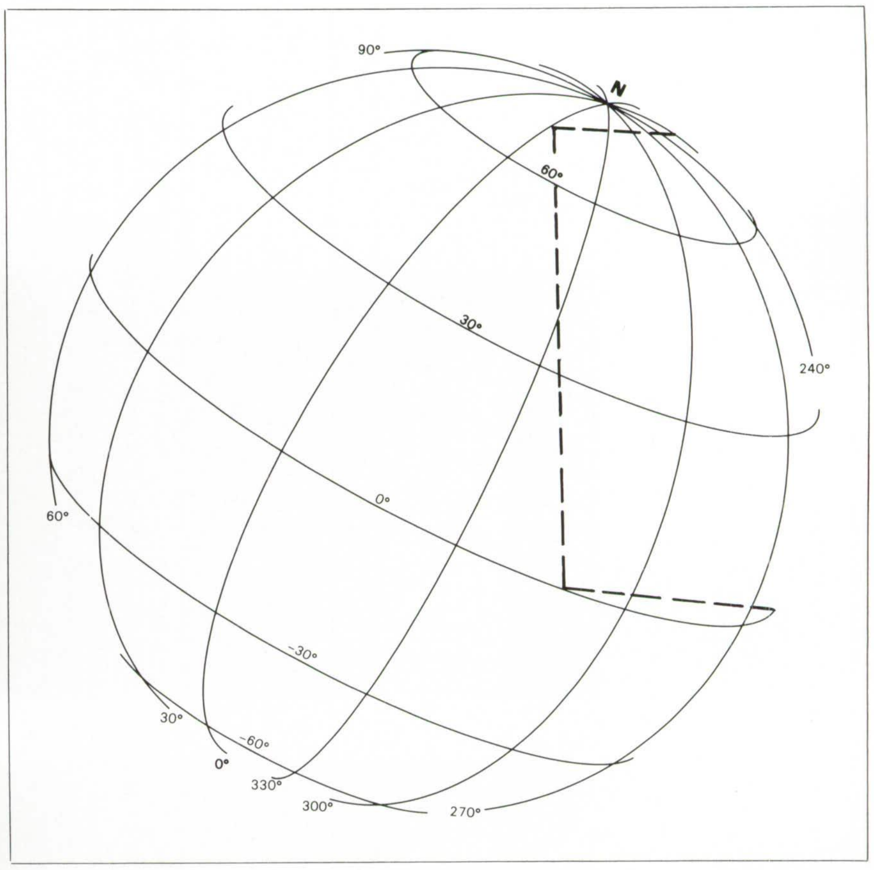

(c)

Picno	0405S1+000
FDS	34950.41
Range, km	109 056
Subspacecraft latitude/longitude, degrees	14/11
Subsolar latitude/longitude, degrees	3/23
Resolution, km/pixel	1
Filter size, pixels	101 × 101
Filter size, km	102
Scale	1:15 000 000

Figure 5–17. Picno 0405S1+000. (*a*) Unfiltered image. (*b*) High-pass filtered image. (*c*) Perspective grid.

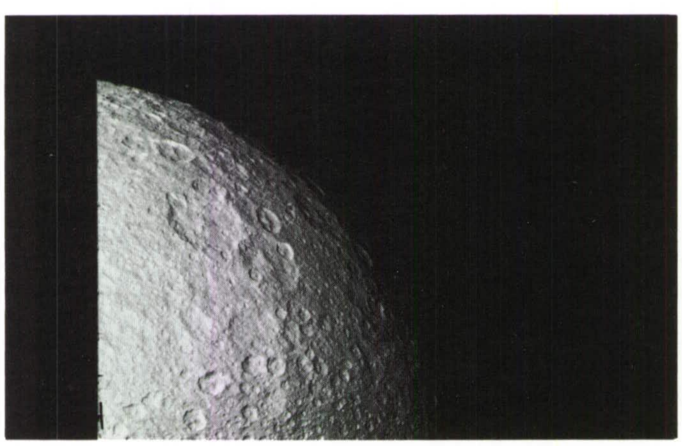

(a)

(b)

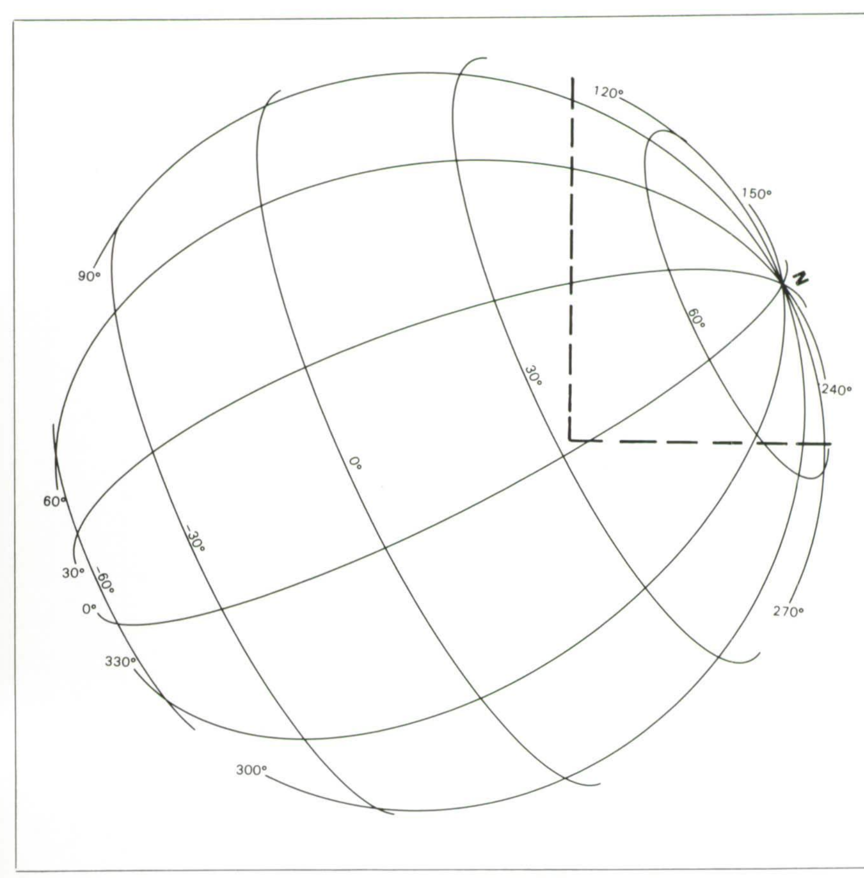

(c)

Picno	0411S1+000
FDS	34950.47
Range, km	105 294
Subspacecraft latitude/longitude, degrees	15/12
Subsolar latitude/longitude, degrees	3/23
Resolution, km/pixel	1
Filter size, pixels	101 × 101
Filter size, km	98
Scale	1:15 000 000

Figure 5–18. Picno 0411S1+000. (*a*) Unfiltered image. (*b*) High-pass filtered image. (*c*) Perspective grid.

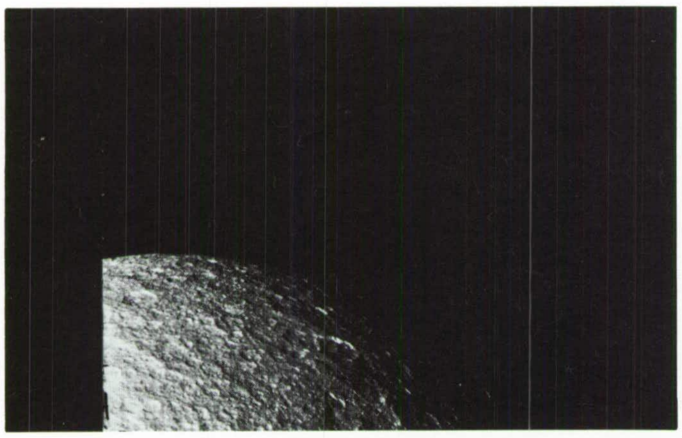

(a)

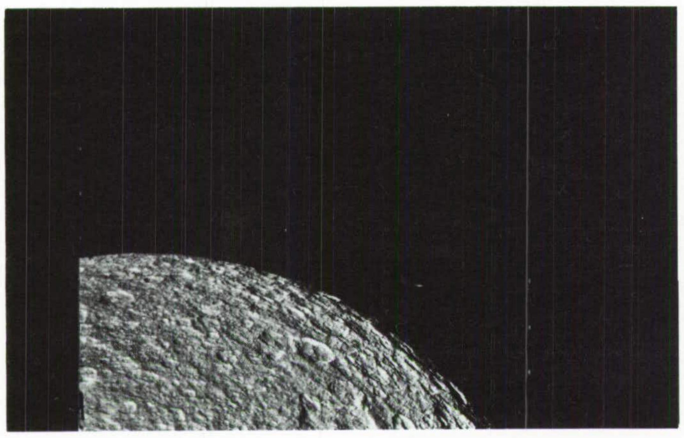

(b)

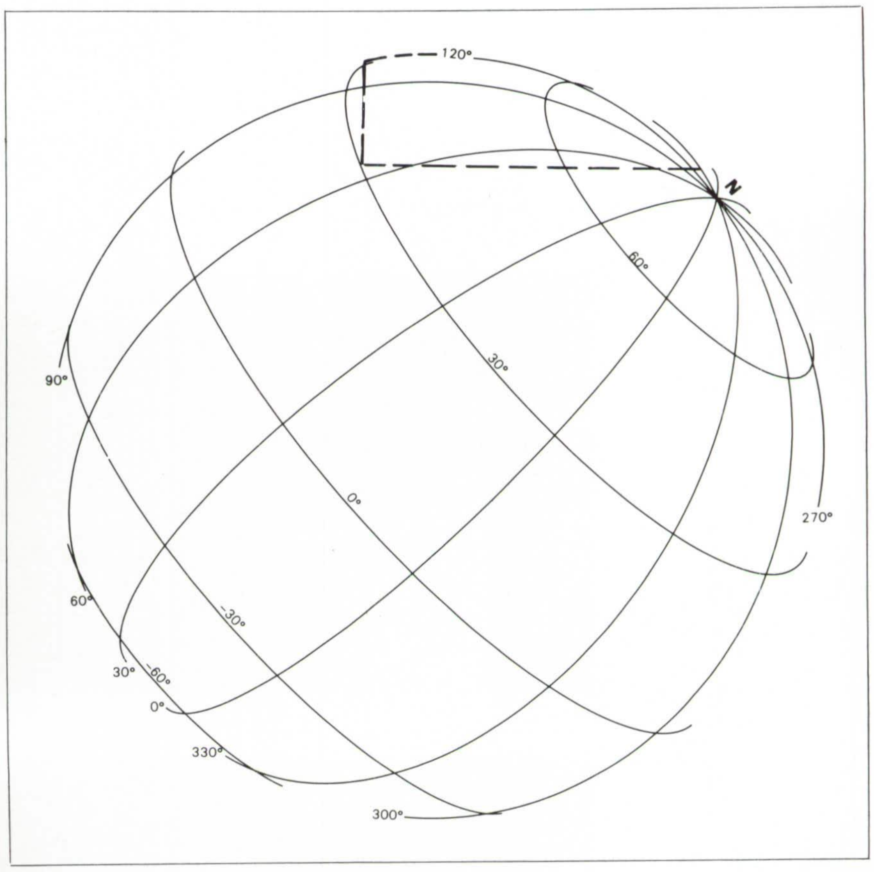

(c)

Picno	0417S1+000
FDS	34950.53
Range, km	101 664
Subspacecraft latitude/longitude, degrees	17/13
Subsolar latitude/longitude, degrees	3/24
Resolution, km/pixel	1
Filter size, pixels	101 × 101
Filter size, km	95
Scale	1:15 000 000

Figure 5–19. Picno 0417S1+000. (*a*) Unfiltered image. (*b*) High-pass filtered image. (*c*) Perspective grid.

(*a*)

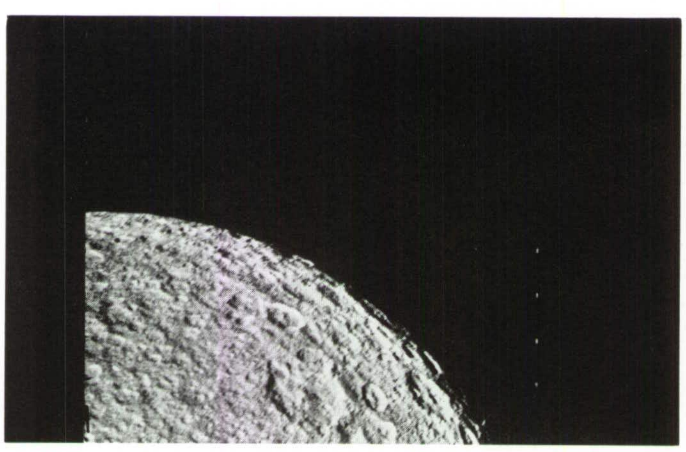

(*b*)

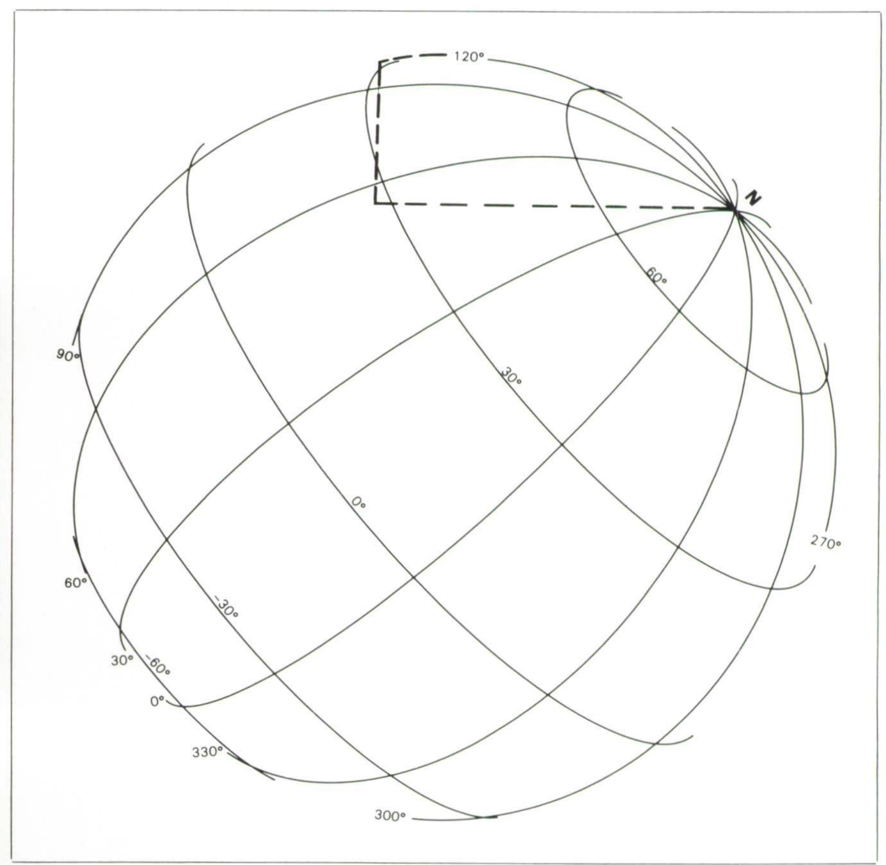

(*c*)

Picno	0419S1+000
FDS	34950.55
Range, km	100 486
Subspacecraft latitude/longitude, degrees	18/13
Subsolar latitude/longitude, degrees	3/24
Resolution, km/pixel	1
Filter size, pixels	101 × 101
Filter size, km	94
Scale	1:15 000 000

Figure 5–20. Picno 0419S1+000. (*a*) Unfiltered image. (*b*) High-pass filtered image. (*c*) Perspective grid.

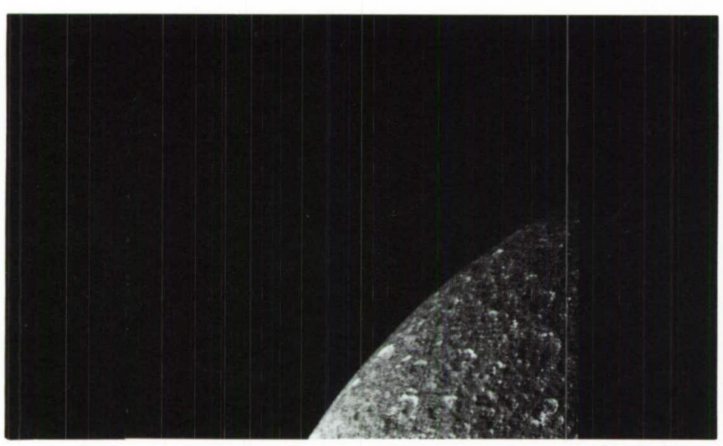

(a)

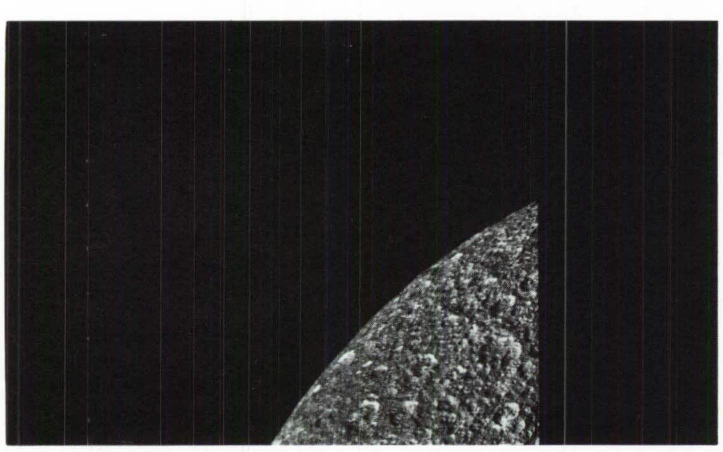

(b)

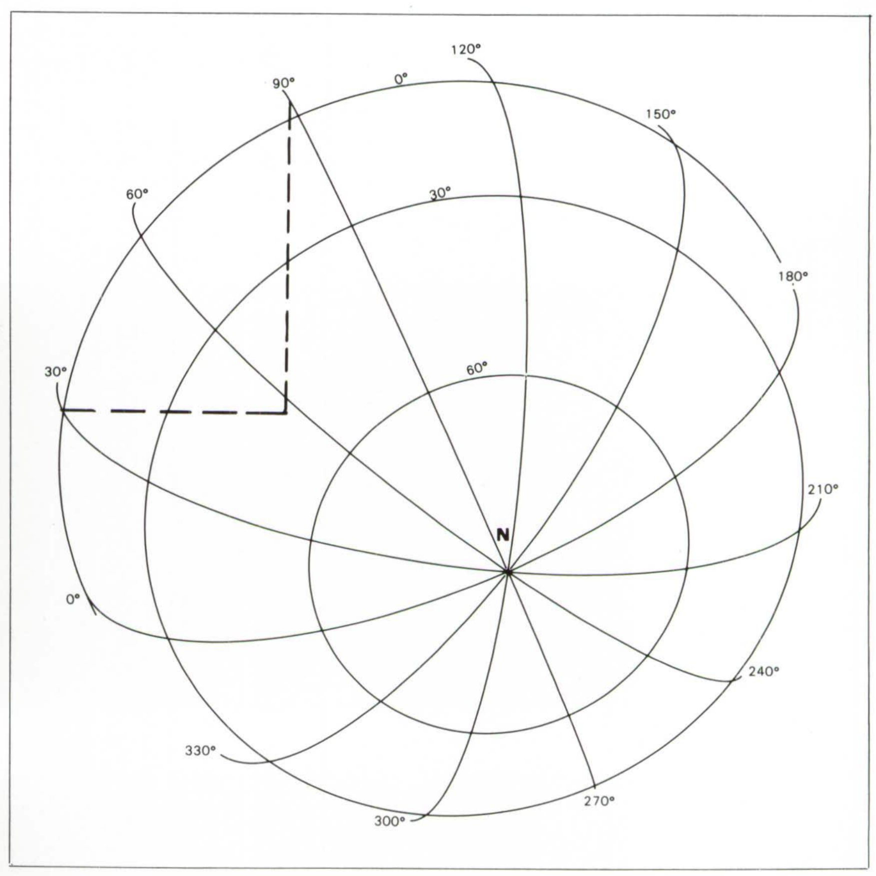

(c)

Picno	0517S1+000
FDS	34952.33
Range, km	75 746
Subspacecraft latitude/longitude, degrees	67/56
Subsolar latitude/longitude, degrees	3/28
Resolution, km/pixel	1
Filter size, pixels	101 × 101
Filter size, km	71
Scale	1:15 000 000

Figure 5–21. Picno 0517S1+000. (*a*) Unfiltered image. (*b*) High-pass filtered image. (*c*) Perspective grid.

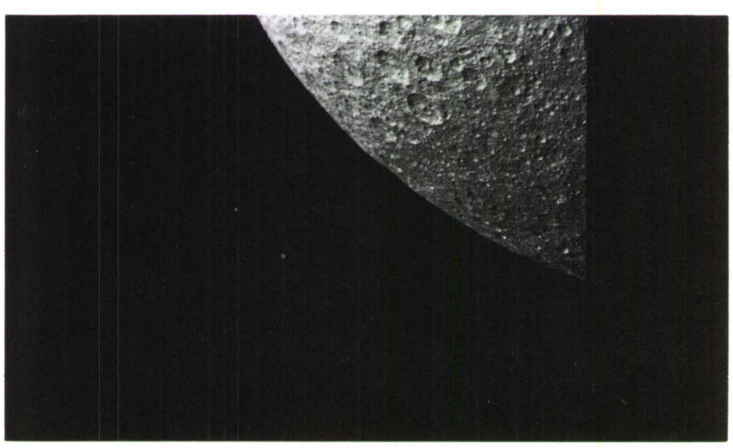

(a)

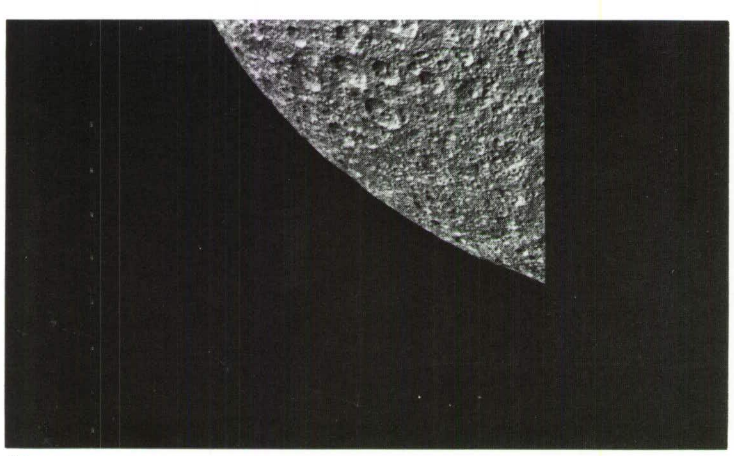

(b)

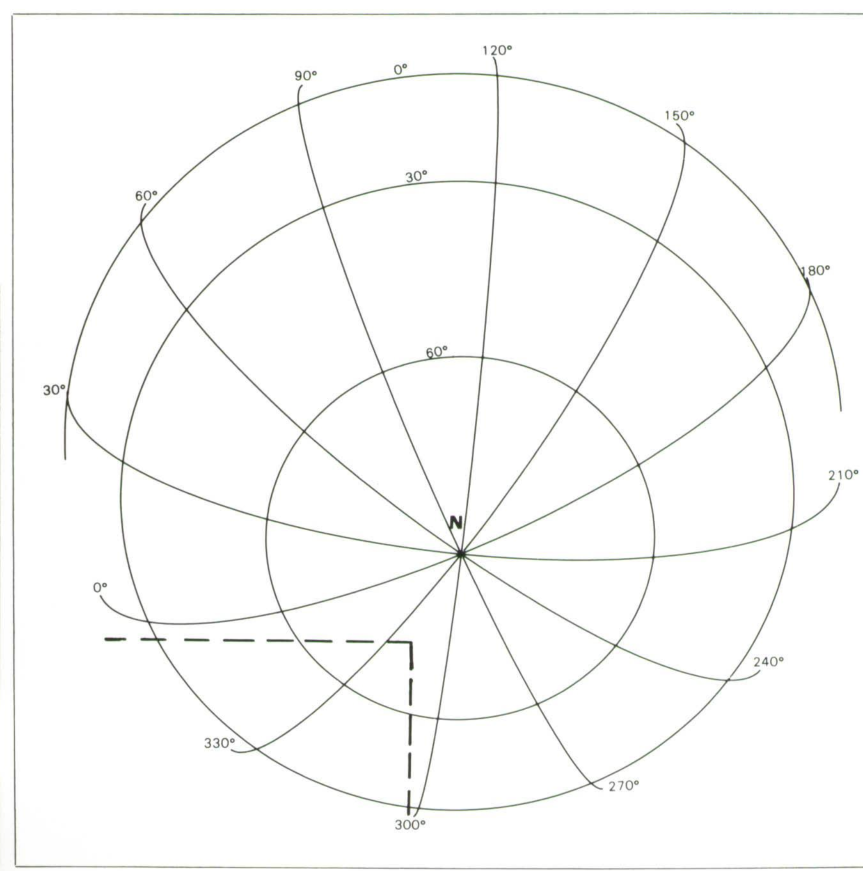

(c)

Picno	0533S1+000
FDS	34952.49
Range, km	79 796
Subspacecraft latitude/longitude, degrees	72/80
Subsolar latitude/longitude, degrees	3/29
Resolution, km/pixel	1
Filter size, pixels	101 × 101
Filter size, km	74
Scale	1:15 000 000

Figure 5–22. Picno 0533S1+000. (*a*) Unfiltered image. (*b*) High-pass filtered image. (*c*) Perspective grid.

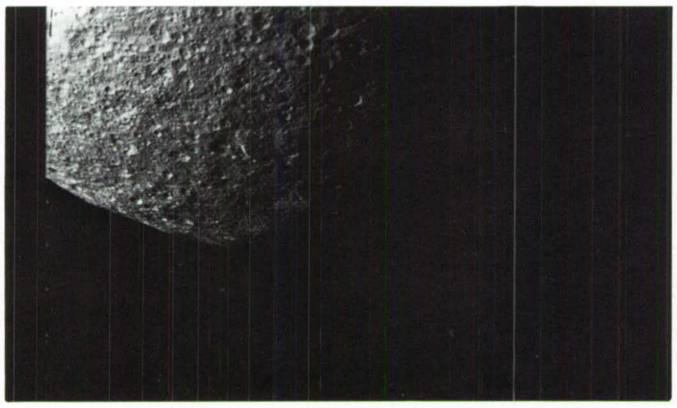

(*a*)

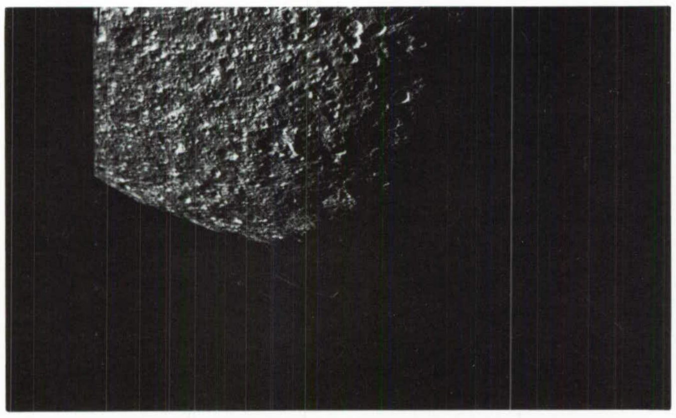

(*b*)

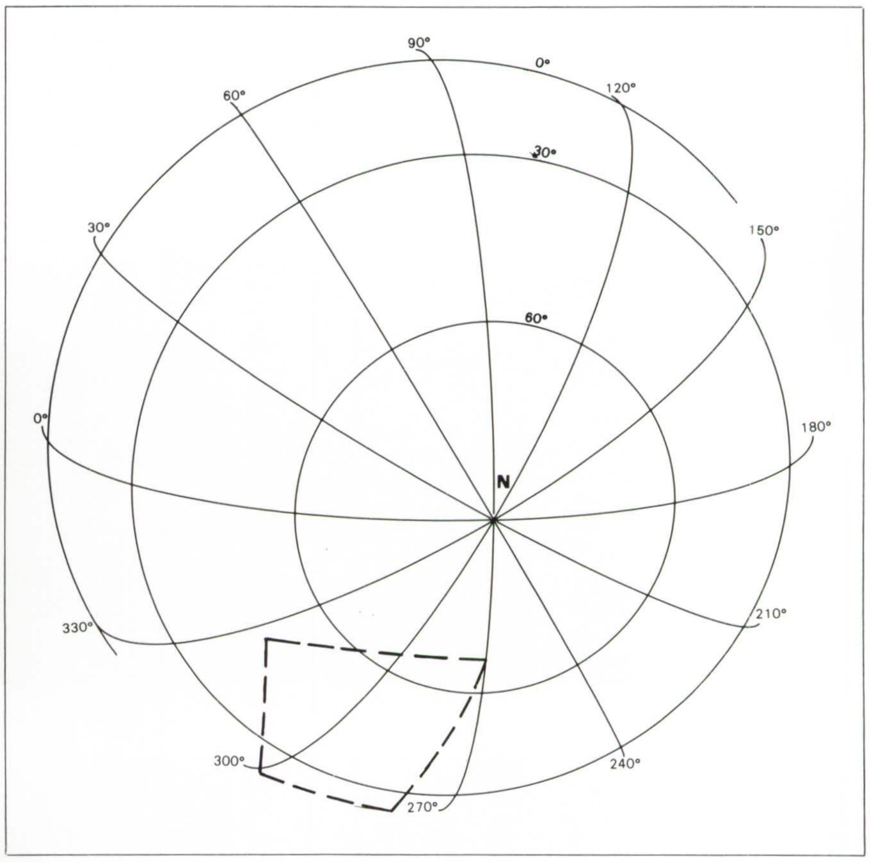

(*c*)

Picno	0535S1+000
FDS	34952.51
Range, km	80 452
Subspacecraft latitude/longitude, degrees	73/84
Subsolar latitude/longitude, degrees	3/29
Resolution, km/pixel	1
Filter size, pixels	101 × 101
Filter size, km	75
Scale	1:15 000 000

Figure 5–23. Picno 0535S1+000. (*a*) Unfiltered image. (*b*) High-pass filtered image. (*c*) Perspective grid.

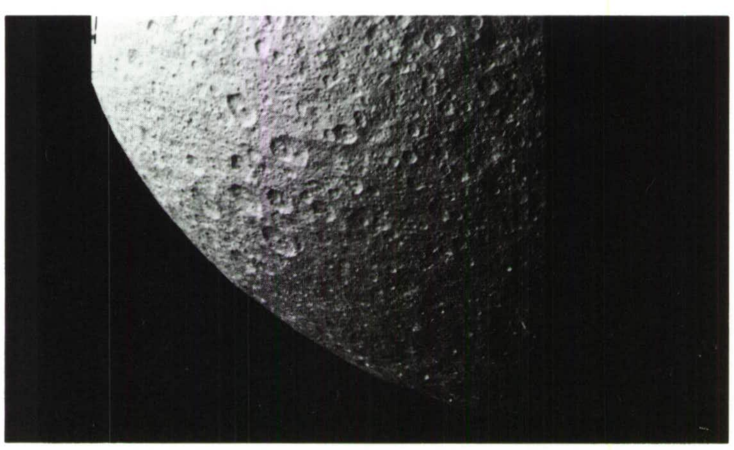

(a)

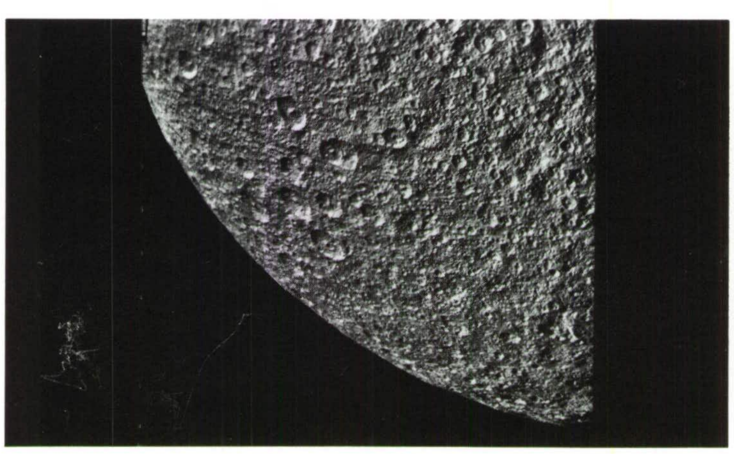

(b)

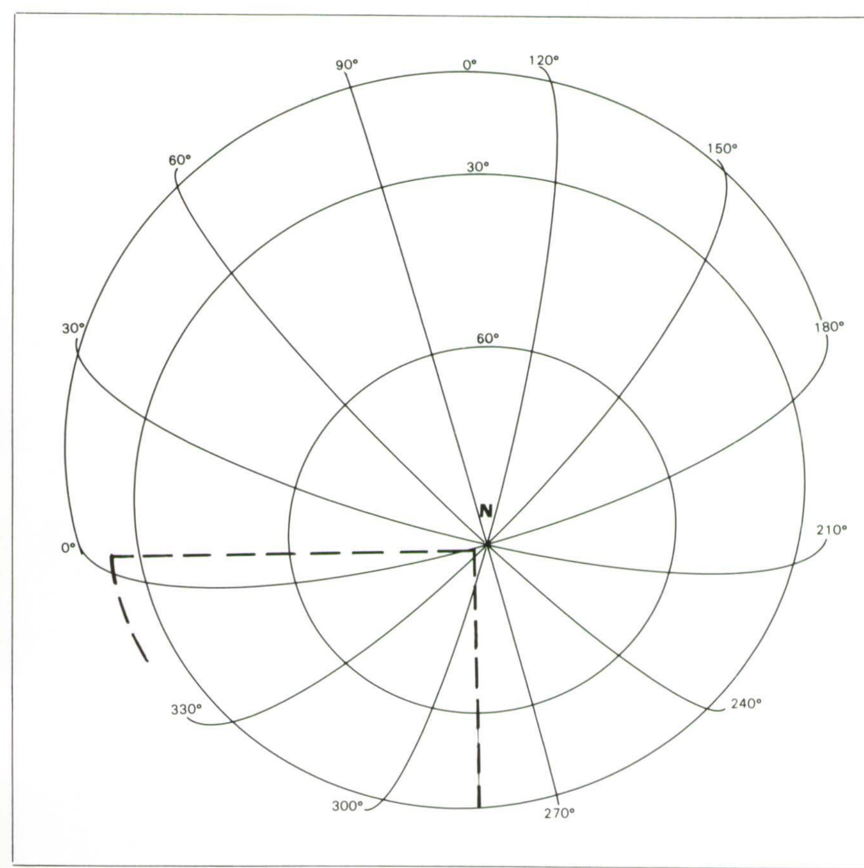

(c)

Picno	0537S1+000
FDS	34952.53
Range, km	81 138
Subspacecraft latitude/longitude, degrees	73/88
Subsolar latitude/longitude, degrees	3/29
Resolution, km/pixel	1
Filter size, pixels	101 × 101
Filter size, km	76
Scale	1:15 000 000

Figure 5–24. Picno 0537S1+000. (*a*) Unfiltered image. (*b*) High-pass filtered image. (*c*) Perspective grid.

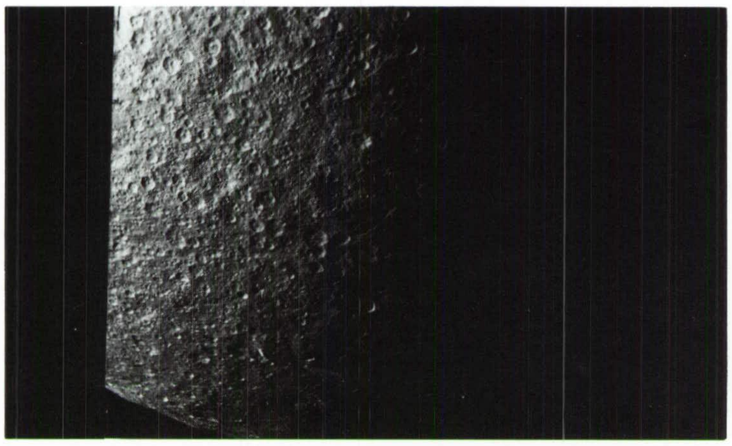

(a)

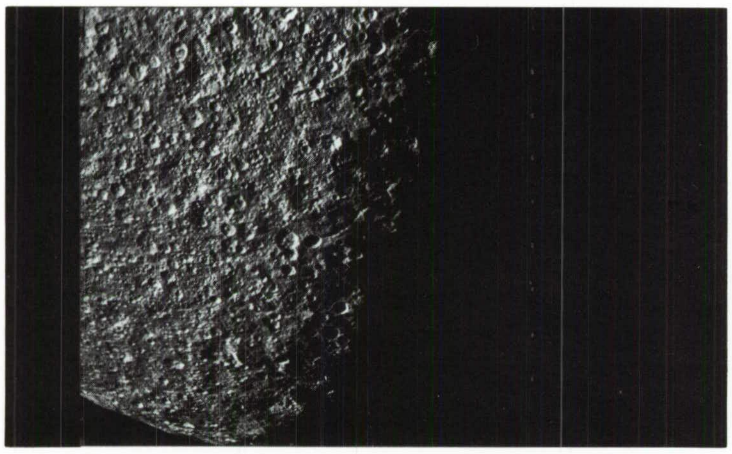

(b)

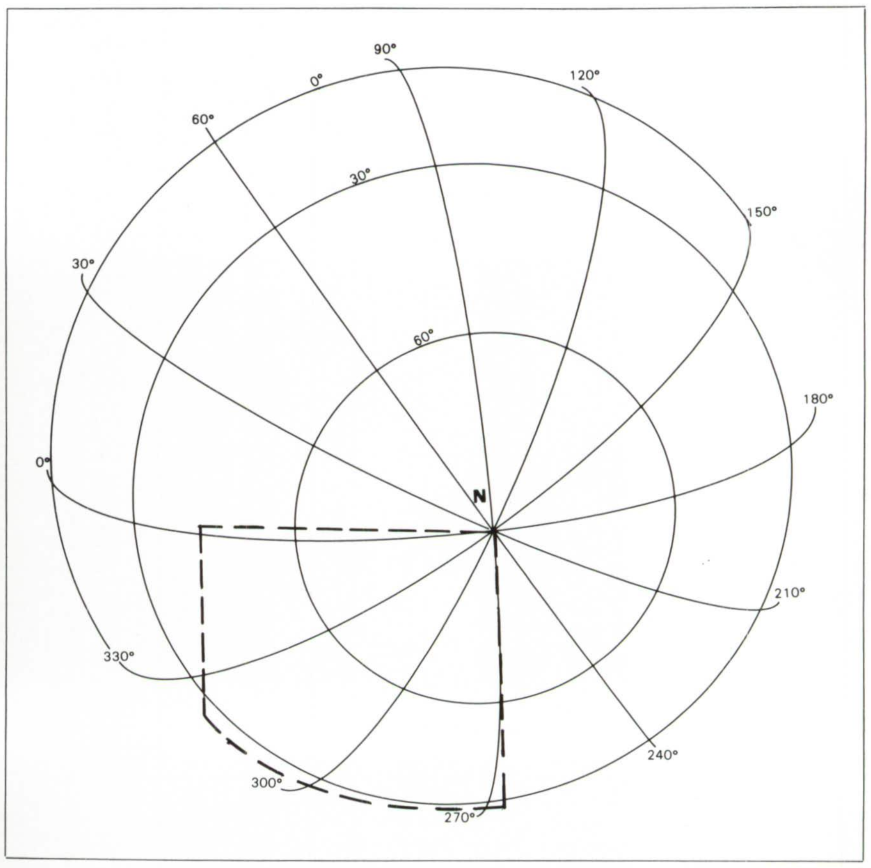

(c)

Picno	0539S1+000
FDS	34952.55
Range, km	81 854
Subspacecraft latitude/longitude, degrees	73/92
Subsolar latitude/longitude, degrees	3/29
Resolution, km/pixel	1
Filter size, pixels	101 × 101
Filter size, km	76
Scale	1:15 000 000

Figure 5–25. Picno 0539S1+000. (*a*) Unfiltered image. (*b*) High-pass filtered image. (*c*) Perspective grid.

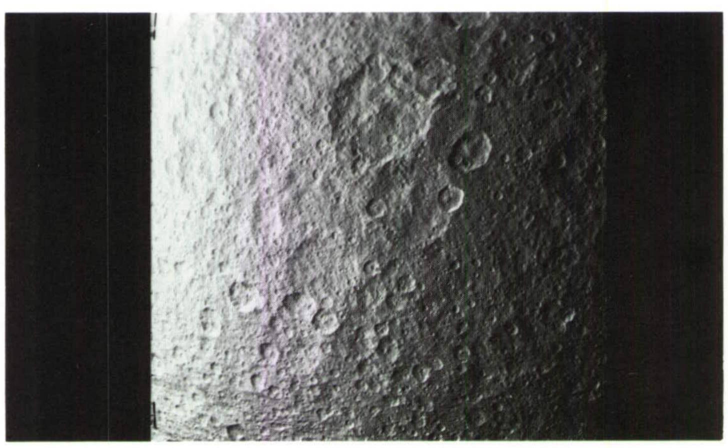

(a)

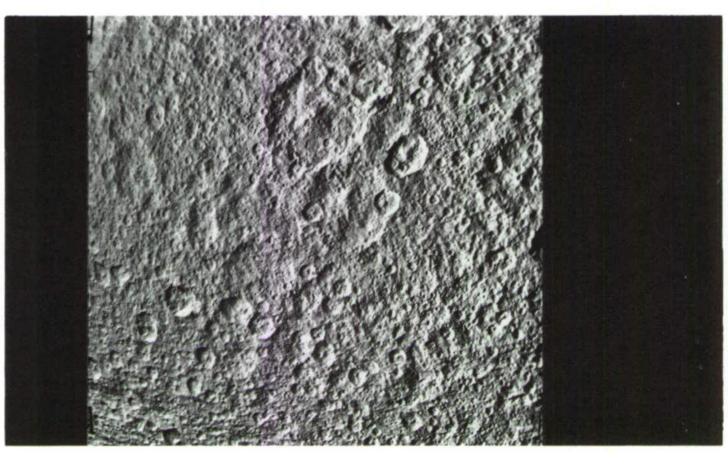

(b)

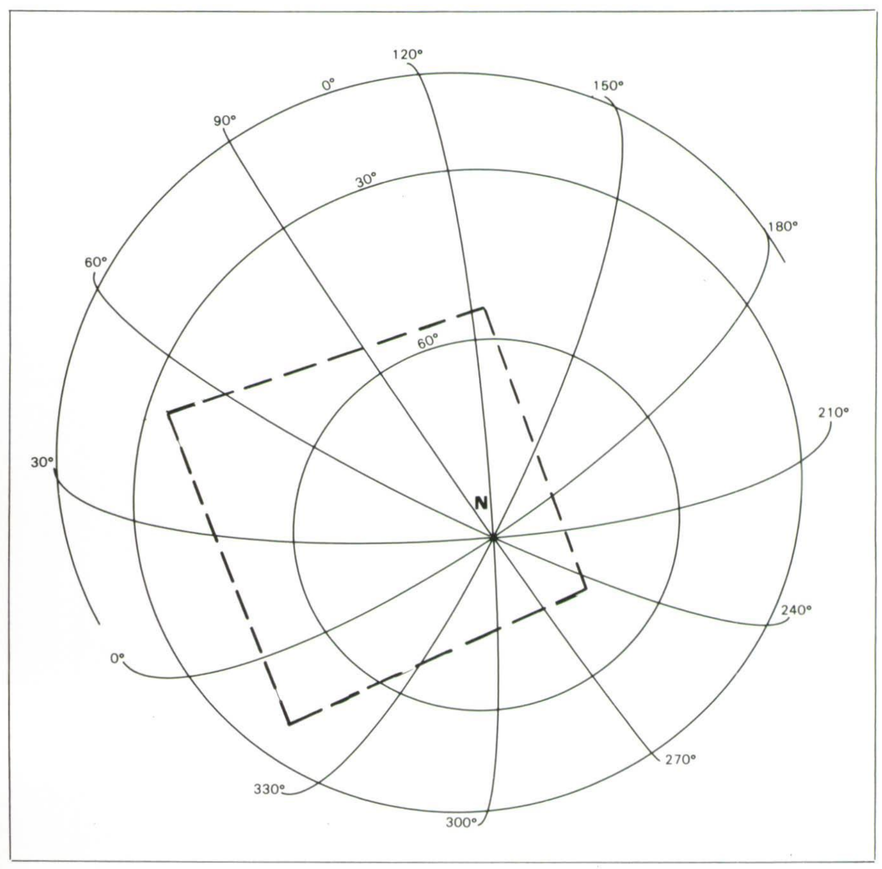

(c)

Picno	0541S1+000
FDS	34952.57
Range, km	82 599
Subspacecraft latitude/longitude, degrees	74/96
Subsolar latitude/longitude, degrees	3/29
Resolution, km/pixel	1
Filter size, pixels	101 × 101
Filter size, km	77
Scale	1:15 000 000

Figure 5–26. Picno 0541S1+000. (*a*) Unfiltered image. (*b*) High-pass filtered image. (*c*) Perspective grid.

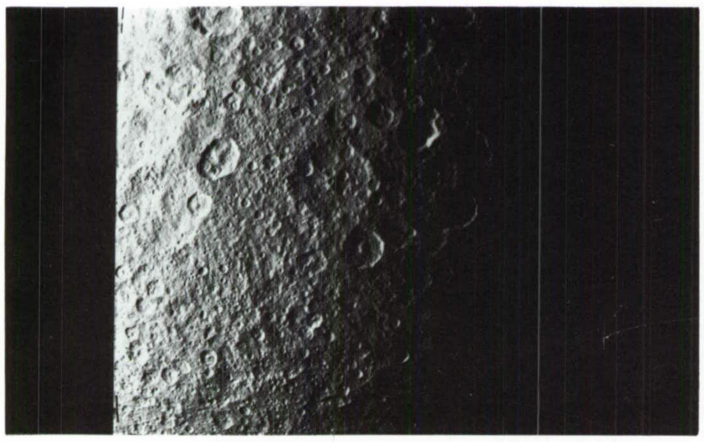

(a)

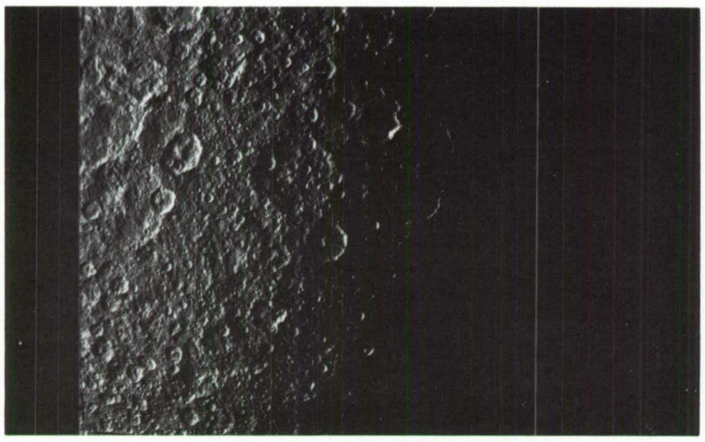

(b)

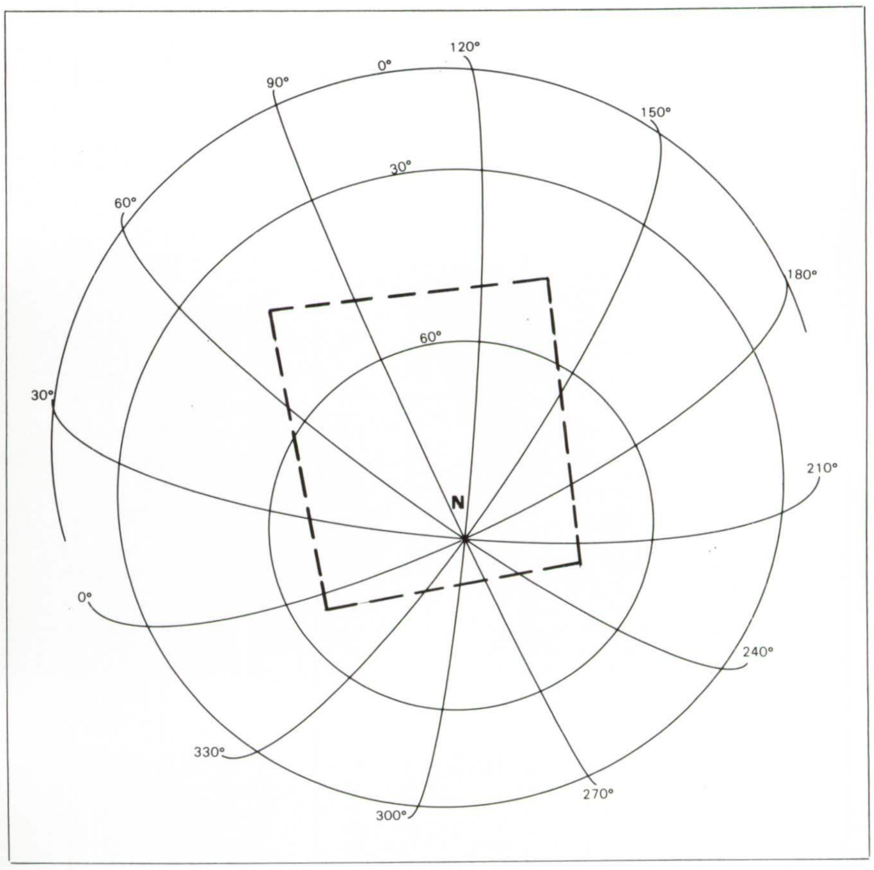

(c)

Picno	0543S1+000
FDS	34952.59
Range, km	83 373
Subspacecraft latitude/longitude, degrees	74/99
Subsolar latitude/longitude, degrees	3/29
Resolution, km/pixel	1
Filter size, pixels	101 × 101
Filter size, km	78
Scale	1:15 000 000

Figure 5–27. Picno 0543S1+000. (*a*) Unfiltered image. (*b*) High-pass filtered image. (*c*) Perspective grid.

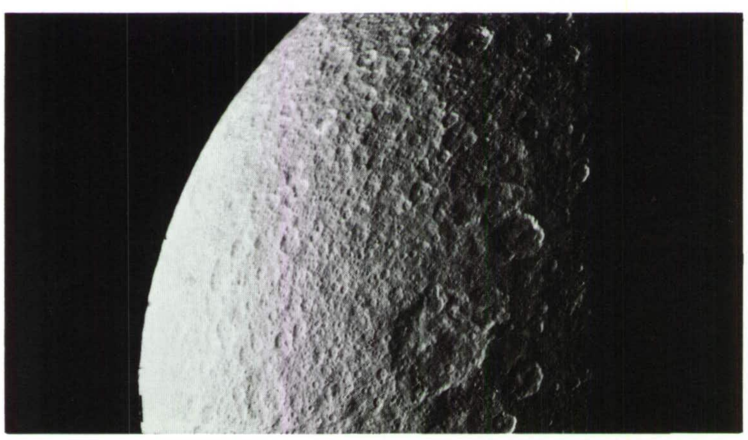

(a)

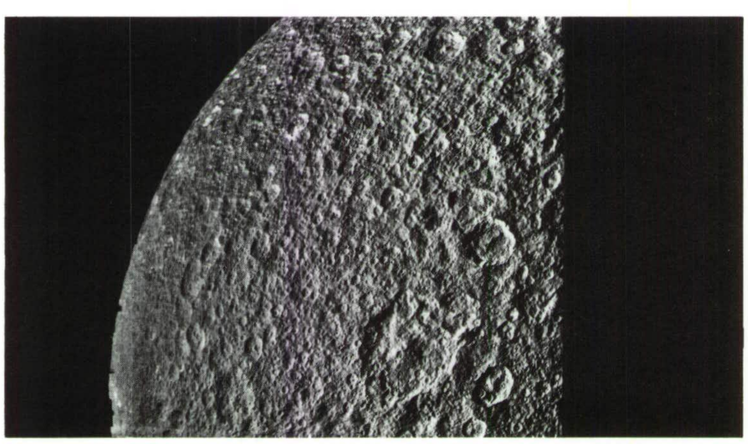

(b)

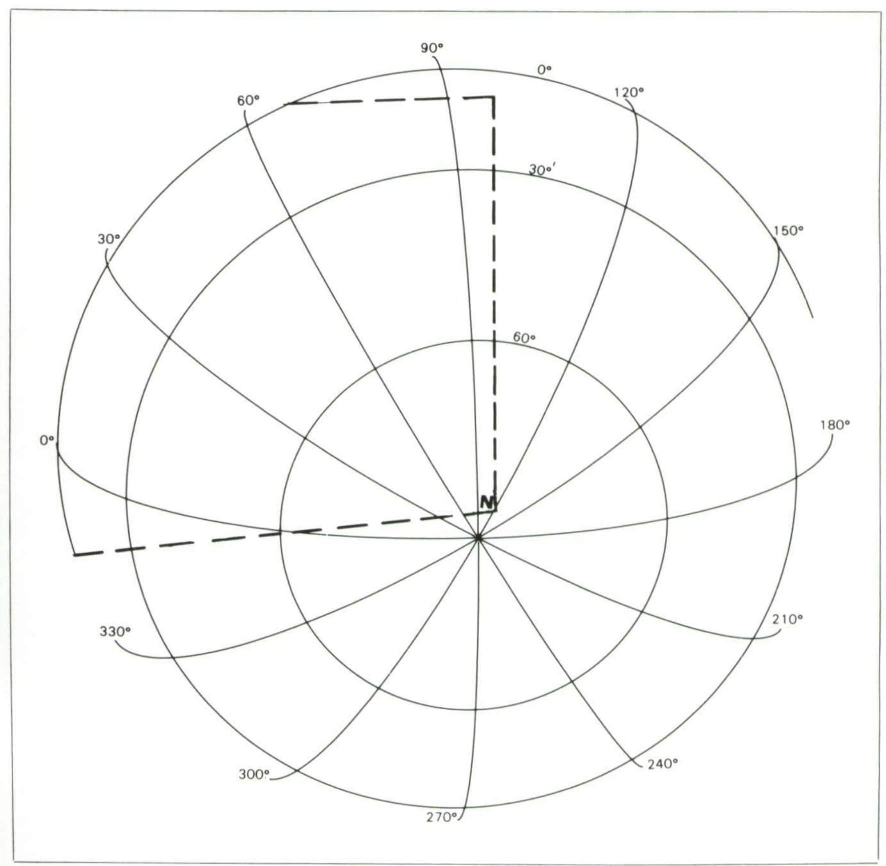

(c)

Picno	0545S1+000
FDS	34953.01
Range, km	84 174
Subspacecraft latitude/longitude, degrees	74/103
Subsolar latitude/longitude, degrees	3/29
Resolution, km/pixel	1
Filter size, pixels	101 × 101
Filter size, km	78
Scale	1:15 000 000

Figure 5–28. Picno 0545S1+000. (*a*) Unfiltered image. (*b*) High-pass filtered image. (*c*) Perspective grid.

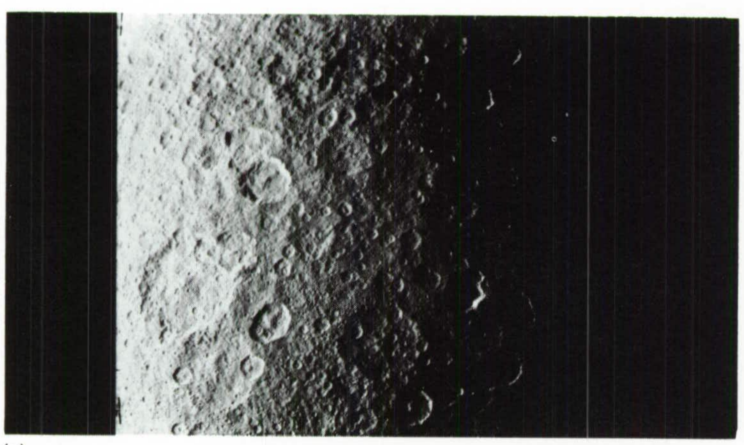

(a)

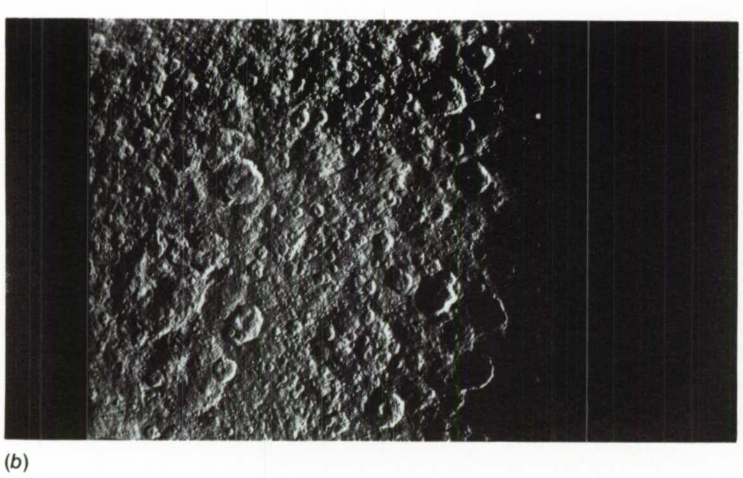

(b)

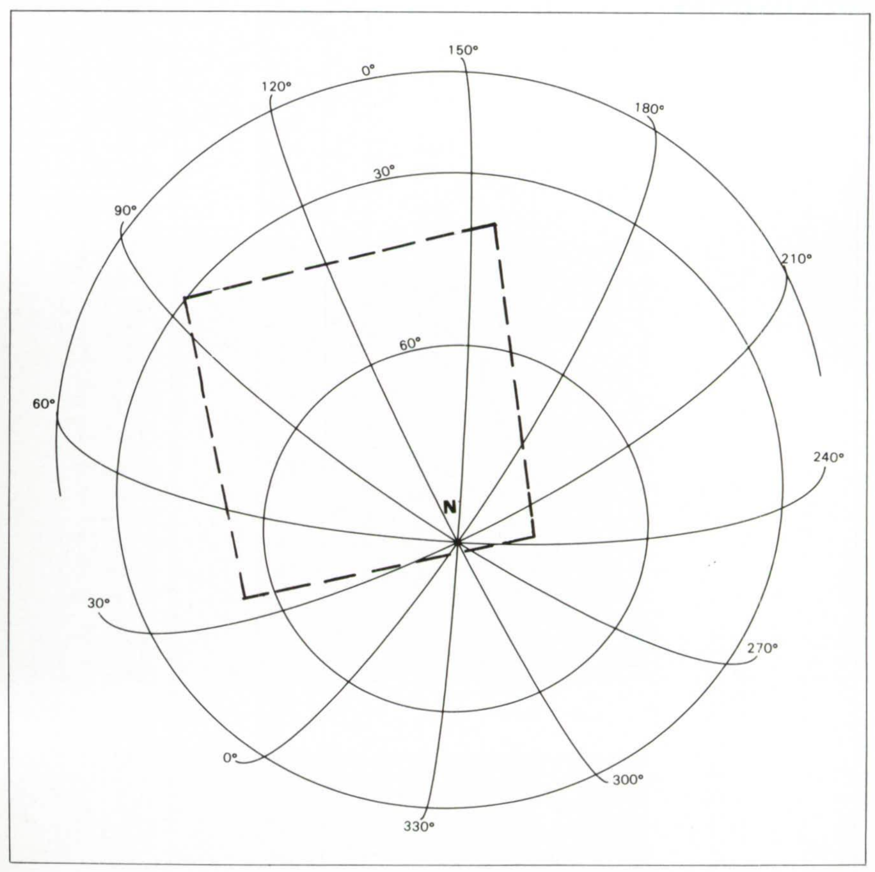

(c)

Picno	0547S1+000
FDS	34953.03
Range, km	85 001
Subspacecraft latitude/longitude, degrees	74/107
Subsolar latitude/longitude, degrees	3/29
Resolution, km/pixel	1
Filter size, pixels	101 × 101
Filter size, km	79
Scale	1:15 000 000

Figure 5–29. Picno 0547S1+000. (*a*) Unfiltered image. (*b*) High-pass filtered image. (*c*) Perspective grid.

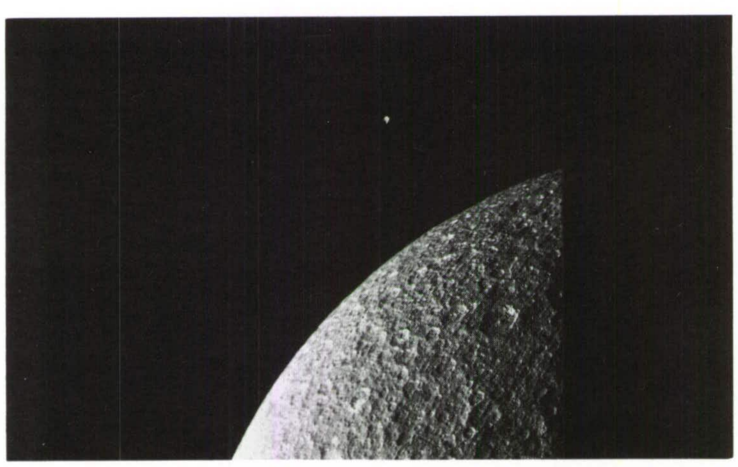

(a)

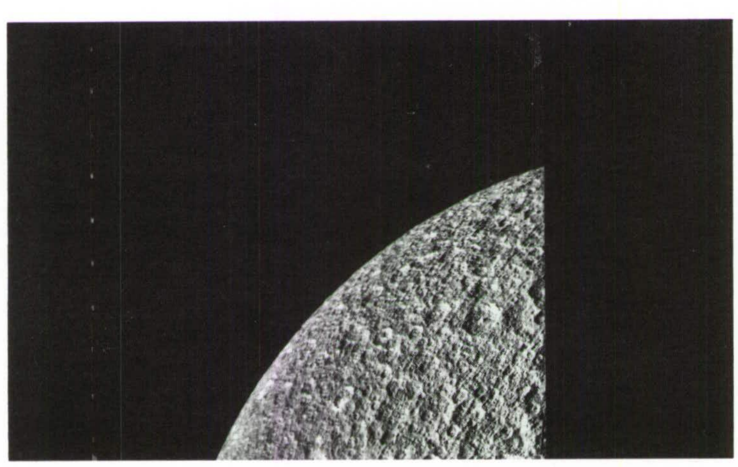

(b)

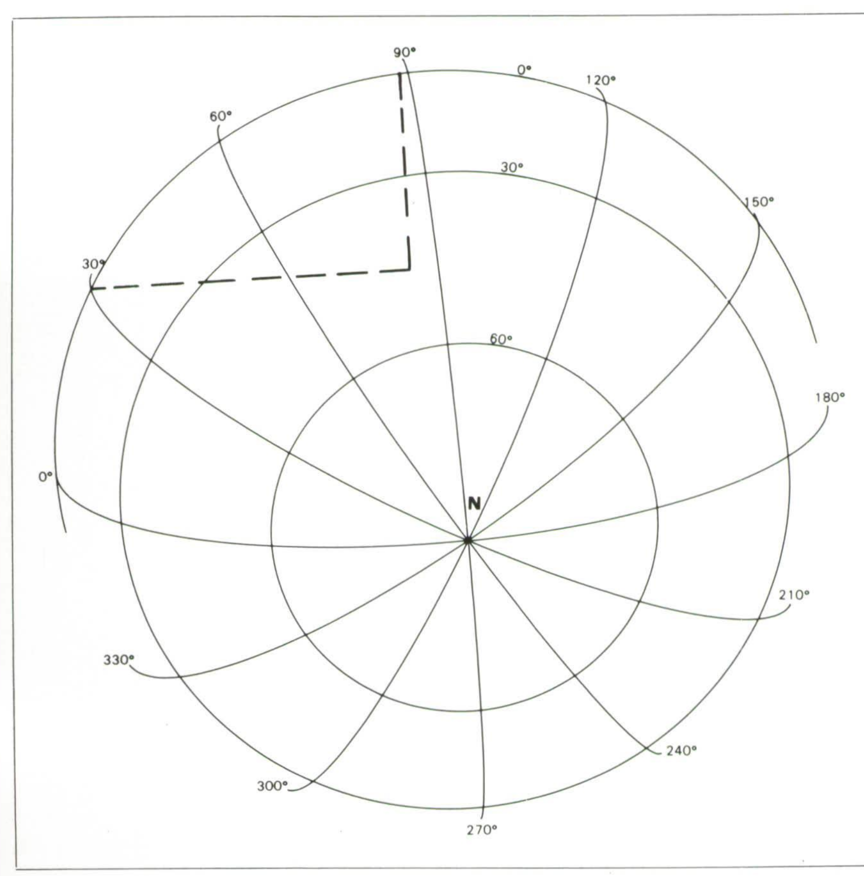

(c)

Picno	0549S1+000
FDS	34953.05
Range, km	85 855
Subspacecraft latitude/longitude, degrees	74/111
Subsolar latitude/longitude, degrees	3/29
Resolution, km/pixel	1
Filter size, pixels	101 × 101
Filter size, km	80
Scale	1:15 000 000

Figure 5–30. Picno 0549S1+000. (*a*) Unfiltered image. (*b*) High-pass filtered image. (*c*) Perspective grid.

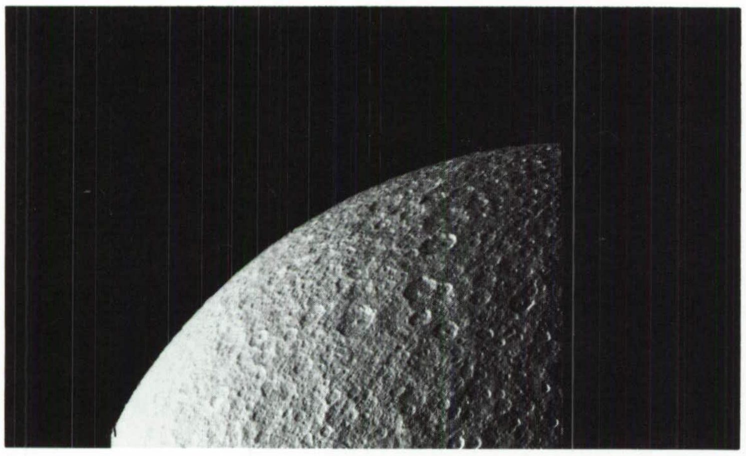

(a)

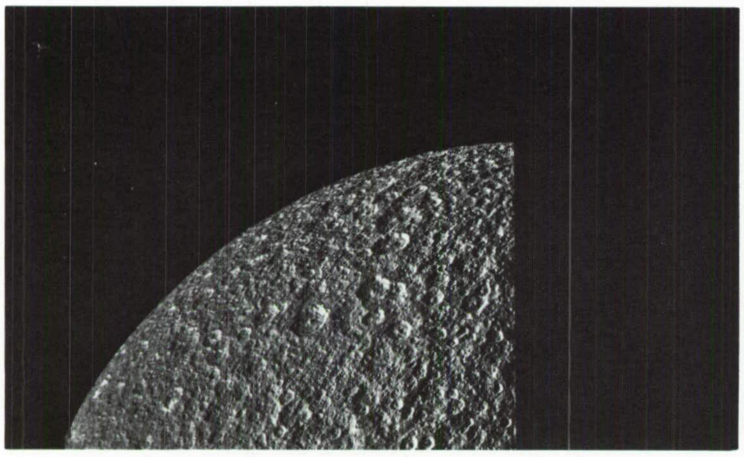

(b)

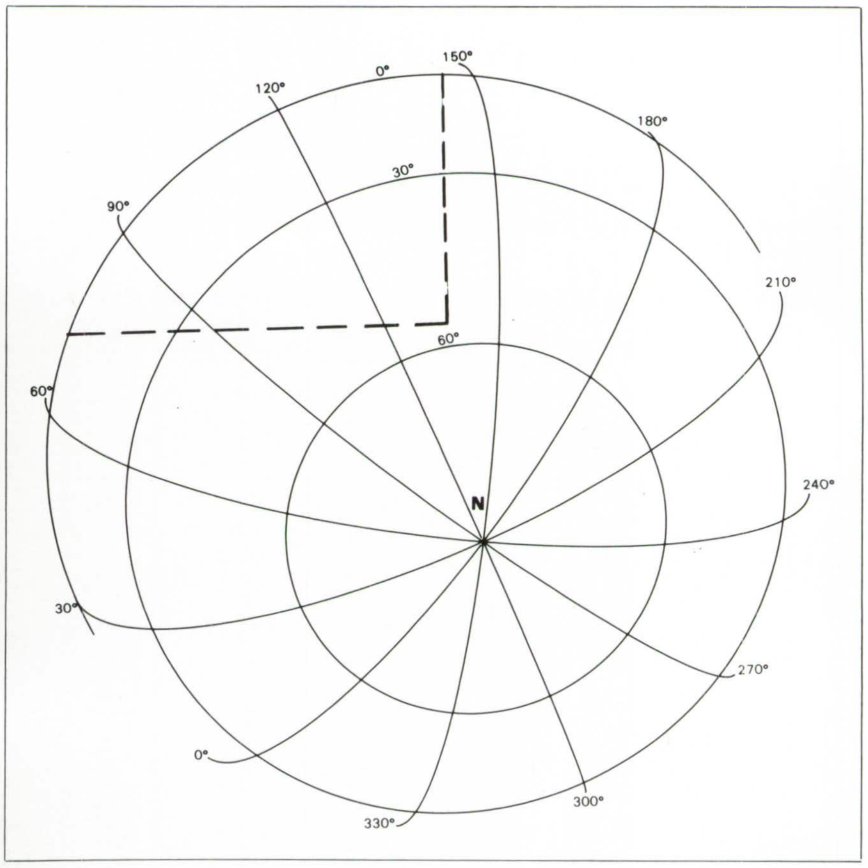

(c)

Picno	0551S1+000
FDS	34953.07
Range, km	86 734
Subspacecraft latitude/longitude, degrees	73/114
Subsolar latitude/longitude, degrees	3/29
Resolution, km/pixel	1
Filter size, pixels	101 × 101
Filter size, km	81
Scale	1:15 000 000

Figure 5–31. Picno 0551S1+000. (*a*) Unfiltered image. (*b*) High-pass filtered image. (*c*) Perspective grid.

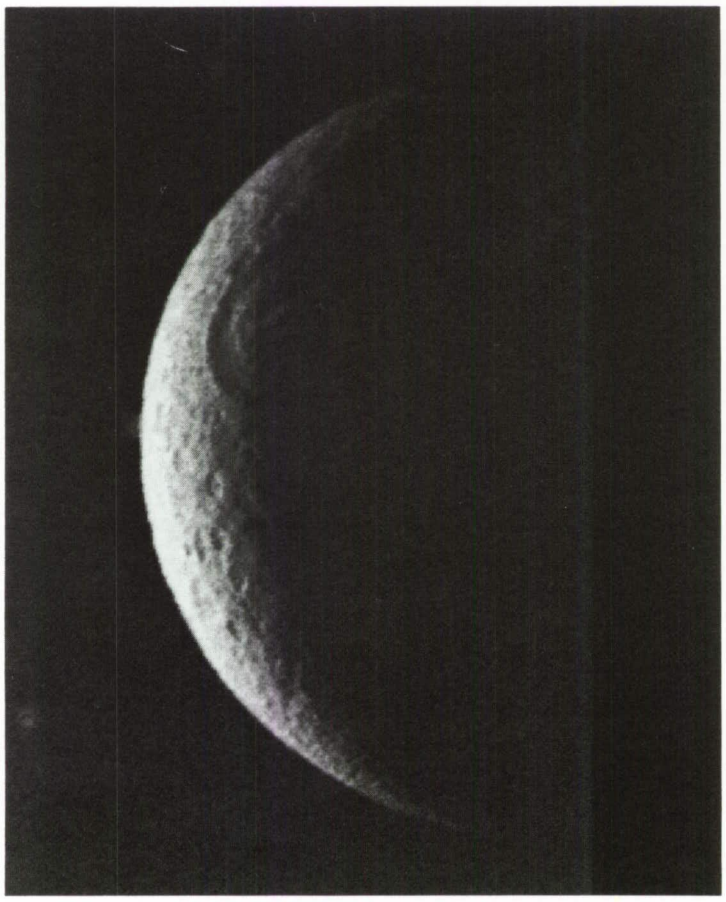

(a)

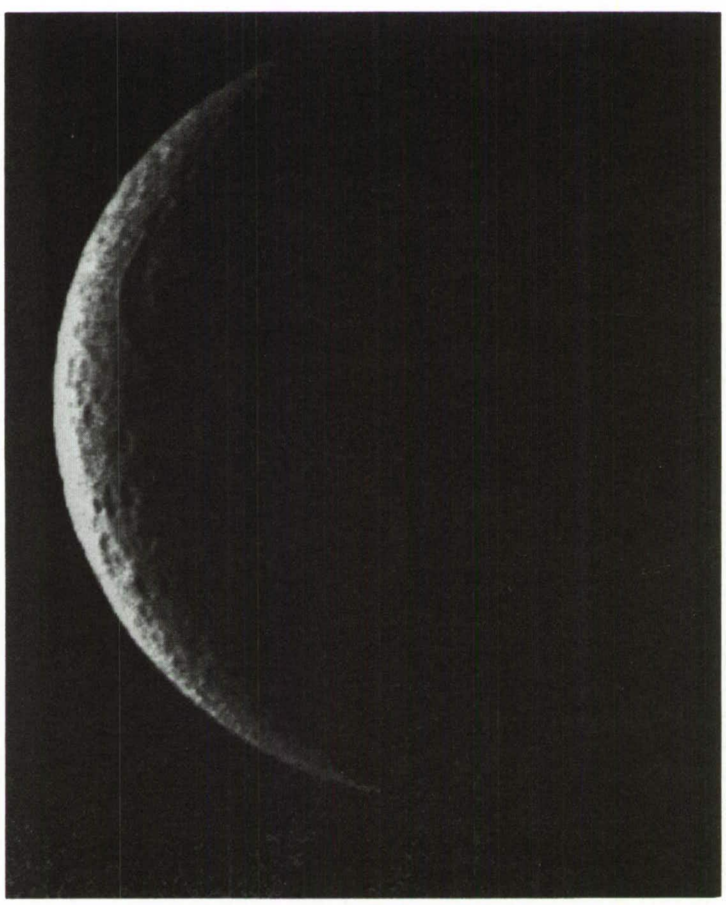

(b)

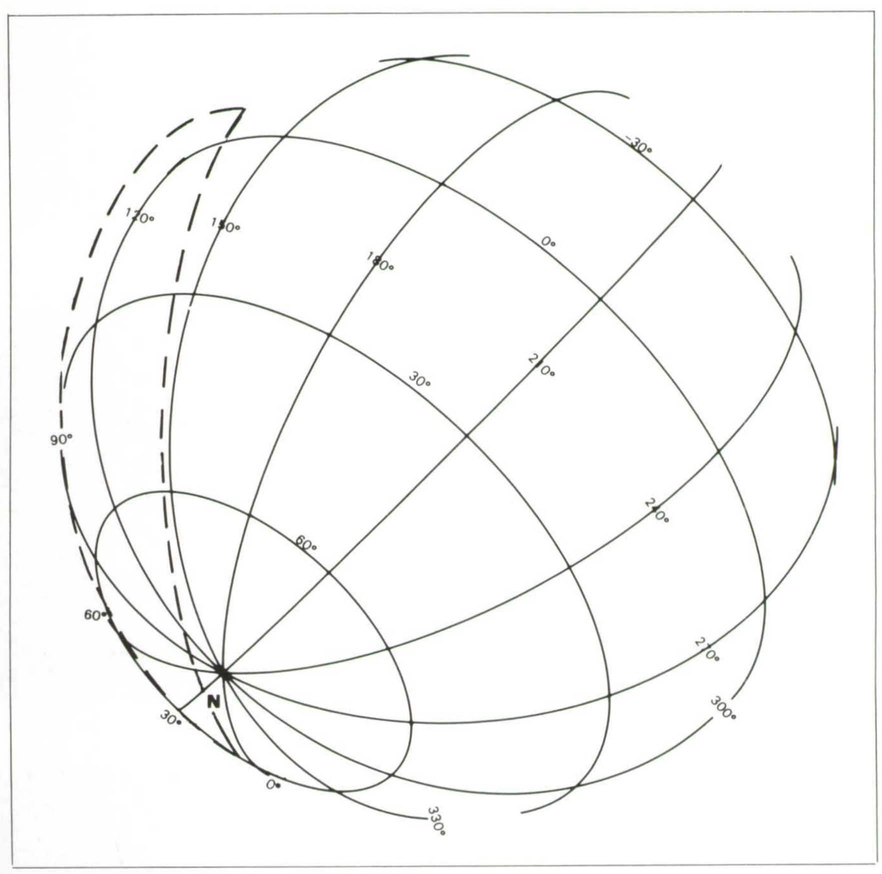

(c)

Picno	1152S1+000
FDS	34963.08
Range, km	579 771
Subspacecraft latitude/longitude, degrees	32/208
Subsolar latitude/longitude, degrees	3/56
Resolution, km/pixel	5
Filter size, pixels	101 × 101
Filter size, km	542
Scale	1:15 000 000

Figure 5–32. Picno 1152S1+000. (*a*) Unfiltered image. (*b*) High-pass filtered image. (*c*) Perspective grid.

PART 6

Iapetus

Diameter	1448 km (900 miles)
Density	1.2
Albedo:	
Bright side	0.5
Dark side	0.05
Distance from Saturn	3 559 400 km (2 211 704 miles)
Orbital period	1901 hr, 49 min, 12 sec
Voyager 1 closest approach	2 470 000 km (1 534 784 miles)
Voyager 1 pictures used in mapping	3
Voyager 2 closest approach	909 070 km (564 870 miles)
Voyager 2 pictures used in mapping	8

One of the unique phenomena discovered on Iapetus is the extreme difference in albedo between the hemisphere that always faces in the direction of orbital movement (leading hemisphere) and the opposite hemisphere (trailing hemisphere). The leading hemisphere is about the color and brightness of coal, while the trailing hemisphere has the approximate brightness and color of somewhat dirty snow. Because of the extreme differences in brightness, Voyager 1 and 2 were able to resolve data only in the trailing hemisphere. Several theories have been proposed to explain this difference, but no really convincing explanation has been found.

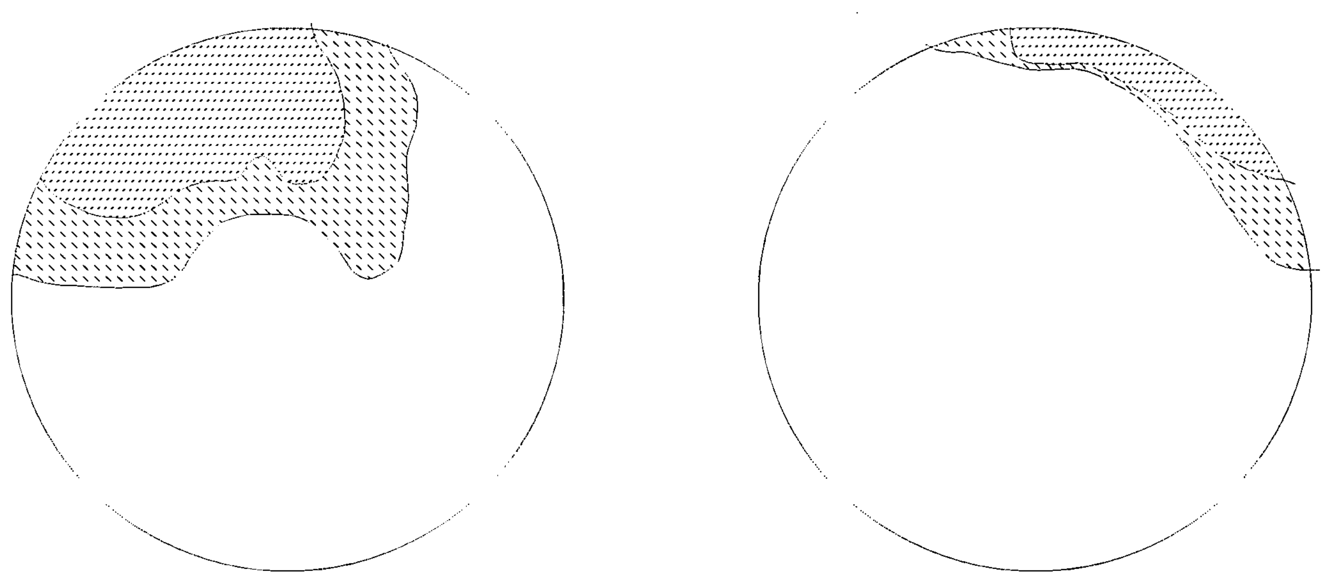

Resolution, km/pixel	Area, km2	Percent of total
0.5 to 2	—	—
2 to 5	—	—
5 to 20	696 000	10.4
20 to 40	670 000	10.0
>40	5 330 000	79.6

Figure 6–1. Resolution of Voyager pictures of Iapetus in terms of aerial coverage.

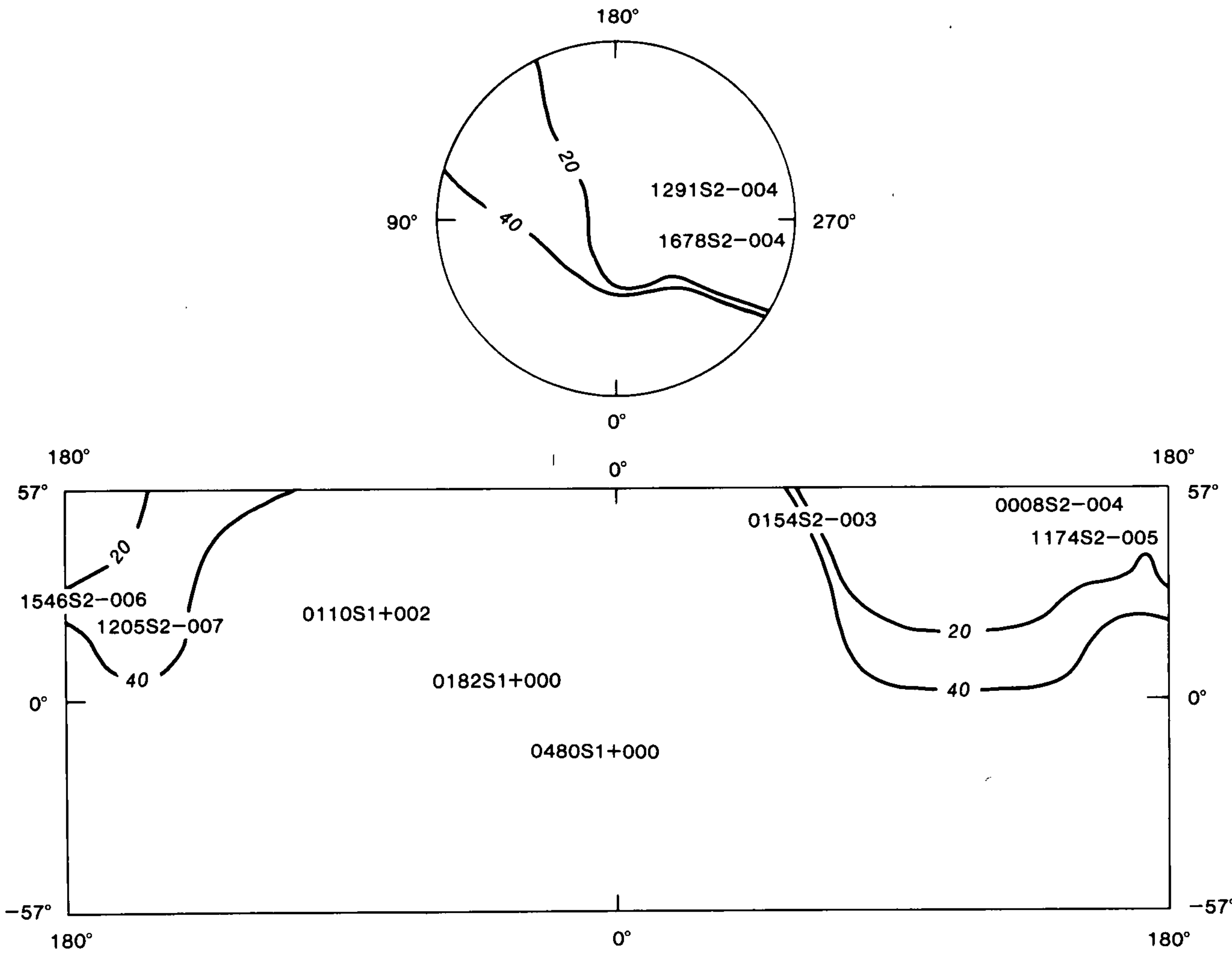

Figure 6–2. Index of Voyager 1 and 2 pictures used to compile the maps of Iapetus. Picture numbers indicate the subspacecraft point at the time the pictures are taken. Contour lines indicate the approximate resolution of available images in kilometers per picture element. (See also fig. 6–1.)

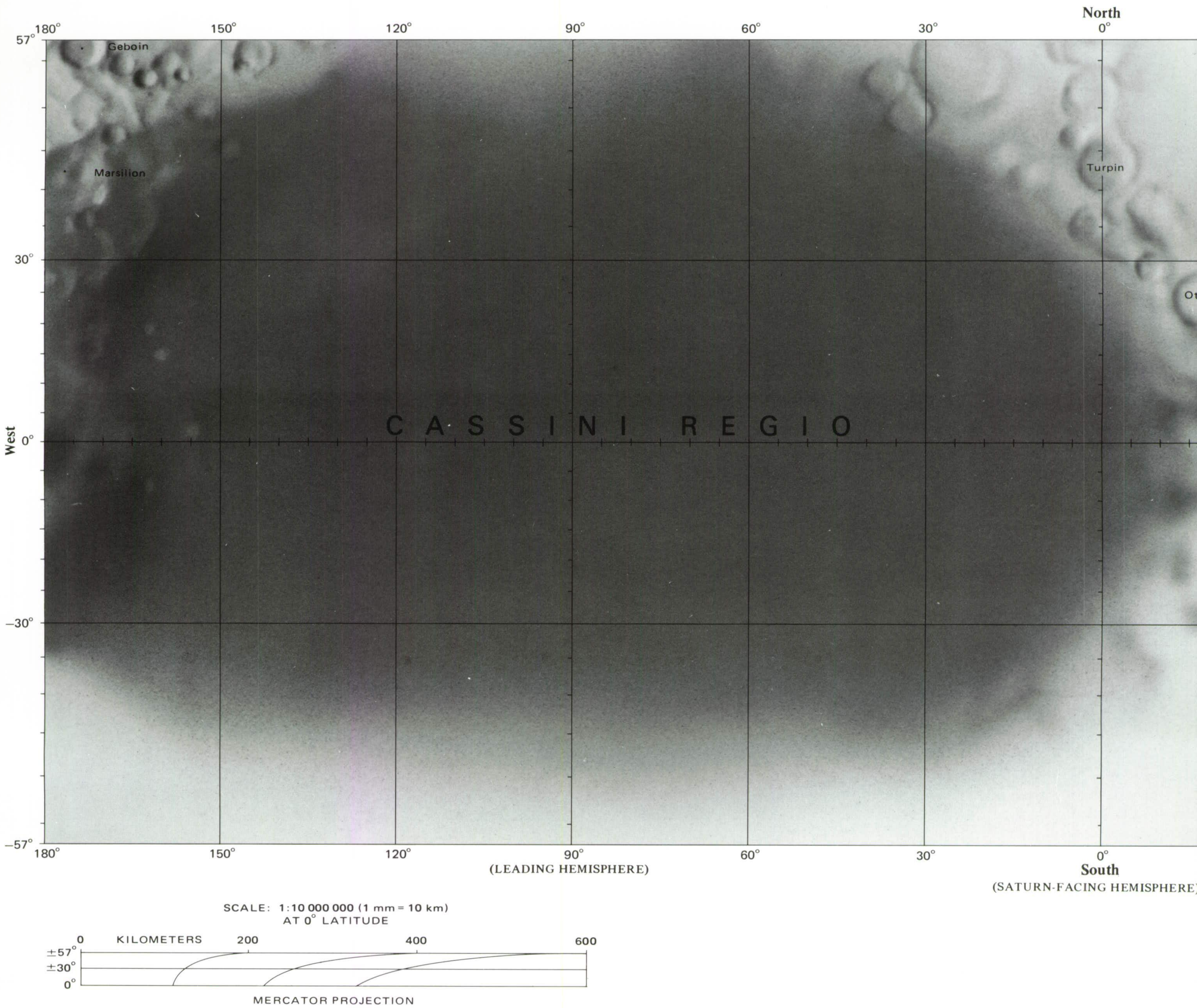
North
South
West
180°
150°
120°
90°
60°
30°
0°
57°
30°
0°
−30°
−57°
Geboin
Marsilion
Turpin
C A S S I N I   R E G I O
(LEADING HEMISPHERE)
(SATURN-FACING HEMISPHERE)
SCALE: 1:10 000 000 (1 mm = 10 km)
AT 0° LATITUDE
0 KILOMETERS 200 400 600
±57°
±30°
0°
MERCATOR PROJECTION

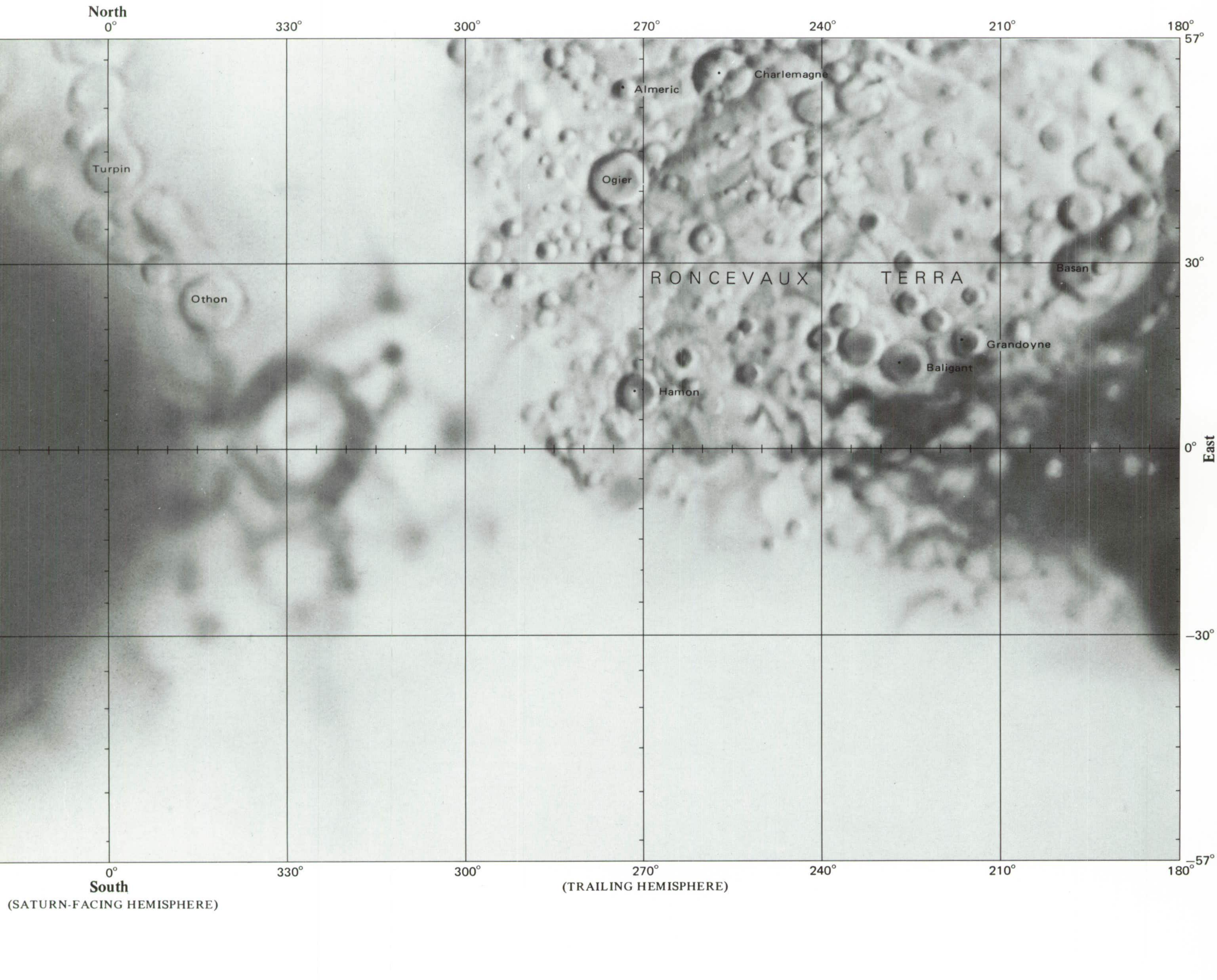

Figure 6–3. Map of the equatorial region of Iapetus on a Mercator projection (part of map I–1486).

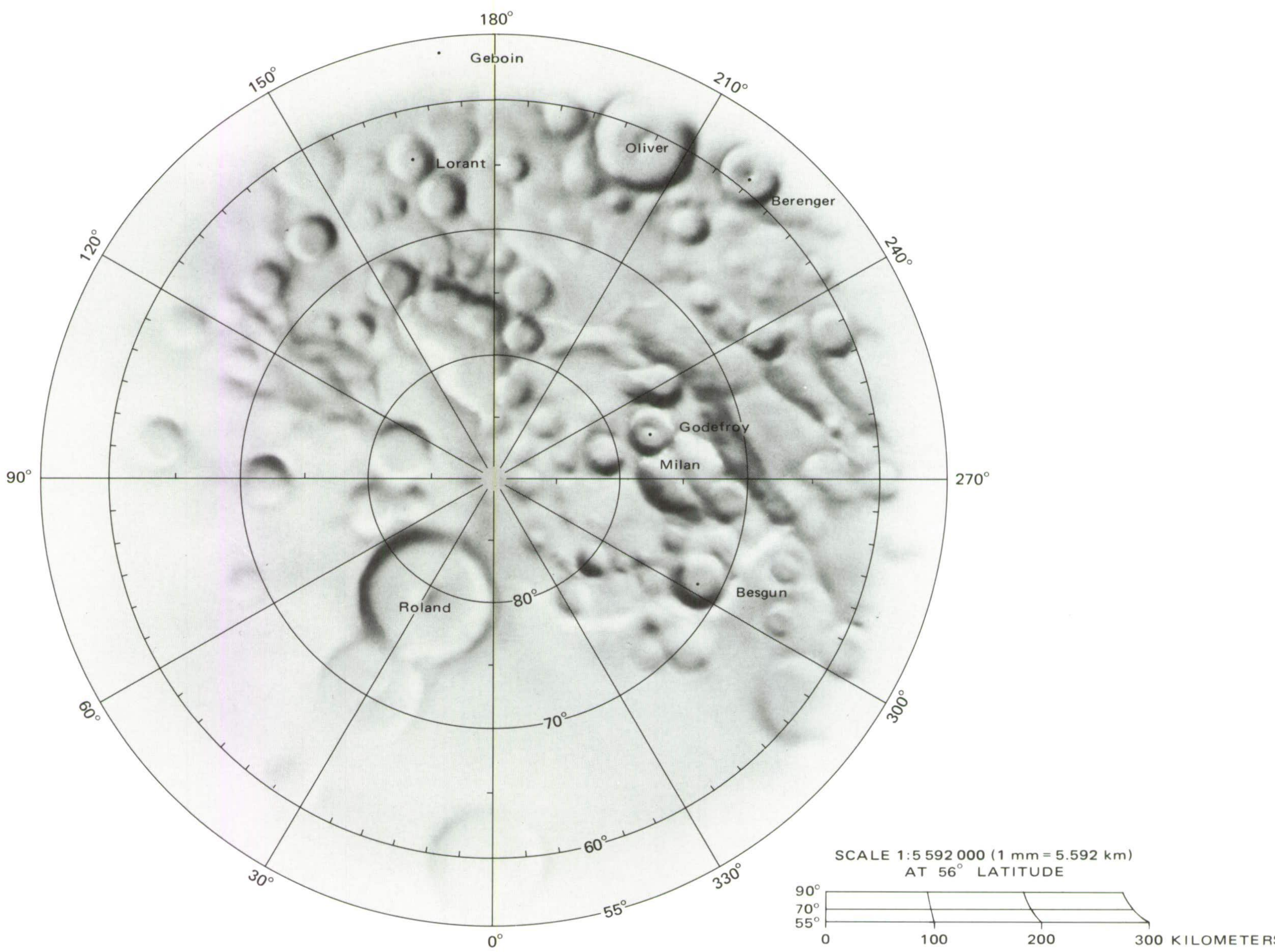

Figure 6–4. Map of the north polar region of Iapetus on a polar stereographic projection (part of map I–1486).

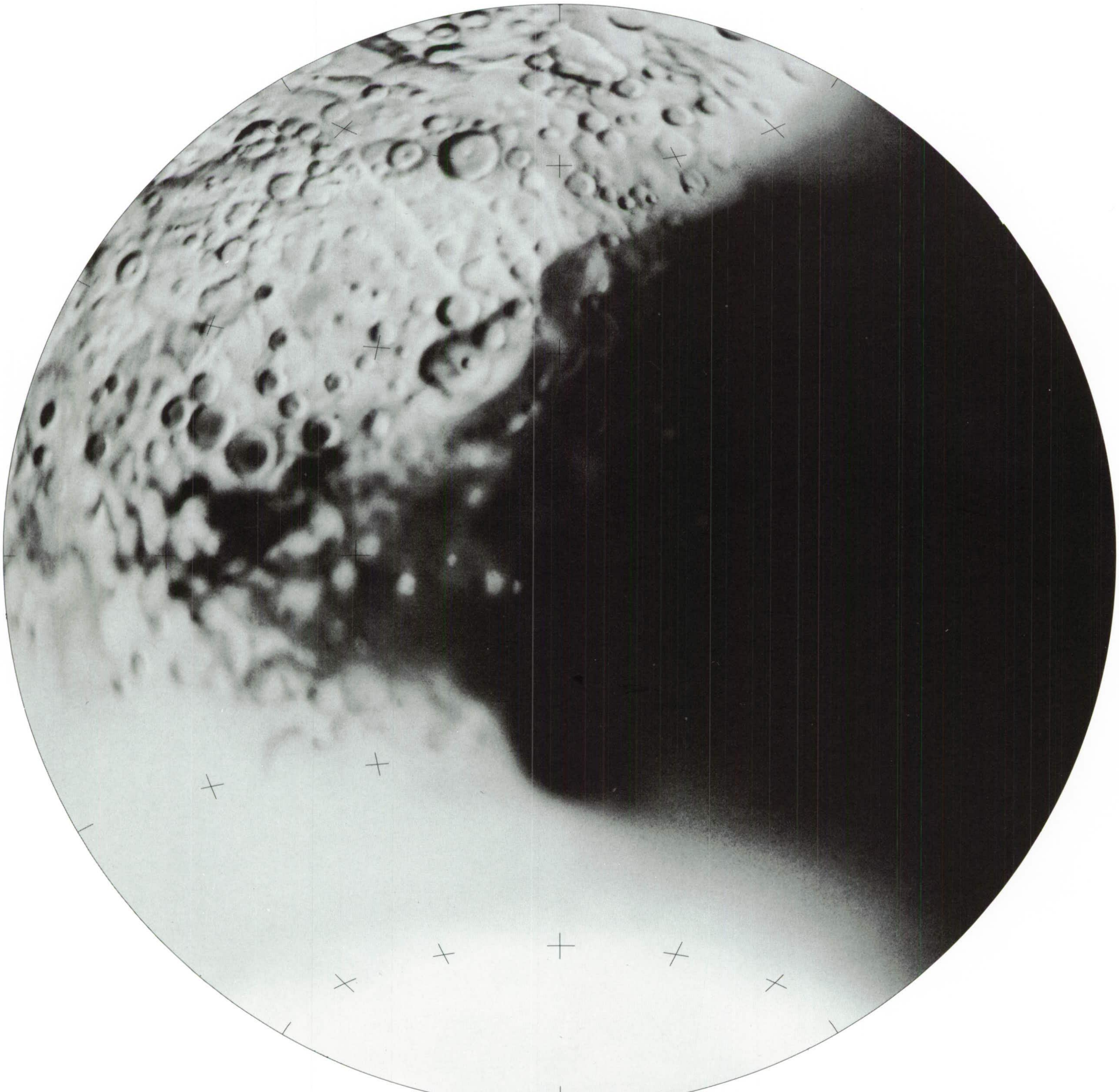

Figure 6–5. Map of the anti-Saturn-facing hemisphere of Iapetus on a Lambert azimuthal equal-area projection. Nomenclature is not shown, to avoid obscuring detail. Scale 1:10 000 000 (1 mm^2 = 100 km^2; 1 in^2 = ~25 000 mi^2).

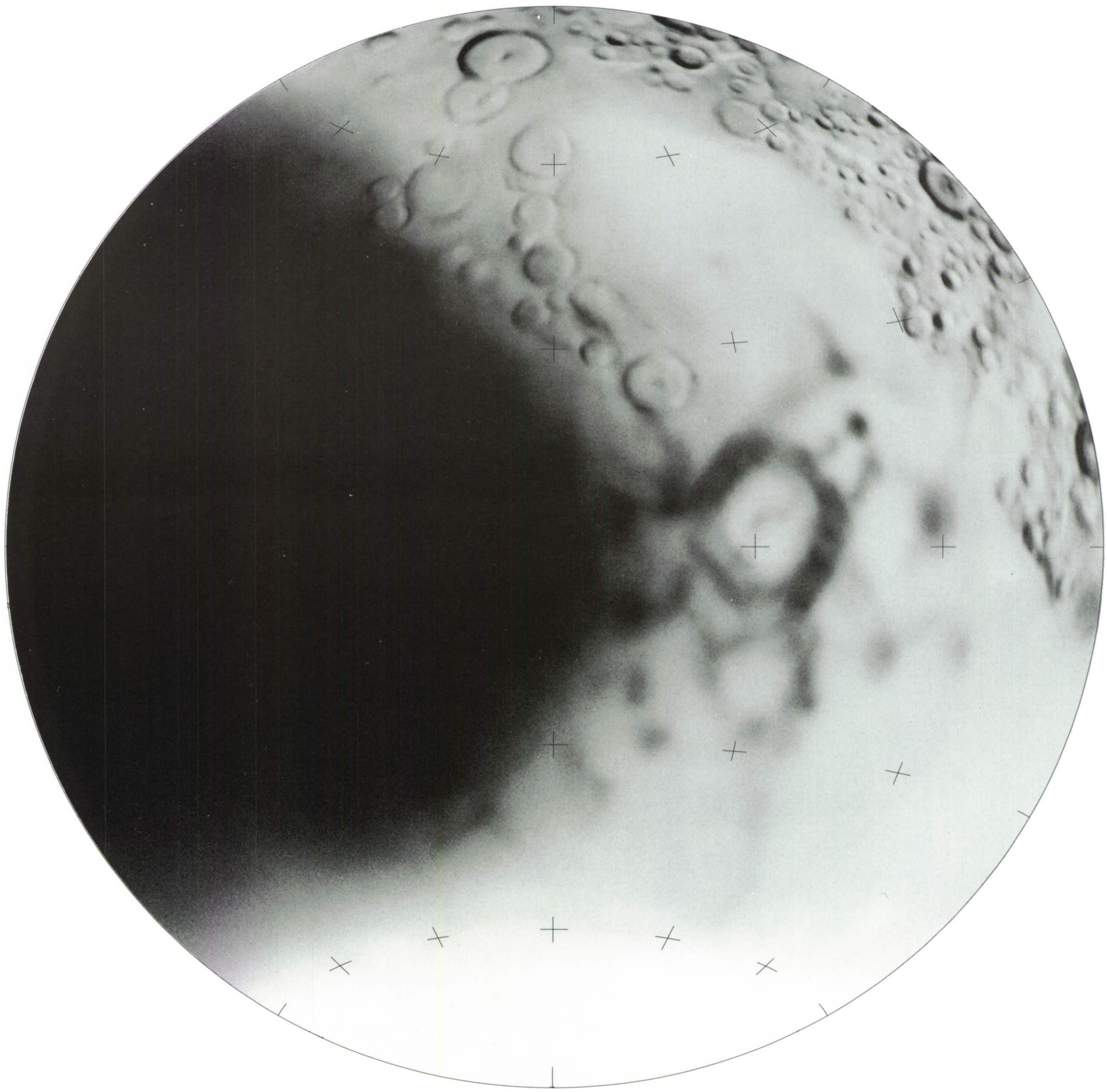

Figure 6–6. Map of the Saturn-facing hemisphere of Iapetus on a Lambert azimuthal equal-area projection. Nomenclature is not shown, to avoid obscuring detail. Scale 1:10 000 000 (1 mm^2 = 100 km^2; 1 in^2 = ~25 000 mi^2).

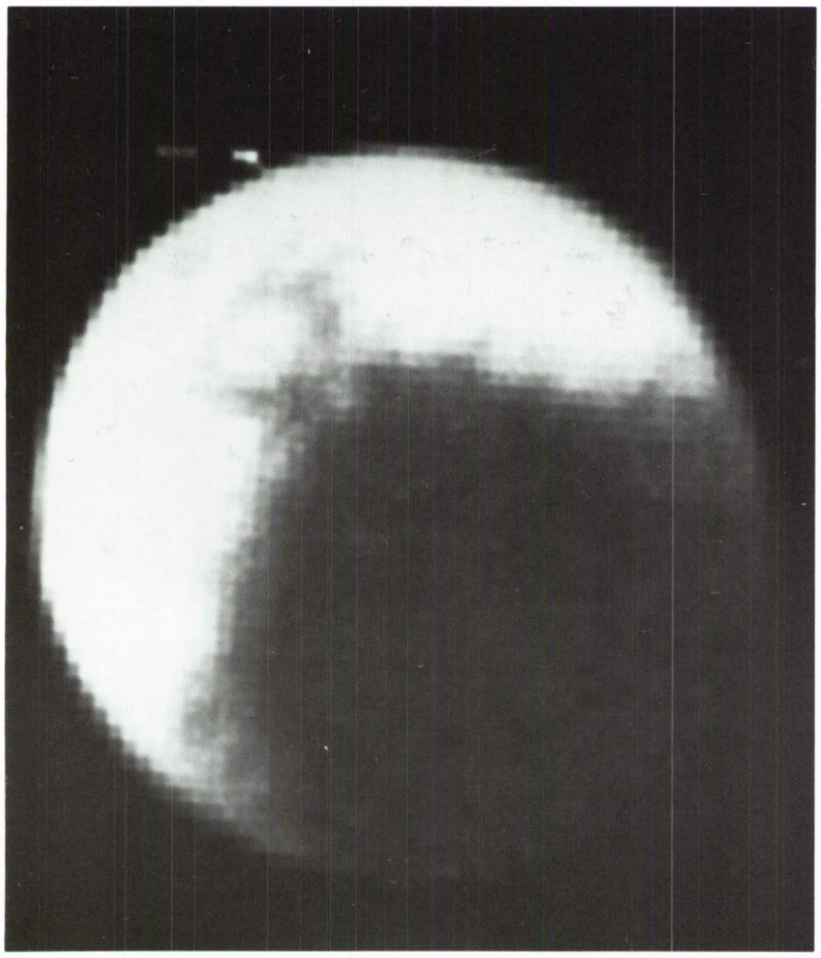

(a)

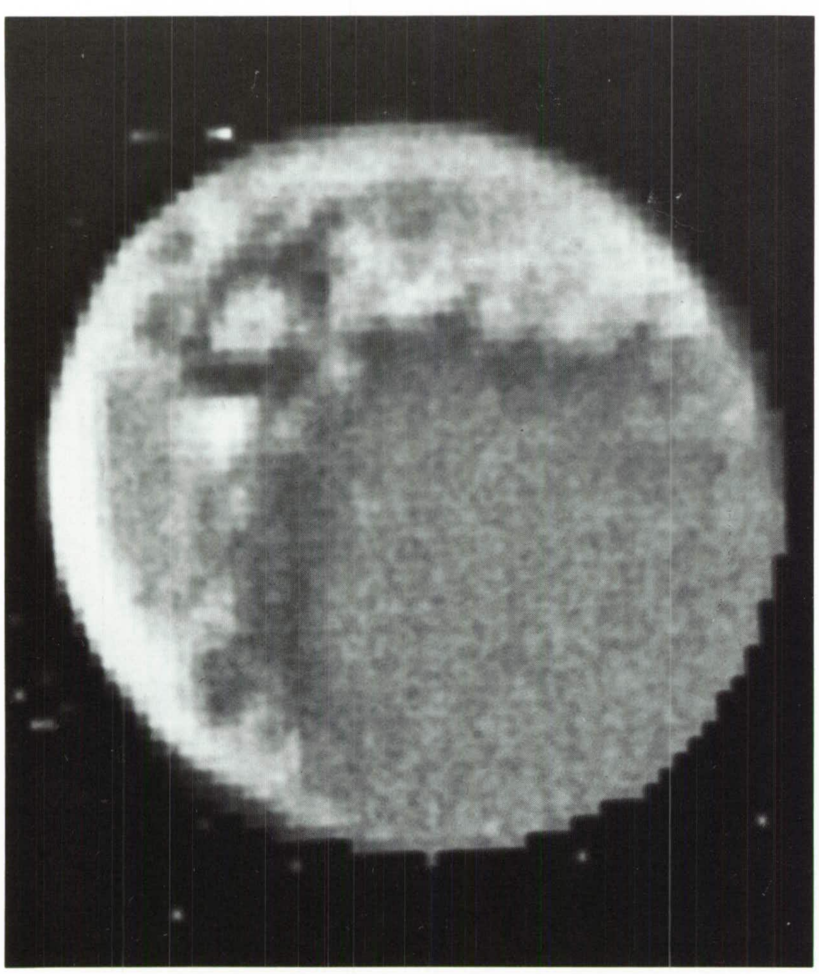

(b)

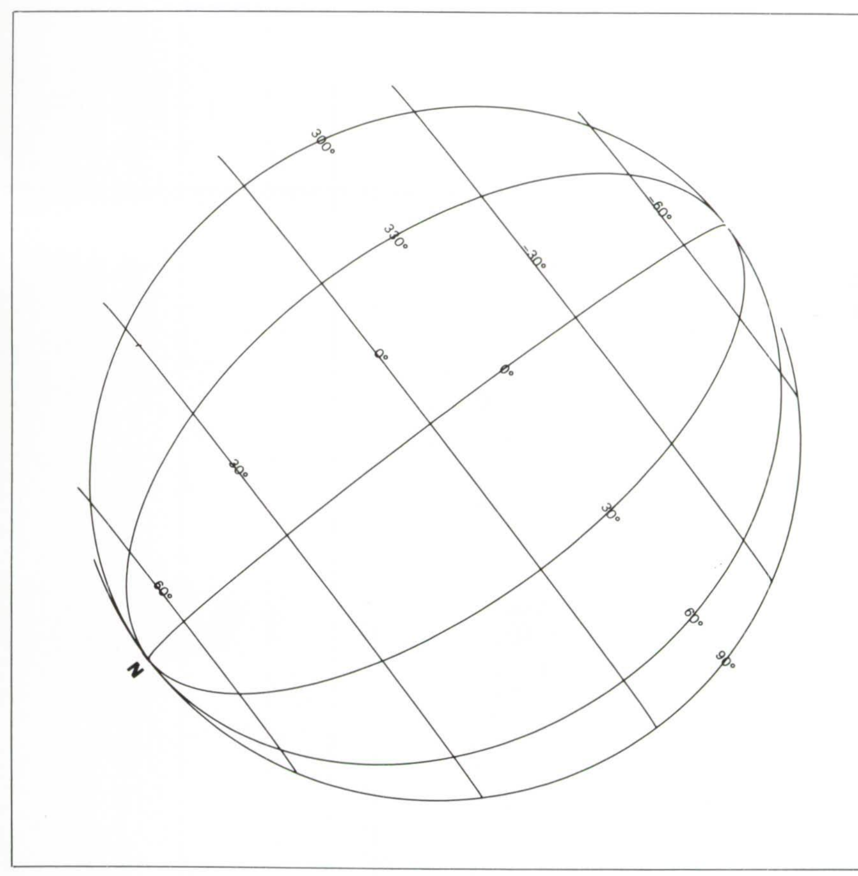

(c)

Picno	0480S1+000
FDS	34951.56
Range, km	3 221 033
Subspacecraft latitude/longitude, degrees	1/13
Subsolar latitude/longitude, degrees	9/3
Resolution, km/pixel	30
Filter size, pixels	9 X 9
Filter size, km	268
Scale	1:15 000 000

Figure 6–7. Picno 0480S1+000. (*a*) Unfiltered image. (*b*) High-pass filtered image. (*c*) Perspective grid.

(a)

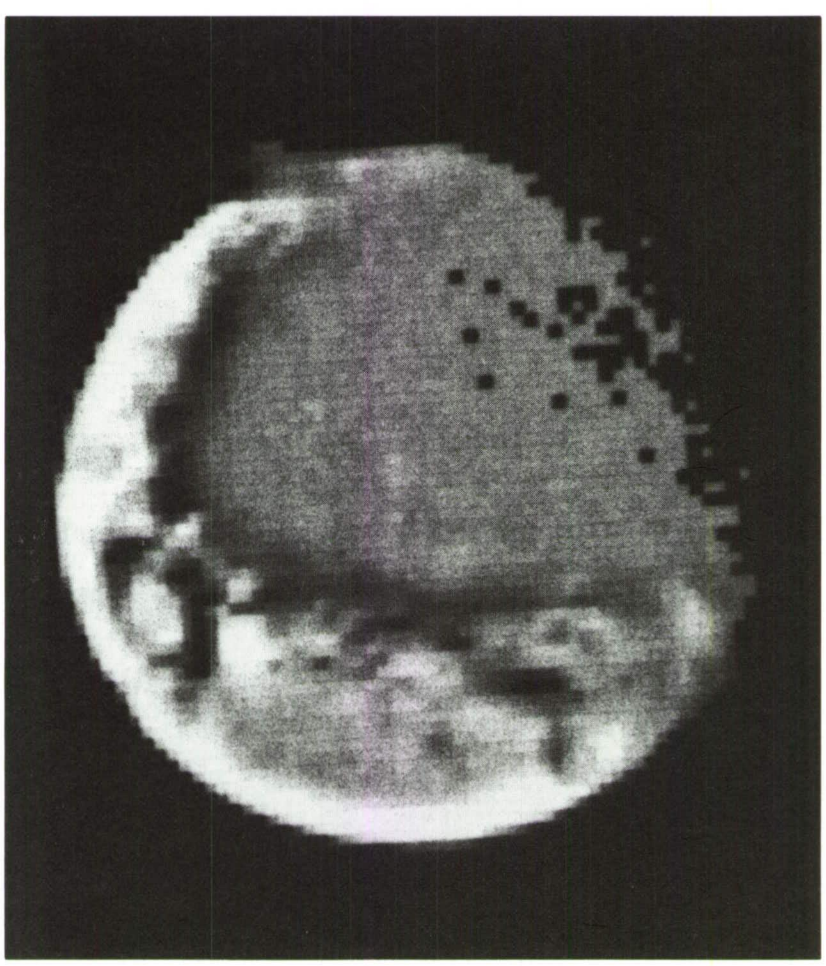

(b)

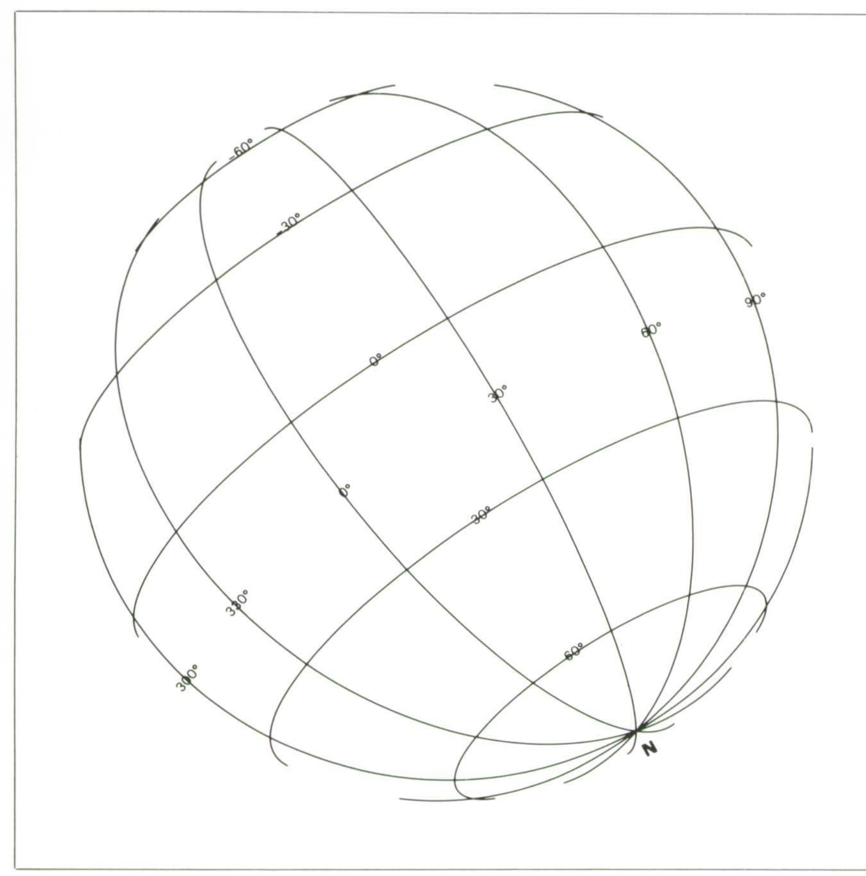

(c)

Picno	0182S1+001
FDS	34976.58
Range, km	2 635 830
Subspacecraft latitude/longitude, degrees	17/19
Subsolar latitude/longitude, degrees	9/7
Resolution, km/pixel	24
Filter size, pixels	9 X 9
Filter size, km	219
Scale	1:15 000 000

Figure 6–8. Picno 0182S1+001. (*a*) Unfiltered image. (*b*) High-pass filtered image. (*c*) Perspective grid.

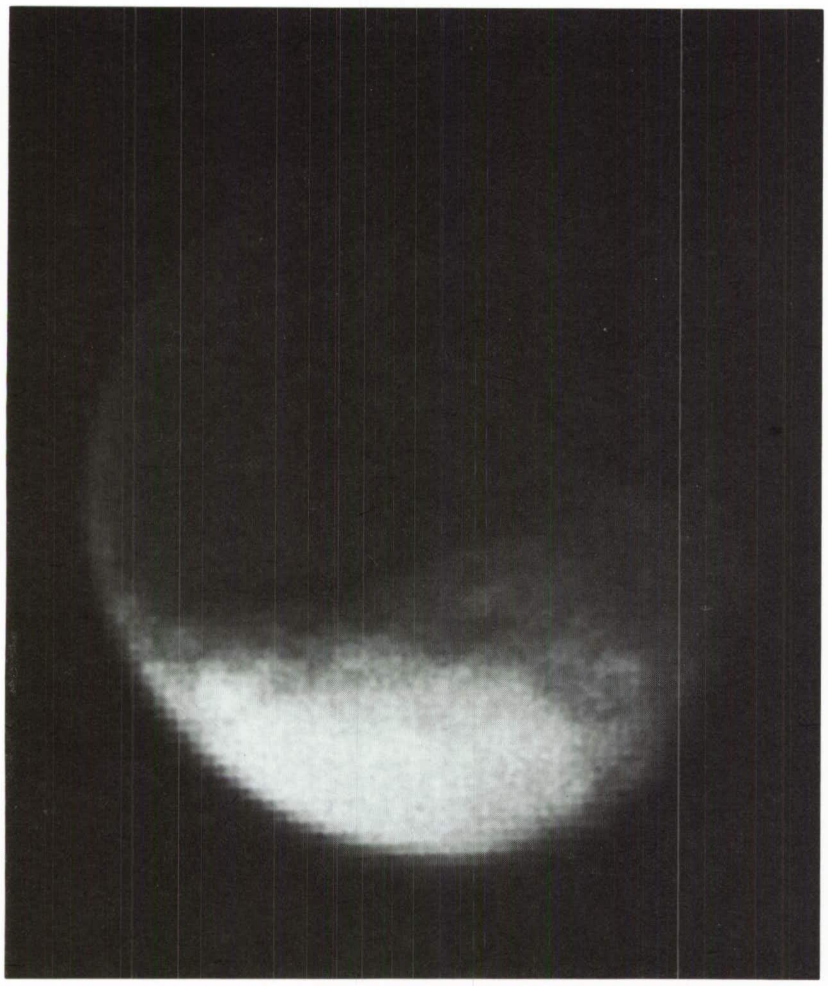

(a)

(b)

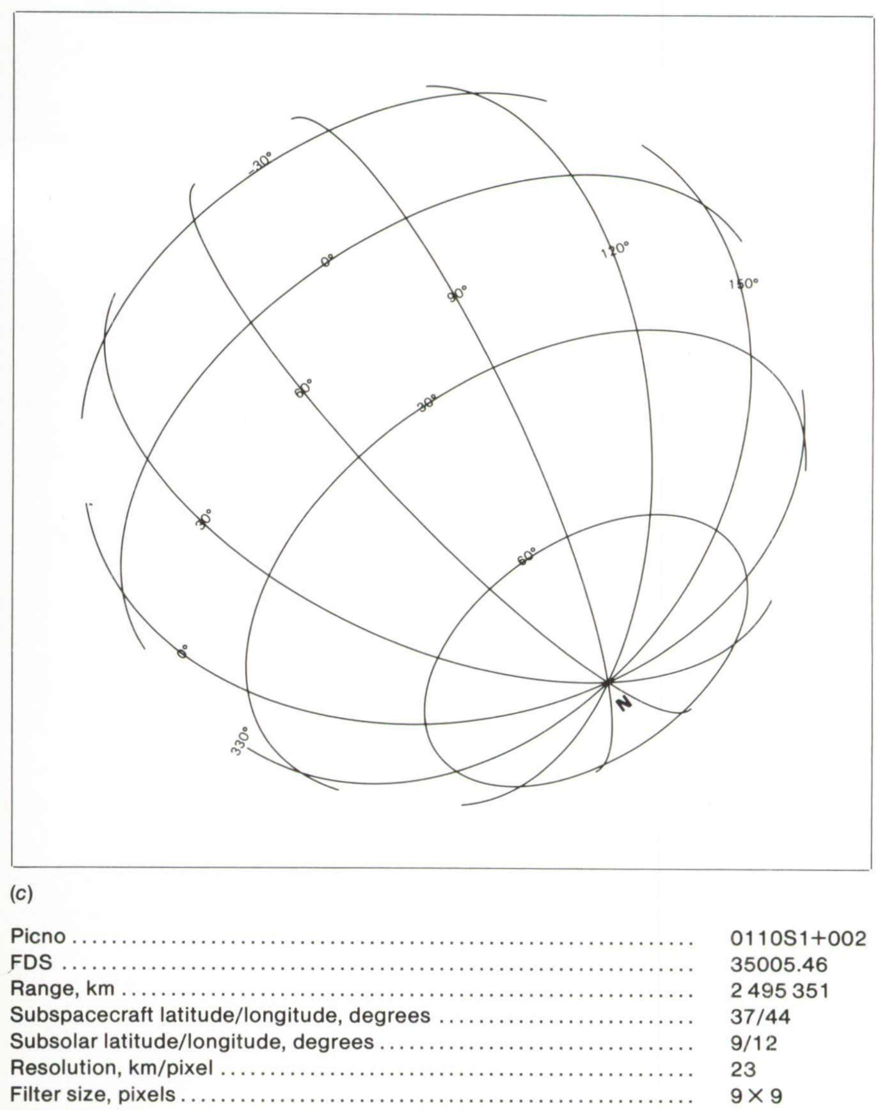

(c)

Picno	0110S1+002
FDS	35005.46
Range, km	2 495 351
Subspacecraft latitude/longitude, degrees	37/44
Subsolar latitude/longitude, degrees	9/12
Resolution, km/pixel	23
Filter size, pixels	9 X 9
Filter size, km	208
Scale	1:15 000 000

Figure 6–9. Picno 0110S1+002. (*a*) Unfiltered image. (*b*) High-pass filtered image. (*c*) Perspective grid.

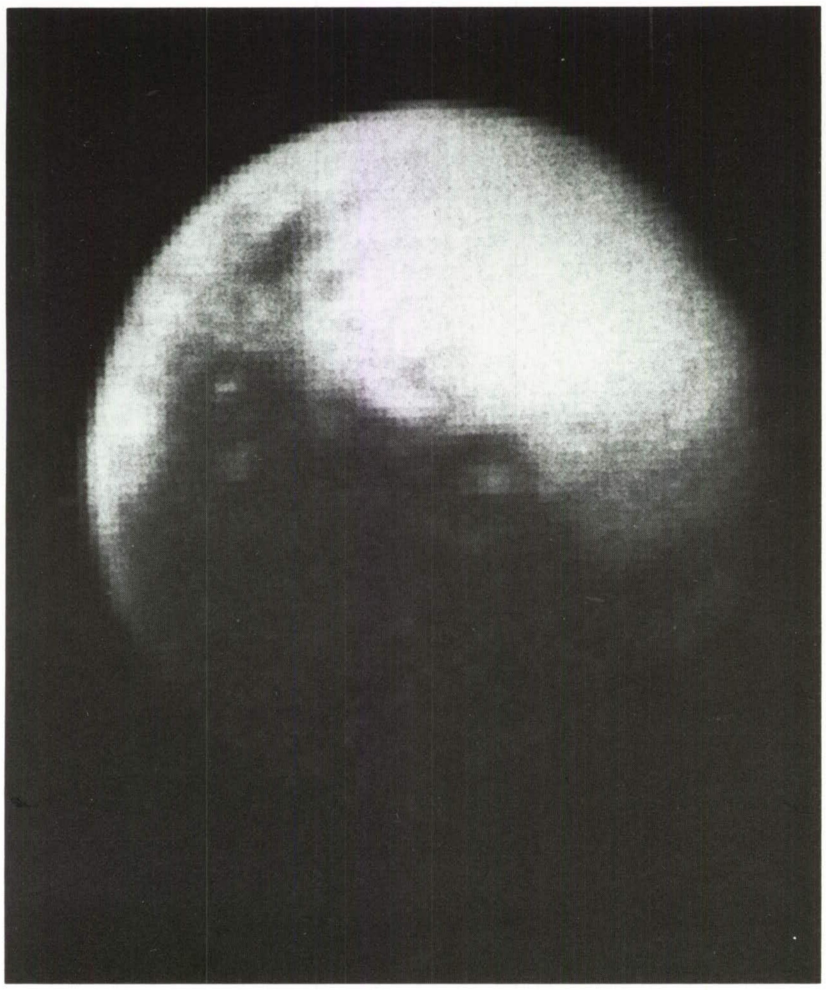

(a)

(b)

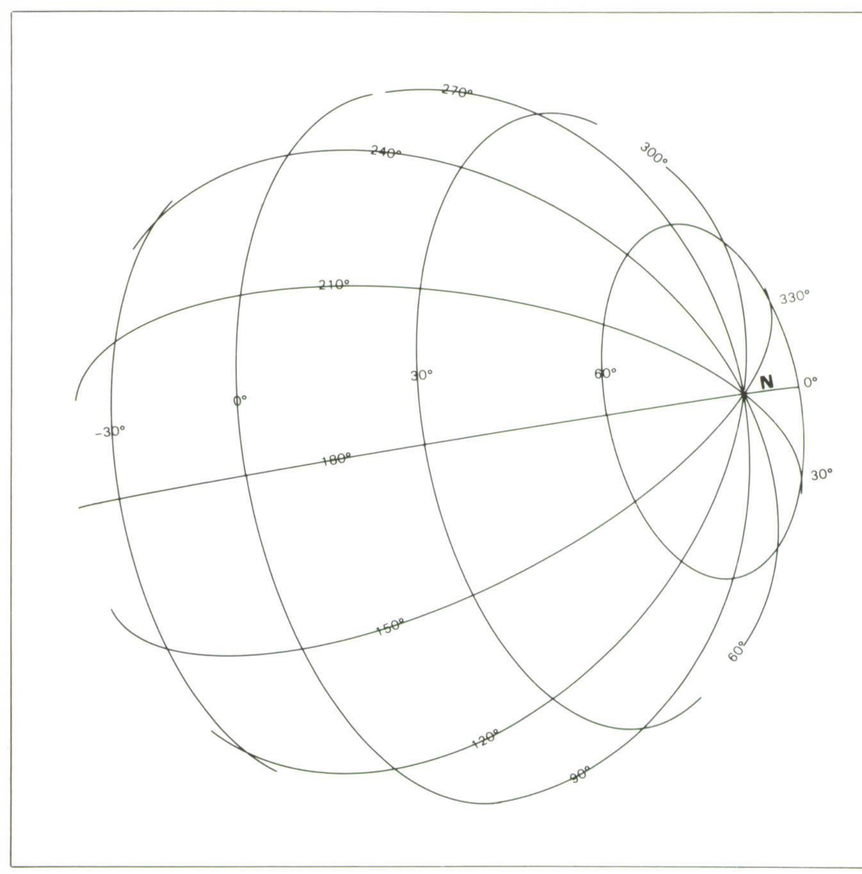

(c)

Picno	1562S2–006
FDS	43851.39
Range, km	2 226 309
Subspacecraft latitude/longitude, degrees	32/179
Subsolar latitude/longitude, degrees	11/188
Resolution, km/pixel	20
Filter size, pixels	19 × 19
Filter size, km	391
Scale	1:15 000 000

Figure 6–10. Picno 1562S2–006. (*a*) Unfiltered image. (*b*) High-pass filtered image. (*c*) Perspective grid.

(a)

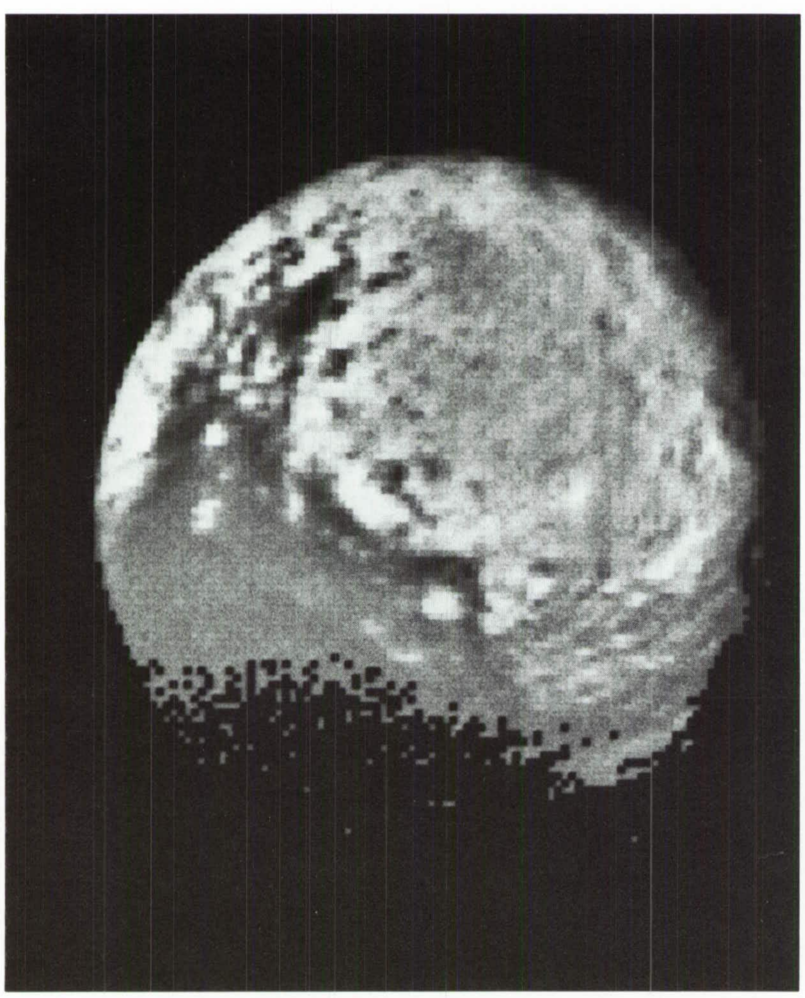

(b)

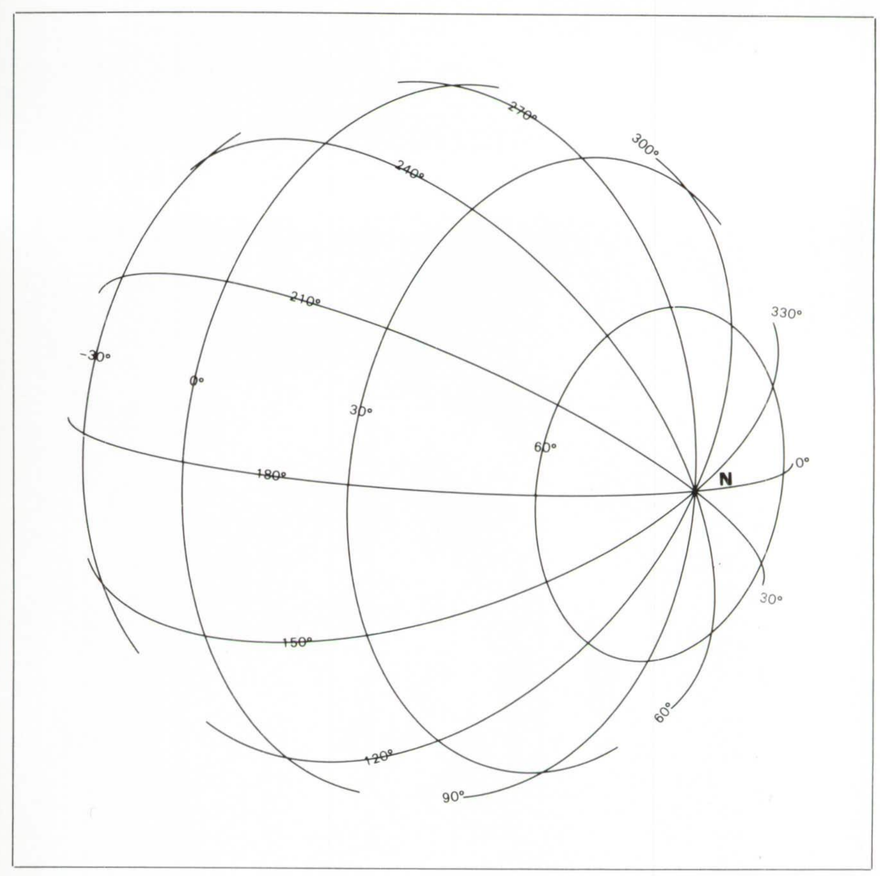

(c)

Picno	1174S2–005
FDS	43875.11
Range, km	1 545 842
Subspacecraft latitude/longitude, degrees	42/191
Subsolar latitude/longitude, degrees	11/192
Resolution, km/pixel	14
Filter size, pixels	15 × 15
Filter size, km	214
Scale	1:15 000 000

Figure 6–11. Picno 1174S2—005. (*a*) Unfiltered image. (*b*) High-pass filtered image. (*c*) Perspective grid.

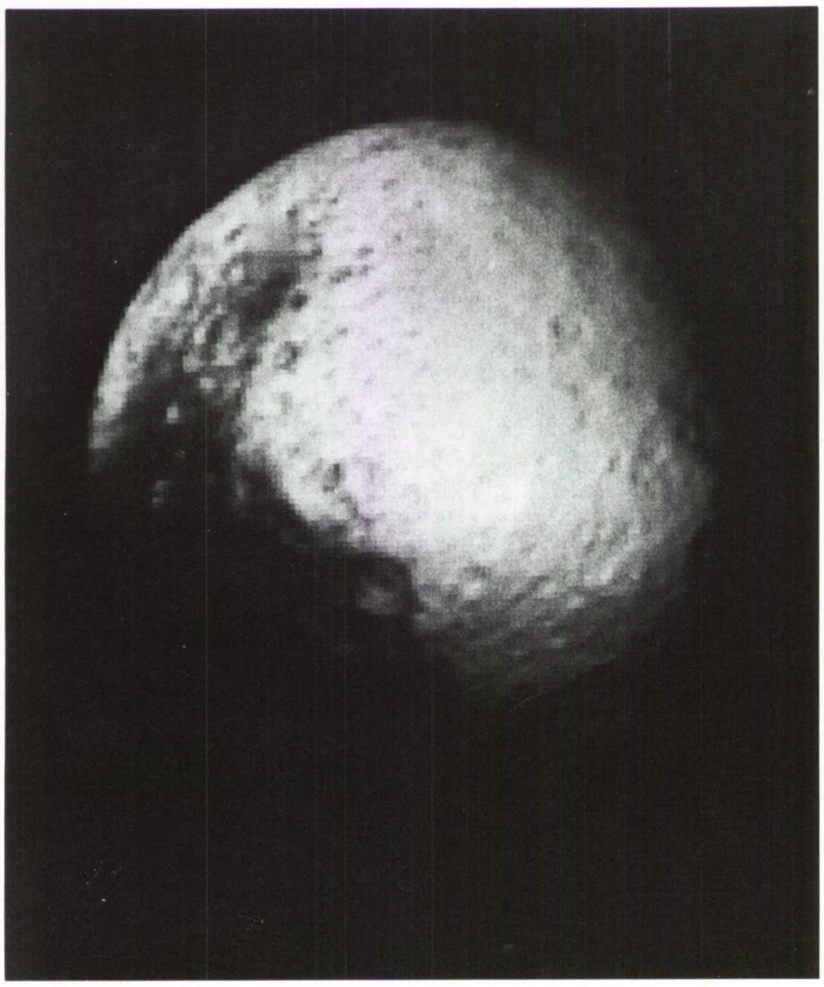

(a)

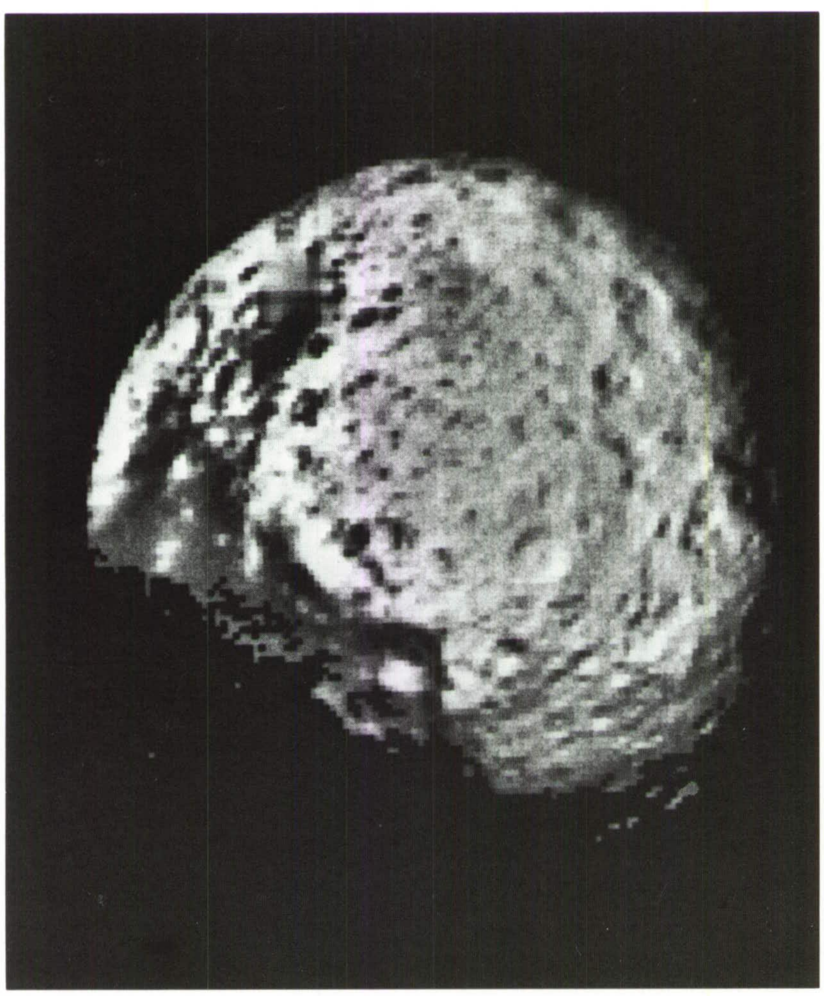

(b)

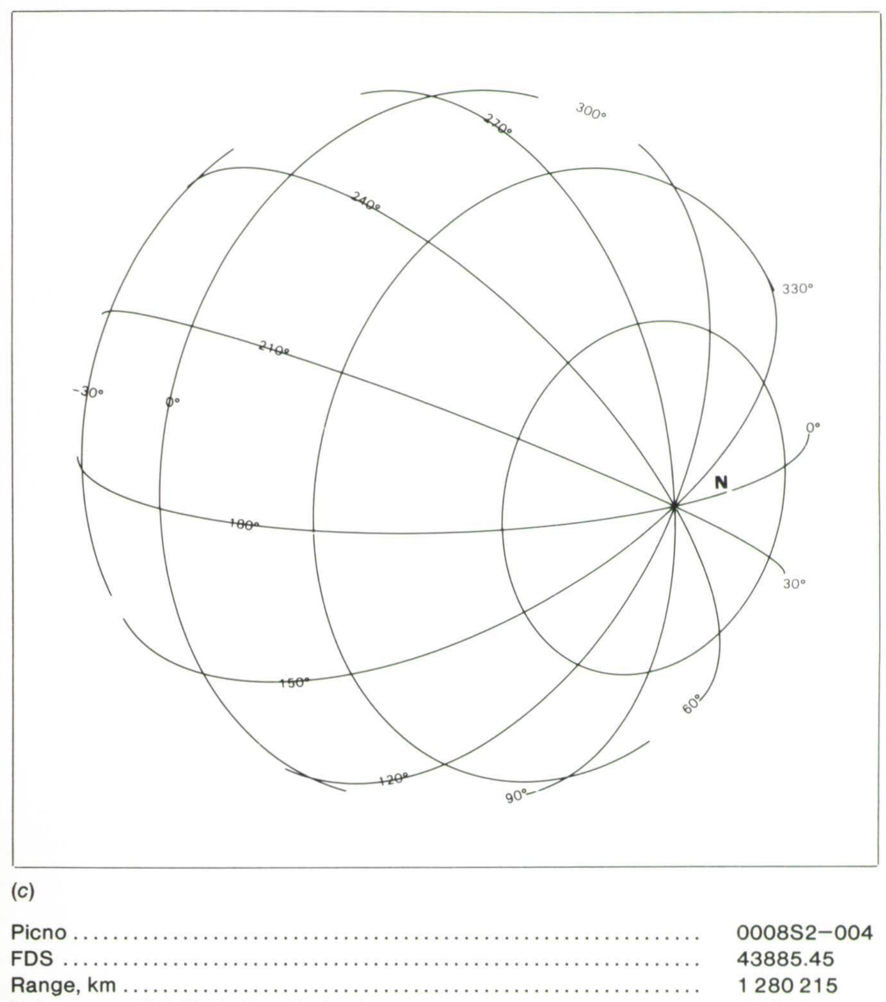

(c)

Picno	0008S2—004
FDS	43885.45
Range, km	1 280 215
Subspacecraft latitude/longitude, degrees	49/201
Subsolar latitude/longitude, degrees	11/193
Resolution, km/pixel	12
Filter size, pixels	17 × 17
Filter size, km	201
Scale	1:15 000 000

Figure 6–12. Picno 0008S2—004. (*a*) Unfiltered image. (*b*) High-pass filtered image. (*c*) Perspective grid.

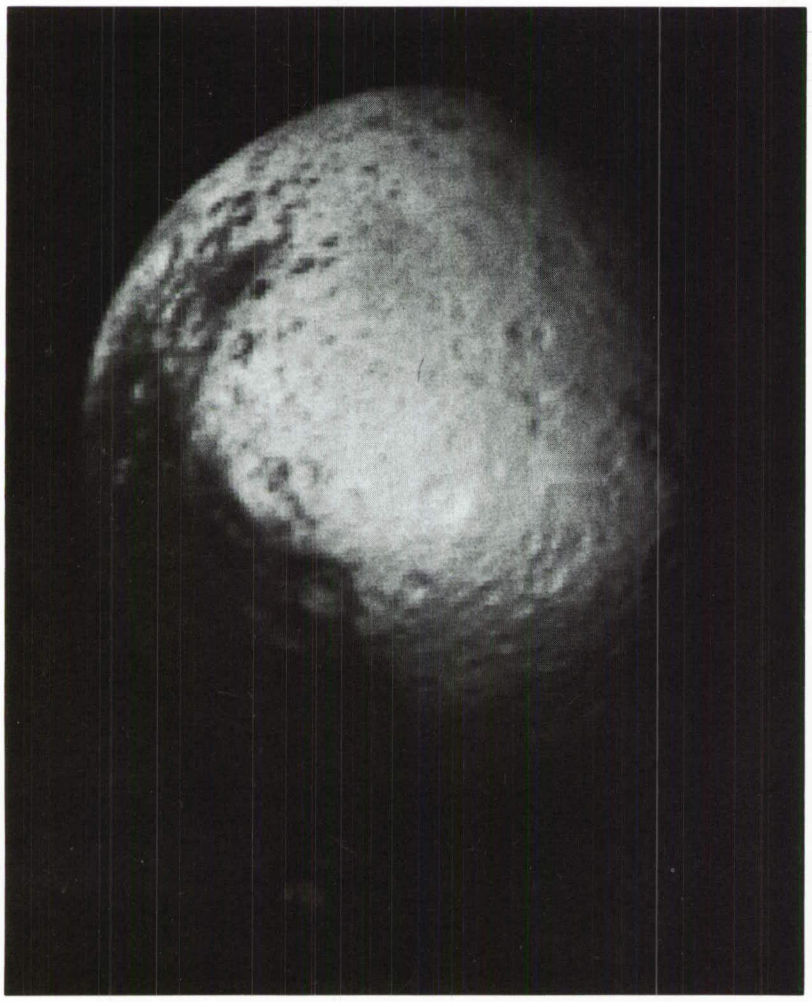

(a)

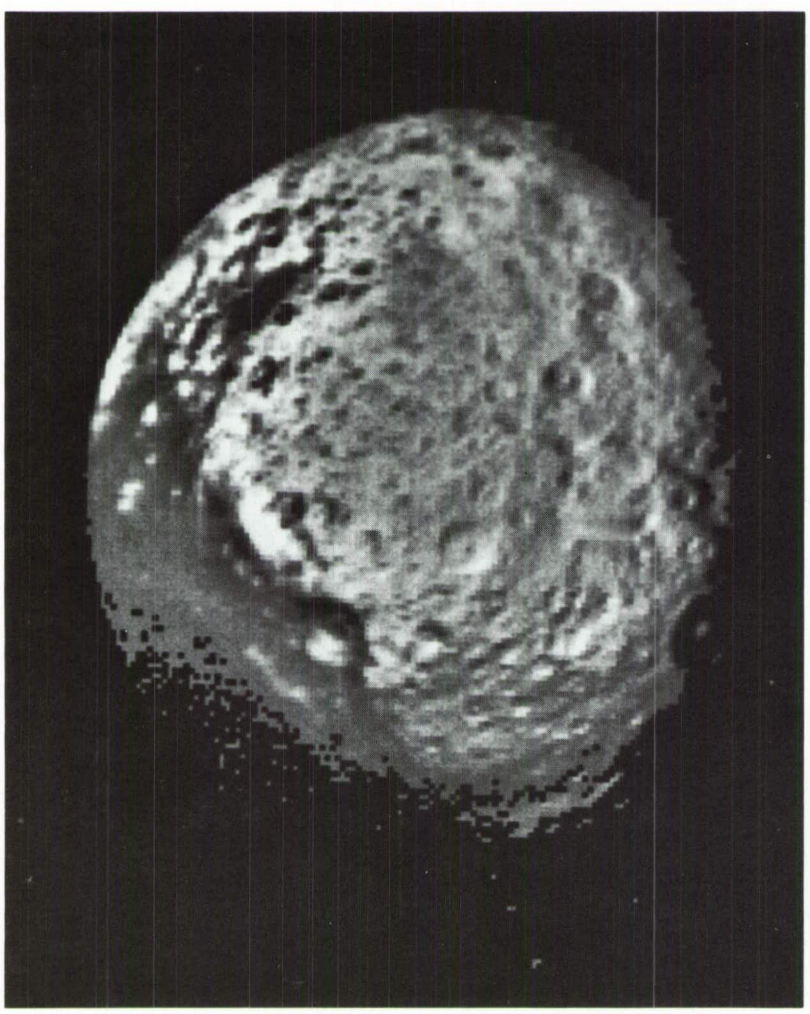

(b)

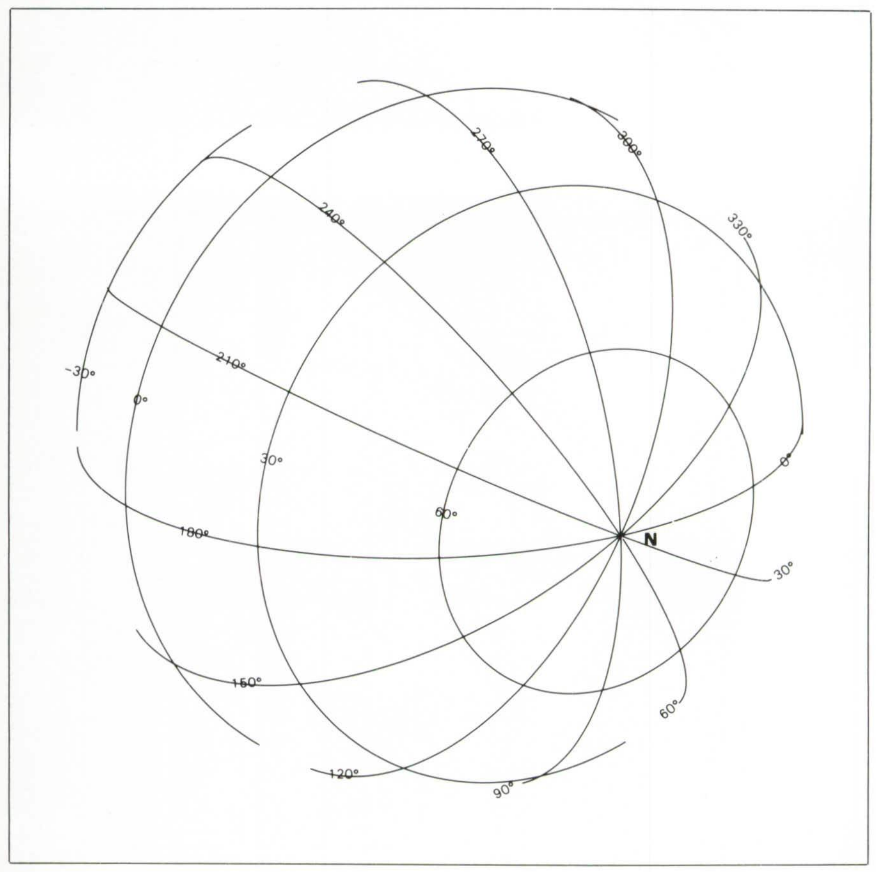

(c)

Picno	0523S2–004
FDS	43894.20
Range, km	1 099 661
Subspacecraft latitude/longitude, degrees	55/217
Subsolar latitude/longitude, degrees	11/194
Resolution, km/pixel	10
Filter size, pixels	21 × 21
Filter size, km	214
Scale	1:15 000 000

Figure 6–13. Picno 0523S2–004. (*a*) Unfiltered image. (*b*) High-pass filtered image. (*c*) Perspective grid.

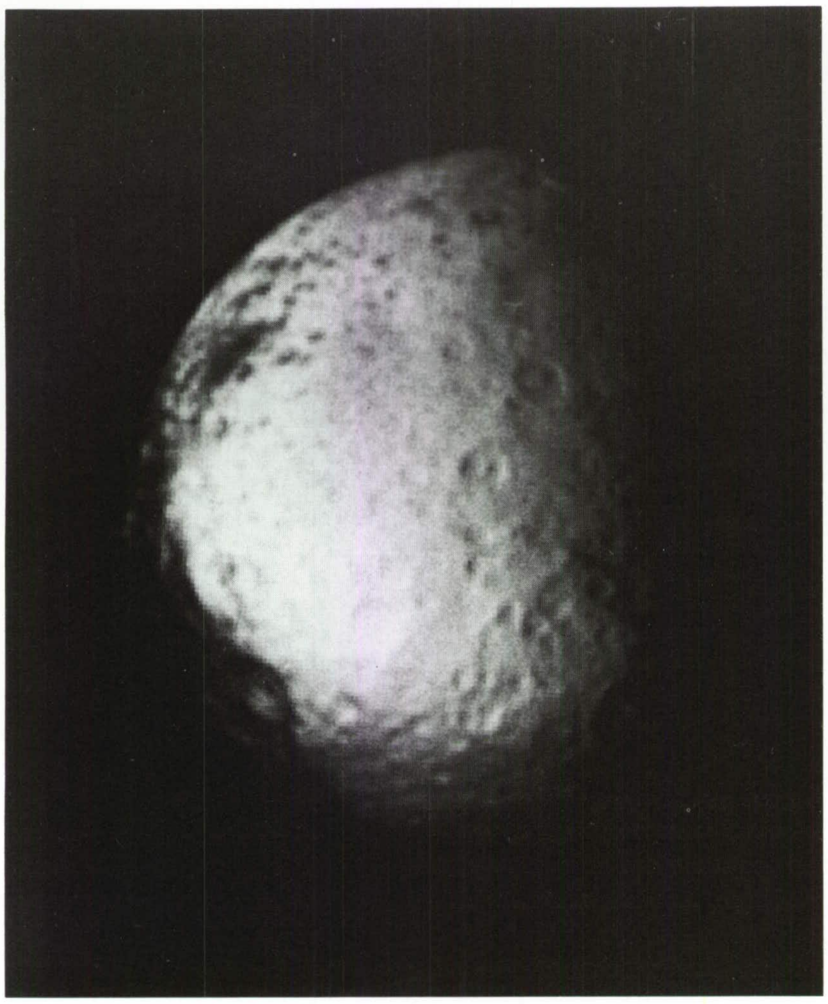

(a)

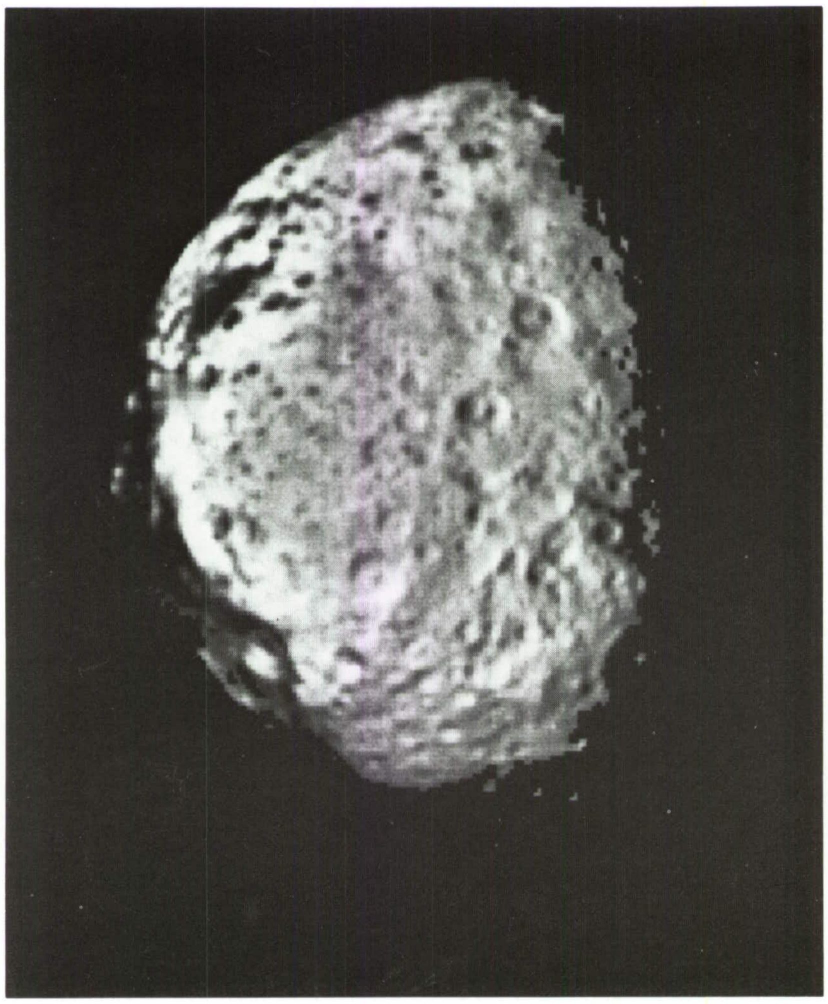

(b)

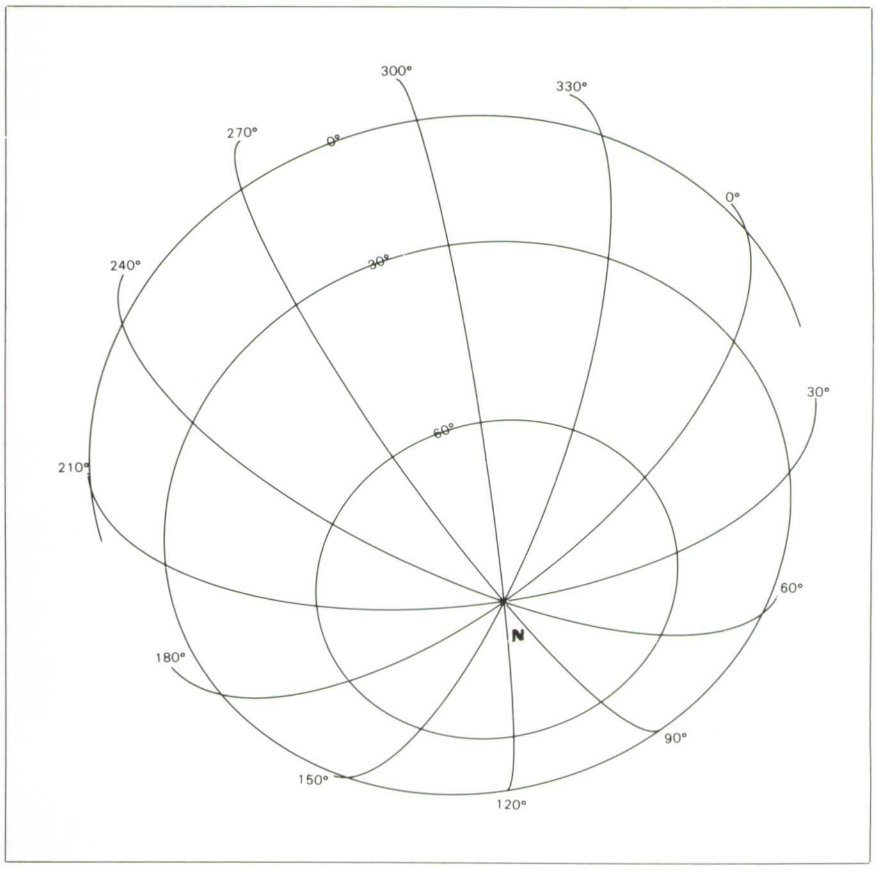

(c)

Picno	1291S2—004
FDS	43907.08
Range, km	930 228
Subspacecraft latitude/longitude, degrees	61/260
Subsolar latitude/longitude, degrees	11/196
Resolution, km/pixel	9
Filter size, pixels	23 × 23
Filter size, km	198
Scale	1:15 000 000

Figure 6–14. Picno 1291S2—004. (*a*) Unfiltered image. (*b*) High-pass filtered image. (*c*) Perspective grid.

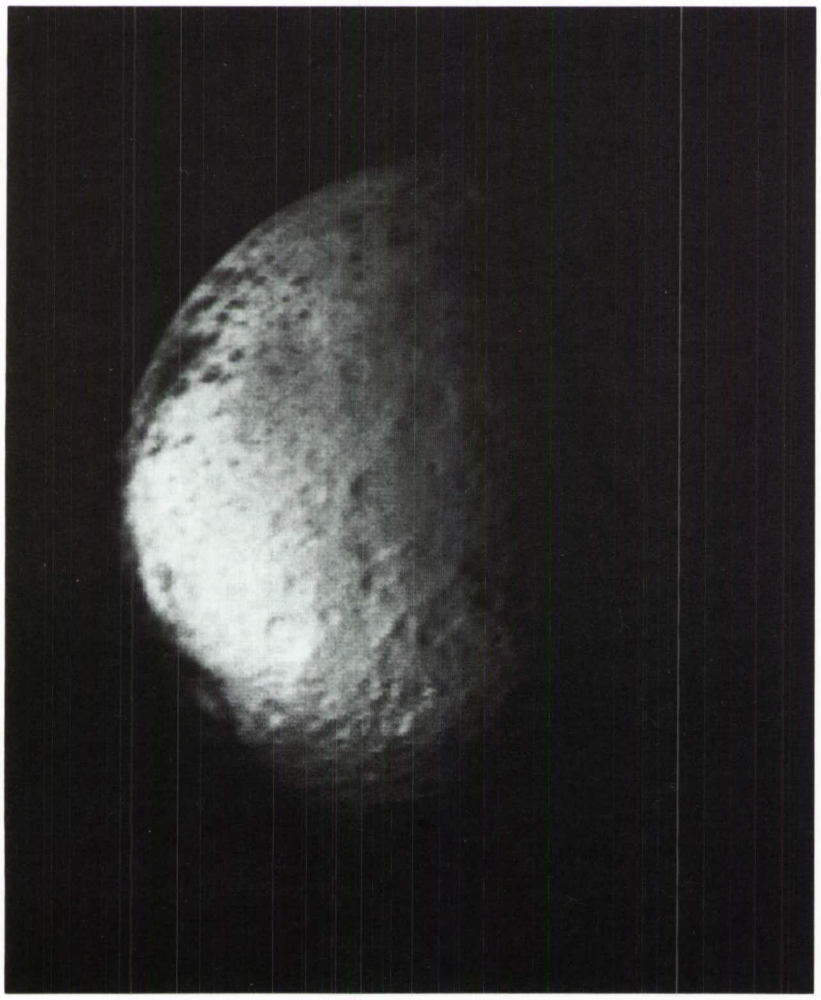

(a)

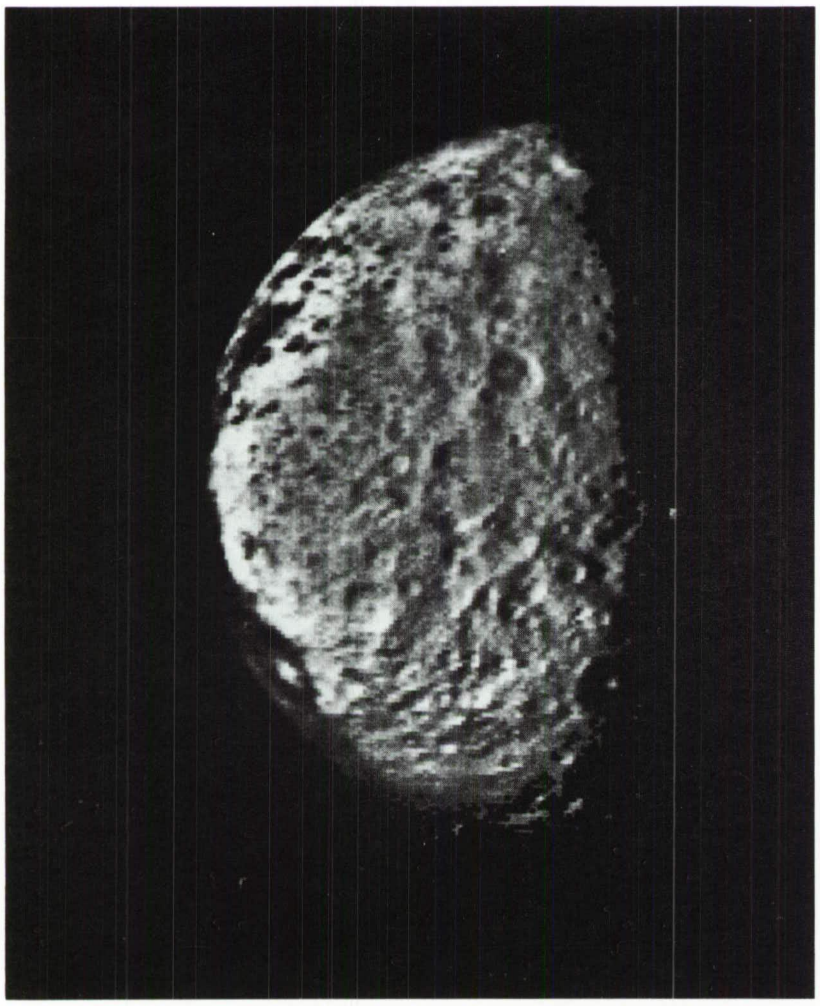

(b)

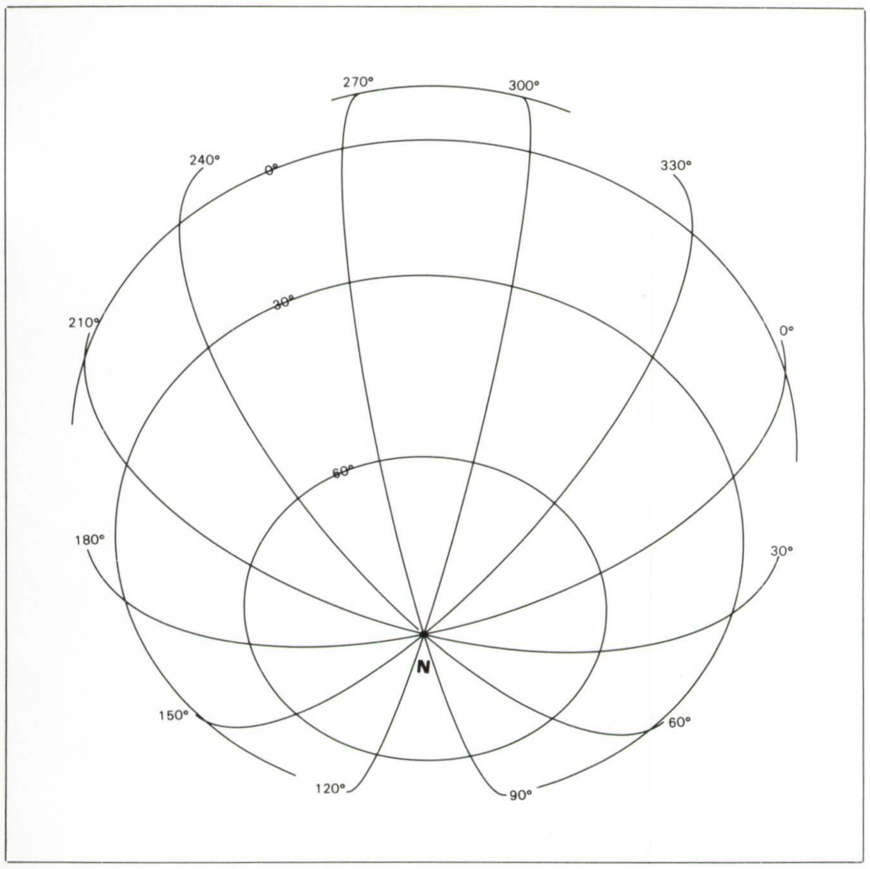

(c)

Picno	1678S2–004
FDS	43913.35
Range, km	908 777
Subspacecraft latitude/longitude, degrees	58/287
Subsolar latitude/longitude, degrees	11/197
Resolution, km/pixel	8
Filter size, pixels	19 × 19
Filter size, km	160
Scale	1:15 000 000

Figure 6–15. Picno 1678S2–004. (*a*) Unfiltered image. (*b*) High-pass filtered image. (*c*) Perspective grid.

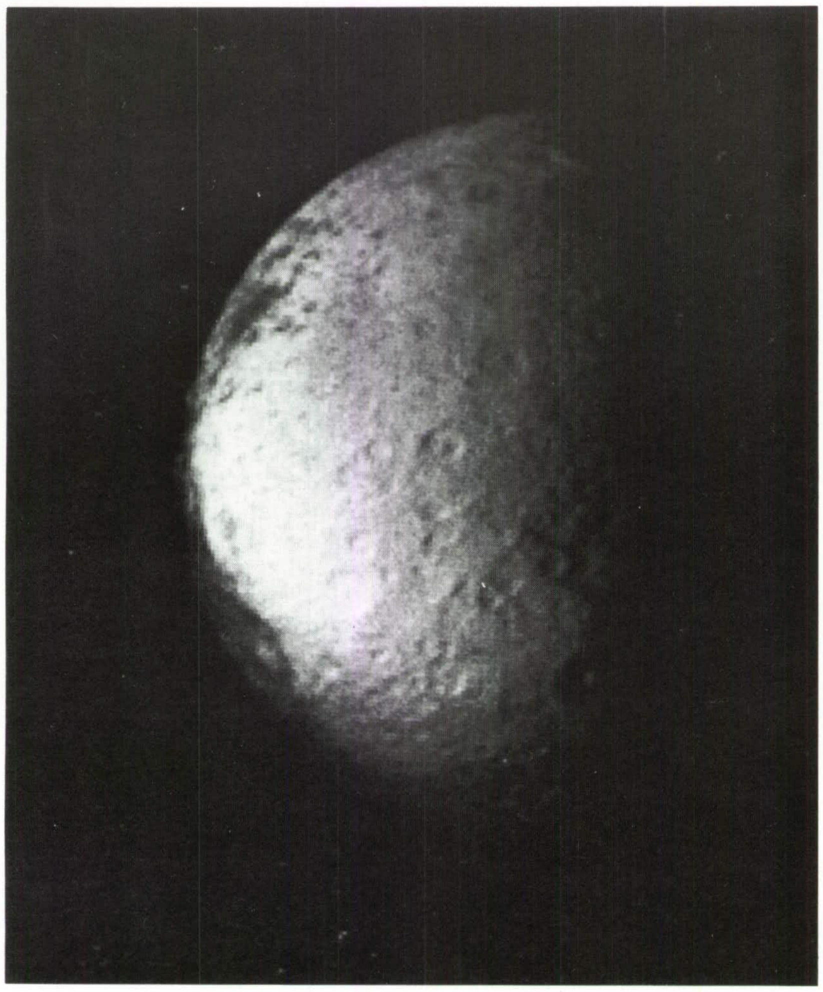

(a)

(b)

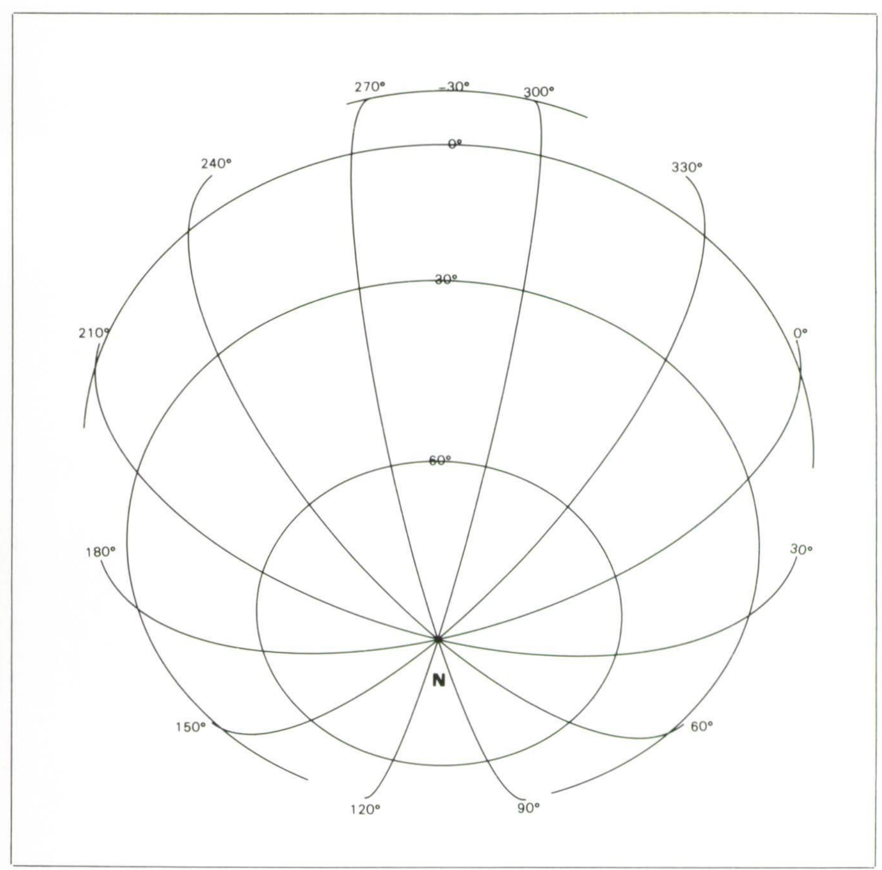

(c)

Picno	1690S2–004
FDS	43913.47
Range, km	908 891
Subspacecraft latitude/longitude, degrees	58/288
Subsolar latitude/longitude, degrees	11/197
Resolution, km/pixel	8
Filter size, pixels	29 × 29
Filter size, km	244
Scale	1:15 000 000

Figure 6–16. Picno 1690S2–004. (*a*) Unfiltered image. (*b*) High-pass filtered image. (*c*) Perspective grid.

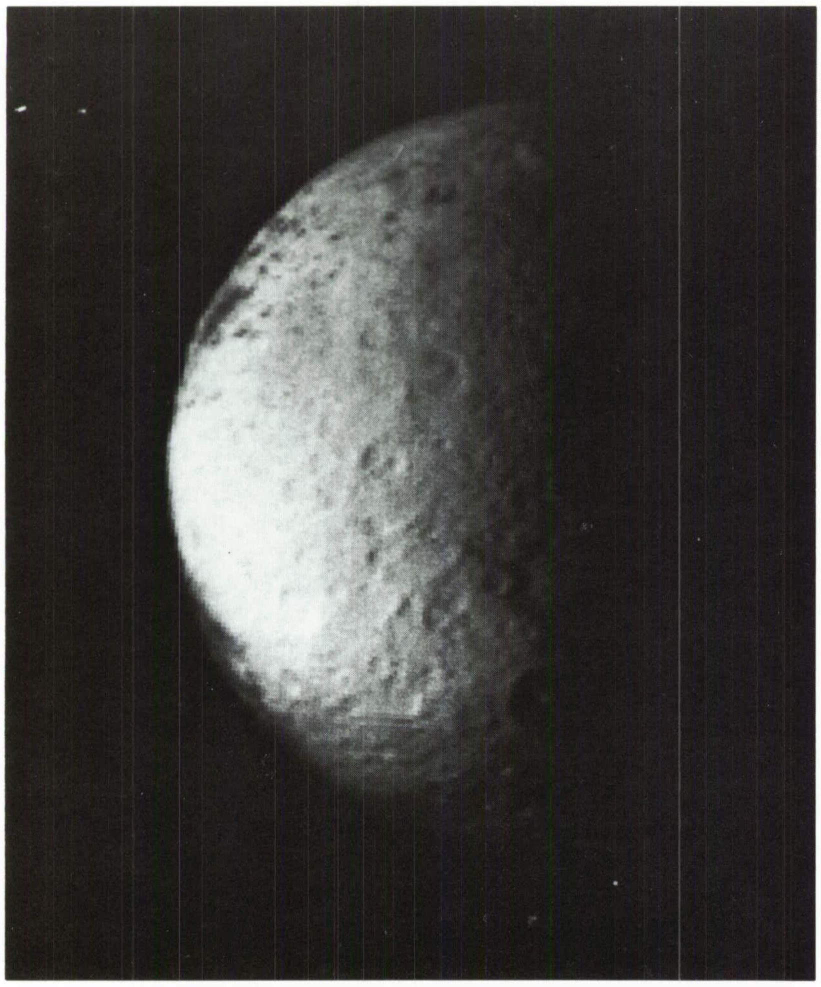

(a)

(b)

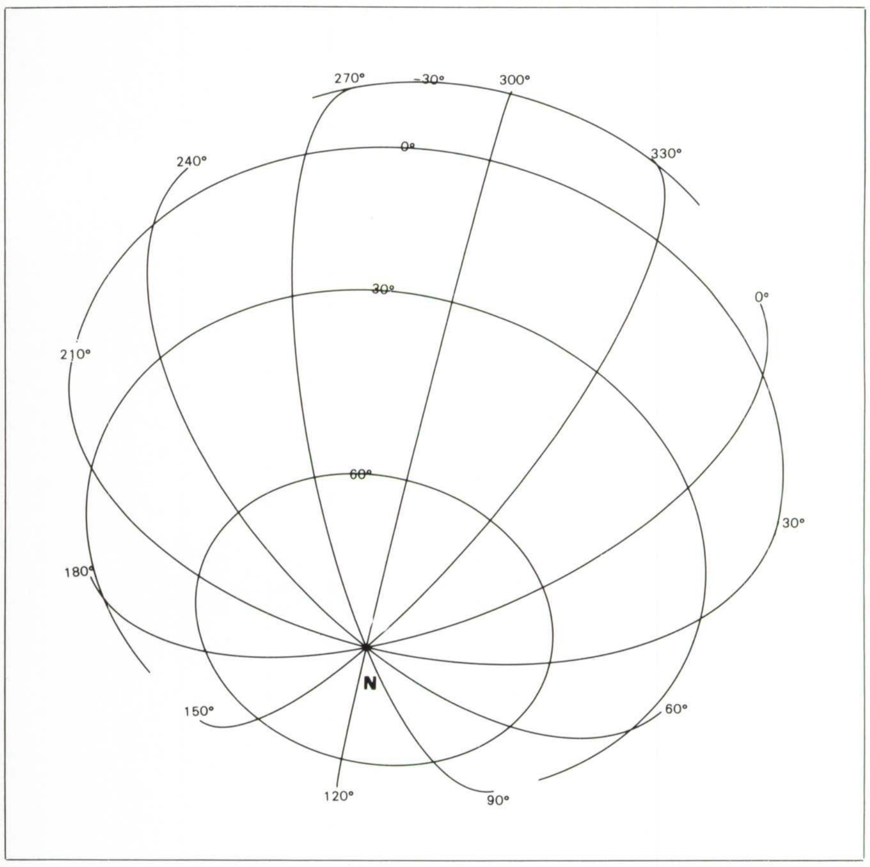

(c)

Picno	0154S2—003
FDS	43918.11
Range, km	923 264
Subspacecraft latitude/longitude, degrees	53/302
Subsolar latitude/longitude, degrees	11/198
Resolution, km/pixel	8
Filter size, pixels	17 × 17
Filter size, km	145
Scale	1:15 000 000

Figure 6–17. Picno 0154S2—003. (*a*) Unfiltered image. (*b*) High-pass filtered image. (*c*) Perspective grid.

Page intentionally left blank

References

Baines, Keith. 1962, *Malory's Le Morte d'Arthur.* Mentor. New York.

Bates, Herbert. 1900, *The Odyssey of Homer.* Harper and Brothers. New York.

Batson, R. M. 1978, Planetary Mapping With the Airbrush. *Sky and Telescope* **55**(2): 109–112.

Batson, R. M. 1980, Status and Future of Extraterrestrial Mapping Programs. *Int. Arch. Photogram.,* Commission IV, XIVth Congr. Int. Soc. Photogram. Hamburg, West Germany, pp. 36–55. Also NASA CR–3390.

Benesh, M; and Jepsen, F. 1978, *Voyager Imaging Science Subsystem Calibration Report.* Jet Propulsion Laboratory Rept. 618–802, pp. 3–14 and 3–32.

Burton, Richard F. 1900, *The Thousand Nights and a Night.* Carson-Harper Press, Denver.

Collins, S. A.; Cook, A. F., II; Cuzzi, J. N.; Danielson, G. E.; Hunt, G. E.; Johnson, T. V.; Morrison, D.; Owen, T.; Pollack, J. B.; Smith, B. A.; and Terrile, R. J. 1980, First Voyager View of the Rings of Saturn. *Nature* **288**: 439–442.

Davies, M. E. 1983, Updated Diameters for the Saturnian Satellites. Personal communication.

Davies, M. E.; Abalakin, V. K.; Cross, C. A.; Duncombe, R. L.; Masursky, H.; Morando, B.; Owen, T. C.; Seidelmann, P. K.; Sinclair, A. T.; Wilkins, G. A.; and Tjuflin, Y. S. 1980, Report of the IAU Working Group on Cartographic Coordinates and Rotational Elements of the Planets and Satellites. *Celestial Mechanics* **22**: 205–230.

Davies, M. E.; and Katayama, F. Y. 1983*a*, The Control Networks of Mimas and Enceladus. *Icarus* **53**(2): 332–340.

Davies, M. E.; and Katayama, F. Y. 1983*b*, The Control Networks of Tethys and Dione. *J. Geophys. Res.* **88**(A11): 8729–8735.

Graves, Robert. 1955, *The Greek Myths,* vol. 1. Penguin Books Inc. Baltimore.

Inge, J. L. 1972, *Principles of Lunar Illustration.* Aeronaut. Chart and Inf. Center Ref. Pub. RP–72–1.

Inge, J. L.; and Bridges, P. M. 1976, Applied Photointerpretation for Airbrush Cartography. *Photogram. Eng. Remote Sensing* **42**(6): 749–760.

International Astronomical Union, Commission 16. 1971, Physical Study of Planets and Satellites. 14th Gen. Assem., 1970, Proc., *Int. Astron. Union Trans.* **XIVB**: 128–137.

International Astronomical Union, Working Group for Planetary System Nomenclature. 1983, 18th Gen. Assem., Patras, 1982, Proc., *Int. Astron. Union Trans.* **XVIIB**: 337–344.

Mandelbaum, Allen. 1972, *The Aeneid of Virgil.* Bantam. New York.

Moik, Johannes G. 1980, *Digital Processing of Remotely Sensed Images.* NASA SP–431.

Morrison, David. 1982, *Voyages to Saturn.* NASA SP–451.

Sayers, Dorothy L. 1967, *The Song of Roland.* Penguin Books Inc. Baltimore.

Science. 1980, Special Pioneer Saturn issue. Vol. **207**: 400–453.

Science. 1981, Special Voyager 1 issue. Vol. **212**(4491): 159–243.

Science. 1982, Special Voyager 2 issue. Vol. **215**(4532): 498–594.

Smith, B. A.; Soderblom, L. A.; Beebe, R.; Boyce, J.; Briggs, G.; Bunker, A.; Collins, S. A.; Hansen, C. J.; Johnson, T. V.; Mitchell, J. L.; Terrile, R. J.; Carr, M.; Cook, A. F., II; Cuzzi, J. N.; Pollack, J. B.; Danielson, G. E.; Ingersoll, A.; Davies, M. E.; Hunt, G. E.; Masursky, H.; Shoemaker, E.; Morrison, D.; Owen, T.; Sagan, C.; Veverka, J.; Strom, R.; and Suomi, V. E. 1982, Encounter With Saturn: Voyager 1 Imaging Science Results. *Science* **212**(4491): 163–191.

Space Science Reviews. 1977, Special Voyager instrumentation issue. Vol. **21**(2): 75–232. (See especially Kohlhase and Penzo, Voyager Mission Description, pp. 77–101; and Smith et al., Voyager Imaging Experiment, pp. 103–127.)

Space Science Reviews. 1977, Special Voyager instrumentation issue. Vol. **21**(3): 234–376.
Stone, E. C.; and Miner, E. D. 1981, Voyager 1 Encounter With the Saturnian System. *Science* **212**(4491): 159–163.

APPENDIX A

The Voyager Mission

The Voyager 2 and 1 spacecraft were launched on August 20, 1977, and September 5, 1977, respectively, to explore the planets and satellites in the outer solar system. After extremely successful traverses through the Jovian system in March and July of 1979, the two Voyagers continued on to Saturn, where they arrived in November of 1980 and August of 1981. Figure 3 in the section entitled "Introduction" diagrams the trajectories of the Voyagers through the Saturnian system. At the time of Voyager 1's closest encounter with Saturn, it was 1524 million km (947 million miles) from Earth. The radio signals from the spacecraft, traveling at the speed of light, required 1 hr and 25 min to reach tracking stations on Earth. Voyager 2 was 1556 million km (967 million miles) from Earth during the Saturnian encounter, and its readio signals required 1 hr and 27 min to reach Earth.

Many remote sensing instruments are carried on each spacecraft, including two television cameras with telephoto lenses. Figure A–1 is a diagram showing the locations of various instruments on the Voyager spacecraft.

Each Voyager spacecraft carries a wide-angle camera, with a field of view of about 3°, and a narrow-angle camera with a field of view of less than ½°. The optical configuration of the Voyager cameras is diagrammed in figure A–2. Tables A–1 and A–2 show selected specifications of the cameras. Objects as small as 1 km in diameter (about 0.6 mile) can be detected on the surface from a distance of 55 000 km (about 34 000 miles). Figure A–3 is a telescopic picture of the Moon that has been digitized and modified to illustrate what the Voyager narrow-angle camera could have resolved from

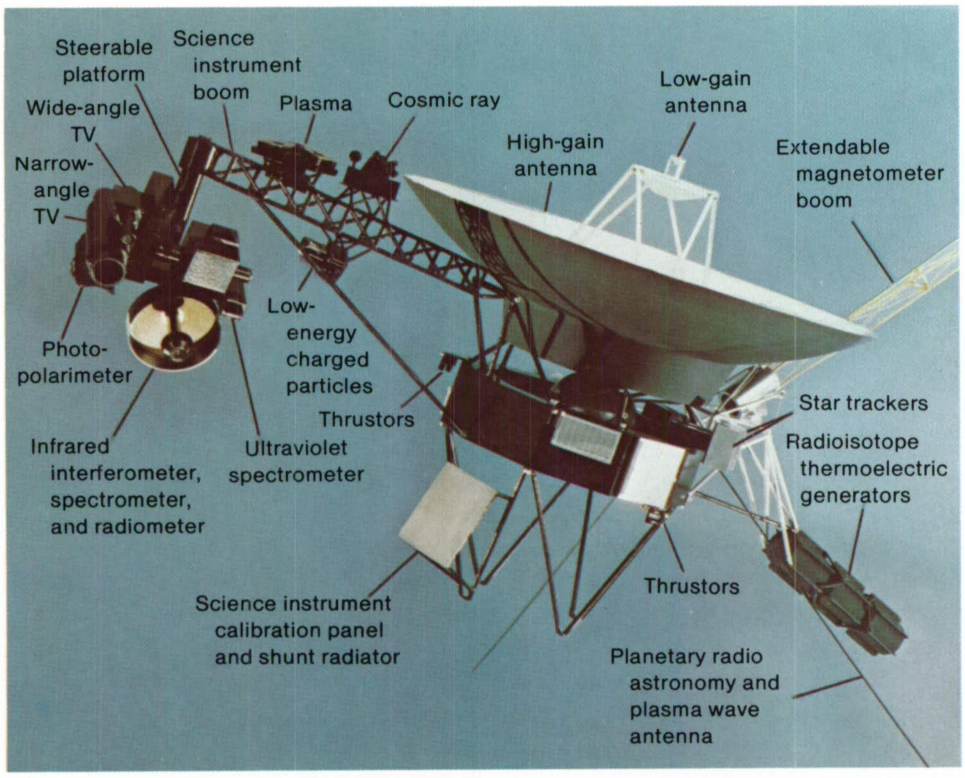

Figure A–1. The Voyager spacecraft, showing locations of the various instruments (JPL photo P 1881AC).

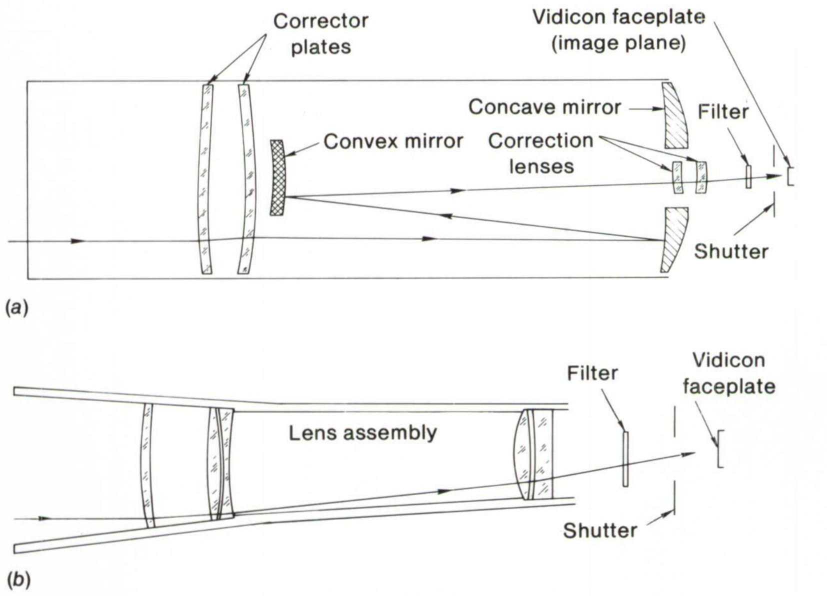

Figure A–2. Optical configuration of the Voyager cameras. (*a*) The narrow-angle cameras have nominal focal lengths of 1500 mm and use catadioptric mirror telescopes for imaging. (*b*) The wide-angle cameras have 200-mm focal lengths and use conventional transmission-type lenses.

Table A–1. Specifications of the Voyager Cameras

Parameter	Wide-angle camera	Narrow-angle camera
Nominal focal length, mm.	200	1500
Focal ratio	*f*/3.5	*f*/8.5
Angular field of view:		
Milliradians	56 × 56	7.4 × 7.4
Degrees	3.2 × 3.2	0.42 × 0.42
Nominal shutter speeds:		
Milliseconds	5, 12.5, 25, 50, and 97.5	5, 12.5, 25, 50, and 97.5
Seconds	1/200, 1/80, 1/40, 1/20, and 1/10	1/200, 1/80, 1/40, 1/20, and 1/10
Active target raster (image size on vidicon tube), mm	11.14 × 11.14	11.14 × 11.14
Active scan lines per frame.	800	800
Active pixels per line	800	800
Field of view of a single pixel:		
Microradians	70	9.25
Degrees	4.0×10^{-3}	5.3×10^{-4}
Bits per picture element	8	8
Number of filters	8	8

Source: Benesh and Jepsen (1978).

Table A–2. Color Filters on the Voyager Cameras

Type of camera	Filter wheel position	Filter	Wavelength, nm
Narrow-angle	0	Clear	—
	1	Violet	50 to 400
	2	Blue	50 to 480
	3	Orange	570
	4	Clear	—
	5	Green	530
	6	Green	530
	7	Ultraviolet	45 to 325
Wide-angle	0	Methane	5 to 619
	1	Blue	50 to 480
	2	Clear	—
	3	Violet	50 to 400
	4	Sodium D	589
	5	Green	>530
	6	Methane	5 to 541
	7	Orange	>590

Source: Benesh and Jepsen (1978).

a range comparable to that between Earth and the Moon. The pixels are approximately 3.5 km square on the Moon, and the complete lunar disk will not quite fit in one frame. For comparison, the best Earth-based telescopes can resolve features with dimensions as small as about 1 km on the Moon. Figure A–4 is a simulated Voyager wide-angle picture of the Moon from Earth.

Voyager images are identified by a picture number, or "picno." This number contains information identifying the spacecraft that took the picture, planetary system being traversed at the time the picture was taken (Jovian or Saturnian), and the location (in time) of the spacecraft with respect to the major planet when the picture was taken. The cameras are capable of taking 1800 pictures in one Earth day; each picture is, therefore, coded first by a number between 1 and 1800, denoting one of the 1800 opportunities to take a picture during a given day. Not all opportunities were taken, so many gaps exist in the numeric sequence. This number is followed by a "J" or an "S," depending upon whether the spacecraft was nearer to the Jovian or Saturnian system when the picture was taken, and a "1" or a "2," depending upon whether the picture was taken by Voyager 1 or 2. The final number contains three digits, including leading zeros, and indicates the number of days from closest approach to the primary planet of the system. This number is separated from the preceding ones by a "+" or a "–," depending on whether the picture was taken before or after closest approach to the planet. Thus, picno "0272S1+000" was taken on the 272d opportunity, by Voyager 1, on the day the spacecraft made its closest approach to Saturn.

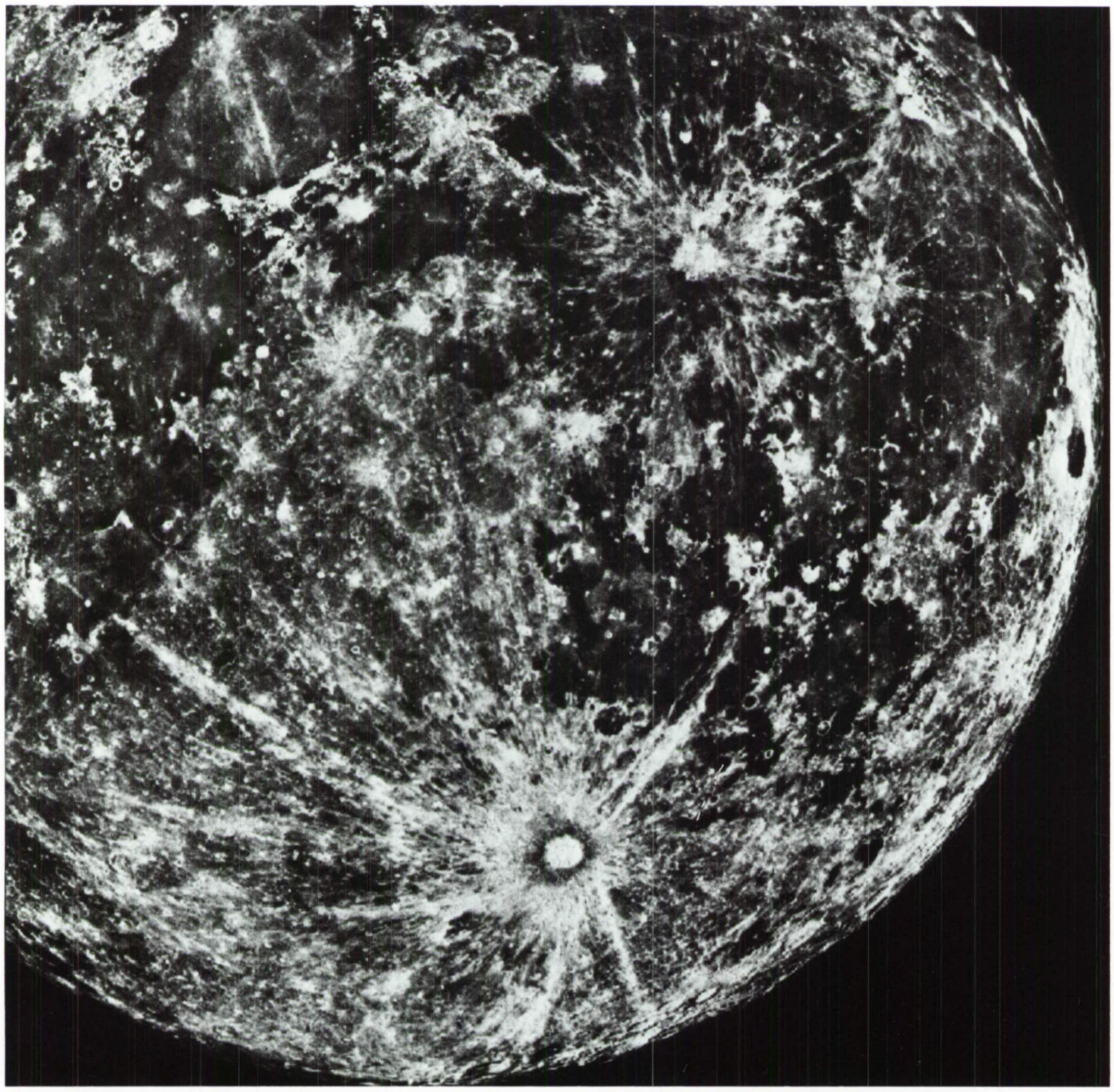

Figure A–3. Simulated Voyager narrow-angle picture of the Moon that approximates the resolution and field of view (0.42° × 0.42°) of a narrow-angle Voyager picture taken from the distance of Earth. The film image, taken through an Earth-based telescope, was scanned and digitally encoded at 8-bit format (256 gray shades) with pixel dimensions of 3.5 × 3.5 km on the Moon. (Lick Observatory full-Moon photo taken on January 16, 1946, by J. H. Moore and J. F. Chapel)

The Voyager cameras can be used to take black and white pictures through a variety of color filters (table A–2). The primary purpose of the filters was to permit analysis of target reflectance in different color bands, not the construction of true color pictures. Nevertheless, a reasonable approximation of true color could often be made in the photolab by matching spacecraft filters as closely as possible with the primary darkroom color filters and printing the composite photographically (fig. A–5).

More details on the Voyager missions are available in two special issues of *Space Science Reviews* (1977), *Science* (1981, 1982), and Morrison (1982).

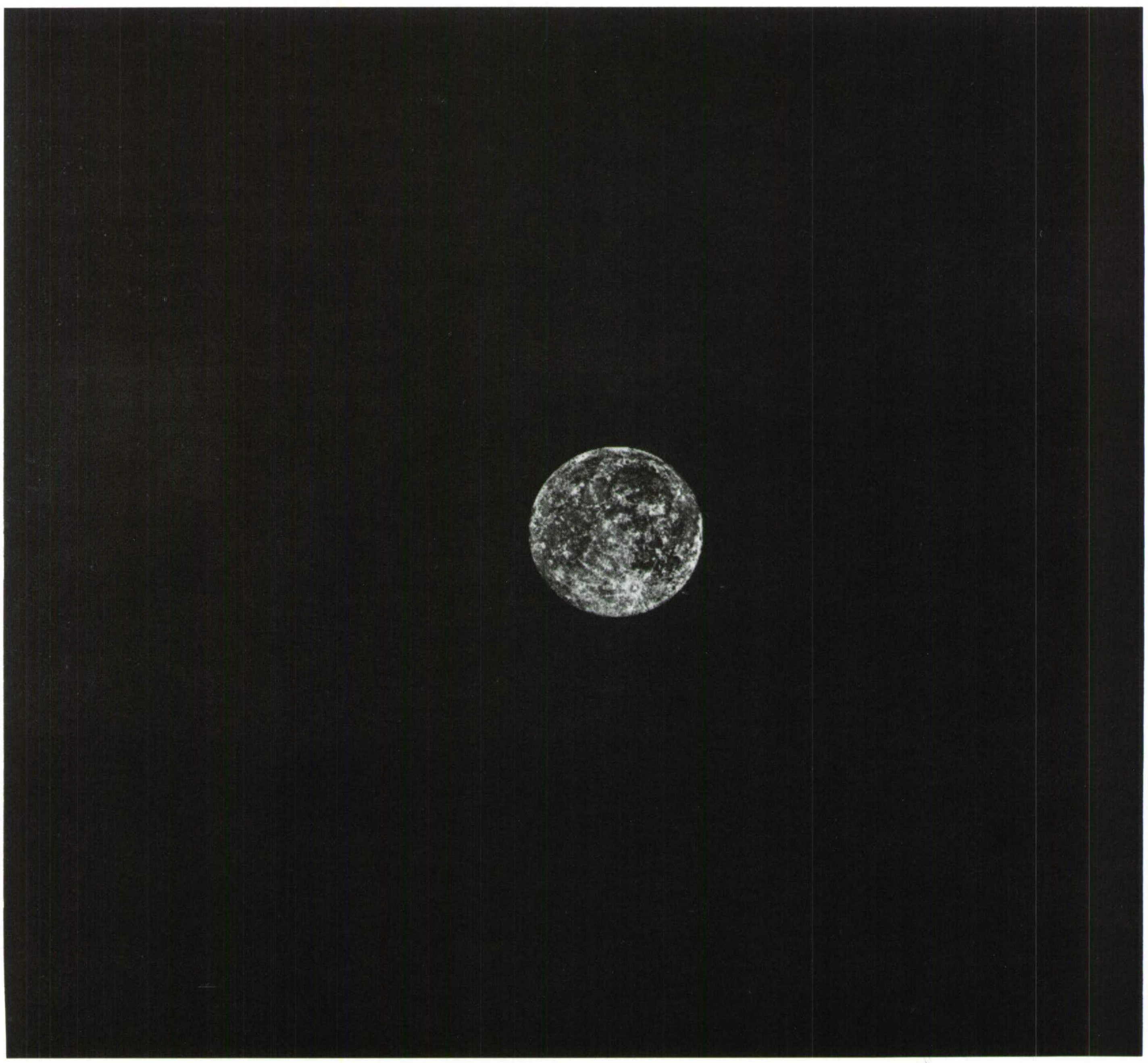

Figure A–4. Simulated Voyager wide-angle picture of the Moon. This digital treatment of the photograph used for figure A–3 approximates the resolution and field of view (3.2° × 3.2°) of a Voyager wide-angle picture taken from the distance of Earth. The pixel dimensions are 27 × 27 km on the Moon.

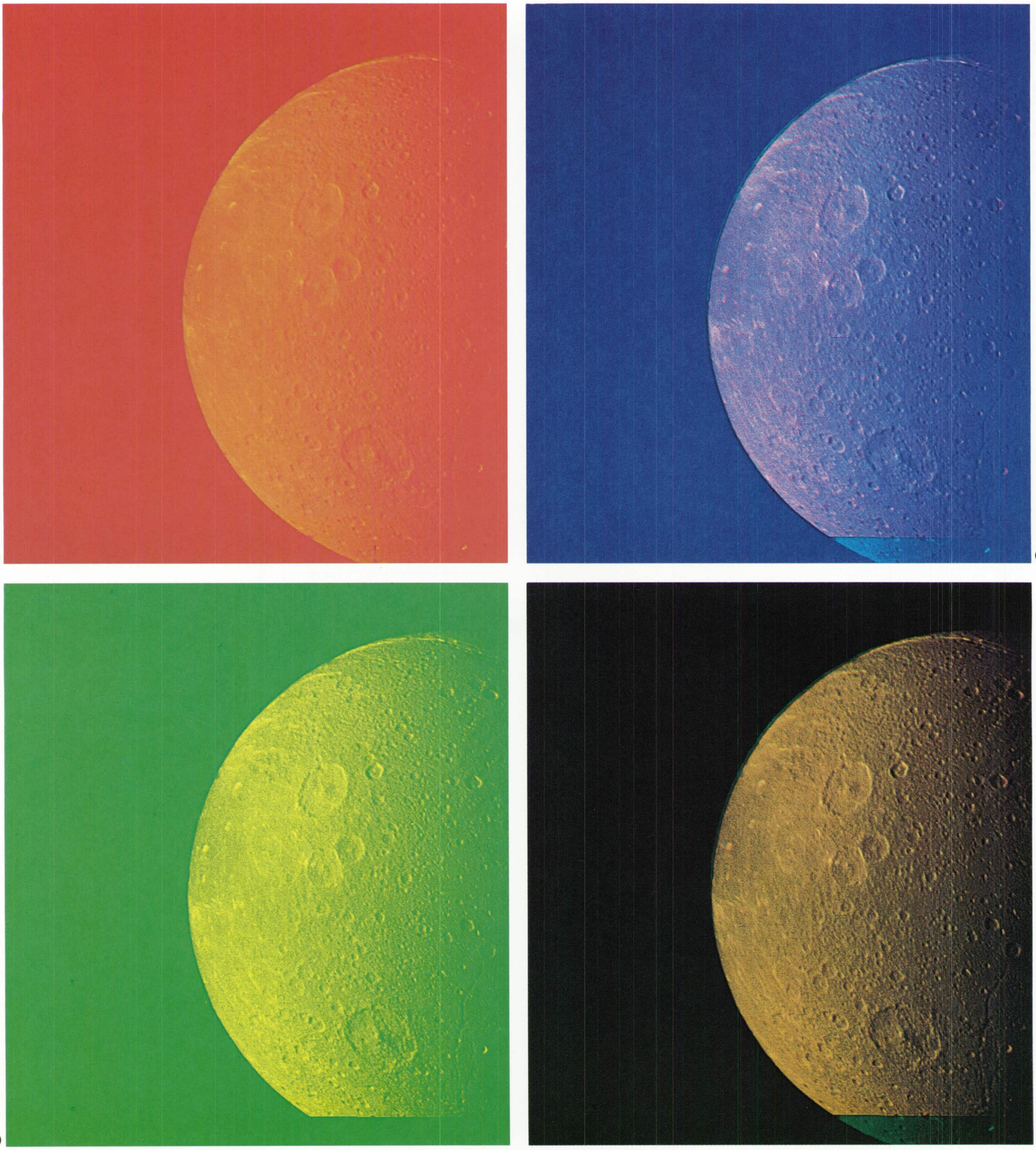

(a) (c) (b) (d)

Figure A–5. A color picture of Dione, made with three black and white Voyager pictures taken through different filters. (*a*) Picno 0274S1+000, taken through the violet filter, printed in red. (*b*) Picno 0276S1+000, taken through the green filter. (*c*) Picno 0272S1+000 taken through the clear filter, which actually has a bluish cast and is printed in blue. (*d*) Composite full-color picture of frames (*a*), (*b*), and (*c*).

PAGE MISSING FROM AVAILABLE VERSION

APPENDIX B

The Saturnian System

The highly successful missions of the Pioneer and Voyager 1 and 2 (*Science,* 1980, 1981, 1982; Morrison, 1982) spacecraft have tremendously expanded our knowledge about the planet Saturn, its rings, and its satellites. The system has been found to be an extremely complex group of at least 17 satellites and thousands of rings orbiting a huge planet (120 000 km or 74 500 miles in diameter). The size of this system may be more fully appreciated if it is realized that the orbit of Earth's Moon would extend only to the outer limit of Saturn's ring system (Ring E) or that the largest moon, Titan, is almost half the diameter of Earth. Saturn itself is composed mostly of lighter gases such as hydrogen, deuterium, methane, ammonia, ethane, phosphene, and probably helium. Because of its rapid rotation (10 hr, 14 min), these gases are forced outward, resulting in an equatorial diameter 11 percent greater than the polar diameter. Because of its composition, the planet has a very low density; "average" Earth material weighs almost eight times as much as average Saturn material. Given a large enough body of water, we could float Saturn in it. Because of this low density and size, Saturn's gravity near the top of the atmosphere is only 0.9 times that of Earth; that is, anything that weighs 100 lb on Earth would weigh only 90 lb on Saturn. Temperatures in the outer atmosphere of Saturn range from −130° C (−265° F) to −180° C (−355° F). Ring particles and satellites appear to be frozen gases and water ice, and their densities indicate that the term "dirty snowball" is a reasonably accurate description for most of them. Ice at these low temperatures is as brittle as most rock, and eons of impacts have scarred the surfaces of the satellites with craters and massive fractures.

Saturn is the most distant planet known to the ancients, and its name is a Latin term for the Roman god of agriculture. From Earth, it is a bright object (magnitude −0.4 at greatest brilliancy) with a slightly orange color. More than 29 years (29.485 years to be exact) are required for this planet to complete one revolution about the Sun, and its path can be traced in our night sky as it slowly moves through the constellations of the ecliptic. In 1610, when Galileo first turned his crude telescope on Saturn, he was mystified by what he described as "companions" of Saturn. He drew Saturn as a planet with two handlelike protuberances. As telescopes were improved, the rings were resolved more clearly, and in 1655 Huygens finally perceived their geometry. In 1675, Cassini noted a "gap" in the rings, which today bears the name Cassini Division. Voyager found that this is not a gap at all, but a ring that appears from Earth to be darker than adjacent rings. The rings separated by this "division" were named Rings A and B by W. Struve. An additional division was found in Ring A by J. Encke in 1837 and is now called Encke's Division. A third ring inside Ring B was noted in 1838 by J. G. Galle and is known as the Crepe or Ring C. Other rings and ring features were suspected by observers, but were not resolved until spacecraft traversed the Saturnian system in 1980 and 1981.

The satellites of Saturn were discovered by painstaking observation over a period of 250 years. The moon Iapetus has been of great interest to astronomers because of its significant variations of brightness (magnitude variation of 1.92) at different positions in its orbit. In 1944, G. Kuiper noted the presence of a methane atmosphere on Titan, further expanding the mysteries of the Saturnian system. The satellites are all fairly substantial

Table B–1. Saturnian System Statistics (Earth Included for Comparison)

Object	Diameter or dimensions, km	Density[a]	Gravity	Albedo	Distance from Saturn, km		Orbital period, hr	Closest approach, km		Discoverer	Year of discovery
					Minimum	Maximum		Voyager 1	Voyager 2		
Earth	[b]12 756 [c]12 713	5.5	1.0								
Saturn	[b]120 000 [c]107 000	.7	.9								
Ring D					67 000	73 200	4.91				
Ring C					73 200	92 200	5.61			Galle	1838
Ring B					92 200	117 500	7.93			Huygens	1655
Cassini Division					117 500	121 000				Cassini	1675
Ring A					121 000	136 200	11.93			Huygens	1655
Encke Division					133 500	133 700	13.82			Encke	1837
1980S28	30				137 300		14.45	219 000	287 000		
1980S27	220				139 400		14.71	300 000	247 000		
Ring F					140 600		14.94				
1980S26	200				141 700		15.08	270 000	107 000		
1980S3	90 × 40				151 422		16.66	121 000	147 000		
1980S2	100 × 90				151 472		16.67	297 000	223 000		
Ring G					170 000		19.90				
Mimas	394	1.4	.005	.6	188 224	184 440	23.14	88 400	309 990	W. Herschel	1789
Ring E					210 000	300 000	27.30				
Enceladus	502	1.1		1.0	240 192		33.36	202 040	87 140	W. Herschel	1789
1980S13	34 × 28 × 26				294 700		45.31				
1980S25	34 × 22 × 22				294 700		45.31				
Tethys	1 048	1.0		0.8	296 563		45.76	415 670	93 000	Cassini	1684
1980S6	160				378 600		65.73	230 000	270 000		
Dione	1 118	1.4		0.6	379 074		66.13	161 520	502 250	Cassini	1684
Rhea	1 528	1.2		0.6	527 828		108.66	73 980	645 280	Cassini	1672
Titan	5 150	1.9			1 221 432		382.50	6 490	665 960	Huygens	1655
Hyperion	205 × 130 × 110			0.3	1 502 275		521.74	880 440	470 840	Bond and Lassell	1848
Iapetus	1 448	1.2		0.5	3 559 400		1901.82	2 470 000	909 070	Cassini	1671
Pheobe	220				10 583 200		9755.67	13 537 000	1 473 000	Pickering	1899

[a]Water = 1.
[b]Equatorial.
[c]Polar.
Sources: Stone and Miner, 1981; Smith et al., 1981; Collins et al., 1980; Davies, 1983.

bodies, larger than the outer irregular satellites of Jupiter and five are larger than the largest asteroid, Ceres.

The sizes and other statistics regarding objects in the Saturnian system are listed in table B–1 and further illustrated in figures 3 (Introduction) and B–1. Comparison of the total known solid surface area in the Saturnian system with that in the whole solar system is illustrated in figure 2.

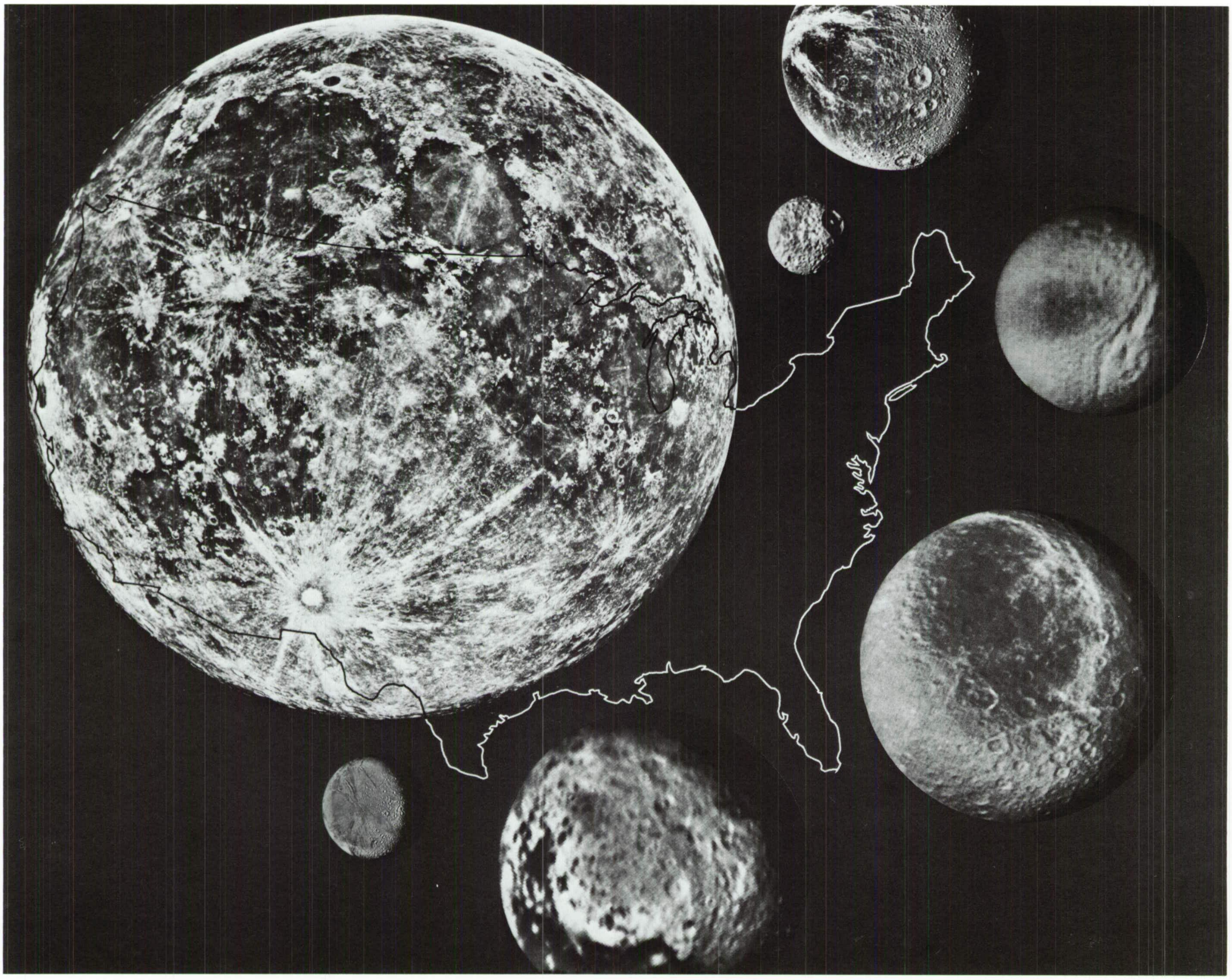

Figure B–1. Relative sizes of six Saturnian satellites. The Moon and an outline of the United States are included for scale.

Page intentionally left blank

APPENDIX C

Image Processing

The Voyager pictures of the Saturnian satellites are digital images; they are transmitted from the spacecraft as a stream of numbers, each representing a shade of gray of a specific point in the picture. When these numbers are placed in their proper location in an array of rows and columns, and each number replaced by a tone of the correct gray shade, an image is formed that is visible to the human observer (fig. C–1). These operations are performed with computers and computer-driven film-writing devices. The technique is called "digital image processing." (See Moik, 1980.) Although the methods were originally developed by space scientists for processing lunar pictures, they are now used in medicine for enhancing X-ray photographs, by resource scientists for enhancing aerial and spacecraft views of Earth, and by a variety of other specialists.

Two levels of digital processing are commonly used for planetary mapping. Level 1 is intended to remove all image artifacts, including noise and shading. Level 2 processing changes the geometric shape of the image to match an appropriate map projection. The level 1 and 2 images are carefully preserved on magnetic tape without contrast enhancement. Contrast enhancements are then applied to film images as needed, without modifying the digital tapes. Each Voyager picture contains 800 rows of 800 picture elements, called "pixels" (fig. C–2). Each pixel is assigned a density number (DN) by the spacecraft imaging system, according to the brightness of an image projected on the vidicon tube by the Voyager camera. (See app. A.) The Voyager imaging system is capable of discriminating and transmitting 256 shades of gray. The DNs in a Voyager picture thus range from 0 (black) to 255 (white). The camera can be commanded to take pictures at shutter speeds ranging from 1/10th to 1/200th of a second (table A–1).

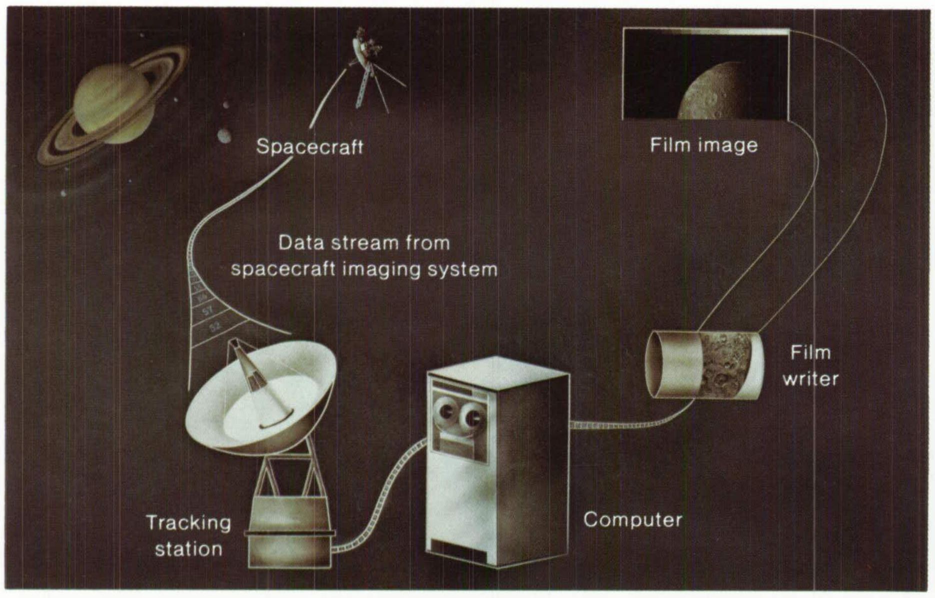

Figure C–1. The principle of the digital image. A stream of numbers (density numbers (DNs)) representing shades of gray is received from the spacecraft by tracking stations on Earth. Each DN is placed in its correct location in an array of rows and columns ("raster") by a computer and is then replaced by its correct gray shade and printed on film by a computer-driven film-writing device. (Illustration by Susan L. Davis)

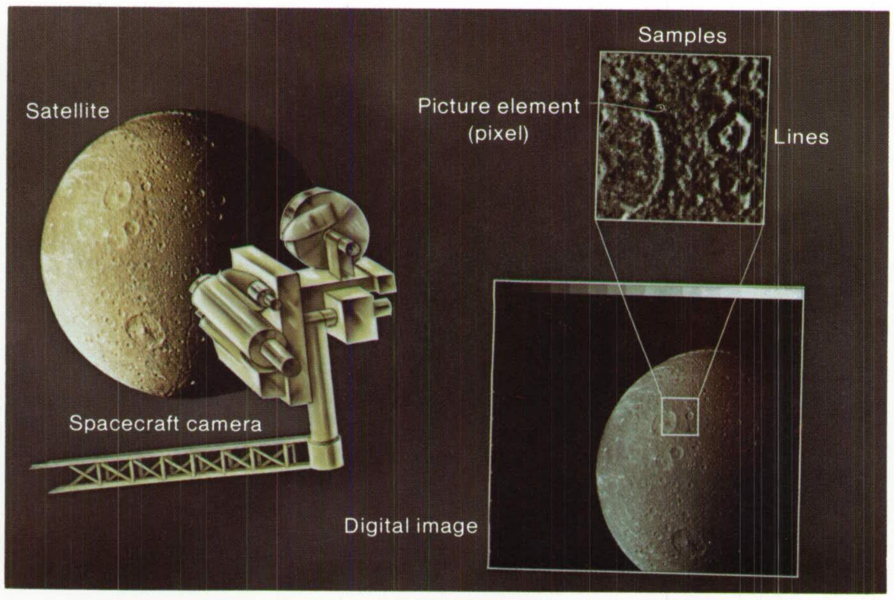

Figure C–2. Spacecraft digital imaging system. Picture elements, or pixels are visible on the enlarged inset. (Illustration by Patricia M. Bridges)

A variety of factors degrade any spacecraft television picture. Electronic fluctuations within the spacecraft cause a variation in the sensitivity of the system and make the DN that should represent black, or no signal, larger than 0. Spurious DN values are often injected into an image by fluctuations in electrical currents or magnetic fields in or near the camera. Segments of a string of DN values may be lost during transmission. Although lens distortions are virtually negligible in the Voyager cameras, geometric distortions are introduced into the pictures by the electronic recording and transmitting systems. All of these problems can be corrected, or significantly reduced, by digital image processing techniques. For example, pictures of empty space will contain many DN values other than 0 in a pattern that does not vary significantly from one frame to the next (fig. C–3). Because it is known that all these values should equal 0, subtracting DN values in black-sky pictures from the DN values in the same rows and columns on pictures of a planet or satellite results in a picture that has been corrected for radiometric distortions.

Spurious DN values (bit errors and dropped lines) can be detected by computer programs that examine the rate of change in DN values that are adjacent to each other in an image. Abrupt changes do not usually occur in images of natural surfaces, but are likely to result from data anomalies. They are corrected by replacing the DN values of pixels that deviate significantly from their surroundings with the average DN value of neighboring pixels.

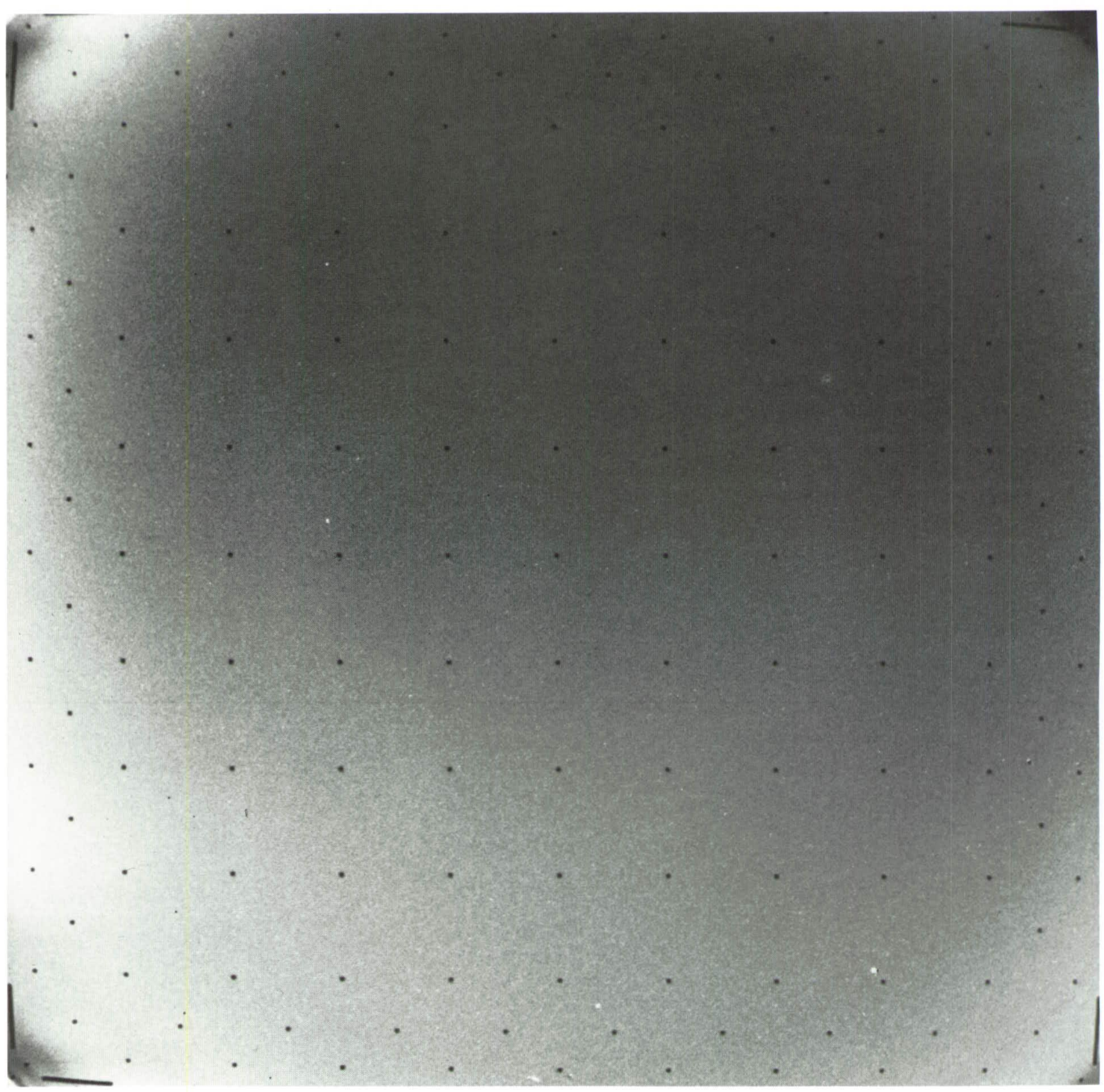

Figure C–3. A picture of black, featureless space used for in-flight calibration of Voyager cameras. Nonblack tones (exaggerated in this illustration for emphasis) are artifacts of the spacecraft imaging system. The DNs in this image are subtracted from raw images to produce radiometrically corrected pictures. Picno 0998J1–025.

The purpose of level 1 processing is to restore the pictures to the quality that would have been produced by a "perfect" camera transmission and film recording system. Figures C–4 and C–5 illustrate this processing phase. Figure C–4 is a "raw," or uncorrected, Voyager picture of Dione. Figure C–5 is the same picture after radiometric correction, reseau and blemish removal, and contrast enhancement. This atlas is intended to show the preliminary cartographic products of the Voyager mission, and hence contains only level 1 images.

Final map compilations are being done with level 2, or geometrically processed, images. This processing entails removal of camera distortions and transformation of the images to appropriate map projections. Distortion corrections are based on the known positions of calibration dots (reseau marks) in an image. These marks are etched in the photosensitive surface on the vidicon faceplate so that they appear in every picture. The positions of the reseau marks were measured on Earth before the spacecraft was launched. When the pictures were received on Earth, the reseau marks were located in each image and their positions recorded. The reseau pattern is clearly visible in figures C–3 and C–4. Although the marks themselves are removed during the level 1 phase by processing similar to that used for bit errors and dropped lines, their recorded positions can still be used to control geometric transformations. In correcting distortions, each image is stretched like a rubber sheet in such a way as to restore the reseau marks to their original, correct locations.

Each geometric correction of a digital image results in a slight loss in resolution. For this reason the correction of camera distortions is done

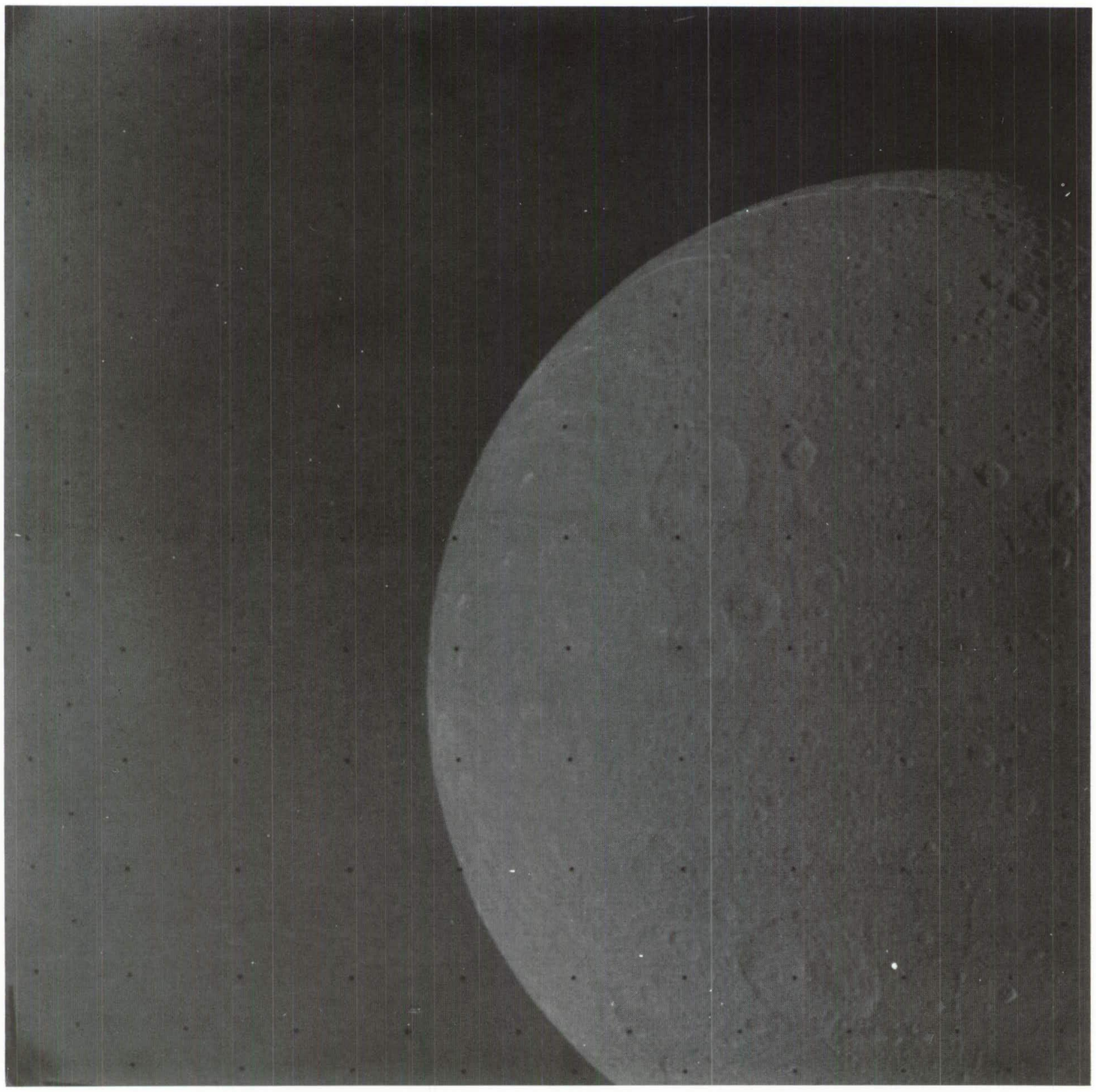

Figure C–4. An untreated Voyager picture of Dione. Picno 0272S1+000.

Figure C–5. Voyager picture of Dione with bit errors, dropped lines, and reseau marks removed and contrast enhanced (level 1 processing). Picno 0272S1+000.

simultaneously with transformation to a map projection, so that the actual geometric correction is performed only once.

Transformation to map projections is based on orientation matrices derived by analytical photogrammetry (Davies and Katayama, 1983*a,b*). This process involves a complex mathematical analysis of the positions of images of selected features (control points) on several spacecraft television pictures. The final results of this calculation include precise latitudes and longitudes for the control points and a set of linear equations that precisely define the orientation of the spacecraft camera with respect to the satellite at the time each picture was taken. These equations are used to change the shape of mapping pictures so that they will fit specified projections. Figure C–6 is a geometrically corrected, map-projected version of the Dione image of figure C–5.

A digital television image, with its 256 shades of gray, frequently contains far more information than can be discriminated by the human eye or shown on film. Before it is printed on film (with or without geometric correction), a decision must be made as to which aspect of the image to emphasize. If it contains both very dark and very light areas, its contrast must be modified in the computer so that detail in both light and dark areas will be visible.

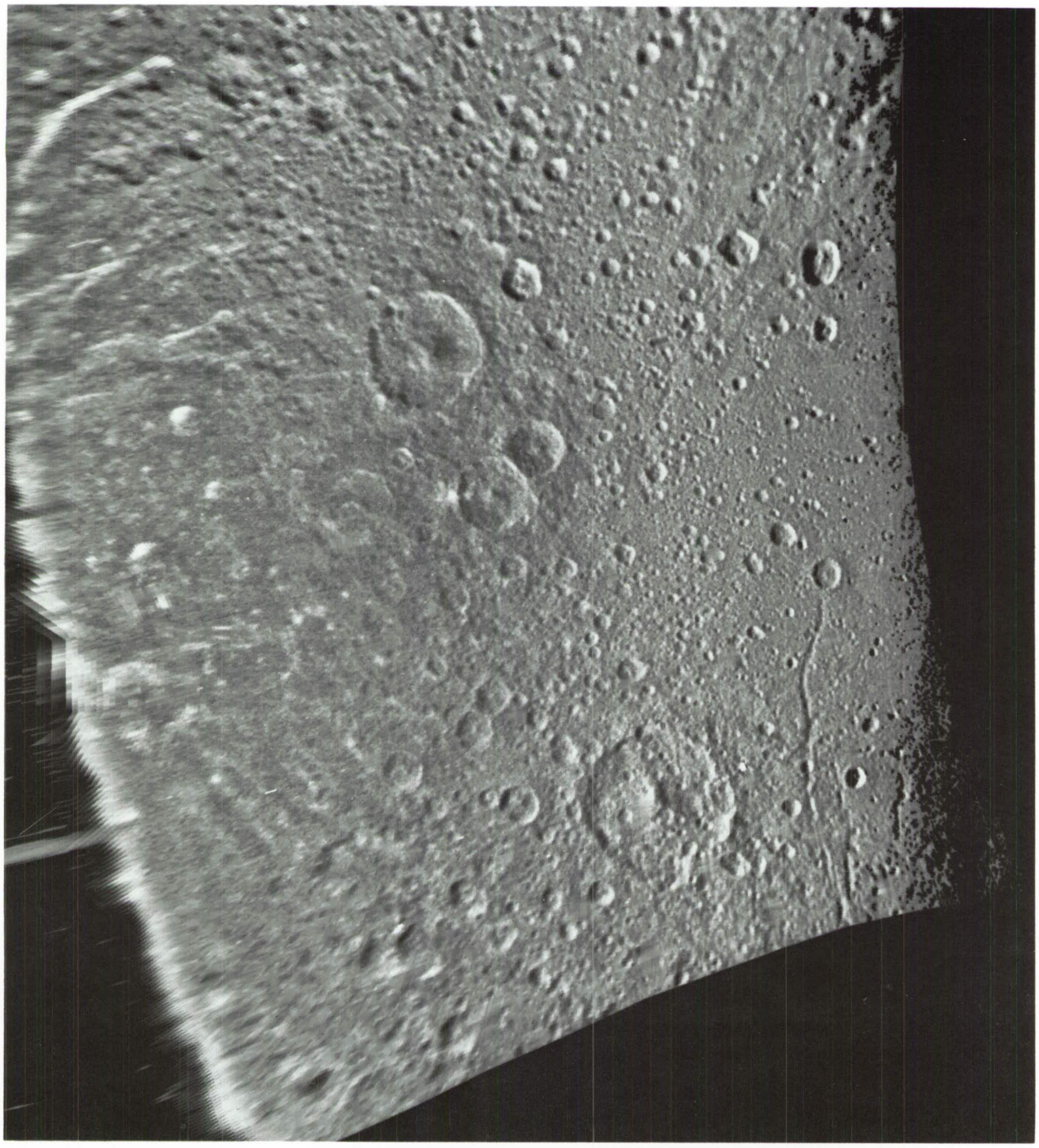

Figure C–6. Geometrically corrected Mercator projection of figure C–5 (level 2 processing). High-pass filter and contrast stretch have been applied to this image.

Two kinds of contrast manipulation are commonly used either singly or in combination on digital images. The first is a simple contrast change ("stretch") applied to the whole image. This is analogous to the photographic processing operation in which photographic papers of different contrast grades are used.

Contrast-stretch parameters for a given image are selected on the basis of a histogram of DN values in the image (figure C–7). This histogram is a graph that shows the number of pixels of each DN value in the image. The lowest DN recorded for a significant number of pixels in the original image is set to 0 for the stretched image. The highest DN recorded for a significant number of pixels in the original image is set to 255 DN for the stretched image. Intermediate DNs are reset in proportion to the newly defined high and low values. Figures C–4 and C–5 illustrate the effect of contrast stretching.

The second method of contrast enhancement, called high-pass filtration, changes local contrasts throughout the picture in such a way that small

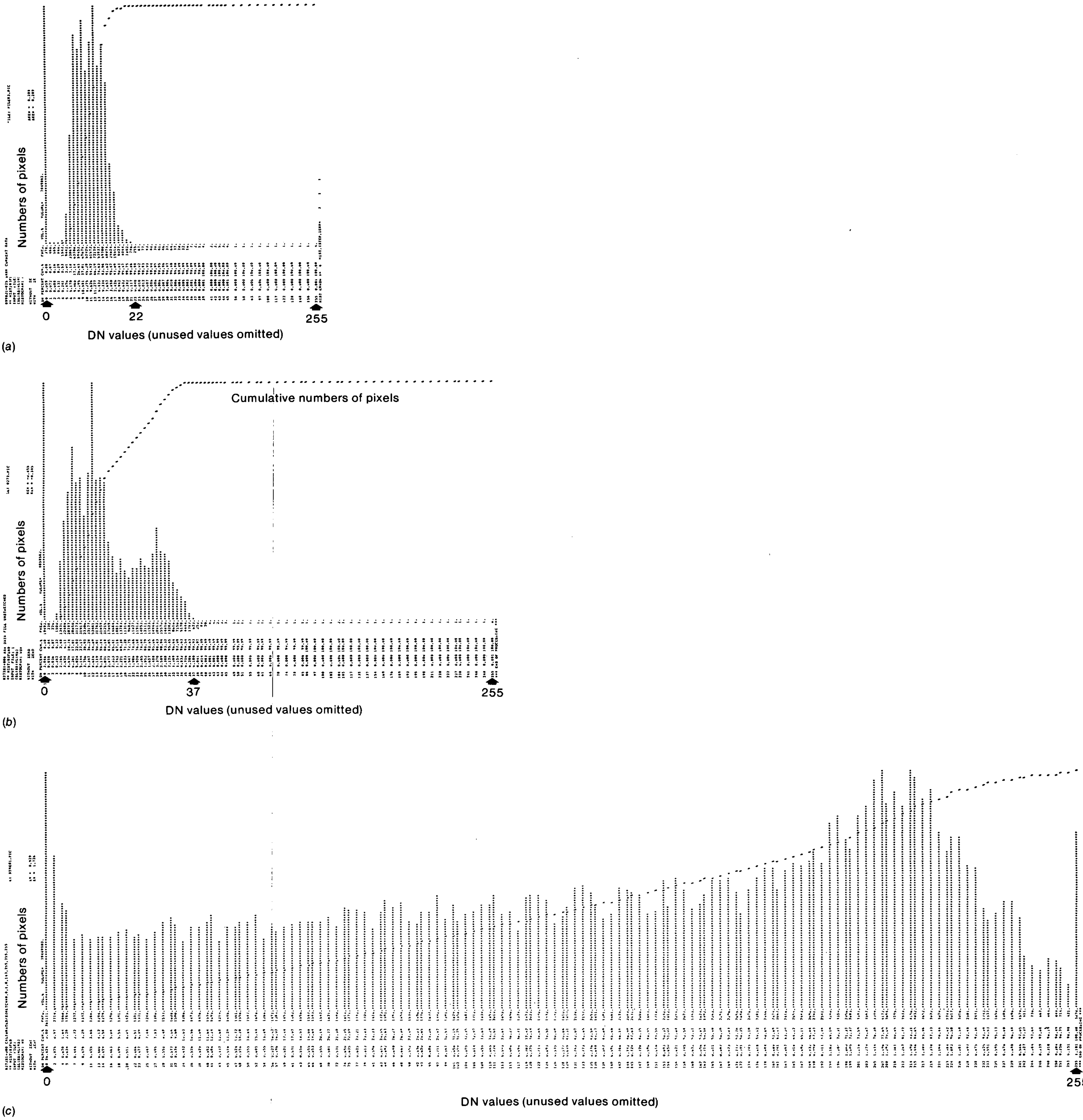

Figure C–7. Histograms of DNs in picno 0272S1+000. (*a*) The calibration image of figure C–3. (*b*) The raw, untreated version. Note that all DN values are clustered in a 37-DN range, including the DNs in (*a*), representing black sky. This is the histogram for the image of figure C–5. (*c*) The contrast-stretched version of the level 1 image in which the black-sky frame has been subtracted and the DNs in the raw image with values of 37 or greater have been converted to 255. Intermediate values are modified in proportion. This is the histogram for the image of figure C–8.

details, bright or dark, are adjusted to the same average gray tone. The effect of this computer technique is analogous to that of electronic dodging devices available on some photographic printers and enlargers, or the photographic technique of "unsharp masking." The small details are emphasized while broader tonal variations in the picture are subdued (figs. C–5 and C–8).

The following procedure is used to make high-pass filtered versions of digital images (fig. C–9):

(1) The filter size is selected on the basis of the size of image features to be emphasized. This size is defined in terms of pixel dimensions: a filter might be 3 pixels wide by 3 pixels high, or 51 pixels wide by 31 pixels high. The filter dimensions are odd numbers so that there is always a pixel in the exact center of the filter.

(2) The high-pass filter computer program computes the average DN value of all pixels within the filter beginning at its first location in the upper left corner of the picture. The actual DN of the pixel in the upper left corner of the filter box is subtracted from this average. Because there is about a 50-percent chance that this new filtered

Figure C–8. High-pass-filtered version of figure C–5. A 101-X-101-pixel filter (300 X 300 km on Dione) was used on this image, thus subduing tonal variations covering areas larger than 300 X 300 km. Note also that midtones are uniform across the image, even near the terminator where the unfiltered image of figure C–5 is much darker.

56	37	32	10	15	48	40
53	44	38	18	15	30	32
60	55	43	10	14	28	32
75	62	60	61	8	16	25
70	65	54	48	32	18	20
65	71	66	55	46	38	41
51	58	59	54	49	41	43

(a)

x	*x*	*x*	*x*	*x*	*x*	*x*
x	46	32	22	21	29	*x*
x	54	43	30	22	23	*x*
x	60	38	23	26	21	*x*
x	65	60	48	36	27	*x*
x	62	59	51	42	36	*x*
x	*x*	*x*	*x*	*x*	*x*	*x*

(b)

x	*x*	*x*	*x*	*x*	*x*	*x*
x	125	133	123	121	128	*x*
x	128	127	107	119	132	*x*
x	129	149	165	109	122	*x*
x	127	121	127	123	118	*x*
x	136	134	131	131	129	*x*
x	*x*	*x*	*x*	*x*	*x*	*x*

(c)

Figure C–9. The arithmetic of high-pass filtration. (*a*) An array of DNs representing a hypothetical raw image seven pixels wide and seven pixels long. (*b*) 3-X-3-pixel low-pass filter image of (*a*). The average DN value of the 3 X 3 block of pixels in the upper left corner of the image was calculated, and the result used as the value of the pixel in the center of the 3-X-3-pixel block. The block was then moved one pixel to the right and the process repeated until the entire image, except for the edges, was filled with the average values for the blocks. Because the pixels at the edge of the image are not at the center of any blocks, they are either lost or treated separately. The effect of this process is to defocus the image. The larger the filter, the greater the defocussing effect. (*c*) The 3-X-3-pixel high-pass filter image of (*a*). Each value in the low-pass filter picture (*b*) is subtracted from its corresponding value in the raw image (*a*) and added to 127, so that negative values do not result and so that the midtone of the image will have an average value of 127, in the middle of the 255-DN tonal range.

DN will have a negative value, a DN value representing a medium gray (127) is then added to it. The filter is then moved one pixel to the right, and the process is repeated. When filtered values for the first row of pixels have been computed, the filter box is moved down one row and filtered values for the second row of pixels are computed. The process is repeated until new values have been computed for each pixel in the image. The filters are affected by frame edges and abrupt contrast changes, so special program steps must be devised to deal with these problems. Several high-pass-filter algorithms are in use, but they produce similar results.

Filter sizes for the Voyager pictures in this atlas were selected primarily on the basis of image scale so that landforms would be uniformly emphasized. In other words, rather than using, for example, a 101-X-101-pixel filter for all pictures, a 21-X-21-km filter might be used. To achieve this uniformity, a picture taken when Voyager was 22 500 km from a satellite might be treated with a 101-X-101-pixel high-pass filter, whereas a picture taken from five times farther away (112 000 km) might have a 21-X-21-pixel filter applied. No single filter size, however, was appropriate for the full range of available image resolutions. It was, therefore, necessary to group the images as to high, medium, and low resolution and select the best filter for each group by trial and error.

APPENDIX D

Mapping

Requirements

Preliminary maps are required by scientists and Voyager mission planners immediately after images are received from a spacecraft for planning further data-gathering sequences and for preliminary scientific interpretations that will lay the foundation for more detailed investigations. Geometric controls have not been rigorously defined when these kinds of maps are prepared, and time is not availble for thorough image interpretation. Data arrive from spacecraft in fragments. Preliminary maps allow users to view the spatial context of the new information they have received.

Final mapping is done over a period of several years. It is tied to an accurate control net, which is now being developed for the Saturnian satellites (Davies and Katayama, 1983*a,b*). Final maps are made at larger scales and display more meticulous interpretations of surface detail than do preliminary ones.

The maps contained in this atlas are preliminary; a second edition is planned for release in 3 or 4 years that will contain final maps from the Voyager 1 and 2 missions.

Methods

The first stage in planetary mapping after data reception is the digital processing (see app. C) of pictures to be used in the mapping. Second, image locations must be determined. Third, a coherent pictorial representation of all the available surface information is prepared in the form of a map. Finally, a set of names is selected and applied to newly discovered features. (See app. E.) The two sources of information used to determine the location of the part of a planet appearing in a given picture are the location and orientation of the planet or satellite and the location of the spacecraft. The satellites of Saturn have been observed and their orbits timed by astronomers for many years. Their orbital periods, the fact that they always present the same face to Saturn, and their location within the solar system were accurately known long before Voyager arrived. The location of the spacecraft at any given instant was determined by the character of its radio signals (the time it took them to reach Earth, their doppler shift, and so on). From these data sources alone, it is possible to draw the latitude and longitude system of the satellite in proper orientation with respect to the Voyager camera for use in making preliminary maps. These are the perspective grids that accompany each pair of Voyager pictures of each satellite. Once a grid has been drawn for each picture, preliminary maps are made by sketching image details on a map-projection graticule by manually transferring information grid cell by grid cell. This is the process used to make the preliminary maps contained in this atlas.

Final maps are controlled by precise latitude and longitude locations of a selected set of features (usually craters) determined by methods of analytical photogrammetry (Davies and Katayama, 1983*a,b*). The precise camera orientation at the time each picture was taken is determined as part of this process. This information is used to transform pictures to appropriate map projections in the computer (fig. C–6) so that they can be placed in photomosaics.

The surfaces of the Saturnian satellites are portrayed with the airbrush by specially trained cartographic illustrators. These drawings show details visible in the Voyager pictures, with their correct relative emphasis, in a coherent fashion. This is possible because a human interpreter is able to examine many different pictures of the same area and to build a mental image of what that area would look like in a picture taken by a "perfect" camera. A proficient cartographic illustrator can draw an accurate representation of that mental image in the form of a map. The airbrushing technique is described in more detail by Inge (1972), Inge and Bridges (1976), and Batson (1978). The difference between preliminary and final airbrush maps is a function of the time available to make the drawings. Meticulous and detailed interpretation of all available image data is usually postponed until the final mapping phase. Preliminary airbrush maps are made at smaller scales and with more generalization of image detail than final ones; they are also made in a matter of weeks, rather than months or years.

Airbrush portrayal of the Saturnian satellites with Voyager images differs from that used for most planetary map series because of the unique character of the Voyager data set. Albedo features dominate the maps because most of the pictures have low resolution and were taken under high solar illumination. If portrayals were restricted to relief only, as is done in standard planetary mapping with more uniform coverage, only a very small part of each satellite could be mapped.

Projections and scales

The airbrush map drawings were originally compiled on conformal projections, which preserve the correct shapes of most mapped features, although map scale changes rapidly with latitude. For example, a crater at 60° latitude on a Mercator projection will appear to be twice as large as a crater of the same size at the equator. The drawings were then digitized; that is, their brightness values were measured at regular intervals and recorded on magnetic tape in the same format as digital television pictures, allowing them to be modified by digital image processing techniques discussed in appendix C. A computer program that changes one map projection to another was used to transform the original conformal projections to Lambert azimuthal equal-area projections. Forms are somewhat foreshortened near the edges of a global equal-area projection, but surface areas can be measured easily. For example, a dime placed anywhere on the Rhea equal-area map covers about 25 000 km^2 (almost 10 000 mi^2).

Preliminary planetary maps must be compiled in a short time period and be easily reproduced for distribution to mission scientists and engineers. The number of map sheets and total map area must, therefore, be kept to a minimum, mandating scales that are smaller than those that will be used for the final mapping.

The selection of scales for final planetary maps is based on image resolution. It is assumed that at least five picture elements, or pixels, are required to resolve a feature, and that mapped features should not have dimensions smaller than 1 mm at map scale. Consistent scales within map series are necessary for comparison of features. Scales are, therefore, selected on the basis of the availability of a few high-resolution images, with the result that some image areas are enlarged far beyond the five pixel per millimeter optimum scale.

Image resolution

The term "resolution" as it is used in this atlas refers to the size of a picture element on the surface of the body being imaged. The size of the pixel can be computed by multiplying the field of view of a single pixel (in radians) by the distance between the camera and the satellite (fig. D–1). True resolution is a much more complicated concept and is not discussed here. Even this simplified concept of pixel resolution is complicated by viewing and illumination geometry. For example, a pixel is square (and therefore covers a minimum area on a planet) only when the surface being viewed is perpendicular to the line of sight of the camera. The "viewing angle" of 90° is therefore optimum. As that angle becomes smaller, the

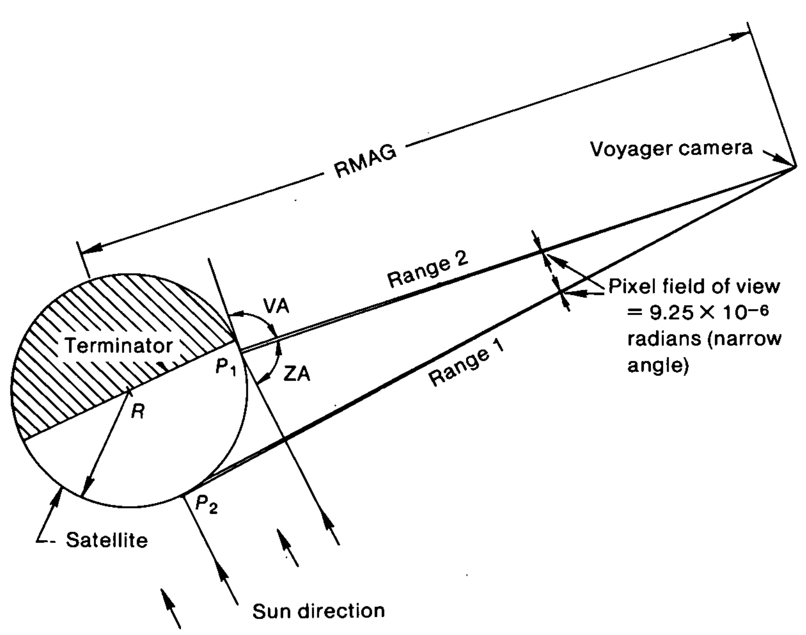

Figure D–1. Voyager camera viewing geometry. Pixel dimension = 9.25 × 10^{-6} rad × range for the narrow-angle camera used for all Voyager pictures of the Saturnian satellites. The value of range is so large compared with the radii of the satellites R that RMAG is usually used for the computation. Viewing angle VA is the angle between the line of sight to the camera and the planetary surface. It is nearly 90° at P_1 and nearly 0° at P_2. Zenith angle ZA is the angle between the direction to the Sun and the local zenith. ZA is approximately 90° at P_1 and approximately 0° at P_2. Image resolution will be much better at P_1 than at P_2.

footprint of the pixel on the ground becomes elongated and covers a larger area, so less surface detail is resolved. At the limb, or edge, of the disk of a satellite or planet, the viewing angle is zero and resolution is very poor except occasionally for profiles of mountains.

Resolution of surface landforms is usually best under low-Sun illumination, because shadows add contrast to surface relief. In a picture such as figure C–8, images are most clearly resolved near the terminator, where the viewing angle is nearly 90° and features are illuminated by grazing sunlight. The resolution in that picture is poorest at the limb, where the viewing angle is small and the solar zenith angle is small. When such an image is reprojected for viewing from an overhead perspective, as in figure C–6, the resolution loss near the limb causes the images to appear to be smeared.

The resolution figures shown in the diagrams at the beginnings of parts 1 through 6 were computed by dividing the nominal pixel size by the sine of the viewing angle or by the sine of the solar zenith angle, whichever resulted in the lowest resolution value. Images are not resolved at all, obviously, when solar zenith angles are greater than 90°; that is, when it is night at the site being photographed.

PAGE MISSING FROM AVAILABLE VERSION

APPENDIX E

Feature Nomenclature

Odysseus, Aeneas, Launcelot, Aladdin, Roland—names of features on the Saturnian satellites bring to mind some of the best-known myths and epics of European literature. Other names, such as Izanagi, Bumba, Xamba, and Yu-ti, are equally recognizable to Asian, African, or South American audiences. These and other names for features discriminated by the Voyager mission cameras are the persons and places memorialized in the epic stories and legends of ethnic groups throughout the world.

In naming the features on the Saturnian satellites, the Working Group for Planetary System Nomenclature within the International Astronomical Union (IAU) has expanded the mythological theme first used on the Jovian satellites. On the Saturnian satellites, however, the features bear names derived from the great epics and legends of the world. The convention of naming a prominent feature on each satellite for the discoverer of the satellite, developed for the satellites of Jupiter, also has been continued, wherever possible, at Saturn. Thus, the enormous crater on Mimas is named for William Herschel, famous astronomer and musician, who discovered the satellite in 1789. The extensive, dark, apparently featureless area on Iapetus is named Cassini Regio for Giovanni Cassini, who found this satellite in 1672. Hyperion's prominent ridge bears a double name, Bond-Lassell Dorsum, to honor the unusual circumstance of its discovery by William and George Bond, and by William Lassell, on the same night in 1848. Discoverers of Janus and Epimetheus are not honored on these satellites because they are both still living, and the IAU does not allow commemorative names for living persons on planetary bodies. Other satellites photographed by Voyager do not bear their discoverer's name on a feature because of another IAU constraint that duplication of names should be avoided: Cassini discovered Tethys, Dione, and Rhea as well as Iapetus, and Herschel discovered Enceladus as well as Mimas. Instead, prominent features are named for important places in the appropriate epics or legends: Ithaca (home of Odysseus), Latium (Aeneas' promised land), Kun Lun (Chinese promised land) Chasma, and Bassorah Fossae (town from which Sindbad left on his third voyage) on Tethys, Dione, Rhea, and Enceladus, respectively.

In some cases, the nationality of the epic is matched to the nationality of the discoverer. Names on Dione are taken from the great Roman epic, the *Aeneid* of Virgil; names derived from the great—some think the greatest—epic of all time, Homer's *Odyssey*, are found on Tethys; and names from the French *Song of Roland*, the great medieval story of a battle of Charlemagne, are found on Iapetus. Because the cultures of the East have not produced an epic of worldwide renown, a majority of the features on Rhea were assigned names from far-Eastern legends and myths. Other features were named from African, South American, or Oceanic legends. In this way, the strong European bias of names on the other satellites is offset. In some cases, the theme for naming features is determined by the satellite name or position: Hyperion, the Sun god, displays names of other Sun and Moon gods; the satellites that share a common orbit, Janus and Epimetheus, display names taken from the Greco-Roman myth about the twins, Castor and Pollux.

Mankind has always expressed by myth, epic, and legend its concern with the basic questions concerning man's place in the universe. It is fitting that names that embody these questions are now memorialized as names of mountains, craters, and plains on the planetary bodies.

Table E–1 contains many of the approved names (IAU, 1983) that have been assigned to features on the Saturnian satellites. Positions are shown in degrees of longitude and latitude as they are positioned on the maps in this atlas. Southern latitudes are shown as negative, and all longitudes are west of the prime meridian. The coordinates will be improved when final maps are made.

Table E–1. Gazeteer of Saturnian Satellites

Type and name of feature	Origin of name	Longitude, degrees	Latitude, degrees
MIMAS Names from Baines' (1962) translation of Malory's *Le Morte d'Arthur.*			
Craters:			
Accolon	Companion of Arthur; tricked into jousting with Arthur	166	−68
Arthur	King of the Round Table assemblage	190	−35
Balin	Knight of "matchless courage and virtue"	82	22
Ban	King of Benwick; father of Sir Launcelot	149	47
Bedivere	Arthurian knight	145	10
Bors	King of Gaul; father of Sir Ector de Marys, Sir Bors, and Sir Lyonel; godfather of Sir Blamoure and Sir Bleobris	165	45
Dynas	A knight of the Round Table	75	8
Elaine	Daughter of King Pelles; lover of Sir Launcelot; and mother, by Launcelot, of Sir Galahad	102	44
Gaheris	Older son of King Lot; killed by Sir Launcelot in his rescue of Gwynevere from burning at the stake	287	−46
Galahad	Bastard son of Launcelot and Elaine; sinless and invincible, he went on the quest for the Holy Grail	135	−47
Gareth	Youngest son of King Lot; killed by Sir Launcelot in his rescue of Gwynevere	280	−44
Gawain	Eldest son of King Lot; Arthur's favorite cousin	254	−60
Gwynevere	Queen; wife of Arthur; lover of Launcelot	312	−12
Herschel (William)	1738–1822; German-British astronomer who discovered Mimas and Enceladus in 1789	104	00
Igraine	Wife of Uther; Mother of Arthur	225	−40
Iseult	Loved by Tristram	35	−48
Kay	Royal seneschal at Arthur's court	116	48
Lamerok	Pellinore's son; sent testing horn to King Mark to expose adultery of Sir Tristram	283	−65
Launcelot	King Arthur's favorite; champion and lover of Queen Gwynevere	317	−10
Lot	Leader of the rebel kings of the North and West; married Margawse and fathered Sir Gawain, Sir Aggravayne, Sir Gaheris, and Sir Gareth; killed in the battle of Terrabyl by King Pellinore; his death avenged by Sir Gawain	227	−30
Mark	King of Cornwall	297	−28
Merlin	Magician and prophet; son of the devil; Arthur's mentor	215	−38
Modred	Arthur's bastard son and mortal enemy; delivered fatal wound to Arthur but was also killed by him	213	5
Morgan	Arthur's half sister; enchantress; plotted to destroy Arthur but failed	240	25
Palomides[a]	Saracen enemy of Tristram	157	4
Pellinore	A king whose duty it was to pursue the "questing beast" (a mythical creature with the head of a serpent, body of a leopard, buttocks of a lion, and the feet of a hart), and either run it to earth or lose his strength	128	35
Percivale	Very pure knight; went on the quest for the Holy Grail	171	−1
Tristram	Saved Iseult; fell in love with her	26	−58
Uther	Ruler of all Britain; Arthur's father	244	−35

NOTE.—See footnotes at end of table.

Table E–1. Gazeteer of Saturnian Satellites—Continued

Type and name of feature	Origin of name	Longitude, degrees	Latitude, degrees
Chasma:			
Avalon	Arthurian paradise	160 to 120	20 to 57
Camelot	Home of the Round Table assemblage	0 to 45	−25 to −60
Oeta	Mountain in Greece; was shaken by a Titan in the war between Titans and Olympians	130 to 105	10 to 35
Ossa	Mt. Ossa was piled on Mt. Pelion in the war between the Titans and the Gods	305 to 280	−10 to −30
Pangea	Mountain picked up by a Titan in the war with the Gods	340 to 290	−25 to −55
Pelion	Mountain on which Mt. Ossa was piled in war between the Titans and the Gods	235 to 200	−20 to −25
Tintagil	Home of Igraine, Arthur's mother	235 to 190	−43 to −60
ENCELADUS Most names from Burton's (1899–1901) *The Thousand Nights and a Night*			
Craters:			
Ahmad	Youngest son; brought father a magic apple	304	58
Aladdin	Hero of the tale of "Aladdin, or, the Wonderful Lamp"	17	63
Ali Baba	Hero of the tale of "Ali Baba and the Forty Thieves"; found a great treasure owned by 40 thieves	11	55
Dalilah	Crafty old crone who fooled a series of men in the tale of "The Rogueries of Dalilah and Her Daughter Zaynab"	244	53
Duban	Sage who cured King Yunan of leprosy and was poisoned by the King by a trick in the tale of "The Wazir and the Sage Duban"	276	58
Dunyazad	Sister of Shahrazad (means "world freer" in Persian)	200	43
Gharib	Hero of many tales	245	81
Julnar	"The Seaborn"; mermaid heroine of story told on nights 738 to 756	340	54
Musa	Went to get the vessels that contain Jinni in "The City of Brass"	3	73
Peri-Banu	Genie who married Ahmad and helped him fulfill the demands of his father in the tale of "Prince Ahmad and Peri-Banu"	315	63
Salih[b]	Brother of Julnar	−6	0
Samad	Shayk who guided Musa and Talib to the mountains in "The City of Brass"	353	61
Shahrazad	Daughter of Wazir who told king Shahryar the tales of a thousand nights and a night to keep from being killed (means "city freer" in Persian)	200	49
Shahryar	King whom Shahrazad beguiled with the tales of a thousand nights and a night	222	58
Sindbad	Voyager who had many marvelous adventures on 7 voyages in "Sindbad the Seaman"	210	66
Fossa:			
Bassorah	Town from which Sindbad embarked on his 3d voyage	23 to 345	40 to 50
Daryabar	"Ocean region" land from which princess Daryabar (Kudadad's wife) came in the tale of "Khudadad and His Brothers"	20 to 335	5 to 10
Isbanir	Fakir Taj's home; may be ancient Ctesiphon	0 to 350	20 to −10
Planitia:			
Diyar	Country where Khudadad's father ruled in the tale of "Khudadad and His Brothers"	250	0
Sarandib	Ceylon, the island visited by Sindbad on his 6th voyage	300	5
Sulci:			
Harran	City where Khudadad's father ruled in tale of "Khudadad and His Brothers"	270 to 210	35 to −5
Samarkand	Country ruled over by Zaman, brother of Shahryar	300 to 340	75 to −5
CO-ORBITAL SATELLITES: EPIMETHEUS AND JANUS[c] Names from Greek and Gemini myths (Graves, 1955).			
Epimetheus (1980S3; S11)			
Craters:			
Hilairea	Wife of Pollus		
Pollus	Latin name for Polydeukes, Castor's twin		

Table E–1. Gazeteer of Saturnian Satellites—Continued

Type and name of feature	Origin of name	Longitude, degrees	Latitude, degrees
	Janus (1980S01; S10)		
Craters:			
Castor	One of the Dioskuroi; Pollux's twin; famous as a tamer of horses		
Idas	Twin of Lynceus, cousin of Gemini		
Lynceus	Twin of Idas, cousin of Gemini		
Phoibe	Daughter of Leukippos		
	TETHYS Most names from *The Odyssey of Homer* (Bates, 1900).		
Craters:			
Ajax	Greek hero second only to Achilles; met by Odysseus in the underworld	285	−30
Anticleia	Mother of Odysseus	38	55
Antinous	Chief of the wooers of Penelope; slain by Odysseus	265	−62
Arete[b]	Wife of Alcinous (King of Phaeacia); mother of Nausicaa	300	−4
Circe	Changed Odysseus' companions into swine	49	−8
Elpenor	Follower of Odysseus	268	54
Eumaeus	Faithful swineherd who greeted Odysseus, gave warm cloak, and guided him to palace	47	27
Eurycleia	Faithful old nurse of Odysseus	247	56
Laertes	Father of Odysseus	60	−50
Melanthius	Disloyal goatherd; insulted Odysseus; was slain	204	−62
Mentor	Friend of Odysseus	39	3
Nausicaa	Daughter of Alcinous; advised Odysseus	352	80
Nestor	A wise old king of ancient Greece	58	−57
Odysseus	Hero of *The Odyssey*	130	30
Penelope	Faithful wife of Odysseus	252	−10
Phemius	Minstrel to the wooers of Penelope; spared by Odysseus	290	12
Polyphemus	Cyclops who fought with Odysseus	285	−5
Teiresias	Aged prophet; Odysseus consulted him among the dead	5	62
Telemachus	Son of Odysseus	338	56
Chasma:			
Ithaca	An Ionian island, home of Odysseus	30 to 340	50 to −80
	DIONE Most names from *The Aeneid of Virgil* (Mandelbaum, 1972).		
Craters:			
Adrastus	King of Argos, one of the Seven against Thebes, and the only one to return alive	40	−64
Aeneas	Hero of *The Aeneid;* the son of Anchises and Venus and a member of the royal family of Troy; a secondary figure in the Iliad, which notes that "his might shall reign among the Trojans"; escaped to some place in Italy when Troy fell (according to early tradition)	47	26
Amita	Mother of Lavinia, Aeneas' wife	287	7
Anchises	Aeneas' father	63	−35
Antenor	Nephew of Priam, king of Troy; escaped the fall of Troy and reached Italy before Aeneas; founded Padua	8	−6
Butes	Famous boxer who had been defeated by Dares	50	68
Caieta	A nurse of Aeneas	80	−25
Cassandra	Daughter of Priam; she could foretell the future	242	−42
Catillus	Brother of Tiburtus and twin brother of Coras, the three brothers who founded the city of Tibur (on the Tiber River)	275	−1
Coras	Brother of Tiburtus and twin brother of Catillus; a founder of the city of Tibur and an ally of Turnus against Aeneas	268	3
Creusa	Daughter of Priam; first wife of Aeneas	78	48
Dido	Tyrian princess; also called Elissa; founded Carthage	15	−22
Halys	A Trojan defending Aeneas' camp against the Rutulian attack; killed by Turnus	45	−60

Table E-1. Gazeteer of Saturnian Satellites—Continued

Type and name of feature	Origin of name	Longitude, degrees	Latitude, degrees
Ilia	Also known as Rhea Silvia; mother by the god Mars of Romulus and Remus, the founders of Rome	344	3
Italus	Ancient hero and eponymous ancestor of the Italians	76	−20
Latagus	Soldier of Aeneas	26	16
Lausus	Son of Mezentius; handsome, brave, and full of promise	23	38
Magus	King of the Rutulians; Aeneas' rival for the hand of Lavinia	24	20
Massicus	An Etruscan ally of Aeneas	52	36
Palinurus[b]	Pilot of Aeneas' fleet	62	−5
Remus	Brother of Romulus, cofounder of Rome	30	−10
Ripheus	A Trojan; fought at the side of Aeneas during Troy's last night	29	−56
Romulus	Mythical cofounder of Rome in 754 or 753 B.C., son of Mars by Ilia (Rhea Silvia)	24	−8
Sabinus	Fabled ancestor of the Sabines	190	−44
Turnus	Rutulian king; Aeneas' rival for hand of Lavinia	342	21
Chasma:			
Larissa	A town in Thessaly, Achilles' native region	15 to 65	20 to 48
Latium	The Trojans' promised land in Italy, supposedly so named because Saturn was "hidden" (or "latent") there	64 to 75	3 to 45
Palatine	One of the seven hills of Rome	75 to 320	−55 to −73
Tibur	Ancient town of Italy not far from Rome on the river of the same name	60 to 80	48 to 80
Linea:			
Carthage	An Etruscan city thought to have been founded by colonists from the city of Pisa in Elis, Greece, which stood on the River Alpheus	337 to 310	20 to 10
Padua	City in northern Italy founded by Antenor	245 to 190	5 to −40
Palatine	One of the seven hills of Rome	285 to 320	10 to −55

RHEA

Names are characters and places from creation myths selected from various cultures around the world; Asian names were emphasized.

Type and name of feature	Origin of name	Longitude, degrees	Latitude, degrees
Craters:			
Aananin	Korean god of the heavens	330	39
Adjua	Mythical heroine and ancestor of the Ulci tribe (Union of Soviet Socialist Republics)	126	46
Agunua	San Cristobal (Melanesia) god who made sea, land, and people	65	70
Ameta	Ceram (Indonesia) ancestor whose blood made Hainuwele	14	59
Arunaka	Inca creator of all things	21	−14
Atum	Old creator god of Heliopolos; became son of Ptah (primal Egyptian god)	0	−45
Bulagat	Mythological ancestor of the Buriat tribe (Mongolian people living near Lake Baikas)	14	−35
Bumba	Bushongo (Africa) god who dwelt in primordial waters; vomited up Sun, Moon, stars, animals, and men; showed man how to make fire from trees	40	70
Burkhan	Buriat (Siberia) god who created world	288	69
Con	South American (coastal) creator god	10	−24
Djuli	Ukrainian; first man—ancestor of the Neghidahan (Ukranian) people	46	−26
Ellyay	Yakutian (Soviet Far East) ancestor of the people	95	78
Faro	Mande (Africa); his sacrificial killing in heaven atoned for Pemba's sin; purified Earth; his 60 parts became trees; sent back to Earth in an ark	121	52
Haik	Mythological ancestor of the Armenian people	27	−34
Haoso	Manchurian creator of all things	8	9
Heller	Araucanian (South American) creator of men and bringer of civilization	310	9
Iraca	Incan creator god who became the Moon	120	45
Izanagi	Japanese creator god; brother and husband of Izanami	298	−49
Izanami	Sister and wife of Izanagi; creator goddess of Japan	310	−46

Table E–1. *Gazeteer of Saturnian Satellites*—Continued

Type and name of feature	Origin of name	Longitude, degrees	Latitude, degrees
Jumo	Marijan (Russian people living near the Volga River) sky god	65	56
Karora	Aranda (Australia) ancestor who, in his dreams, gave birth to animals and male children	16	7
Khado	Nanajan (people living on the border between the Union of Soviet Socialist Republics and China) mythological hero who built the world; first shaman	349	45
Kiho	Tuamotu (Society Islands) progenitor being; existed in void; made land and sea	354	−10
Kumpara	Jivaro (Ecuador) creator god	321	11
Leza	Tonga (Africa) god of heaven and nature	304	−19
Lowa	Marshall Islands (Melanesia) great creator god	9	45
Malunga	Yao (Bantu, Africa) first god; left Earth to live in sky when man was cruel to animals; creator god; progenitor god	49	74
Manoid	Negrito (Malay Peninsula) female progenitress goddess; wife of Pedn	2	33
Melo	Minyong (India) original human male	6	−51
Mubai	Tibetan god of heaven	11	61
Num	Samoyed god of heaven	93	23
Ormazd	Persian progenitor god of light	52	62
Pan Ku	Miao (aboriginal Chinese) creator of all things	115	72
Pedn	Negrito (Malay Peninsula) god who created first men	340	48
Oat	New Hebrides (Melanesia); born from a stone; formed men out of trees	347	23
Sholmo	Buriat (Siberia); devil who created harmful creatures of the world	340	13
Taaroa	Tahitian creator god; existed alone in the void	99	14
Thunupa	Inca creator of all things	15	51
Tika	Abkhaz (west of the Caucasus Mountains) supreme being	87	25
Tore[d]	Pygmy (Africa) lord of the world, creator of all things	335	1
Torom (Turm)	Ostya (Finno-Ugric people of Western Siberia) sky god	345	−68
Uku	Estonian supergod	115	85
Whanin	Korean creator of all things	121	74
Wuraka	Kakadu (Australia) ancestor of all people; a giant	357	28
Xamba	Bushman (Africa) supreme being, creator of all things	347	4
Xu (Huwe)	Bushman (Africa) creator	70	61
Yu-ti	"August personage of jade"; supreme primal Chinese god	85	55
Chasma:			
Kun Lun	Mountain dwelling place of the immortals (Chinese)	275 to 300	37 to 50
Pu Chou	Mountain attacked by Kung Chung; sky fell (Chinese)	85 to 115	10 to 35
	HYPERION[c] Names of Sun and Moon gods.		
Craters:			
Bahloo[3]	The Moon; maker of girl babies		
Helios	Son of Hyperion; Greek Sun god		
Jarilo	The god of the Sun and fertility (Union of Soviet Socialist Republics)		
Meri	Bororo (southern Brazil) folk hero; the Sun		
Dorsum:			
Bond-Lassell	William and George Bond (American astronomers) and William Lassell (British astronomer) who discovered Hyperion on the same night in 1848		
	IAPETUS Names from *The Song of Roland* (Sayers, 1967).		
Craters:			
Almeric[f]	One of 12 peers; killed by Marsilion	274	53
Baligant	Emir of Babylon; Marsilion enlisted his help against Charlemagne, King of France	225	15

Table E–1. Gazeteer of Saturnian Satellites—Concluded

Type and name of feature	Origin of name	Longitude, degrees	Latitude, degrees
Basan	French baron; brother of Basilie; murdered with Basilie while serving as ambassador of Marsilion	197	30
Berenger	One of 12 peers; killed Estramarin; killed by Grandoyne	220	59
Besgun	Chief cook for Charlemagne's army; guarded Ganelon after Ganelon's treachery was discovered	296	72
Charlemagne	King of France; his forces conquered Spanish towns for 7 years	266	54
Geboin	Guarded French dead; became leader of Charlemagne's 2d column; killed by Baligant	175	56
Godefroy	Bearer of Charlemagne's gonfalcon; brother of Tierri, Charlemagne's defender against Pinabel	253	78
Grandoyne	Son of Cappadocian king Capuel; killed Gerin, Gerier, Berenger, Guy St. Antoine, and Duke Astorge, who were all allies of Charlemagne; killed by Roland	215	18
Hamon	Joint commander of Charlemagne's 8th division	271	10
Lordnt	French commander of one of first divisions against Baligant (enemy of Charlemagne), killed by Baligant	165	64
Marsilion	Saracen king of Spain; vassal of Emir Baligant; killed Bevon, Ivon, Ivor, and Gerard; returned to Sargasso when Roland cut off his hand; died of wound later	177	41
Milon	Guarded French dead while Charlemagne pursued Spanish forces	270	75
Ogier	Dane assigned to vanguard position in Charlemagne's army; later led 3d column against Baligant's forces	274	42
Oliver	Roland's friend; killed Falsarun, Justin, Climborin, and Alfayen (all enemies of Charlemagne); mortally wounded by Marganice, also an enemy of Charlemagne	203	61
Othon	One of 12 peers; guarded French dead while Charlemagne pursued Spanish forces; 6th column leader	344	24
Roland	Charlemagne's nephew; led rear guard of French forces; killed Chernubles, Adelroth, Valdebond, Grandoyne, and Faldron de Puys (all enemies of Charlemagne); last to die at the Roncevaux battleground	30	78
Turpin	Archbishop of Rheims; killed Siglorel, Corsablis, Abisme, and Maliquant, all enemies of Charlemagne	0	43
Regio:			
Cassini	Italian-French astronomer (1625–1712) who discovered Iapetus in 1671, Rhea in 1672, and Tethys and Dione in 1684	210 to 340	55 to −48
Terra:			
Roncevaux	Pass where Roland and his forces were ambushed by the Spaniards	300 to 130	90 to −30

[a]Rand control point 43.
[b]Rand control point 100.
[c]Coordinates of Epimetheus, Janus, and Hyperion have not yet been specified.
[d]Rand control point 65; too small to show on map; position marked by open cross.
[e]Rand control point 1.
[f]Rand control point 40.

PAGE MISSING FROM AVAILABLE VERSION

APPENDIX F

Index of Voyager Pictures

The Voyager pictures reproduced in this atlas show essentially all surface features that could be included in the preliminary maps. Many other pictures were taken, but they are virtual duplicates of the illustrations. The following is a listing, in order of acquisition, of all Voyager pictures that show useful detail. Figure numbers are provided for pictures shown in this book.

Picno	FDS	Satellite	Figure No.
0087S1−003 ...	34855.23	Rhea	—
0004S1−002 ...	34884.00	Rhea	—
0011S1−002 ...	34884.07	Rhea	5–8
0966S1−002 ...	34900.02	Rhea	—
0973S1−002 ...	34900.09	Rhea	—
0982S1−002 ...	34900.18	Tethys	—
0986S1−002 ...	34900.22	Tethys	—
0990S1−002 ...	34900.26	Tethys	—
0994S1−002 ...	34900.30	Tethys	—
0998S1−002 ...	34900.34	Tethys	—
1002S1−002 ...	34900.38	Tethys	3–6
1136S1−002 ...	34902.52	Tethys	3–7
1140S1−002 ...	34902.56	Tethys	—
1144S1−002 ...	34903.00	Tethys	—
1148S1−002 ...	34903.04	Tethys	—
1152S1−002 ...	34903.08	Tethys	—
1156S1−002 ...	34903.12	Rhea	5–9
1163S1−002 ...	34903.19	Rhea	—
1414S1−002 ...	34907.30	Tethys	3–8
1417S1−002 ...	34907.33	Tethys	—
1420S1−002 ...	34907.36	Rhea	—
1424S1−002 ...	34907.40	Rhea	—
1428S1−002 ...	34907.44	Rhea	—
1432S1−002 ...	34907.48	Rhea	—
1436S1−002 ...	34907.52	Rhea	—
1440S1−002 ...	34907.56	Rhea	—
0011S1−001 ...	34914.07	Dione	4–6
0055S1−001 ...	34914.51	Rhea	5–10
0015S1−001 ...	34914.11	Dione	—
0019S1−001 ...	34914.15	Dione	—
0023S1−001 ...	34914.19	Dione	—
0061S1−001 ...	34914.57	Rhea	—
0690S1−001 ...	34925.26	Dione	4–7
0696S1−001 ...	34925.32	Rhea	5–11
0702S1−001 ...	34925.38	Rhea	—
0708S1−001 ...	34925.44	Rhea	—
0718S1−001 ...	34925.54	Rhea	—
0722S1−001 ...	34925.58	Rhea	—
0726S1−001 ...	34926.02	Rhea	—
0730S1−001 ...	34926.06	Rhea	—
0734S1−001 ...	34926.10	Rhea	—
0737S1−001 ...	34926.13	Rhea	—
0742S1−001 ...	34926.18	Tethys	3–9
0907S1−001 ...	34929.03	Mimas	1–6
0967S1−001 ...	34930.03	Dione	—
0971S1−001 ...	34930.07	Dione	4–8
0975S1−001 ...	34930.11	Dione	—
0979S1−001 ...	34930.15	Dione	—
0983S1−001 ...	34930.19	Dione	—
0987S1−001 ...	34930.23	Dione	—
0990S1−001 ...	34930.26	Dione	—
1004S1−001 ...	34930.40	Mimas	1–7
1088S1−001 ...	34932.04	Mimas	1–8
1182S1−001 ...	34933.38	Dione	4–9
1194S1−001 ...	34933.50	Mimas	1–9
1339S1−001 ...	34936.15	Mimas	1–10
1390S1−001 ...	34937.06	Tethys	3–10
1394S1−001 ...	34937.10	Tethys	3–11
1398S1−001 ...	34937.14	Tethys	—
1402S1−001 ...	34937.18	Tethys	—
1406S1−001 ...	34937.22	Tethys	—
1446S1−001 ...	34938.02	Mimas	1–11
1462S1−001 ...	34938.18	Mimas	1–12
1558S1−001 ...	34939.54	Rhea	5–12
1561S1−001 ...	34939.57	Rhea	—
1598S1−001 ...	34940.34	Mimas	1–13
0025S1+000 ...	34944.21	Mimas	1–14
0055S1+000 ...	34944.51	Dione	—
0058S1+000 ...	34944.54	Dione	—
0062S1+000 ...	34944.58	Dione	4–10
0066S1+000 ...	34945.02	Dione	4–11
0252S1+000 ...	34948.08	Dione	—
0260S1+000 ...	34948.16	Dione	—
0262S1+000 ...	34948.18	Dione	—
0264S1+000 ...	34948.20	Dione	—
0266S1+000 ...	34948.22	Dione	4–12
0268S1+000 ...	34948.24	Dione	—
0270S1+000 ...	34948.26	Dione	—
0272S1+000 ...	34948.28	Dione	4–13
0274S1+000 ...	34948.30	Dione	—
0276S1+000 ...	34948.32	Dione	4–14
0369S1+000 ...	34950.05	Rhea	—
0371S1+000 ...	34950.07	Rhea	—
0373S1+000 ...	34950.09	Rhea	—
0376S1+000 ...	34950.11	Rhea	—
0376S1+000 ...	34950.12	Rhea	—
0377S1+000 ...	34950.13	Rhea	—
0378S1+000 ...	34950.14	Rhea	—
0379S1+000 ...	34950.15	Rhea	—
0380S1+000 ...	34950.16	Rhea	—
0381S1+000 ...	34950.17	Rhea	—
0383S1+000 ...	34950.19	Rhea	—
0385S1+000 ...	34950.21	Rhea	—
0387S1+000 ...	34950.23	Rhea	5–13
0389S1+000 ...	34950.25	Rhea	5–14
0391S1+000 ...	34950.27	Rhea	—
0393S1+000 ...	34950.29	Rhea	5–15
0395S1+000 ...	34950.31	Rhea	—
0397S1+000 ...	34950.33	Rhea	—
0399S1+000 ...	34950.35	Rhea	—
0401S1+000 ...	34950.37	Rhea	5–16
0403S1+000 ...	34950.39	Rhea	—
0405S1+000 ...	34950.41	Rhea	5–17
0407S1+000 ...	34950.43	Rhea	—

Picno	FDS	Satellite	Figure No.
0409S1+000 ...	34950.45	Rhea	—
0411S1+000 ...	34950.47	Rhea	5–18
0413S1+000 ...	34950.49	Rhea	—
0415S1+000 ...	34950.51	Rhea	—
0417S1+000 ...	34950.53	Rhea	5–19
0419S1+000 ...	34950.55	Rhea	5–20
0421S1+000 ...	34950.57	Rhea	—
0480S1+000 ...	34951.56	Iapetus	6–7
0489S1+000 ...	34952.05	Rhea	—
0493S1+000 ...	34952.09	Rhea	—
0497S1+000 ...	34952.13	Rhea	—
0501S1+000 ...	34952.17	Rhea	—
0505S1+000 ...	34952.21	Rhea	—
0509S1+000 ...	34952.25	Rhea	—
0513S1+000 ...	34952.29	Rhea	—
0517S1+000 ...	34952.33	Rhea	5–21
0520S1+000 ...	34952.36	Rhea	—
0524S1+000 ...	34952.40	Rhea	—
0533S1+000 ...	34952.49	Rhea	5–22
0535S1+000 ...	34952.51	Rhea	5–23
0537S1+000 ...	34952.53	Rhea	5–24
0539S1+000 ...	34952.55	Rhea	5–25
0541S1+000 ...	34952.57	Rhea	5–26
0543S1+000 ...	34952.59	Rhea	5–27
0545S1+000 ...	34953.01	Rhea	5–28
0547S1+000 ...	34953.03	Rhea	5–29
0549S1+000 ...	34953.05	Rhea	5–30
0551S1+000 ...	34953.07	Rhea	5–31
1152S1+000 ...	34963.08	Rhea	5–32
1156S1+000 ...	34963.12	Rhea	—
1160S1+000 ...	34963.16	Rhea	—
1164S1+000 ...	34963.20	Rhea	—
1168S1+000 ...	34963.24	Rhea	—
0134S1+001 ...	34976.10	Iapetus	—
0140S1+001 ...	34976.16	Iapetus	—
0146S1+001 ...	34976.22	Iapetus	—
0152S1+001 ...	34976.28	Iapetus	—
0158S1+001 ...	34976.34	Iapetus	—
0164S1+001 ...	34976.40	Iapetus	—
0170S1+001 ...	34976.46	Iapetus	—
0176S1+001 ...	34976.52	Iapetus	—
0182S1+001 ...	34976.58	Iapetus	6–8
0191S1+001 ...	34977.07	Iapetus	—
0196S1+001 ...	34977.12	Iapetus	—
0201S1+001 ...	34977.17	Iapetus	—
0206S1+001 ...	34977.22	Iapetus	—
0062S1+002 ...	35004.58	Iapetus	—
0079S1+002 ...	35005.15	Iapetus	—
0085S1+002 ...	35005.21	Iapetus	—
0091S1+002 ...	35005.27	Iapetus	—
0097S1+002 ...	35005.33	Iapetus	—
0103S1+002 ...	35005.39	Iapetus	—
0110S1+002 ...	35005.46	Iapetus	6–9
0115S1+002 ...	35005.51	Iapetus	—
1546S2−006 ...	43851.23	Iapetus	—
1550S2−006 ...	43851.27	Iapetus	—
1554S2−006 ...	43851.31	Iapetus	—
1558S2−006 ...	43851.35	Iapetus	—
1562S2−006 ...	43851.39	Iapetus	6–10
1566S2−006 ...	43851.43	Iapetus	—
1570S2−006 ...	43851.47	Iapetus	—
1574S2−006 ...	43851.51	Iapetus	—
1578S2−006 ...	43851.55	Iapetus	—
1581S2−006 ...	43851.58	Iapetus	—
1174S2−005 ...	43875.11	Iapetus	6–11
1178S2−005 ...	43875.15	Iapetus	—
1182S2−005 ...	43875.19	Iapetus	—
1186S2−005 ...	43875.23	Iapetus	—
1190S2−005 ...	43875.27	Iapetus	—
1194S2−005 ...	43875.31	Iapetus	—
1198S2−005 ...	43875.35	Iapetus	—
1202S2−005 ...	43875.39	Iapetus	—
1206S2−005 ...	43875.43	Iapetus	—
1209S2−005 ...	43875.46	Iapetus	—
0008S2−004 ...	43885.45	Iapetus	6–12
0012S2−004 ...	43885.49	Iapetus	—
0016S2−004 ...	43885.53	Iapetus	—
0020S2−004 ...	43885.57	Iapetus	—
0024S2−004 ...	43886.01	Iapetus	—
0028S2−004 ...	43886.05	Iapetus	—
0032S2−004 ...	43886.09	Iapetus	—
0036S2−004 ...	43886.13	Iapetus	—
0040S2−004 ...	43886.17	Iapetus	—
0043S2−004 ...	43886.20	Iapetus	—
0523S2−004 ...	43894.20	Iapetus	6–13
0527S2−004 ...	43894.24	Iapetus	—
0531S2−004 ...	43894.28	Iapetus	—
0535S2−004 ...	43894.32	Iapetus	—
0539S2−004 ...	43894.36	Iapetus	—
0543S2−004 ...	43894.40	Iapetus	—
0547S2−004 ...	43894.44	Iapetus	—
0551S2−004 ...	43894.48	Iapetus	—
0555S2−004 ...	43894.52	Iapetus	—
1259S2−004 ...	43906.36	Iapetus	—
1263S2−004 ...	43906.40	Iapetus	—
1267S2−004 ...	43906.44	Iapetus	—
1271S2−004 ...	43906.48	Iapetus	—
1275S2−004 ...	43906.52	Iapetus	—
1279S2−004 ...	43906.56	Iapetus	—
1283S2−004 ...	43907.00	Iapetus	—
1287S2−004 ...	43907.04	Iapetus	—
1291S2−004 ...	43907.08	Iapetus	6–14
1678S2−004 ...	43913.35	Iapetus	6–15
1682S2−004 ...	43913.39	Iapetus	—
1682S2−004 ...	43913.43	Iapetus	—
1690S2−004 ...	43913.47	Iapetus	6–16
1694S2−004 ...	43913.51	Iapetus	—
1698S2−004 ...	43913.55	Iapetus	—
1702S2−004 ...	43913.59	Iapetus	—
1706S2−004 ...	43914.03	Iapetus	—
0154S2−003 ...	43918.11	Iapetus	6–17
0158S2−003 ...	43918.15	Iapetus	—
0162S2−003 ...	43918.19	Iapetus	—
0166S2−003 ...	43918.23	Iapetus	—
0170S2−003 ...	43918.27	Iapetus	—
0174S2−003 ...	43918.31	Iapetus	—
0178S2−003 ...	43918.35	Iapetus	—
0182S2−003 ...	43918.39	Iapetus	—
0186S2−003 ...	43918.43	Iapetus	—
0816S2−002 ...	43959.13	Tethys	—
0820S2−002 ...	43959.17	Tethys	—
0824S2−002 ...	43959.21	Tethys	3–12
0828S2−002 ...	43959.25	Tethys	—
1060S2−002 ...	43963.17	Tethys	3–13
1063S2−002 ...	43963.20	Tethys	—
1281S2−002 ...	43966.58	Rhea	—
1285S2−002 ...	43967.02	Rhea	—
1289S2−002 ...	43967.06	Rhea	—
1293S2−002 ...	43967.10	Rhea	—
1297S2−002 ...	43967.14	Rhea	—
1352S2−002 ...	43968.09	Tethys	3–14
1356S2−002 ...	43968.13	Tethys	—
1360S2−002 ...	43968.17	Tethys	—
1364S2−002 ...	43968.21	Tethys	—
1766S2−002 ...	43975.03	Tethys	—
1770S2−002 ...	43975.07	Tethys	3–15
1774S2−002 ...	43975.11	Tethys	—
1778S2−002 ...	43975.15	Tethys	—
1782S2−002 ...	43975.19	Tethys	—
1786S2−002 ...	43975.23	Tethys	—
0097S2−001 ...	43977.14	Rhea	—
0404S2−001 ...	43977.21	Dione	—
0408S2−001 ...	43977.25	Dione	—
0112S2−001 ...	43977.29	Dione	—
0116S2−001 ...	43977.33	Dione	—
0120S2−001 ...	43977.37	Enceladus	—
0124S2−001 ...	43977.41	Enceladus	—
0128S2−001 ...	43977.45	Enceladus	—
0132S2−001 ...	43977.49	Enceladus	—
0136S2−001 ...	43977.53	Enceladus	—
0140S2−001 ...	43977.57	Enceladus	—
0272S2−001 ...	43980.09	Tethys	—
0278S2−001 ...	43980.15	Tethys	—
0284S2−001 ...	43980.21	Tethys	—
0290S2−001 ...	43980.27	Tethys	3–16
0466S2−001 ...	43983.23	Enceladus	—
0472S2−001 ...	43983.29	Enceladus	—
0478S2−001 ...	43983.35	Enceladus	—
0484S2−001 ...	43983.41	Enceladus	—
0490S2−001 ...	43983.47	Enceladus	—

Picno	FDS	Satellite	Figure No.	Picno	FDS	Satellite	Figure No.
0496S2−001 ...	43983.53	Enceladus	—	1225S2−001 ...	43996.02	Enceladus	2–10
0596S2−001 ...	43985.33	Tethys	—	1228S2−001 ...	43996.05	Enceladus	—
0600S2−001 ...	43985.37	Tethys	—	1308S2−001 ...	43997.25	Enceladus	2–11
0604S2−001 ...	43985.41	Tethys	3–17	1312S2−001 ...	43997.29	Enceladus	2–12
0608S2−001 ...	43985.45	Tethys	—	1316S2−001 ...	43997.33	Enceladus	2–13
0612S2−001 ...	43985.49	Tethys	—	1320S2−001 ...	43997.37	Enceladus	—
0616S2−001 ...	43985.53	Tethys	—	1403S2−001 ...	43999.00	Enceladus	2–14
0800S2−001 ...	43988.57	Tethys	3–18	1505S2−001 ...	44000.42	Enceladus	2–15
0809S2−001 ...	43989.06	Enceladus	—	1507S2−001 ...	44000.44	Enceladus	2–16
0813S2−001 ...	43989.10	Enceladus	—	1509S2−001 ...	44000.46	Enceladus	2–17
0817S2−001 ...	43989.14	Enceladus	—	1511S2−001 ...	44000.48	Enceladus	2–18
0821S2−001 ...	43989.18	Enceladus	—	1513S2−001 ...	44000.50	Enceladus	—
0825S2−001 ...	43989.22	Enceladus	—	1700S2−001 ...	44003.57	Tethys	3–21
0993S2−001 ...	43992.10	Enceladus	2–6	1703S2−001 ...	44004.00	Tethys	—
0999S2−001 ...	43992.16	Tethys	3–19	1707S2−001 ...	44004.04	Mimas	—
1003S2−001 ...	43992.20	Tethys	—	1710S2−001 ...	44004.07	Mimas	—
1007S2−001 ...	43992.24	Tethys	—	1715S2−001 ...	44004.12	Enceladus	2–19
1011S2−001 ...	43992.28	Tethys	—	1719S2−001 ...	44004.16	Enceladus	—
1015S2−001 ...	43992.32	Tethys	—	1723S2−001 ...	44004.20	Enceladus	2–20
1055S2−001 ...	43993.12	Enceladus	2–7	1727S2−001 ...	44004.24	Enceladus	2–21
1059S2−001 ...	43993.16	Enceladus	2–8	1731S2−001 ...	44004.28	Enceladus	2–22
1063S2−001 ...	43993.20	Enceladus	2–9	1735S2−001 ...	44004.32	Enceladus	2–23
1067S2−001 ...	43993.24	Enceladus	—	1739S2−001 ...	44004.36	Enceladus	2–24
1221S2−001 ...	43995.58	Tethys	3–20	0115S2+000 ...	44007.32	Tethys	3–22